

Mont Terri Project – Hydrogeological Synthesis, Osmotic Flow

Berichte des BWG, Serie Geologie – Rapports de l'OFEG, Série Géologie – Rapporti dell'UFAEG, Serie Geologia – Reports of the FOWG, Geology Series

No. 6 – Bern 2004



Bundesamt für Wasser und Geologie **BWG**
Office fédéral des eaux et de la géologie **OFEG**
Ufficio federale delle acque e della geologia **UFAEG**
Uffizi federal per aua e geologia **UFAEG**
Federal Office for Water and Geology **FOWG**

Eidgenössisches Departement für Umwelt, Verkehr,
Energie und Kommunikation
Département fédéral de l'environnement, des transports,
de l'énergie et de la communication
Dipartimento federale dell'ambiente, dei trasporti,
dell'energia e delle comunicazioni
Federal Department of Environment, Transport,
Energy and Communications

Mont Terri Project – Hydrogeological Synthesis, Osmotic Flow

P. Heitzmann (editor)

Berichte des BWG, Serie Geologie – Rapports de l'OFEG, Série Géologie – Rapporti dell'UFAEG, Serie Geologia –
Reports of the FOWG, Geology Series

No. 6 – Bern 2004



Bundesamt für Wasser und Geologie **BWG**
Office fédéral des eaux et de la géologie **OFEG**
Ufficio federale delle acque e della geologia **UFAEG**
Uffizi federal per aua e geologia **UFAEG**
Federal Office for Water and Geology **FOWG**

Contents

Synthesis of Hydrogeological Investigations at the Mont Terri Site (Phases 1 to 5)

P. Marschall, J. Croisé, L. Schlickenrieder, J.-Y. Boisson, P. Vogel & S. Yamamoto

7

An Experimental and Modelling Study of Chemico-osmotic Effects in the Opalinus Clay of Switzerland

D.J. Noy, S.T. Horseman, J.F. Harrington, P. Bossart & H.R. Fisch

95

Impressum

Editor Federal Office for Water and Geology,
FOWG

ISSN / ISBN ISSN 1660-0754 / ISBN 3-906723-70-4

Recommended quotation Heitzmann, P., editor (2004):
Mont Terri Project – Hydrogeological Synthesis – Osmotic Flow. Reports of the Federal
Office for Water and Geology (FOWG),
Geology Series No. 6.

For individual articles:

Marschall, P.
et al. (2004):
Synthesis of Hydrogeological Investigations
at the Mont Terri site (Phases 1 to 5). In:
Heitzmann, P. ed. (2004): Mont Terri Project
– Hydrogeological Synthesis, Osmotic Flow.
Reports of the Federal Office for Water and
Geology (FOWG), Geology Series No. 6.

Noy, D. J. et al. (2004): An experimental and modelling study of
chemico-osmotic effects in the Opalinus
Clay of Switzerland. In: Heitzmann, P. ed.
(2004): Mont Terri Project – Hydrogeological
Synthesis – Osmotic Flow. Reports of the
Federal Office for Water and Geology
(FOWG), Geology Series No. 6.

Cover photos

© Nagra, © Comet

Internet

This report is available in PDF format at
www.bwg.admin.ch

Impression

1200 copies

Distribution

BBL, Vertrieb Publikationen, CH-3003 Bern
www.bbl.admin.ch/bundespublikationen

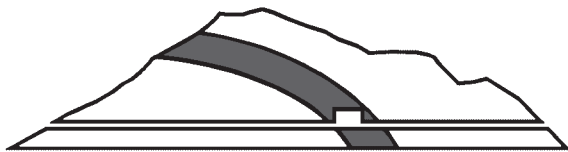
Order Number

804.606.eng

Copyright

© FOWG, Bern-Ittigen, 2004

Organizations involved in the Mont Terri Project



Mont Terri Project Underground Rock Laboratory Laboratoire souterrain

FOWG/SGS ANDRA BGR CRIEPI ENRESA GRS HSK IRSN JNC NAGRA OBAYASHI SCK•CEN

Responsible for the Mont Terri motorway tunnel system and authorizations

RCJU

République et Canton du Jura
Département de l'Environnement et de l'Équipement

Project Partners

ANDRA

Agence nationale pour la gestion des déchets radioactifs, France

BGR

Bundesanstalt für Geowissenschaften und Rohstoffe, Germany

CRIEPI

Central Research Institute of Electric Power Industry, Japan

ENRESA

Empresa Nacional de Residuos Radiactivos, S.A., Spain

FOWG/SGS

Federal Office for Water and Geology, Swiss Geological Survey

GRS

Gesellschaft für Anlagen- und Reaktorsicherheit mbH, Germany

HSK

Swiss Federal Nuclear Safety Inspectorate

IRSN

Institut de radioprotection et de sûreté nucléaire, France

JNC

Japan Nuclear Cycle Development Institute, Japan

NAGRA

National Cooperative for the Disposal of Radioactive Waste, Switzerland

OBAYASHI

Obayashi Corporation, Japan

SCK•CEN

Studiecentrum voor Kernenergie, Centre d'étude de l'énergie nucléaire, Belgium

Direction of the Project

FOWG

Federal Office for Water and Geology, Switzerland

Project Management

GI

Geotechnical Institute Ltd., St-Ursanne, Switzerland

List of authors

Hydrogeological Synthesis: List of authors

J.-Y. Boisson
I.R.S.N. / D.E.S. / S.E.S.I.D.
Bat. UIS / pièce 224
60–68 Avenue du Général Leclerc BP n°17
F-92 262 Fontenay-aux-Roses Cedex France
jean-yves.boisson@irsn.fr

J. Croisé
Colenco Power Engineering AG
Täferstrasse 26
CH-5405 Baden, Switzerland
jean.croise@colenco.ch

P. Marschall
Nagra
Hardstrasse 73
CH-5430 Wettingen, Switzerland
paul.marschall@nagra.ch

L. Schlickenrieder
Colenco Power Engineering AG
Täferstrasse 26
CH-5405 Baden, Switzerland
liane.schlickenrieder@colenco.ch

P. Vogel
BGR
Stilleweg 2
CH-30655 Hannover, Germany
p.vogel@bgr.de

S. Yamamoto
Obayashi Corporation
Shinagawa Intercity Tower B, 2-15-2 Konan,
Minatoku,
Tokyo 108-8502, Japan
yamamoto.shuichi@obayashi.co.jp

Editor

Peter Heitzmann
Federal Office for Water and Geology
Swiss Geological Survey
CH-3003 Bern
Switzerland
peter.heizmann@bwg.admin.ch

Osmotic Flow: List of authors

P. Bossart
Geotechnisches Institut AG
Gartenstr. 13
CH-3007 Bern, Switzerland
paul.bossart@geo-online.com

H.R. Fisch
Solexperts AG
Schulstrasse 5
CH-8603 Schwerzenbach, Switzerland

J.F. Harrington
British Geological Survey
Kingsley Dunham Centre
Keyworth
Nottingham
NG12 5GG
United Kingdom

St.T. Horseman
British Geological Survey
Kingsley Dunham Centre
Keyworth
Nottingham
NG12 5GG
United Kingdom

D.J. Noy
British Geological Survey
Kingsley Dunham Centre
Keyworth
Nottingham
NG12 5GG
United Kingdom

Preface of the Editor

The international research project Mont Terri (St-Ursanne, Canton Jura) started in January 1996. Research is carried out in a gallery and in niches excavated from the security gallery of the Mont Terri road tunnel. The aim of the project is the geological, hydrogeological, geochemical and geotechnical characterisation of a clay formation, specifically of the Opalinus Clay. Twelve partners from six different countries participate today in the project. The Swiss Geological Survey, a division of the Federal Office for Water and Geology (FOWG), supports hydrogeological research projects in low-permeability formations and is one of the Mont Terri partners since the beginning of the project. The FOWG is in charge of the project direction since July 2001 and is also responsible for the publication of the reports. For geological reasons, a repository for radioactive waste in the Mont Terri region has been ruled out.

After the completion of different experiments in the field of hydrogeology during phases 1 to 5, the results obtained were compiled in an extensive synthesis. Following the publication of a general synthesis (SNHGS, Geological Report No. 23, 1999), the geological description of the Mont Terri region (Reports of the FOWG, Geology Series No. 4, 2003) and the geochemical synthesis (Reports of the FOWG, Geology Series No. 5, 2003), we are pleased to present now the hydrogeological synthesis and a special report on osmotic flow to a broader scientific audience. The editor would like to express his best thanks to the authors and all others contributing to this volume for their special effort. We would also like to thank the Mont Terri Partners for their excellent collaboration and the federal and cantonal authorities for their support in the project. Dr. P. Heitzmann (FOWG) is gratefully acknowledged for the edition of this report.

The authors alone are responsible for the content of the text and the illustrations.

Further information can be found on the Internet site www.mont-terri.ch.

Préface de l'éditeur

Depuis 1996, des expériences dans le cadre du projet de recherche international du Mont Terri (St-Ursanne, Canton du Jura) sont réalisées dans une galerie et des niches excavées à partir de la galerie de sécurité du tunnel autoroutier du Mont Terri. L'objectif principal du projet est la caractérisation géologique, hydrogéologique, géochimique et géotechnique d'une formation argileuse, les Argiles à Opalinus. Douze partenaires de six différents pays collaborent aujourd'hui au projet. Le Service géologique national (Office fédéral des eaux et de la géologie, OFEG) soutient l'étude des formations géologiques à faible perméabilité et collabore dès le début comme partenaire au Projet Mont Terri. La direction du projet est depuis juillet 2001 placée sous la responsabilité de l'OFEG, auquel incombe également la publication des rapports. Pour des raisons géologiques, il n'est pas question d'entreposer des matériaux radioactifs dans la région du Mont Terri.

Après l'achèvement des différentes expériences hydrogéologiques des phases 1 à 5, les résultats obtenus ont été mis en valeur sous la forme d'une vaste synthèse. C'est un plaisir de présenter ici à un large public de spécialistes cette synthèse hydrogéologique, accompagnée d'un rapport spécial sur le flux osmotique, après la publication d'une première synthèse générale (SHGN, Rapport géologique No 23, 1999), la description géologique de la région du Mont Terri (Rapports de l'OFEG, Série géologie No 4, 2003) et la synthèse géochimique (Rapports de l'OFEG, Série géologie No 5, 2003). L'éditeur tient à remercier les auteurs ainsi que les personnes qui, par leur compétence et leur engagement, ont permis la réalisation de cette synthèse. Nos remerciements s'adressent aussi à nos partenaires du Projet Mont Terri pour leur précieuse collaboration et aux autorités fédérales et cantonales pour leur soutien dans le projet. P. Heitzmann, dr.sc.nat. (OFEG) est remercié du suivi de l'édition du rapport.

Les auteurs sont seuls responsables du contenu du texte et des illustrations.

Pour toute information supplémentaire, veuillez consulter le site Internet www.mont-terri.ch.

Vorwort des Herausgebers

Seit 1996 werden im Rahmen des internationalen Forschungsprojektes Mont Terri (St-Ursanne, Kanton Jura) in einem erweiterten Teil des Sicherheitsstollens des Mont-Terri-Autobahntunnels Untersuchungen durchgeführt. Das Hauptziel dieses Projektes ist die geologische, hydrogeologische, geochemische und geotechnische Charakterisierung von Tongesteinen, im Speziellen des Opalinus-Tons; heute sind zwölf Partner aus sechs Ländern daran beteiligt. Die Landesgeologie im Bundesamt für Wasser und Geologie (BWG) unterstützt die hydrogeologischen Untersuchungen geringdurchlässiger geologischer Formationen und arbeitet deshalb von Beginn an als Partnerin im Mont-Terri-Projekt mit. Die Leitung des Projektes liegt seit Mitte 2001 beim BWG. Dieses ist auch für die Veröffentlichung der Berichte verantwortlich. Aus geologischen Gründen ist im Mont-Terri-Gebiet jegliche Planung eines Endlagers für radioaktive Abfälle ausgeschlossen.

Nach der Durchführung verschiedener hydrogeologischer Experimente während der Phasen 1 bis 5 sind deren Ergebnisse zu einer umfassenden Synthese verarbeitet worden. Es freut uns, im Rahmen der Mont-Terri-Publikationen nach der einführenden Zusammenfassung (LHG, Geologische Berichte Nr. 23, 1999), der geologischen und hydrologischen Beschreibung des Mont-Terri-Gebietes (Berichte des BWG, Serie Geologie Nr. 4, 2003) und der Geochemie-Synthese (Berichte des BWG, Serie Geologie Nr. 5, 2003) jetzt auch die hydrogeologische Synthese sowie den Spezialbericht über Osmose einem breiten Fachpublikum vorlegen zu können. Das BWG als Herausgeber möchte den Autoren und allen andern, die an diesem Band beteiligt waren, für ihren grossen Einsatz bestens danken. Ebenfalls danken möchten wir unseren Mont-Terri-Partnern für die wertvolle Zusammenarbeit sowie den eidgenössischen und kantonalen Behörden für ihre Unterstützung im Projekt. Dr. P. Heitzmann sei für die Begleitung der Herausgabe gedankt.

Für den Inhalt des Textes und die Illustrationen sind die Autoren allein verantwortlich.

Weitere Informationen zum Mont-Terri-Projekt finden Sie unter www.mont-terri.ch.

Prefazione dell'editore

Dal gennaio 1996, ricerche effettuate nell'ambito del progetto di ricerca internazionale Mont Terri (St-Ursanne, Canton Giura) sono realizzate in un cunicolo e nelle nicchie scavate a partire dalla galleria di soccorso del tunnel autostradale del Mont Terri. L'obiettivo principale del progetto è la caratterizzazione geologica, idrogeologica, geochemica e geotecnica di una particolare formazione argillosa: l'Argilla ad Opalinus. A tutt'oggi collaborano al progetto dodici partner di sei diverse nazioni. Il Servizio geologico nazionale dell'Ufficio federale delle acque e della geologia (UFAEG) promuove gli studi di formazioni geologiche a bassa permeabilità, collaborando fin dall'inizio come partner del progetto Mont Terri. Dal luglio 2001, il progetto è sotto la direzione dell'UFAEG, al quale compete anche la pubblicazione dei rapporti. La pianificazione di un deposito finale per le scorie radioattive sotto il Mont Terri è da escludere per ragioni geologiche.

Dopo aver concluso diverse ricerche idrogeologiche durante le fasi da 1 a 5, i risultati sono stati presentati in un'ampia sintesi. La sintesi e il rapporto speciale sul flusso osmotico, destinati a un largo pubblico di specialisti, fanno seguito alla sintesi introduttiva (SIGN, Rapporti geologici, n. 23, 1999), alla descrizione geologica della regione (Rapporti dell'UFAEG, Serie geologia n. 4, 2003) e alla sintesi geochemica (Rapporti dell'UFAEG, Serie geologia n. 5, 2003). Ringrazio tutti gli autori e le persone che, con le loro conoscenze e il loro impegno, hanno contribuito alla riuscita dell'opera. I ringraziamenti vanno estesi anche ai partner del Mont Terri e alle autorità cantonali e federali per la preziosa collaborazione e il sostegno al progetto. Un ringraziamento particolare va al Dr. P. Heitzmann (UFAEG) per l'edizione del rapporto.

Gli autori sono gli unici responsabili del contenuto dei testi e delle illustrazioni.

Ulteriori informazioni sono pubblicate all'indirizzo www.mont-terri.ch.

Federal Office for Water and Geology
The Head of the Swiss Geological Survey

Dr. Christoph Beer

Synthesis of Hydrogeological Investigations at Mont Terri Site (Phases 1 to 5)

P. Marschall, J. Croisé, L. Schlickenrieder, J.-Y. Boisson, P. Vogel & S. Yamamoto

Recommended quotation:

Marschall, P. et al. (2004): Synthesis of Hydrogeological Investigations at the Mont Terri Site (Phases 1 to 5).

In: Heitzmann, P. ed. (2004): Mont Terri Project – Hydrogeological Synthesis, Osmotic Flow. Reports of the Federal Office for Water and Geology (FOWG), Geology Series No. 6.

Abstract

The Mont Terri project has provided the opportunity to assess hydrogeological testing procedures in the clay-rich Opalinus Clay formation and to shed light on the hydrogeological setting of the Mont Terri region of Northern Switzerland. The hydrogeologically relevant field methodologies applied, data analyses performed and results obtained from experiments conducted in the Mont Terri rock laboratory in the years 1996 to 2000 served as a data base for the three objectives of this synthesis:

- Assessment of the achievements of the hydrogeological investigations both in terms of *development of investigation techniques* and in terms of *geoscientific data analysis*.
- Development of a *conceptual model of groundwater flow* at the Mont Terri site.
- Development of a *conceptual model of gas migration mechanisms* in the Opalinus Clay.

The intended audience of this report includes readers with a hydrogeological background, in general, and an interest in the hydrodynamics of clay-rich formations, in particular. The introduction to the Mont Terri rock laboratory and its geological environment is brief. However, comprehensive literature on the Mont Terri project is referenced.

Various types of hydraulic long-term monitoring systems, e.g. classical inflatable multipacker systems, PP system and minipacker piezometers, were tested in the rock laboratory and evaluated with special focus on their applicability in clay-rich formations. Design criteria were established which prove particularly useful for investigations in Opalinus Clay, such as the minimisation of the effective volume of the observation interval and the appropriate selection of the materials for the downhole equipment to prevent corrosion and to allow for representative porewater sampling.

The results from the hydraulic packer testing were assessed for possible clay-specific artifacts which could be introduced as a consequence of drilling techniques and testing methodologies. The experiments demonstrated that chemico-osmotic effects may influence the transmissivity of the formation zone immediately beyond the borehole wall. The effect is minor, however, and does not significantly affect the formation-property estimates.

A preliminary conceptual hydrogeological model of the Mont Terri site was developed. The hydrogeological units of main concern for the underground laboratory and its vicinity are the karstified “Lower Dogger” aquifer and the Opalinus Clay formation, a highly efficient flow barrier. The hydraulic significance of the Jurensis Marls and Posidonia Shales to the North has

not been established very well. The main fault, which intersects the rock laboratory, does not affect the barrier function of the Opalinus Clay. The hydraulic conductivity of the Opalinus Clay generally shows low spatial variability and lies in the range of 2×10^{-14} – 2×10^{-12} m/s. The expected range of specific storage is 2×10^{-7} – 3×10^{-5} 1/m. The primary driving force for porewater flow in the Opalinus Clay at the Mont Terri site is gravity: the long-term observations of hydraulic head depict a clear cone of depression towards the gallery system. Also, the “Lower Dogger” aquifer to the South represents a sort of constant pressure boundary for the hydraulic system.

An assessment of the gas transport mechanisms with results from laboratory and in-situ experiments showed evidence of both non-dilatant and dilatant gas transport. The observed gas entry pressure for the Opalinus Clay was generally low (< 1 MPa). Enhancement of gas permeability was observed at elevated gas injection pressures (2–3 MPa), suggesting that gas flow is entailed by microscopic pathway dilation processes. Hydrofrac experiments exhibited frac pressures of 9 MPa and refrac pressures in the order of 4–5 MPa.

Acknowledgements

The authors would like to thank Prof. G. de Marsily (Laboratoire Geologie Appliquée, Université Pierre et Marie Curie, Paris / France), Dr. P. Bossart (Mont Terri Project, St. Ursanne / Switzerland) and Dr. M. Thury (Mont Terri Project and Nagra, Wettingen/Switzerland) for inspiring discussions and for valuable review comments on this manuscript. Their contributions to the facts and interpretations greatly improved the overall value of the report and are gratefully acknowledged.

Contents

Abstract	9	4.5.4	The sub-millimeter scale.....	55
Acknowledgments	10	4.6	Pore pressure distribution at the Mont Terri site	58
List of Contents	11	4.6.1	Data base	58
List of Tables	12	4.6.2	Interpretation of the pore pressure distribution in the Opalinus Clay formation	61
List of Figures	13	4.6.3	Simple assessment of the galleries' drainage effects with numerical simulations	62
1 Introduction	15	4.7	Evaluation of current hydrogeological site understanding	66
1.1 The Mont Terri project: Phases 1 to 5..	15	5 Gas Migration Mechanisms in the Opalinus Clay	67	
1.2 Scope and objectives	17	5.1 Introduction	67	
1.3 Report organisation	17	5.2 Conceptual approaches of gas migration in clay formations	67	
2 Hydrogeological Site Investigations in Phases 1 to 5	18	5.3 Quality assurance of gas related experiments	69	
2.1 Geological setting	18	5.4 Modelling of gas related experiments ..	71	
2.2 Program overview	18	5.4.1 Two-phase flow modelling of the gas threshold pressure test in BGP-4	71	
2.3 Experiments of hydrogeological relevance	20	5.4.2 Hydro-mechanical modelling of the BGS-2 gas injection experiment Objectives	73	
3 Developments in Hydrogeological Investigation Techniques and Data Analysis	23	5.4.3 Long-term gas injection tests	76	
3.1 Particular issues of interest	23	5.4.4 Hydrofrac an gasfrac experiments	76	
3.2 Suitability assessment of hydrogeologi- cally relevant data	23	5.5 Evaluation of achievements.....	79	
3.3 Developments in long-term monitoring systems for pore pressure and water sampling	24	5.5.1 Two phase flow modelling of the gas threshold pressure test in BGP-4 Objectives	79	
3.3.1 Problems related to the clay-rich environment	24	5.5.2 Hydro mechanical modelling of the BGS-2 gas injection experiment Objectives	82	
3.3.2 Equipment portraits	24	6 Summary and Conclusions	86	
3.3.3 Equipment performance	27	6.1 Summary of achievements	86	
3.3.4 Concluding remarks.....	28	6.2 Unresolved issues and outlook	87	
3.4 Impact of drilling technique on packer test results	29	7 References	88	
4 Conceptual Model of Groundwater Flow at the Mont Terri Site	31	Mont Terri technical Notes	89	
4.1 Introduction	31			
4.2 General outline of the synthesis approach	31			
4.3 Hydrogeological data base from Phases 1 to 4	32			
4.3.1 Packertests.....	32			
4.3.2 Permeameter tests	35			
4.4 Assessment of coupled processes.....	37			
4.4.1 Threshold gradient.....	37			
4.4.2 Osmosis	41			
4.4.3 Coupled hydro-mechanical processes..	43			
4.5 Groundwater flow at different scales ..	49			
4.5.1 Site scale ($10^1 - >10^3$ m)	50			
4.5.2 The scale of tunnel investigations ($10^{-1} - 10^1$ m)	53			
4.5.3 The scale of core mapping ($10^{-3} - 10^{-1}$ m)	55			

List of Tables

Table 1.1: Organisations involved in the Mont Terri project	16
Table 2.1: Main contributing experiments to the hydrogeological investigations at the Mont Terri site	19
Table 3.1: Summary of the suitability assessment with resulting suitability typing.	24
Table 3.2: Summary of the results from the final hydraulic test sequence after fluid replacement with Pearson water in boreholes BDB-1, BDB-2 and BDB-3	35
Table 4.1: Overview of the relevant packer test results in the Opalinus Clay formation at the Mont Terri rock laboratory.....	35
Table 4.2: Summary of results from the permeameter tests and structural investigations.....	36
Table 4.3: Range of validity of Darcy's law and threshold gradient estimates.....	41
Table 4.4: Hydrogeological classification of the lithostratigraphic units in the Mont Terri region (after Thury & Bossart 1999).....	52
Table 4.5: Ranges of hydraulic properties in the 3 facies of the Opalinus Clay.....	55
Table 4.6: Mineralogy of the clay-rich shaly facies of the Opalinus Clay at Mont Terri after Mazurek (2001).	56
Table 4.7: Microstructural properties of the Opalinus Clay at Mont Terri after Nagra 2002.....	57
Table 5.1: Overview of potential gas migration mechanisms.	57
Table 5.2: Summary of the quality review of the field and laboratory methods.	70
Table 5.3: Summary of the quality review of the data analysis of gas tests performed in Phases 1 to 5.....	71
Table 5.4: Two-phase flow parameters as derived from laboratory experiments on core samples of the Opalinus Clay from the Mont Terri rock laboratory.	72
Table 5.5: Two-phase flow parameters as derived from gas threshold pressure tests at the Mont Terri rock laboratory.	74
Table 5.6: Hydraulic fracturing experiment in interval I2.2 of borehole BGS-2: stages of the complex test sequence.	78

List of Figures

Figure 1.1: Location map of the Mont Terri Rock Laboratory (Thury & Bossart eds. 1999).....	15	interval pressures.....	49
Figure 1.2: Overview of the organisational structure and distribution of responsibilities for the Mont Terri project as of July 2001	16	Figure 4.13: Hydraulically relevant structural and stratigraphic elements at various scales of observation.....	50
Figure 2.1: (a) View toward the North, with St-Ursanne in the foreground and Mont Terri in the center with the red arrow indicating the southern entrance of the motorway tunnel. (b) 3D view of the Mont Terri rock laboratory.....	18	Figure 4.14: (a) Simplified geological cross-section through the Mont Terri anticline along the motorway tunnel, showing the location of the Mont Terri rock laboratory (Thury & Bossart 1999) and (b) simplified map of the Mont Terri anticline	51
Figure 2.2: 3D view of the Mont Terri site showing niches and boreholes of relevance for the synthesis of hydrogeological investigations.....	22	Figure 4.15: Chloride profiles as an indirect evidence for groundwater flow conditions in the Opalinus Clay and in the adjacent stratigraphic formations	53
Figure 3.1: Piezometer systems tested in Phases 1 to 4 of the Mont Terri research program.....	26	Figure 4.16: The scale of tunnel investigations ($10^{-1} - 10^1$ m)	54
Figure 3.2: Pressures recorded with inflatable packers and mechanical minipacker piezometers during the interference test of the GP experiment/Phases 1 and 2	27	Figure 4.17: Small scale mapping of structural features in the BF niche of the reconnaissance gallery	55
Figure 3.3: Pressures recorded with inflatable packers and PP equipment in the GP experiment/ Phases 3 and 4.....	28	Figure 4.18: Photographic documentation of drillcores and classification of lithological/structural features.	
Figure 3.4: Map view and cross-section of the set-up for the systematic investigation of the impact of the drilling technique and the chemical composition of the test fluids on packer test results.....	30	Figure 4.19: Visualisation of the microstructure of Opalinus Clay by SEM	57
Figure 4.1: Baseline simulation of pressure response in BGP-1	33	Figure 4.20: Determination of equivalent pore radii by Hg porosimetry and nitrogen desorption	57
Figure 4.2: Baseline simulation of pressure change and derivative during BGP-1 – R12 constant-rate injection test	33	Figure 4.21: Cross-section through the Mont Terri site with piezometric levels.....	58
Figure 4.3: Uncertainty analysis of BGP-1 hydraulic conductivity and specific storage estimates	34	Figure 4.22: Pressure monitoring from mid 1997 to early 1999	59
Figure 4.4: Schematic configuration of the BGS permeameter after Harrington et al. 2001.....	36	Figure 4.23: The pressure transients in the period from July 1999 to June 2000	61
Figure 4.5: Permeameter test conducted in the OP experiment.....	38	Figure 4.24: Compilation of pressure observations in boreholes of the Mont Terri rock laboratory on 30.06.2000	62
Figure 4.6: Simulation of a sequence of rate injection and head injection tests in BGP-4 as part of the GP experiment	39	Figure 4.25: Compilation of pressure observations gathered in boreholes at the Mont Terri rock laboratory on 30.06.2000	63
Figure 4.7: Simulation of the crosshole response in BGP-3/I1 to a sequence of rate injection and head injection tests in BGP-4	40	Figure 4.26: Vertical configuration and 2D finite element mesh used to simulate the pressure head	64
Figure 4.8: Pressures recorded in borehole BOP-1 ...	42	Figure 4.27: Simulation of the distribution of pressure head	64
Figure 4.9: Schematic diagram showing Total Dissolved Solids vs. Distance along the Mont Terri reconnaissance gallery.....	43	Figure 4.28: Comparison of pressure observations and the results of the numerical simulation with $K = 1 \times 10^{-13}$ m/s and $S_s = 1 \times 10^{-6}$ 1/m.....	65
Figure 4.10: Interference test in the FM niche with a water-injection test in BGP-6: test configuration with the four boreholes.....	45	Figure 5.1: Schematic view of the isostatic cell and sample assembly for the Opalinus Clay samples as part of the GP experiment	72
Figure 4.11: Inverse modelling of the packer test conducted in BGP-6	47	Figure 5.2: Photographs of the BED-C5/7 sample taken right after the gas injection test.....	73
Figure 4.12: Hydro-mechanical modelling of the interference test in BGP-6 – simulated		Figure 5.3: Diagnostic analysis of gas threshold pressure test in interval I4.2 of borehole BGP-4	74
		Figure 5.4: Long-term gas injection experiment in the GP-A/GS site	75
		Figure 5.5: Sequence of hydrofrac and re-frac events	

in test interval I2.2 of borehole BGS-2.....	77
Figure 5.6: Hydraulic response in interval I1.2 of borehole BGS-1 to the hydrofrac and re-frac events in test interval I2.2 of borehole BGS-2	78
Figure 5.7: Modelling of the extended gas threshold pressure test in interval I4.2 of borehole BGP-4 with a two-phase flow simulator	81
Figure 5.8: Modelling of the gas test sequence in BGS-2/I2 with TOUGH2	83
Figure 5.9: Coupled 3D hydro-mechanical simulation: Pressure history in BGS-2/I2, BGS-1/I2 and BGS-2/I3, and FIM data in boreholes BGS-3 and BGS-4	84

1 Introduction

1.1 The Mont Terri project: Phases 1 to 5

The Mont Terri project was called to life in 1995. The common interest of the founding organisations concerned argillaceous formations as potential host rocks for repositories of radioactive waste. The hub of the international research project is the Mont Terri rock laboratory in the Mont Terri motorway tunnel in north-western Switzerland (Figure 1.1). Its testing ground is the Opalinus Clay, a Mesozoic shale formation. The organisational structure of the Mont Terri project is sketched out in Figure 1.2. The Director of the Mont Terri project is a member of the Swiss Geological Survey of the Federal Office for Water and Geology (FOWG/SGS). Delegates of the FOWG/SGS as well as of the remaining partner organisations form the program committee which is responsible for the definition of annual research programs (see Table 1.1) and budgets. This way each project partner may bring forward its own experiment proposals or express interest to participate in others. Incidentally, the annual research periods are referred to as Phases which generally span from the beginning of July of one year to the end of June of the following year.

The FOWG/SGS submits the annual research programs to the République et Canton Jura for authorisation. Once the research program for a Phase has been authorised it is the responsibility of the project manager (represented by Geotechnical Institute Ltd of St-Ursanne), to implement it in the laboratory. Each experiment is assigned a principal investigator who is one of the delegates representing the participating project partners for that particular experiment. The principal investigator, together with the experiment delegates and the project manager, ascertains that the scientific goals of the experiment are achieved. In particular, the technical performance of field work and laboratory tests as well as the quality assurance of the project documentation, are their key concerns. Complementary, the project management draws responsible for the on-site coordination of the field work, the book keeping and the distribution of reports. The work is then carried out by a series of contractors of which currently there are about 23 universities and national research institutes plus more than 30 companies from six European countries and Japan.

The research program conducted at the Mont Terri rock laboratory is rather comprehensive. The overall aim, to broaden the geoscientific data base as a prerequisite for comprehensive understanding of the barrier function of argillaceous formations, calls upon the full spectrum of geosciences. It may best be summarised with the following objectives:

- Evaluation of investigation techniques particularly suitable to a low permeability clay-rich medium
- Characterisation of the Opalinus Clay formation in terms of its geological, hydrogeological, geochemical and mechanical properties
- Characterisation of changes in the argillaceous host rock environment as induced by gallery excavation, by exposure to a heat source and by chemically aggressive fluids
- Evaluation of suitable techniques for repository construction, waste emplacement and gallery sealing in the Opalinus Clay

The activities of Phases 1 to 4 of the Mont Terri project were occupied predominantly by the compilation of a broad basis of geoscientific data in a fairly short period of time, rather than at conducting elaborate data analyses and integrated interpretations. At the end of Phase 4 a new type of scientific projects was implemented specifically for the interdisciplinary interpretation of data acquired to that point in time: "Geo-

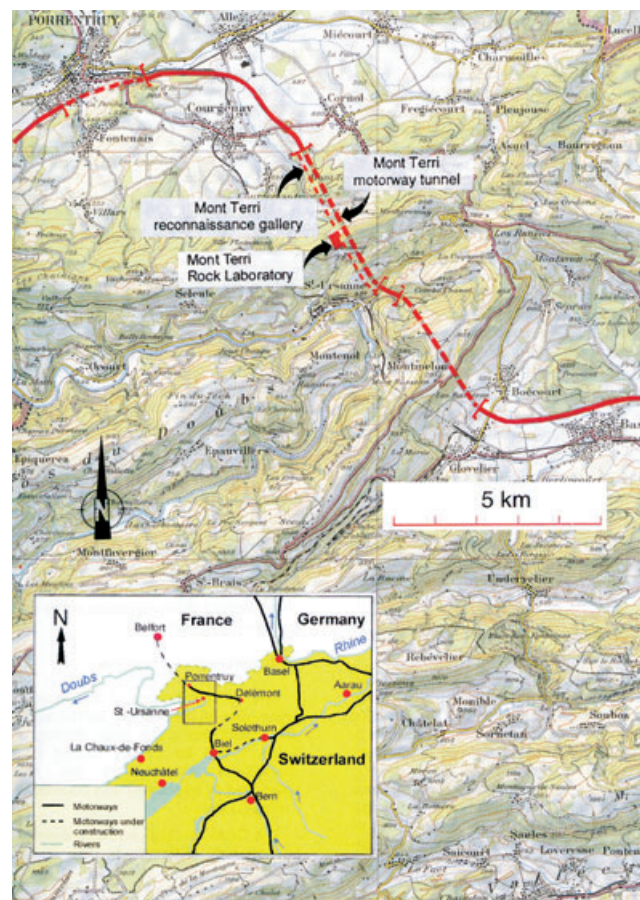


Figure 1.1: Location map of the Mont Terri Rock Laboratory (Thury & Bossart eds. 1999). Published with the permission of swisstopo (BA046450).

chemical Modelling" (GM), "Rock Mechanical Analyses" (RA) and "Hydrogeological Analyses" (HA). This report is part of the HA project and summarises the

interpretation and synthesis of the hydrogeological data base from Phases 1 to 5. Project partners are BGR, IRSN, Nagra and Obayashi Corporation.

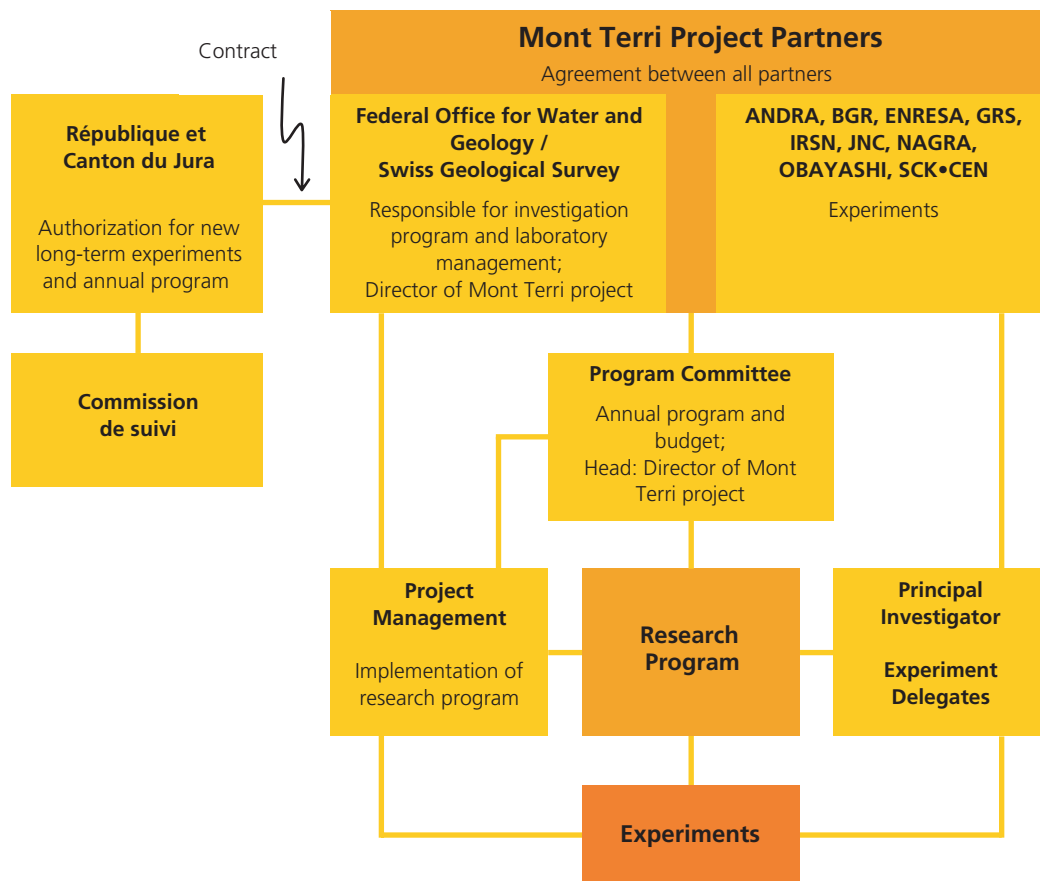


Figure 1.2: Overview of the organisational structure and distribution of responsibilities for the Mont Terri project as of July 2001 (after www.forumvera.ch Bulletin 03/01).

Project Partners

FOWG/SGS	Federal Office for Water and Geology/Swiss Geological Survey (Director of the Mont Terri project)	Switzerland
ANDRA	Agence nationale pour la gestion des déchets radioactifs	France
BGR	Bundesanstalt für Geowissenschaften und Rohstoffe	Germany
CRIEPI*)	Central Research Institute of Electric Power Industry	Japan
ENRESA	Empresa Nacional de Residuos Radiactivos, S.A.	Spain
GRS	Gesellschaft für Anlagen- und Reaktorsicherheit mbH	Germany
IRSN	Institut de radioprotection et de sûreté nucléaire	France
JNC	Japan Nuclear Cycle Development Institute	Japan
NAGRA	National Cooperative for the Disposal of Radioactive Waste	Switzerland
OBAYASHI	Obayashi Corporation	Japan
SCK•CEN	Studiecentrum voor Kernenergie, Centre d'étude de l'énergie nucléaire	Belgium

Project Management

GI	Geotechnical Institute Ltd., St-Ursanne	Switzerland
-----------	-----------------------------------------	-------------

Table 1.1: Organisations involved in the Mont Terri project (* joined in July 2002).

1.2 Scope and objectives

The early Phases of the Mont Terri project emphasised data collection in the field and initial analysis. Integrated approaches to the interpretation of field results had been assigned low priority. Consequently, many of the field and laboratory investigations were documented in a series of Mont Terri Technical Notes without a well-defined level of quality assurance. It was left to the different experimental teams to specify their quality requirements for the contractors' reports. Eventually, at the end of Phase 4 the project partners agreed to implement a new type of scientific projects. These were to stress the synergetic interpretation of the data compiled since the beginnings of the project for the interests of specific disciplines. The experiments initiated for this purpose in the realm of the Mont Terri research program are Geochemical Modelling and Synthesis (GM; Pearson et al. 2003), Rock Mechanical Analyses (RA; Bock 2001, 2002) and Hydrogeological Analyses (HA).

This report is one of the products of the HA experiment. The project partners participating in this experiment have been BGR (Germany), IRSN (France), Nagra (Switzerland) and Obayashi Corporation (Japan). The report's purpose is to provide a synthesis of the hydrogeological investigations conducted at the Mont Terri site in the course of project Phases 1 through 5, i.e. from the project's beginnings in 1996 to mid 2000. The approach chosen to attain this goal divides the synthesis into three subtasks:

- To assess the achievements of the hydrogeological investigations both in terms of *development of investigation techniques* and in terms of *geoscientific data analysis* in low permeability argillaceous formations
- To establish a *conceptual model of groundwater flow* at the site
- To establish a *conceptual model of gas migration mechanisms in Opalinus Clay*

The concluding efforts are dedicated to an assessment of the current level of overall conceptual understanding of groundwater flow at the site, as well as to open issues requiring further attention.

The intended readership of this report includes scientists actively involved in the experimental work at the Mont Terri laboratory and, more generally, hydrogeologists working with shaly aquitards. The synthesis may be of interest particularly to scientists and engineers engaged in projects related to the geological disposal of radioactive waste. For an account of the larger scope and context of the Mont Terri project, the reader

is referred to, for example, Thury & Bossart eds. (1999). This report does not cover the complex hydro-mechanical processes observed in the excavation disturbed zone (cf. Martin & Lanyon 2004), nor those in the unsaturated zone.

1.3 Report organisation

The opening chapter 1 provides general organisational background on the Mont Terri project, outlines the overall goals and motivation of the project, and introduces the objectives for this synthesis of hydrogeological investigations. Beyond that, the report essentially follows the objectives as stated above.

Chapter 2 is an introduction to the hydrogeological site investigations conducted in Phases 1 through 5. It sets the stage for the subsequent chapters with a short outline of the infrastructure of the underground rock laboratory and a brief review of the experiments of relevance for the synthesis of hydrogeological investigations overall.

Chapter 3 then provides a more detailed look of the hydrogeologically relevant investigations with an assessment of three specific aspects: (i) the suitability of hydrogeologically relevant data for consideration in the synthesis; (ii) recent developments in long-term monitoring methodologies for in-situ pore pressures; and (iii) the reliability of packer test results.

Chapter 4 establishes a conceptual model of groundwater flow for the Mont Terri site. The regional extent of the site scale is in the order of several kilometers. More detailed relevant scales addressed in the model are those generally covered in tunnel investigations, in core mapping and in small experimental or microscopic work. These are characterised in terms of groundwater flow mechanisms and site specific hydraulic parameters. The final section discusses the current perception of the distribution of pore water pressure at the site.

Chapter 5 is devoted to gas migration mechanisms in the Opalinus Clay. Relevant mechanisms are assessed, experimental work on gas migration is reviewed and information on the two-phase flow properties of the Opalinus Clay is compiled.

The final chapter summarises the key findings of the synthesis and points out some unresolved issues with an outlook on developments to be expected in the project's future.

2 Hydrogeological Site Investigations in Phases 1 to 5

2.1 Geological setting

There are two main structural domains of the Jura mountains in Switzerland: the Tabular Jura and the Folded Jura. Rocks in the Jura mountains are of Triassic to early Cretaceous age and were deposited mostly in marine environments with generally uniform subsidence. They comprise limestones, evaporitic rocks, and marls/shales. Mont Terri, situated near the town of St-Ursanne (Figure 2.1a) is the northernmost of a series of anticlines of the Folded Jura, and has been overthrust at least 1 km north-westwards over the Tabular Jura. In its total length, the anticline is 50 km along strike and, at Mont Terri, is an asymmetrical dome-shaped fold. Folding took place during the Late Miocene to Pliocene, about 10 to 2 Ma ago.

Rocks of Middle Jurassic to Triassic age (i.e. Dogger to Keuper) are exposed on the present surface of Mont Terri (cf. also Figure 4.14). The formation of interest, the Opalinus Clay, is of Lower Aalenian age (Dogger α , 180 to 178 Ma). In northern Switzerland it forms an 80 to 160 m thick sequence of claystone and marl with intercalated sandy and calcareous layers and lenses. In the Mont Terri underground laboratory, the Opalinus Clay is met at a present overburden of 250 to 320 m. The past overburden is estimated to at least 1000 m. The formation dips from 20 to 60° to the southeast and intersects the reconnaissance gallery for a 243 m long section (Figure 4.14a). It is underlain by the Toarcian Jurensis marl (Lias ζ) and overlain by the so-called Lower Dogger (Lower Bajocian/Upper Aalenian, elsewhere called Murchisonae-Concava Beds, Dogger α , or Blaukalk). Between the Muschelkalk aquifer below and the Malm aquifer above, the shale succession from Keuper/Lias to Dogger forms a 300 to 450 m thick sequence of low to very low permeability rocks. The

Opalinus Clay can be considered to have water-saturated pore space but practically no water circulation. The overlying Malm formation represents a regional karstic aquifer (e.g. Hauptrogenstein), whereas the underlying Liassic marls and limestones (e.g. Gryphaea Limestones) are only weakly karstified with local water inflows. This very brief description of the geological and hydrogeological setting of the laboratory has been taken from Thury & Bossart eds. (1999), however, in depth discussions will follow in sections 4.5 to 4.7. Notably, an excellent summary of the geology of the Mont Terri site is given in Pearson et al. (2003).

2.2 Program overview

The Mont Terri underground laboratory is located in northwestern Switzerland near the town of St-Ursanne (Figure 2.1a). The laboratory is positioned in the reconnaissance gallery for one of the tunnels of the A16 Transjurane motorway. Constructed in 1989, the reconnaissance gallery meanwhile has taken on the function of an escape route, i.e. a safety gallery for the motorists. In order to keep the gallery clear of obstructions, the experimental set-ups of the laboratory and the majority of the drilling activity were placed in eight niches especially excavated for this purpose in 1996. All experiments are carried out within the bounds of the Opalinus Clay.

An expansion of the Mont Terri research program prompted the excavation of the roughly 230 m long "new gallery" in the winter of 1997/98. It, too, lies in the Opalinus Clay and the additionally introduced experiments were again set up in niches. Figure 2.1b shows a schematic of the layout of the Mont Terri rock laboratory.

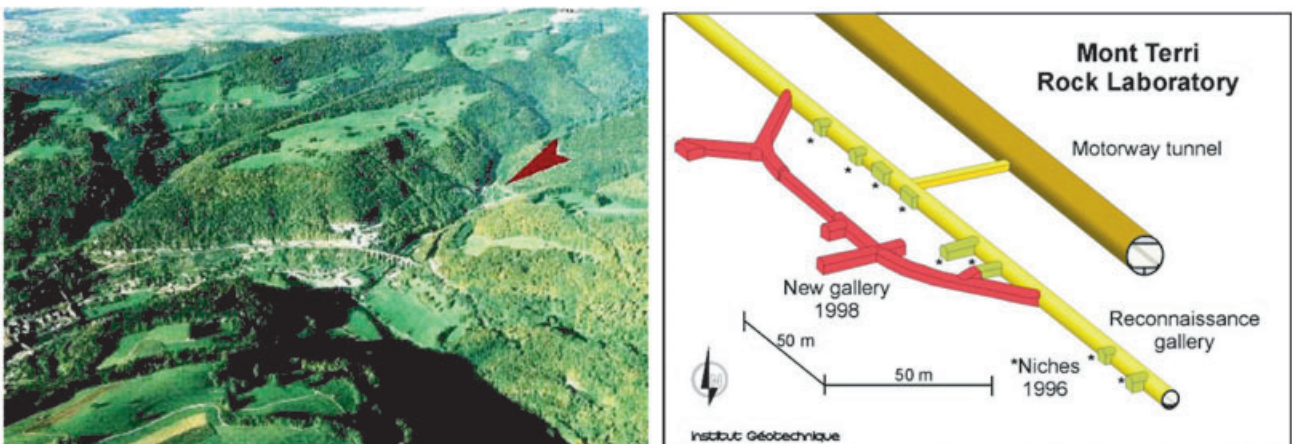


Figure 2.1: (left) View toward the North, with St-Ursanne in the foreground and Mont Terri in the center with the red arrow indicating the southern entrance of the motorway tunnel. (right) 3D view of the Mont Terri Rock laboratory.

The initial set of experiments was run in Phases 1 and 2 between January, 1996 and June, 1997. Hydraulic tests were parts of various experiments designed – at the early stage – primarily to test drilling and measuring techniques in view of the particular challenges posed by the clay-rich mineralogy of the Opalinus Clay formation. From Phase 3 onward, the main focus of the hydrogeologically relevant experiments clearly shifted toward the hydraulic characterisation of the site, i.e. the gathering of representative data. An overview of these experiments is provided in Table 2.1. The experiments' names are an implication of the fact that the investigation approaches and the principal topics of interest have been various. Whereas experiments like the Hydraulic and Gas Permeability experiment (GP), the Pore Pressure experiment (PP), the

Deep Borehole Simulation experiment (DB) and one component of the Flow Mechanism experiment (FM-C) have concentrated on hydraulic packer testing mostly in the undisturbed Opalinus Clay, the ED-A and ED-B experiments were concerned with comparable testing methods but aimed at the excavation disturbed zone. The Gasfrac Self-Healing experiment (GS) and part of GP were devoted mostly to gas testing. The Borehole Fluids Effects (BF) and FM-A experiments shared fluid logging as a common investigation method. The Evaporation Logging experiment (FM-D) was established mainly to test new tools while the Groundwater Sampling experiment (WS-A) was set up primarily for fluid sampling. The Osmotic Pressure experiment (OP) served the analysis of osmotic effects.

Experiment	Hydrogeological relevance	Most pertinent Technical Notes ¹⁾	Phases / Years ²⁾
GP	In-situ hydraulic and gas tests for the determination of the hydraulic and two-phase flow parameters; permeameter tests	96-18, 96-26, 96-27, 97-28, 98-24, 98-25, 99-05, 99-06, 99-07	1 – 5 1996 – 2000
GP-A/GS	Long-term gas injection test/Gasfrac self-healing	2000-06, 2000-07, 2000-10, 2000-11, 2000-12, 2000-13	1 – 6 1996 – 2001
PP	Measurement of the porewater pressure	97-01, 97-02, 97-03	1 – 3 1996 – 1998
DB	Deep borehole hydraulic testing	98-62	4 – 5 1998 – 2000
DT	Drilling techniques (hydraulic test)	96-20	1 – 2 1996 – 1997
BF	Borehole fluid effect	96-05, 96-11, 97-07, 97-36, 98-40, 99-33 (97-29)	1 – 7 1996 – 2002
FM-A	Flow mechanism: fluid logging (& ion-selective logging)		1 – 2 1996 – 1997
WS-A	In-situ groundwater sampling	98-48	1 – 7 1996 – 2002
OP	Hydraulic flow and osmotic pressure	97-39	1 – 6 1996 – 2001
ED-A	EDZ hydraulic and pneumatic tests	97-32	1 – 3 1996 – 1998
ED-B	EDZ porewater pressure monitoring	98-58	4 – 5 1998 – 2000
n.a.	Hydrodynamic characterisation in laboratory	97-38	3 1997
FM-C	Flow mechanism: tracer test (hydraulic testing)	99-49	1 – 7 1996 – 2002
FM-D	Evaporation measurements on tunnel wall and in borehole	96-30, 98-11	3 – 6 1997 – 2001
n.a.	Hydraulic head measurements associated with tunnel excavation	99-22	previous to Mont Terri project

¹⁾ for complete references please refer to chapter 7

²⁾ from Thury & Bossart (1999) and annual work programs

Table 2.1: Main contributing experiments to the hydrogeological investigations at the Mont Terri site with a selection of associated technical notes and an indication of the timeframe within the research program (Note: Some experiments have extended beyond Phase 5. However, only those references are listed which were available by mid 2000).

2.3 Experiments of hydrogeological relevance

It would be beyond the scope of this report to provide detailed descriptions of all relevant experiments. Suffice it then to give a brief overview of the methodology, or at least pertinent parts thereof, for the experiments listed in Table 2.1. For niches and borehole locations, please refer to Figure 2.2.

The GP experiment encompasses hydraulic tests and gas threshold pressure tests in order to investigate single and two-phase flow processes in the Opalinus Clay. The hydraulic tests, including constant rate and constant head injection and pulse tests, have been carried out with various packer configurations in a series of boreholes drilled explicitly for this purpose. The main purpose of the experiments was (i) to investigate the governing flow mechanisms in the Opalinus Clay (possible deviations from Darcy's law), (ii) to determine flow models (flow geometry, coupled processes) and (iii) to estimate representative hydraulic parameters (and two-phase flow parameters).

Attempts have been made to monitor cross-hole pressure responses and responses in intervals located above the test interval, as well as geomechanical reactions to the hydraulic testing. The gas threshold pressure tests have been performed solely in borehole BGP-4. All hydraulic and gas tests have been analysed quantitatively and in detail for formation parameters like hydraulic conductivity, formation storage and gas entry pressure as well as for matrix pressure.

As an independent part of the GP experiment, GP-A is treated in combination with the GS experiment. The hydraulic fracturing tests with hydraulic and gas testing components were conducted in boreholes BGS-1 and BGS-2 and concluded in quantitative estimates of transmissivity for the water phase and of compressibility of the intact formation prior to fracturing. Long-term gas tests are expected to result in two-phase flow properties. Deformations were observed in BGS-3 and BGS-4 in response to hydraulic testing in the adjacent boreholes.

The aim of the PP experiment has been the development and validation of a methodology to measure porewater pressure in formations with very low hydraulic conductivity and free water content. The design of the multi-packer system was to avoid leakage from the test interval, and to minimise the annulus volume and the equipment compressibility in the test section. The very stiff mechanical packers were tested in-situ for their sealing capacity before first pressure build-up measurements were recorded in two test intervals in the Opalinus Clay. The experience gained in the Mol rock laboratory of SCK-CEN con-

cerning PP measurements helped to adequately design the PP equipment for Mont Terri.

The DB experiment was part of the preparation work for the deep borehole project at Benken. Its main concern is the optimisation of the packer testing methodology. Boreholes BDB-1, BDB-2 and BDB-3 at Mont Terri were to simulate the borehole and testing conditions in terms of effects due to different drilling muds and of expected responses to hydraulic testing. The tests included pulse injection, constant head injection and slug withdrawal.

The drilling technique (DT) experiment consisted of three boreholes, BDT-1 to 3 which were all drilled with different fluids. Drilling with compressed air resulted in the most stable boreholes and highest drillcore quality. Of interest to the hydrogeological synthesis are the hydraulic tests performed in three intervals in BDT-2: pulse injection, constant head injection, constant head withdrawal and long-term constant rate injection. The series of tests and the analysis of their observations resulted in transmissivity and corresponding hydraulic conductivity values.

The BF and FM-A experiments are treated in combination for the purpose of the hydrogeological analysis as they share a common investigation method, the fluid logging. In essence, fluid logging entails continuous measurements of electrical conductivity and temperature in a borehole. Ideally, the profiles are then analysed for the location of advective formation water influx as well as the inflow rate and salinity of the formation fluid. Logging took place in numerous boreholes and the records were analysed and interpreted to various degrees. A special type of fluid logging, the ion-selective logging was applied in borehole BGP-4.

As a form of hydrochemical logging it is applied to monitor long-term interaction of the borehole fluid with the borehole walls and allows at least for qualitative interpretations of hydraulically relevant processes. In the course of the WS-A experiment it was possible for the first time to collect formation water of the Opalinus Clay. The observed, temporally variable water inflow into isolated sections of the three boreholes BWS-A1, BWS-A2 and BWS-A3 provided input for estimates of hydraulic conductivity as well as valuable information for the geochemical characterisation of the pore water.

The osmotic properties and effects have been studied in various laboratory and field experiments (OP-experiment). Of particular interest in the current context are the laboratory experiments on hydraulic osmotic flow. The block samples were taken from the shaly facies in the FM-C and SHGN niches. Included in the experiments are the derivation of estimates of hydraulic properties like hydraulic conductivity and specific stor-

age and, in particular, osmotic permeability and osmotic efficiency both under steady-state and transient conditions. In-situ experiments have been carried out using fluids with different chemical potentials, i.e. different salinities. The observed pressure changes served to evaluate the osmotic efficiency of the clay membrane.

The ED-A experiment involves hydraulic and pneumatic tests in the excavation disturbed zone (EDZ). The Modular Mini-Packer System was used in boreholes BED-A1, BED-A3 and BED-A5 for short and long-term constant head testing. The hydraulic conductivity values determined from these tests should provide information on the lateral reaches of the EDZ from the tunnel wall, i.e. could contribute to the definition of the boundary conditions for the conceptual site model.

The ED-B experiment is also associated mostly with the excavation disturbed zone. The main component of the experiment was the monitoring of pressure changes in five horizontal boreholes between the two galleries with various packer configurations before, during and after the excavation of a central section of the new gallery. Some of the intervals are located at a sufficient distance from both galleries to provide estimates on the pore pressure of the undisturbed rock. In other words, given the low hydraulic diffusivity of the Opalinus Clay, it is very likely that these testing intervals are influenced very little by the drainage effect of the tunnel, at least at early observation times.

Laboratory tests have augmented the available information regarding the hydraulic characteristics of the Opalinus Clay. Most notable reference for the current purposes is TN 97-38 which describes tests carried out on a set of samples from the shaly facies with the intention of obtaining the permeability of the natural rock.

The FM-C experiment is focussed on the study of transport mechanisms in the main fault. Hydraulic tests were performed in two intervals in borehole BFM-C1: constant head injection, pressure recovery and pulse injection in the main fault, and pulse injection in the shaly facies. The tests were analysed quantitatively for values of transmissivity and hydraulic conductivity.

The evaporation measurements of the FM-D experiment were conducted in two different set-ups. At first, evapometers were installed on the tunnel wall to check the applicability of the equipment. The results warranted the second experiment, this time in borehole BFM-D1. In simple terms, a probe was driven through an isolated and ventilated test interval, recording humidity and temperature. An attempt was also made to evaluate the suction force acting on the borehole wall using a tensiometer and a psychrometer.

The evaporation logging successfully located points of high evaporation. The quantitative back analyses resulted in first estimates of hydraulic conductivity and storage coefficient.

Hydraulic head measurements recorded before and during the excavation of the reconnaissance gallery and motorway tunnel in piezometers along the tunnel traverse are not part of the experiments conducted at the Mont Terri laboratory but constitute an important source of information and as such are noteworthy in the given context.

3 Developments in Hydrogeological Investigation Techniques and Data Analysis

3.1 Particular issues of interest

The above overview of experiments which were conducted at least in part in Phases 1 to 5 and which bear relevance for the hydrogeological synthesis, sheds light on the first of three subtasks of the hydrogeological synthesis for the Mont Terri site. To re-iterate from chapter 1.2, the subtask concerns an assessment of the achievements of the hydrogeological investigations both in terms of the development of *investigation techniques* and in terms of geoscientific *data analysis* in low permeability argillaceous formations. The achievements from these generic objectives need to be examined for their site-specific components before they may enter the conceptual model of groundwater flow at the Mont Terri site. The particular issues of interest for this task are:

- An assessment of the suitability of hydrogeological information acquired as a result of the contributing experiments in Phases 1 to 5 (see Table 2.1).
- An assessment of the achievements in the development of methodologies for field observations and for the analysis of long-term monitoring of pore pressures.
- An assessment of the impact of the drilling technique and testing fluid on the reliability of packer test results from argillaceous formations.

These issues are each treated separately and in detail in the following sections.

3.2 Suitability assessment of hydrogeologically relevant data

From 1996 to 1999 the Mont Terri project saw the execution of many experiments for a variety of different purposes as defined by the various experiment teams. The organisations' motivation for participation was manifold: training staff members in field investigations, development of site characterisation tools suitable for argillaceous formations, and – last, but not least – compiling a geoscientific data base for the Opalinus Clay at the Mont Terri site. The consequence is a wealth of observations, measurements and analytical results. However, the level of quality assurance achieved for the execution, analysis and documentation of the individual tests is rather non-uniform. A core aspect of the early stage of the HA project was, therefore, the establishment of a well-balanced and reliable hydrogeological information base using a thorough suitability assessment (TN 2000-22A). With the intention to extract the maximum possible

amount of information from the available information pool for integration into the Mont Terri conceptual site model (chapter 4), the HA project team looked clearly beyond the group of experiments specifically designated for the hydrogeological characterisation of the undisturbed Opalinus Clay. A key element of the suitability assessment is, therefore, the scanning of Technical Notes for potentially relevant quantitative and qualitative information and the subsequent assessment of the selected information for its suitability to contribute to the conceptual site model.

The objective of the suitability assessment is, first, to filter out hydraulically relevant information and, second, to assign suitability types to the pertinent information. In an attempt to minimise the bias and to warrant the uniform treatment of all information, the assessment process is designed as a pre-defined and traceable procedure equally applicable to all experiments. The rigorous assessment procedure developed for this purpose consists of the following elements:

- i) Definition of *suitability criteria*, i.e. "What are the deliverables required to build the conceptual site model?"
- ii) Definition of *assessment criteria*, i.e. "Which experimental aspects shall be checked in the assessment?"
- iii) Definition of *suitability levels*, i.e. "How suitable are the data for integration into the Mont Terri site model?"
- iv) *Evaluation* of each individual experiment according to the general definitions i), ii) and iii)

The final products of the assessment process are the *suitability levels* assigned to the reviewed information. They are defined as follows:

- T1 The available results are either unreliable or inconclusive with respect to the hydrogeological characterisation of the Opalinus Clay.
- T2 The experiment or an individual part thereof provides reliable qualitative results which are suitable for integration into the hydrogeological synthesis.
- T3 The experiment or an individual part thereof provides reliable quantitative results which are suitable for integration into the hydrogeological synthesis with appropriate uncertainty ranges.

In cases where information is classified as either T2 or T3, additional analyses and interpretation might be desirable, for example with revised conceptual assumptions, more elaborate tools and methodologies, or sensitivity and uncertainty analyses. This type of recommendation is indicated with an asterisk: T2* and T3*, respectively.

Experiment: Investigation method considered	Testing suitable?	Sufficient documentation? Data sensible?	Adequate data analysis performed?	Suitability type
GP: Hydraulic testing	yes	yes	yes	T3 / T3*
GP-A / GS: Hydraulic & gas testing	yes	yes	yes	T3
PP: Porewater pressure testing	yes	yes	yes	T3
DB: Hydraulic testing	yes	yes	yes	T3 / T3*
DT: Hydraulic testing	yes	yes	yes	T2
FM-A & BF: Fluid logging	yes	yes	yes	T2
FM-A: Ion-selective logging	no	—	—	T1
WS-A: In-situ groundwater sampling	yes	yes	T2	
OP: Hydraulic & osmotic flow	yes	yes	yes	T3
ED-A: Hydraulic testing	no	—	—	T1
ED-B: Porewater pressure testing	yes	yes	no	T3*
n.a.: Hydrodynamic characterisation	yes	yes	yes	T3
FM-C: Hydraulic testing	yes	yes	yes	T3
FM-D: Evaporation logging	no	—	—	T1
n.a.: Hydraulic head measurements	yes	yes	yes	T2

The authors would like to express unambiguously that the assessment scheme applied here is not to be mistaken for a judgement of the equipment's design and general applicability, the workmanship involved in field testing, the know-how introduced into the analysis and interpretation of the raw data, etc.! Instead, it is our attempt to organise the massive amounts of information available according to the suitability for the specific purposes of this report.

Table 3.1: Summary of the suitability assessment with resulting suitability typing.

The experiments presented in Table 2.1 were assessed individually for their suitability in contributing to the hydrogeological characterisation of the Opalinus Clay at the Mont Terri site. The assessment process followed step by step the above described methodology. The results are summarised in Table 3.1 and, incidentally, include practically the entire data base employed in chapter 4. The reader interested in the detailed reasoning and information used in the assessment process for individual tests and experiments is referred to TN 2000-22A. The level of comprehension and quality of the data base attained through the suitability assessment leads to the recommendation of implementing the procedure again in future phases.

3.3 Developments in long-term monitoring systems for pore pressure and water sampling

3.3.1 Problems related to the clay-rich environment

The particular conditions prevalent in argillaceous rock formations turn the monitoring of pore pressure and the long-term monitoring of groundwater chemistry through sampling into non-trivial problems. Several potentials act on the water in the pore space of argillaceous rocks. Horseman et al. (1996) provide a

comprehensive review of these potentials: in addition to the usual pressure and gravitational potential known from typical granular porous media, potentials also found in saturated clays are those due to chemical osmosis and adsorption. The rock's geomechanical behavior causes borehole closure effects due to stress re-distribution and generally associated poor borehole stability. Another source of uncertainty is due to chemical interactions between the rock and the fluid used to flush the observation interval. If the chemical composition of the flushing fluid is not adapted to the porewater chemistry, long-term equilibration processes may bias pressure observations, for example, through the occurrence of chemico-osmotic swelling of clay particles. Some of the factors which may prove to be advantageous for the design of long-term monitoring systems, therefore, are:

- the minimisation of the effective volume of the observation interval
- the introduction of mechanical support along the entire observation interval to prevent borehole collapse (e.g. with a porous screen filter)
- the connection of flow lines at both the top and bottom ends of the observation intervals to allow for a complete flushing
- the appropriate selection of the materials such as stainless steel, teflon or PEEK for the downhole equipment to prevent corrosion and to foster undisturbed porewater sampling.

3.3.2 Equipment portraits

In the early phases of the Mont Terri project (Phases 1 and 2), the development and testing of long-term monitoring systems was an important goal. Particularly the PP experiment focussed on developing a system for long-term monitoring of pore pressure and long-term water sampling (cf. Thury & Bossart 1999). In total, three different types of long-term monitoring systems were applied in the investigation Phases 1 to 4 (Figure 3.1):

- classical inflatable packer systems
- newly developed PP systems
- mini-packer piezometers

More recently, a new PP-type system was developed in Phase 5 as part of the Heater Experiment (TN 2000-01). It is not considered any further in the context of the HA project because comprehensive information for cross-comparison of the new piezometer with the other systems was not yet available at the end of Phase 5.

The selection of one or the other type of long-term monitoring equipment is governed by a variety of issues. Foremost of all are the specific requirements and objectives of an individual experiment. For example, a principal interest in water sampling may favour a different system than a primary interest in pore pressure observations. Other aspects are costs involved, the expected pore pressure limits, the anticipated depth of emplacement for the system, its retrievability, etc. For the HA project the main concern of the assessment of the various equipment systems is their suitability for long-term pore pressure monitoring. The following equipment portraits, therefore, focus on this concern.

Classical inflatable packer system

Many of the Mont Terri boreholes, among these BGS-1, BGS-2, BGP-1, BGP-4 and BGP-5, were equipped with inflatable double or triple packer systems. They served the hydraulic characterisation of the formation with packer testing or long-term monitoring. The packers have a diameter of typically 80–85 mm and a sealing length of 0.5 m or rather 1.0 m. The set-up of a triple packer system is illustrated in Figure 3.1a, at center. The packers are inflated with water through hydraulic lines. The stability of the packer pressure is controlled by manometers at the surface. The length of the testing or observation interval ranges from several decimeters to more than 10 m. The interval volume can be minimised by inserting dummies. The

achievable packer pressures were tested systematically in Phases 1 and 2 of the GP experiment (TN 96-27, TN 97-28). The tests indicated that packer pressures of more than 40 bars could hardly be maintained for prolonged periods. At such elevated packer pressures, frequent re-injection of water was required to stabilise the pressure. This resulted in considerable increases of the packer volume and in changes of the interval volumes.

PP system

The PP system was developed in Phases 1 and 2 (1996/1997) in the PP experiment (TN 97-01). PP systems were installed in the boreholes BPP-1, BDI-1, BED-B1, BED-B2, BED-B3 and BGP-6. The system as installed in borehole BPP-1 is an assemblage of a multipacker system with four packers and two sintered steel filters. The multipacker system consists of two double packer systems, each with a hydraulic and a mechanical packer (Figure 3.1b). A modified, simpler PP system consists only of the stiff mechanical packers and no hydraulic packers. Such systems were used after the PP experiment. It should be noted that PP-systems and mechanical packer systems are “lost” systems which cannot be retrieved. The classical packer systems (including MMPS) are systems which may be de-installed, provided the borehole stability conditions allow for it. The intent for using a double packer system was to inject resin between the hydraulic and the mechanical packers to obtain long-term sealing. The sintered steel element represents the observation interval. This tube has an outer diameter which is only a few millimeters smaller than the borehole diameter. Synthetic porewater can be circulated through this porous steel or porous poly-ethylene filter. The interval lengths were typically in the range of 20–100 cm.

Mechanical minipacker piezometers

As part of the GP experiment in Phase 2 (TN 96-27), low cost minipacker systems were designed to observe pore pressures in the small-diameter boreholes BGP-2 and BGP-3. Mechanical packers with a sealing length of 20 cm and a nominal diameter of 32 mm were installed at depths of 7.5 m and 8.9 m, respectively (Figure 3.1a). The observation intervals extended from these packers to the bottoms of the boreholes. However, before the mechanical packers were set, the observation intervals were filled with a coarse sand to avoid further borehole collapse and to minimise the interval volume. Each of the observation intervals was connected to equipment outside of the borehole with a pressure monitoring line and a flow line.

(a)

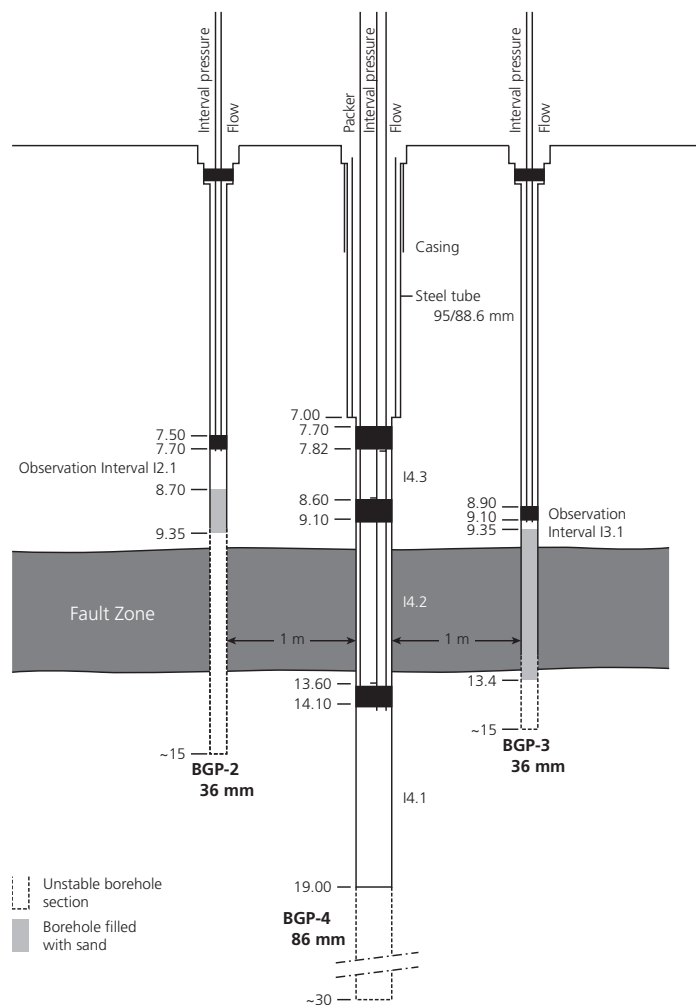
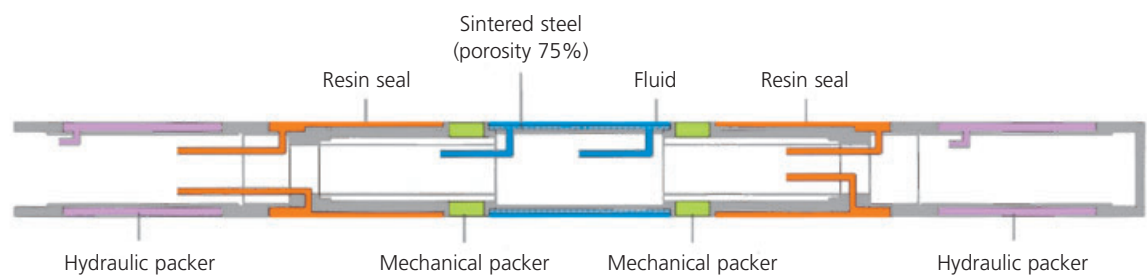


Figure 3.1: Piezometer systems tested in Phases 1 to 4 of the Mont Terri research program: (a) classical inflatable triple packer system in borehole BGP-4 and mechanical minipacker systems in BGP-2 and BGP-3 as applied in the GP experiment / Phase 2 (TN 96-27) and (b) PP system developed in the PP experiment / Phases 1 and 2 (TN 97-01 & TN 97-02).

(b)



3.3.3 Equipment performance

An assessment of the equipment's performance was, in most cases, a by-product of the experiments rather than a separately defined task. As a result, the assessments are of limited scope and detail. Nevertheless, sufficient information is available to comment particularly on the following aspects:

- the performance with respect to the ease of emplacement in the borehole, proper sealing of the observation interval, equipment failure and other potential mechanical problems
- the homogeneity of pore pressure records from different systems

These aspects are discussed here in form of two cross-comparisons between systems. For the comparison of the absolute values of the pore pressure observations one must remember that a certain degree of difference is to be expected due to the different distances between the observation intervals and the galleries.

Classical inflatable packer versus mechanical minipacker piezometer

As part of GP / Phase 2, a comparison of pore pressure measurements was carried out between the classical inflatable triple packer system and the mechanical minipacker piezometer. One of the experiments is an

interference test: a hydrotest sequence was conducted in test interval I4.2 in the main fault of borehole BGP-4 with pressure observations in boreholes BGP-2 and BGP-3 (see Figure 3.1a). The distances between the I4.2 in BGP-4 and the observation intervals were 1 m each. The mechanical minipacker piezometers were used for the observation intervals because of their low-budget maintenance while inflatable packers were used for the test interval because they are relatively easily recoverable and have a movable injection system. Figure 3.2 shows the crosshole pressure reactions monitored in interval I2.1 of BGP-2 and in interval I3.1 of BGP-3. Consistent pore pressures are evident in BGP-3: during the PSR phase prior to the hydraulic test sequence, the pore pressure in BGP-3 is quite similar to the pressure measured in I4.2 of BGP-4 (350 – 400 kPa). Subsequently, clear responses are observed for each test event, indicating that the minipacker piezometer works well.

The interval pressure recorded by the mini-piezometer in BGP-2 is less consistent with the aforementioned observations. Pressures increase from -65 kPa to +25 kPa which corresponds to a water level of 6.5 m below ground and 2.5 m above ground, respectively. This is due to the unsaturated conditions prevailing in the observation interval of BGP-2, which obscure the crosshole response. Therefore, care has to be taken when building this type of mini-piezometer to achieve full water saturation within the interval.

In summary, the experience from the GP experiment

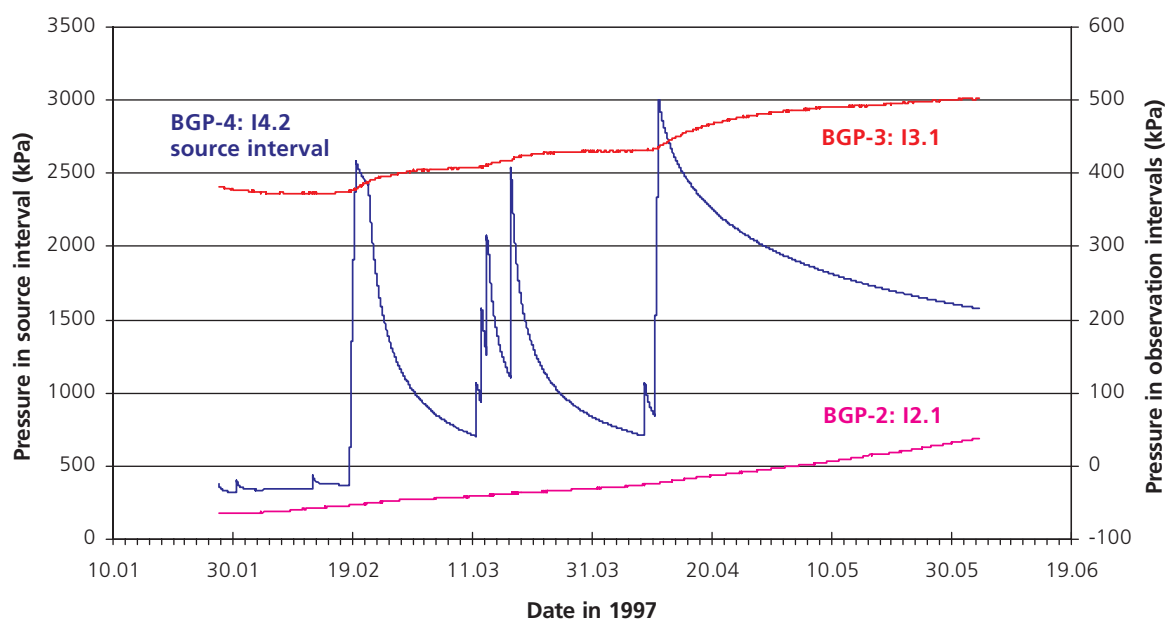


Figure 3.2: Pressures recorded with inflatable packers and mechanical minipacker piezometers during the interference test of the GP experiment/Phases 1 and 2: Pore pressure observations in intervals I2.1 of BGP-2 and I3.1 of BGP-3 in response to a hydrotest sequence in source interval I4.2 of BGP-4.

has proven the minipacker piezometer to be a low-budget system for long-term monitoring of pore pressure which works reasonably well when properly installed. These systems are also easy to install in sub-vertical boreholes of up to 10 m length. Sealing sections of more than 50 cm are favourable. The mechanical minipackers are suitable for low pore pressures of less than 500 kPa; higher pore pressures require inflatable minipackers. Sealing of the borehole section above the packer seat with resin or bentonite may improve the long-term performance of the minipacker piezometer.

Classical inflatable packer versus PP system

In Phases 3 and 4 (1998/1999) of the GP experiment, a PP system with three monitoring intervals and an inflatable triple packer system was installed in boreholes BGP-5 and BGP-6 in the FM niche. The niche lies in the sandy facies and the boreholes' orientation is roughly perpendicular to bedding. The inclined boreholes were drilled parallel to each other. The distance between the boreholes was less than 1 m. The observation intervals isolated with the conventional packer system were intervals I5.1, I5.2 and I5.3 of BGP-5 with their mid-points located at 9.3 m, 8.0 m and 6.6 m from borehole mouth, respectively. The test and observation intervals isolated with the PP system were intervals I6.1, I6.2 and I6.3 of BGP-6 with their mid-points

located at 10.1 m, 7.9 m and 5.5 m from borehole mouth, respectively. Figure 3.3 shows the pressure records in all observation intervals during a hydrotest in interval BGP-6/I2. Prior to testing, some of the corresponding observation intervals exhibit comparable pore pressures (BGP5/I2: 256 kPa, BGP-6/I2: 315 kPa). During the hydrotest sequence, the responses in the observation intervals are extremely weak. Merely the pressure curves for I6.1 and I6.3 of BGP-6, and I5.1 of BGP-5 show sizeable changes.

Nevertheless, the long-term monitoring of pore pressures in boreholes BGP-5 and BGP-6 shows that pore pressure measurements from the PP system and the inflatable packer system are consistent to each other. The PP system is appropriate for continuous monitoring of pore pressures and for water sampling. The inflatable packer equipment is a removable system which is well-suited for site characterisation purposes, but was also shown to be appropriate for long-term monitoring of pore pressures.

3.3.4 Concluding remarks

Inflatable packers are most favourable for site characterisation purposes where the following features and flexibilities are advantageous: removable packer seats, borehole screening, water injection at high pressures, variable packer length etc. The PP system is very suitable for water sampling and long-term monitoring.

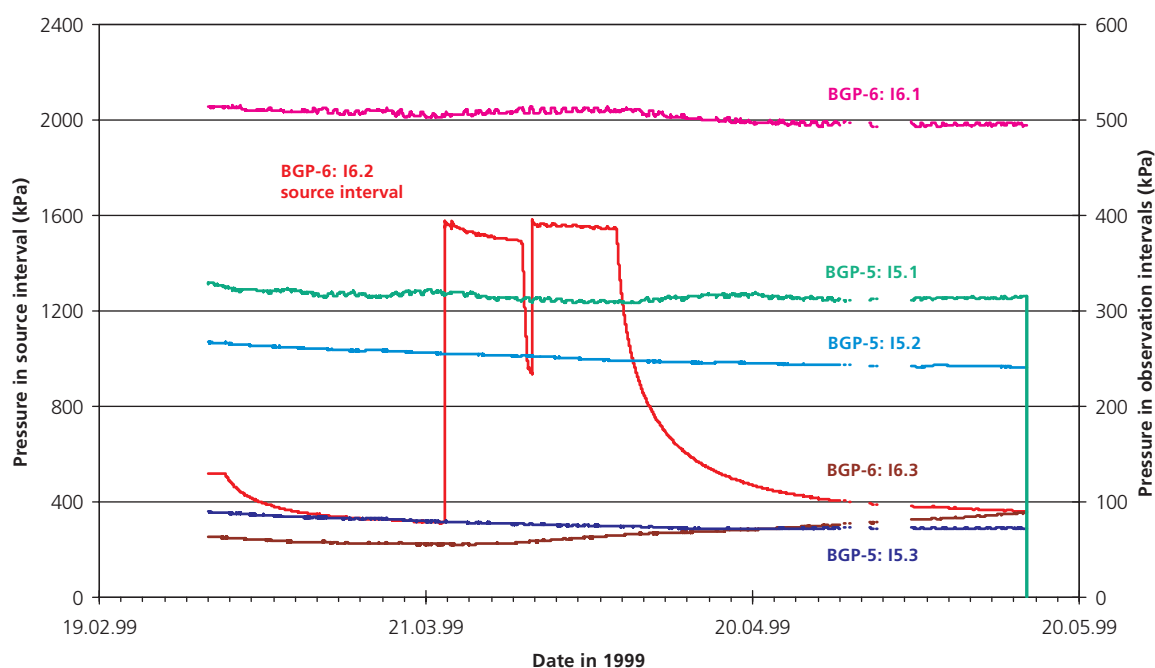


Figure 3.3: Pressures recorded with inflatable packers and PP equipment in the GP experiment / Phases 3 and 4: Pore pressure in the BGP-5 and BGP-6 observation intervals in response to a hydrotest sequence in source interval I6.2 of BGP-6.

Because of its mechanical packers, some flexibility is lost, however, as the tightness of the interval cannot be controlled with the pressure levels applied in the packers. Therefore, it relies heavily on the quality of the resin sealing. The low-budget minipacker piezometers are most appropriate for observation purposes, at low pressures and for rather shallow emplacements in the borehole. Pore pressure monitoring in the excavation disturbed zone is a typical application for the minipacker systems.

3.4 Impact of drilling technique on packer test results

Considerable technical challenges were faced in hydraulic testing of the Opalinus Clay formation at Mont Terri due to the poor borehole stability and the low hydraulic conductivity. The DB experiment was initiated to assess possible distortions of packer test results by effects of the drilling methodology and by impacts of the drilling and test fluids (TN 98-62). Three vertical boreholes were drilled in close proximity of each other in the shaly facies in the OP niche (Figure 3.4). Borehole BDB-1 was drilled with air and BDB-2 and BDB-3 were drilled with a silicate/polymer mud and a potassium-chloride/polymer mud, respectively. Immediately after drilling, the boreholes were equipped with double packer systems. An initial hydraulic testing campaign was performed in BDB-2 and BDB-3 with the drilling mud. Subsequently, the drilling fluids in all three boreholes were replaced by Pearson water, i.e. a synthetic porewater designed to minimise swelling effects, and the test sequence was repeated in the second testing campaign with the

intention of analysing the impact of the testing fluid on the results. Typical test sequences were a succession of initial pressure recovery, pulse injection and constant head injection events sometimes followed by a slug withdrawal and a prolonged pressure recovery. After termination of the second campaign, pore pressure was monitored in the boreholes for more than a month. Finally, the third hydraulic testing campaign was done to assess possible changes in hydraulic parameters due to long-term processes in the boreholes such as borehole closure, swelling or osmotic flow.

Table 3.2 presents the results of the first and second hydraulic testing campaigns. Values of hydraulic conductivity are given in terms of inner zone and outer zone, i.e. analogous to radial shells around the boreholes. The outer zone corresponds to the properties of the undisturbed rock. Significant differences between the inner and outer zone conductivities were not observed. It must be stated that the specific storage values are not the result of interference testing but of single-hole analysis and that they are, therefore, poorly constrained. In summary, the following conclusions were drawn from the DB experiment:

- A comparison of the tests conducted in the three boreholes revealed no relevant differences between the first and second testing campaigns conducted before and after the fluid exchange.
- The most consistent test responses and analysis results were achieved in borehole BDB-2, drilled with silicate/polymer mud, followed by borehole BDB-3, drilled with KCl/polymer mud.
- The only relevant inexplicable test responses were recorded in borehole BDB-1. In this borehole, the

Test interval	Inner zone hydraulic conductivity K_1 [m/s]		Outer zone hydraulic conductivity K_2 [m/s]		Specific Storage S_s [1/m]	
	before	after fluid exchange	before	after fluid exchange	before	after fluid exchange
BDB-1 I1.1 9.9-15.1 m fbm	-	1.2×10^{-12}	-	3.8×10^{-13}	-	3.8×10^{-6}
BDB-1 I1.2 3.0-9.1 m fbm	-	3.3×10^{-13}	-	1.2×10^{-13}	-	8.2×10^{-6}
BDB-2 I2.1 10.5-20 m fbm	2.1×10^{-13}	2.1×10^{-13}	4.2×10^{-14}	3.2×10^{-14}	9.5×10^{-6}	7.4×10^{-6}
BDB-2 I2.2 4.5-9.7 m fbm	3.8×10^{-13}	3.8×10^{-13}	1.3×10^{-13}	1.3×10^{-13}	1.3×10^{-5}	9.6×10^{-6}
BDB-3 I3.1 9.3-16.4 m fbm	2.8×10^{-13}	2.8×10^{-13}	9.9×10^{-14}	9.9×10^{-14}	7.0×10^{-6}	5.6×10^{-6}
BDB-3 I3.2 3.0-8.5 m fbm	1.8×10^{-12}	1.5×10^{-12}	9.1×10^{-13}	9.1×10^{-13}	7.3×10^{-6}	1.8×10^{-6}

Table 3.2: Summary of the results from the final hydraulic test sequence after fluid replacement with Pearson water in boreholes BDB-1, BDB-2 and BDB-3. Test interpretation based on a finite skin flow model, i.e. inner zone/outer zone.

- long-term monitoring phase demonstrates inexplicable changes in slope and roll-over. It would be feasible that this was caused by two-phase flow phenomena induced by air drilling.
- The testing conditions encountered in the Mont Terri Opalinus Clay, neither fluid-rock interaction nor osmosis have significant impact on the transmissivity determination.
- The diagnostic plot comparison between the second and third testing campaigns conducted before and after long-term monitoring showed a slight increase of the near borehole transmissivity by less than half an order of magnitude. It is, however, not clear whether this effect is due to the approximately one month long exposure of the test intervals to synthetic porewater, or to stress redistribution.

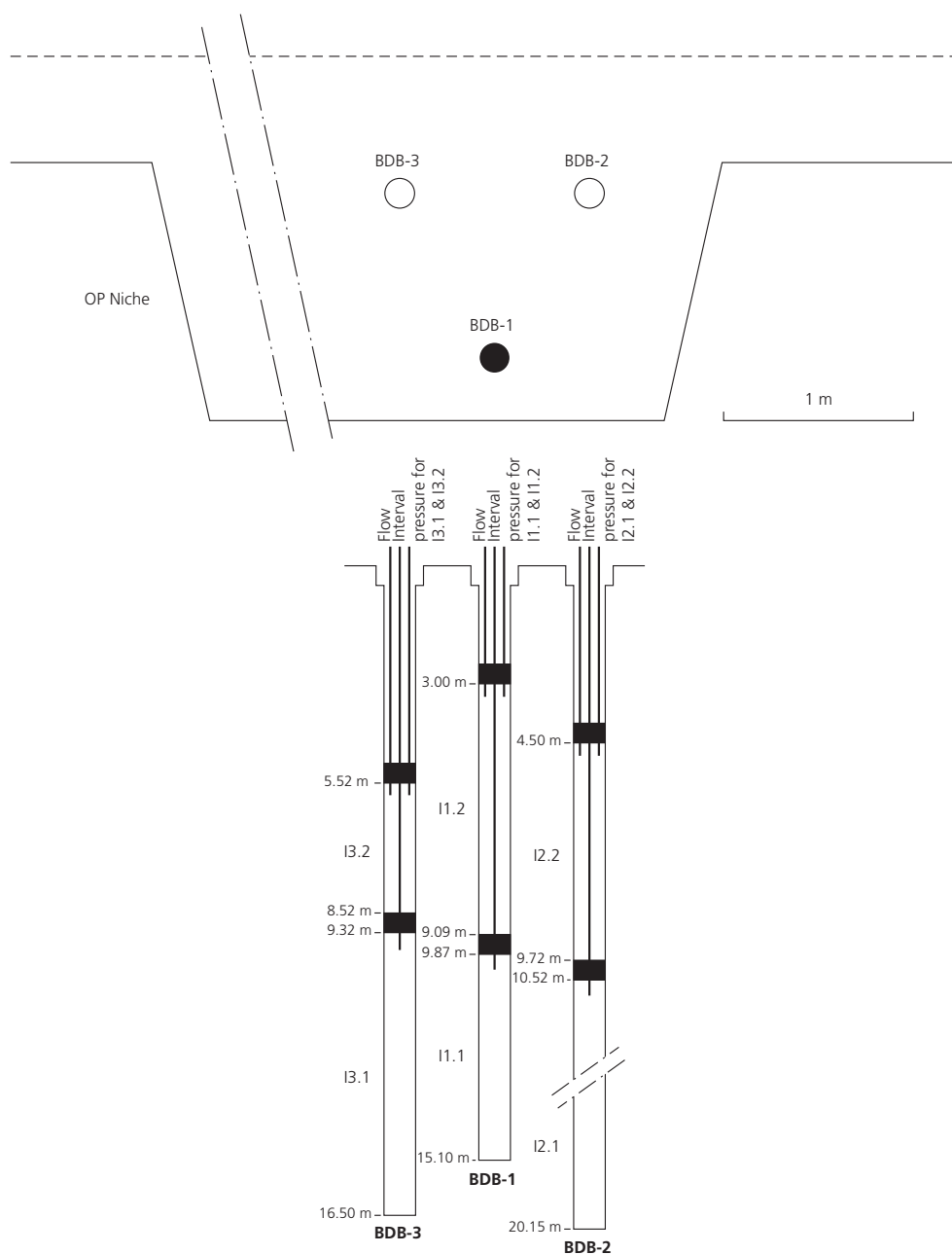


Figure 3.4: Map view and cross-section of the set-up for the systematic investigation of the impact of the drilling technique and the chemical composition of the test fluids on packer test results. The three boreholes BDB-1, BDB-2 and BDB-3 were drilled with air, silicate/polymer mud and potassium-chloride/polymer mud, respectively. Synthetic porewater was used for hydraulic testing.

4 Conceptual Model of Groundwater Flow at the Mont Terri Site

4.1 Introduction

The conceptual model of groundwater flow at the Mont Terri site is based on the accomplishments from Phases 1 to 5, that is from 1996 to 2000, of the Mont Terri research program. The data base is made up of those results of hydrogeological field and laboratory investigations, which have passed the suitability assessment described in chapter 3.2. Furthermore, various geological and geochemical data sets are used, which have been quality assured as part of Nagra's Geosynthesis Project (Nagra 2002). In the process of deriving the conceptual model, the hydrogeological data base is analysed in the context of the given hydrogeological setting, the relevant groundwater flow mechanisms are highlighted, and the different scales of groundwater flow are reviewed. Representative hydraulic properties of the undisturbed Opalinus Clay are assigned to the relevant scales of groundwater flow. Finally, the current level of understanding of the hydraulic head distribution in the Opalinus Clay and the adjacent stratigraphic formations is discussed. The rock properties of interest are: hydraulic conductivity, anisotropy factor, flow threshold gradients (limits of applicability of Darcy's law), specific storage and conceptual hydro-mechanical models (in particular porosity-permeability relationships).

This report covers neither the complex hydro-mechanical processes observed in the excavation disturbed zone (cf. Martin & Lanyon 2004), nor those in the unsaturated zone. Still, the tunnel nearfield forms the inner boundary of the local-scale hydrogeological model and is therefore important for the HA project. Furthermore, as the Opalinus Clay is known to be an overconsolidated clay-rich shale formation (Thury & Bossart 1999), its geomechanical properties and in-situ stress conditions are expected to play a vital role in the groundwater flow systems (Bock 2002). The integration of such information will be the topic of future Phases of the HA project.

4.2 General outline of the synthesis approach

In the context of common hydrogeological applications like the management of groundwater resources, tight claystone formations are treated as aquicludes, assuming that porewater is not mobile at ambient conditions as diffusion is assumed to be the dominant transport process through the aquiclude. In many cases the hydraulic conductivity of the clay formation is below the detection limit of conventional hydraulic measurement methods. Hence, characterisation of

such an aquiclude may be limited to qualitative investigations demonstrating its tightness. The assessment of the long-term barrier function of clay formations in the framework of radioactive waste disposal, however, requires more rigorous quantitative site characterisation procedures (chapter 4.3) and a careful analysis of flow and transport processes. The key elements of this analysis are:

- An assessment of groundwater flow mechanisms and coupled processes (chapter 4.4).
- An assessment of relevant scales (chapter 4.5).
- Evidence for a continuous distribution of porewater pressure in the formation (chapter 4.6).
- An evaluation of hydrogeological site understanding (chapter 4.7).

The range of applicability of Darcy's law is a key issue to be addressed in the *assessment of groundwater flow mechanisms* in clay formations. The phenomenological explanation for deviations from Darcy's law may be founded in coupled processes involving chemical, mechanical, thermal or hydraulic components (Horseman et al. 1996). Coupled processes may significantly influence the regional groundwater flow system, for example, by preventing advective groundwater flow. The context of the Mont Terri project demands detailed consideration of the following two processes:

- Chemico-osmotic flow as a result of membrane effects in the clay formation.
- Hydro-mechanical processes stemming from pore pressure – stress coupling and porosity-permeability coupling of the porous rock.

In tight formations site characterisation delivers hydraulic properties of the rock which are, at most, representative for a scale of centimeters up to meters (packer testing, permeameter testing – cf. chapter 4.3). Modelling groundwater flow, however, requires representative values of rock properties typical on the scale of deka- to hectometers. The *assessment of relevant scales* and detailed geological information about relevant structural features on all scales is a pre-requisite for any upscaling of the measured hydraulic properties. *Spatial distribution of porewater pressure* at the site is a key for testing model concepts including groundwater flow mechanisms, coupled processes and hydraulic boundary conditions, and for confirming the spatial representativity of the measured hydraulic parameters. Hydrodynamic modelling of the observed in-situ pore pressures provides a valuable tool for model discrimination.

4.3 Hydrogeological data base from Phases 1 to 4

The main hydrogeological investigation techniques applied for the characterisation of the Opalinus Clay at the Mont Terri rock laboratory are:

- Hydraulic packer tests in boreholes,
- Permeameter tests of core samples.

Complementary methods based on microstructural analyses (Kozeny-Carman relationship) and on nitrogen adsorption / desorption techniques were applied to check for internal consistency in the hydrogeological data base.

4.3.1 Packertests

The boreholes which were equipped with packer systems for hydraulic testing and long-term monitoring of pore pressure are indicated in Figure 2.2. A multitude of packer tests was conducted in all lithological facies (sandy, shaly and carbonate-rich sandy) of the Opalinus Clay and the main fault zone. The core mapping logs were compared to the results of the packer tests to check whether the hydraulic properties are significantly influenced by the fracture frequency in the test interval. Hydraulic interference tests were conducted at two locations in the GP and GS experiments. For these, very weak hydraulic pressure responses were monitored in observation boreholes at about 1 m distance from the test boreholes, i.e. at a distance where the prevalence of a mobile fluid phase at testing scale could be inferred. An overview of the range of derived values for hydraulic conductivity and specific storage coefficients is provided in Table 4.1. Only such data sets are presented which passed through the suitability assessment procedure (chapter 3.2). The hydraulic conductivities range from 2×10^{-14} m/s to 2×10^{-12} m/s. The spread of values is a result of (i) the spatial variability of the parameter, (ii) the different methods of interpretation, (iii) uncertainty analyses conducted on a few tests, and (iv) different borehole histories. Detailed hydrotest analyses including flow model identification, uncertainty analysis and simulations of the entire test sequence were carried out as part of the GP experiment on boreholes BGP-1 and BGP-4 (TN 98-24). The general approach used to analyse the hydraulic tests was that of a parameter estimation procedure using non-linear optimisation and uncertainty analysis:

- Choose initial conceptual flow model
- Provide initial values of fitting and non-fitting parameters

- Specify constraints and objective function and optimise fitting-parameter estimates using non-linear regression to obtain baseline estimates
- Analyse residuals (evaluate conceptual model)
- Check fitting-parameter uncertainty (joint-confidence regions)
- If uncertainties appear unacceptably large, attempt to better constrain the problem to reduce the uncertainties, e.g. by using an alternative well-formation flow model
- Use Jacobian matrix analysis to better understand how fitting parameters are being constrained
- Perturb baseline estimates and re-optimize the fitting parameters to investigate the uniqueness of the solution (check for local minima)
- Sample from assigned uncertainty distributions for the non-fitting parameters and then re-optimize the fitting parameters to quantify how non-fitting parameter uncertainties affect the fitting-parameter estimates

The fitting parameters selected were hydraulic conductivity, specific storage, static formation pressure and wellbore storage. The non-fitting parameters were borehole radius, pressure history and fluid density. Details of the analysis procedure are documented in TN 98-24.

Figure 4.1 to 4.3 illustrate individual steps of the approach as applied for the analysis of a hydraulic testing sequence performed in borehole BGP-1. The rigorous analysis approach applied to the BGP-1 and BGP-4 packer test data represents an exception for Phases 1 to 4. Further detailed analyses were carried out in support of hydro-mechanical studies of the BGP-6 interference test (cf. chapter 4.4.3) and the BGS-2 gas test analysis (chapter 5.5). Most of the other packer tests were interpreted using simpler approaches based on diagnostic data analysis. Because of the different levels of detail in the interpretations, the compilation of packer test results presented below cannot fully account for parameter and model uncertainties.

Storage coefficients were not determined for all tests. As a matter of fact, the specific storage coefficient can be better constrained with interference tests, while in most cases only single-hole tests were available. This explains the large range of values of the specific storage obtained: from 2×10^{-7} m⁻¹ to 1.7×10^{-4} m⁻¹. In many cases values around 1×10^{-6} and 1×10^{-5} m⁻¹ are obtained, which is in a range of expected values for this parameter.

In addition to hydraulic conductivities and storage coefficients, Table 4.1 also lists the tested facies and the frequency of discontinuities which were obtained

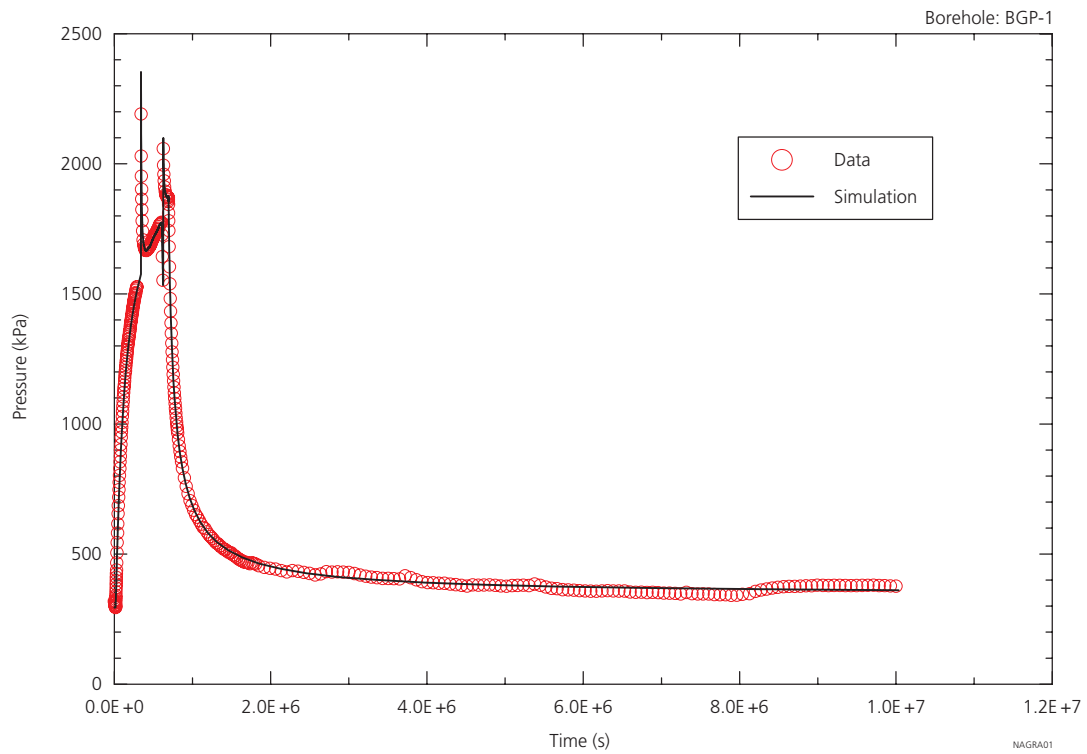


Figure 4.1: Baseline simulation of pressure response in BGP-1 (after TN98-24). The baseline simulation is the result of inverse modelling of the entire test sequence with a given (radial) flow model. Baseline simulations represent the starting point for uncertainty and perturbation analyses.

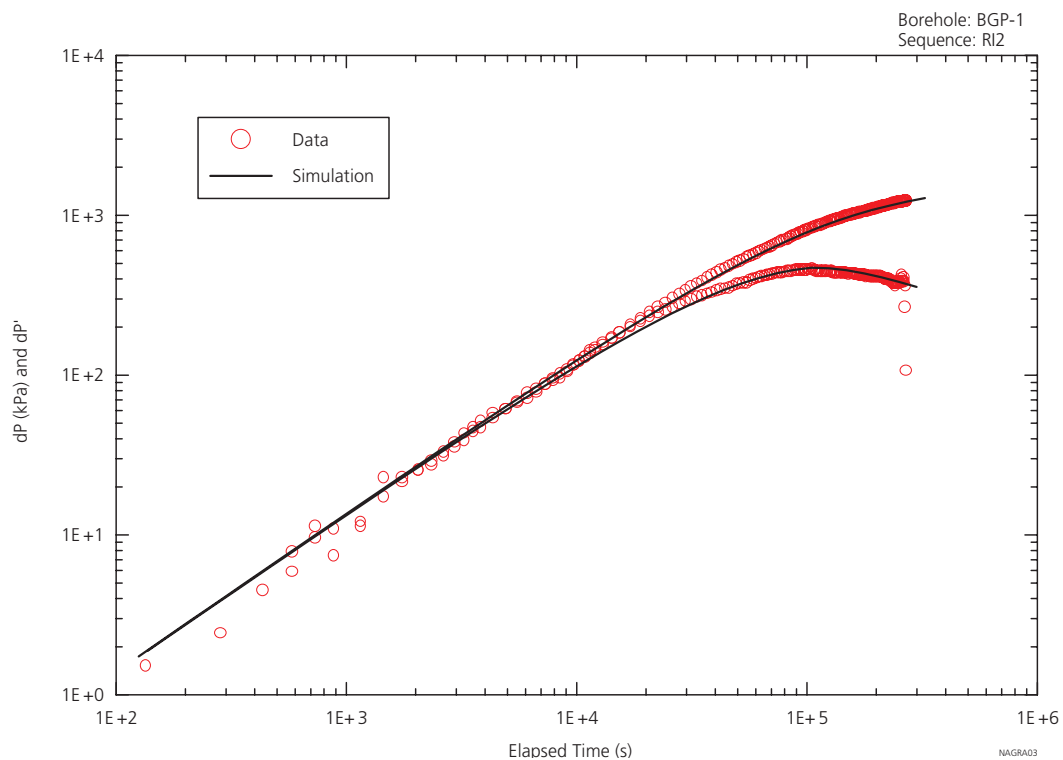


Figure 4.2: Baseline simulation of pressure change (dP) and log-derivative (tdP/dt) during BGP-1 – R12 constant-rate injection test (after TN98-24). The diagnostic log-log derivative plot allows for systematic flow model identification.

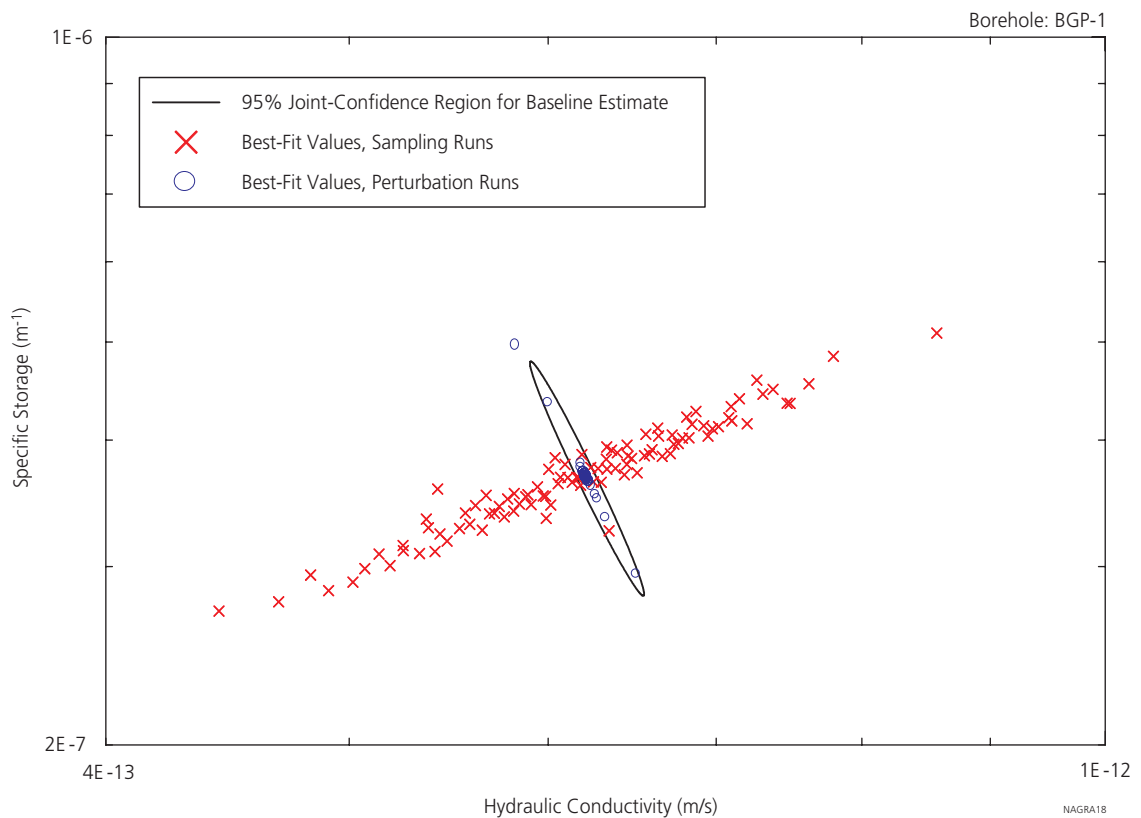


Figure 4.3: Uncertainty analysis of BGP-1 hydraulic conductivity and specific storage estimates (TN98-24): Comparison of the results of the perturbation analyses (perturbation of fitting parameters) and sampling analysis (perturbation of non-fitting parameters) to the 95% confidence regions of the baseline parameters. The best-fit parameter combinations estimated from the perturbation analysis fall within the 95% joint-confidence regions of the baseline parameter set, thus, the inverse problem, as posed, was well constrained.

by locating the test intervals in the core mapping records (see also chapter 4.5.3). Tests were carried out in all facies and the fracture frequency ranged from none to 19 m^{-1} . The data show no significant correlation between the hydraulic conductivity and the lithological facies (cf. chapter 4.5.2). Neither could a definite correlation be detected between the hydraulic conductivity and the fracture frequency in the test section (chapter 4.5.3). The hydraulic tests in the main fault resulted in K values of about 2×10^{-13} to $5 \times 10^{-13} \text{ m/s}$ and, therefore, are within the typical range of Mont Terri values.

Borehole/ Test interval	Borehole dip (up +) (down -)	Bedding dip (orientation is SE)	Lithological unit	Hydraulic conductivity K [m/s]	Specific storage S_s [m ⁻¹]	Frequency of open dis- continuities [m ⁻¹]
BGP-1 I1.2 8-9 m fbm	inclined (-80°)	44°	carbonate rich sandy facies	4.0×10^{-13} – 9.0×10^{-13}	2.0×10^{-7} – 6.0×10^{-7}	0 (0)
BGP-4 I4.2 9.1-13.6 m fbm	vertical (-90°)	44°	main fault: 9.45-12.20 m fbm; in shaly facies	2.0×10^{-13}	3.0×10^{-7} – 3.0×10^{-5}	8.9 (6.2)
BGP-6 I6.2 7.4-8.4 m fbm	inclined (-34°) (⊥ to bedding)	54°	sandy facies	1.5×10^{-14} – 2.7×10^{-13}	not analysed for or fixed at 2×10^{-6}	1 (1)
BGS-1 I1.2 8.0-9.0 m fbm	inclined (-50°)	45°	shaly facies	$\sim 2.0 \times 10^{-12}$	1.7×10^{-4} ¹⁾	n.d.
BGS-1 I1.3 5.0-7.0 m fbm	inclined (-50°)	45°	shaly facies	$\sim 1.0 \times 10^{-13}$	1.6×10^{-4} ¹⁾	n.d.
BGS-2 I2.2 8.0-9.0 m fbm	inclined (-50°)	45°	shaly facies	$\sim 3.0 \times 10^{-13}$	1.7×10^{-5} – 8.4×10^{-5} ¹⁾	n.d.
BGS-2 I2.3 5.0-7.0 m fbm	inclined (-50°)	45°	shaly facies	$\sim 1.5 \times 10^{-13}$	8.5×10^{-5} ¹⁾	n.d.
BFM-C1 I1 8.2-11.2 m fbm	vertical (-90°)	50°	main fault: 8.25-9.21 m fbm; in shaly facies	3.0×10^{-13} – 5.0×10^{-13}	1.5×10^{-6} – 1.0×10^{-5}	19 (18)
BDB-1 I1.1 9.9-15.1 m fbm	vertical (-90°)	n.d.	shaly facies	3.8×10^{-13}	3.8×10^{-6}	6.2 (1)
BDB-1 I1.2 3-9.1 m fbm	vertical (-90°)	n.d.	shaly facies	1.2×10^{-13}	8.2×10^{-6}	13.8 (4.4)
BDB-2 I2.1 10.5-20 m fbm	vertical (-90°)	n.d.	shaly facies	3.2×10^{-14}	7.5×10^{-6}	5.3 (1.8)
BDB-2 I2.2 4.5-9.7 m fbm	vertical (-90°)	n.d.	shaly facies	1.3×10^{-13}	9.6×10^{-6}	8.8 (2.9)
BDB-3 I3.1 9.3-16.4 m fbm	vertical (-90°)	n.d.	shaly facies	9.9×10^{-14}	5.6×10^{-6}	—
BDB-3 I3.2 3-8.5 m fbm	vertical (-90°)	n.d.	shaly facies	9.1×10^{-13}	1.8×10^{-5}	8.9 (6.7)

() in parentheses: frequency of discontinuities excluding artificial discontinuities

¹⁾ values determined based on single-pulse sequence and unusually high test zone compressibility, i.e. most likely strongly overestimated
n.d.: not determined

Table 4.1: Overview of the relevant packer test results in the Opalinus Clay formation at the Mont Terri rock laboratory. Values of parameter ranges either stem from different methods of analysis (i.e. analytical vs. numerical) or are the result of uncertainties determined from sensitivity analysis.

4.3.2 Permeameter tests

Five permeameter tests were conducted successfully as parts of the OP and GP experiments. In the OP experiment conducted by the British Geological Survey (BGS), two samples were tested in isostatic cells, whereby flow was imposed perpendicularly to bedding (TN 97-39, Harrington et al. 2001). Figure 4.4 shows a schematical sketch of the BGS controlled flow-rate permeameter. It consists of five main components: (i) a sample assembly, (ii) a 40 MPa rated pressure vessel and associated confining pressure sys-

tem, (iii) a fluid injection system, (iv) a back pressure system and (v) a micro-computer based data acquisition system. The specimens were sandwiched between two stainless steel end-caps, each with a sintered stainless steel porous disc, and jacketed in heat-shrink teflon to exclude confining fluid. The specimen is subject to an isotropic confining stress – the effective stress varied between 4.2 and 6.4 MPa. The observed K values ranged from 6 to 12×10^{-14} m/s. No significant correlation could be found between the conductivity and the effective stress. The derived storage coefficient was notably high with a value of about 5×10^{-4} m⁻¹.

The permeameter tests as part of the GP experiment were carried out by SCK·CEN (TN 98-15, TN 99-58). The test equipment was similar to the one used by BGS (cf. Figure 5.1). Confining pressure and effective stress were also similar to those for the OP permeame-

ter tests. The flow direction was at about 35°, 50° and normal to bedding. The hydraulic conductivity was derived to be about 1 to 2×10^{-13} m/s. A summary of results from the permeameter tests is provided in Table 4.2.

Experiment	Core sample	Lithological unit	Hydraulic conductivity K [m/s]	Specific storage S_s [1/m]
GP-Experiment	SED-B3 06 (GP)	shaly facies	2.2×10^{-11} (full saturation)	-
	flow parallel to bedding; most probably disturbed sample			
	BFP-16 (GP)	shaly facies	$1.5 \times 10^{-13} - 1.8 \times 10^{-13}$	-
	flow ca. 50° to bedding; effective stress ca. 5 MPa			
	BWS-E4 06	sandy facies	$1.9 \times 10^{-13} - 2.1 \times 10^{-13}$	-
	flow normal to bedding; effective stress ca. 4.5 – 5 MPa			
	BED-C5/7	shaly facies	1.9×10^{-13}	-
OP-Experiment	2 samples from SHGN niche		mean K.L. 7.5×10^{-14} ($6 \times 10^{-14} - 12 \times 10^{-14}$)	4.8×10^{-4}
	for effective stresses, typically in the range of 4 – 5 MPa			

Table 4.2: Summary of results from the permeameter tests and structural investigations.

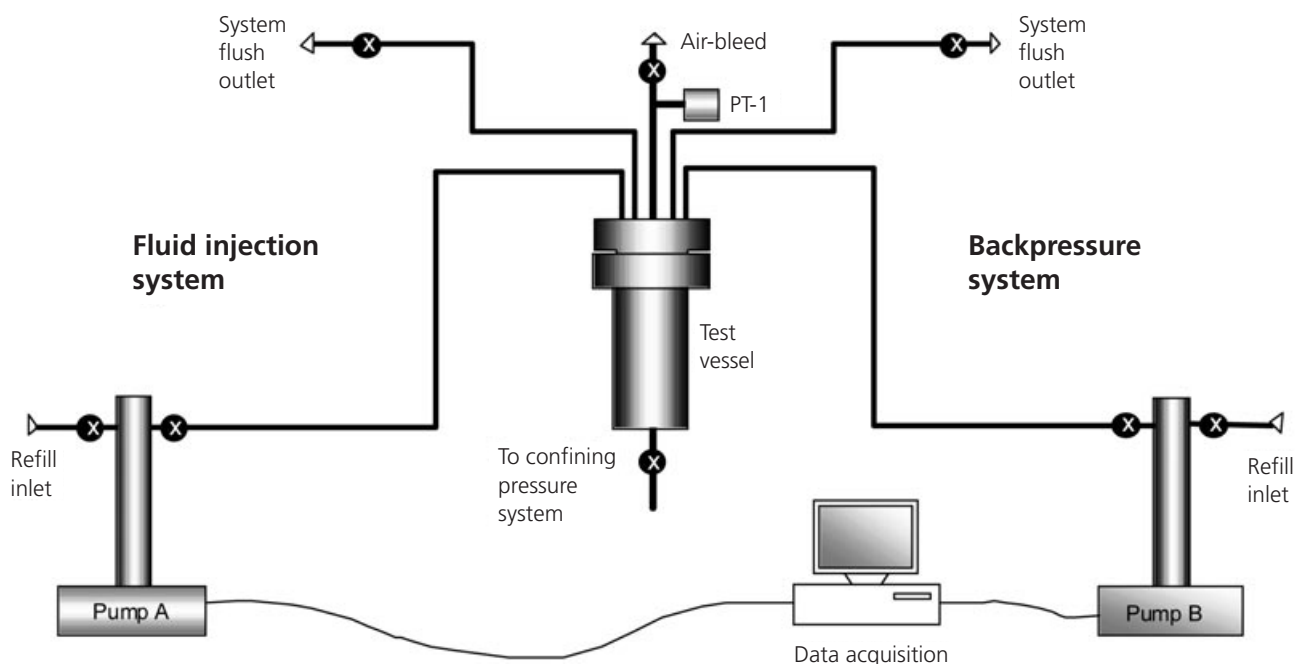


Figure 4.4: Schematic configuration of the BGS permeameter after Harrington et al. (2001).

4.4 Assessment of coupled processes

4.4.1 Threshold gradient

Conceptual framework

Darcy's law represents the general base for quantitative descriptions of groundwater flow. It denotes the linear correlation between the specific discharge v_f through a representative elementary volume and the hydraulic gradient. The proportionality constant for the relationship is provided by the hydraulic conductivity K . Darcy's law is applicable only within certain limitations. For the case of the Opalinus Clay porewater flow at low hydraulic gradient is the range where deviations from the linear flow law may be expected. The small pore radii cause electro-molecular rock-water interactions to gain significance in comparison to the viscous fluid properties, i.e. friction. In response, the formation water no longer behaves like a Newtonian fluid when exposed to a low hydraulic gradient. A comprehensive discussion of possible causes for non-linear porewater flow in clay-rich rock is found in Horseman et al. 1996. In empirical terms, this situation may be accounted for by introducing a hydraulic threshold gradient i_0 (see, e.g. Bear 1972, de Marsily 1986):

$$v_f [\text{m/s}] = \begin{cases} K \cdot \text{grad } h \cdot \left[1 - \frac{i_0}{|\text{grad } h|} \right] & \text{for } |\text{grad } h| \geq i_0 \\ 0 & \text{for } |\text{grad } h| < i_0 \end{cases} \quad (4.1)$$

In clay-rich rock deviations from Darcy's law are often interpreted as a consequence of competing (coupled) flow processes (Miller & Low 1963, Swartzendruber 1962a&b, Russel & Swartzendruber 1971, Horseman et al. 1996). A chemical disequilibrium in the system rock/porewater, for example, gives rise to an osmotic flow. Hence, the hydraulic threshold gradient can be interpreted as the limiting case, below which the osmotic flow due to the chemical disequilibrium dominates the hydraulically driven flow. Therefore, the hydraulic threshold gradient is not an intrinsic rock property, but depends on the geomechanical and geochemical conditions in the porewater / rock system. Literature offers very little quantitative information for threshold gradients which would be appropriate for very low-permeability formations. Voigt & Bamberg (1995) published a compilation of results obtained in laboratory experiments. These indicate threshold hydraulic gradients in the range of 100–1000 m/m for hydraulic conductivities of about 10^{-13} m/s. In the fol-

lowing sections methods and parameter estimates of the threshold gradient are presented for the Opalinus Clay at Mont Terri.

Experimental data base

Experimental evidence for the range of validity of Darcy's law was gained by the following laboratory and field experiments:

- permeameter tests with core samples
- packer tests: single hole and crosshole
- long-term monitoring of pore pressures in piezometer boreholes

Permeameter tests with core samples

Permeameter experiments on core samples of Opalinus Clay from the Mont Terri site generally have been conducted with gradients > 1000 m/m (TN 97-39, TN 98-15, TN 99-58; cf. chapter 4.3.2). At such hydraulic gradients Darcy's law has been proven. Figure 4.5 shows the flow transients of a permeameter experiment, conducted as a multi-step pressure test (TN 97-39). Clear evidence is given for linearity between the stabilised flow rate and water pressure.

Packer tests in boreholes

As part of the GP experiment, long-term packer tests (single hole and crosshole) with flow periods of weeks and recovery periods of months were conducted. These tests were analysed using diagnostic tools (diagnostic plots, straight line analyses, etc.) and by numerical simulation of the entire test sequence (e.g. TN 98-24 and Figure 4.6). In many cases excellent fits of the pressure and flow transients were seen in the test simulations. Figure 4.6a presents a sketch of the pressure gradient radially outward from the testing borehole and Figure 4.6b shows the best fit results of a hydrotest performed in interval I4.2 of borehole BGP-4. The abbreviations for the testing sequences denote the following: PSR = pressure static recovery, RI = constant rate injection, RIS = recovery rate injection, HIS = recovery after head injection. The deviations between simulations and field data are minimal, suggesting an appropriate choice of flow law (Darcy's), well-formation flow model (radially homogeneous) and hydraulic properties. The determination of hydraulic gradients in the immediate vicinity of the borehole, as derived from numerical test simulations, is represented in Figure 4.6c. In the course of the test sequence, hydraulic gradients exhibit typical values in the range 50–500 m/m. It can be concluded that groundwater flow follows Darcy's law at hydraulic gradients higher than 50 m/m.

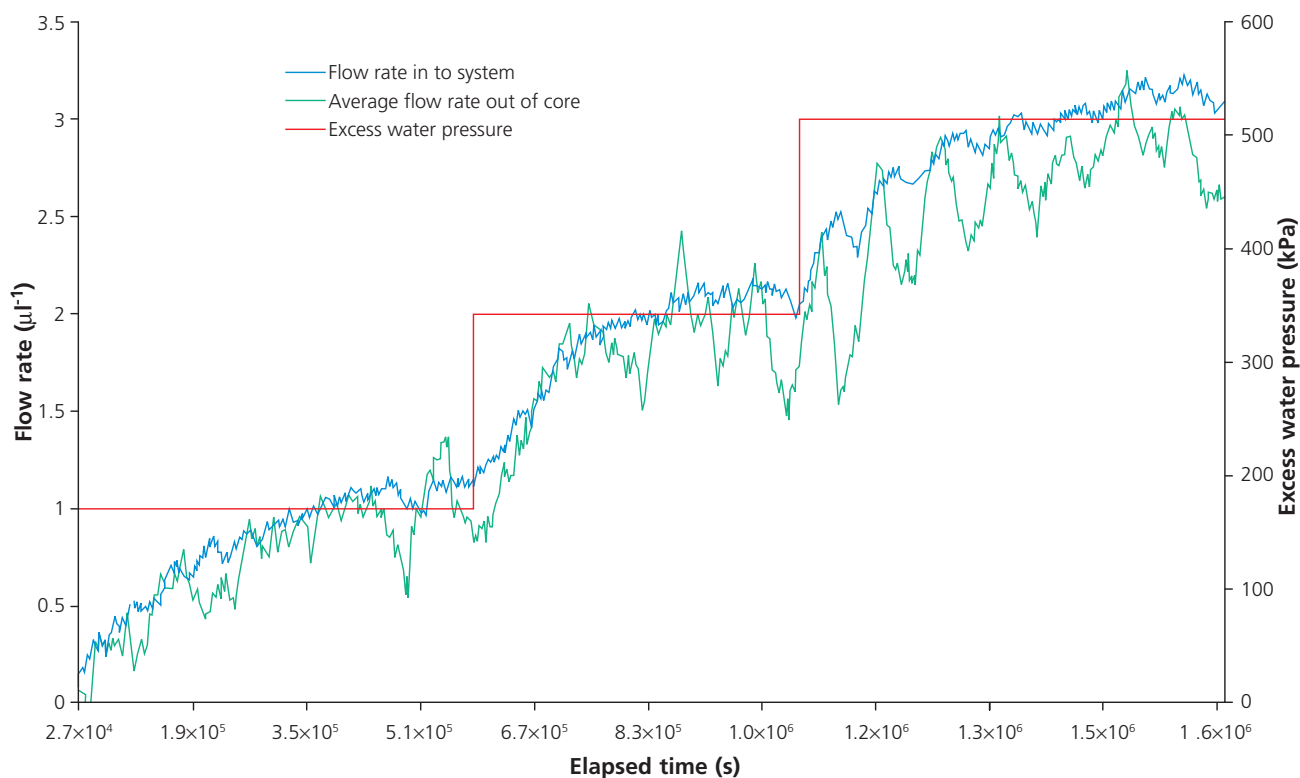


Figure 4.5: Permeameter test conducted in the OP experiment (TN 97-39). Linearity between flow and pressure is proven for hydraulic gradients > 1000 m/m (Figure taken from TN 97-26).

Observations from hydraulic crosshole testing may also be used to explore the range of validity of Darcy's law. The crosshole response in interval I3.1 of borehole BGP-3 on the source signal in BGP-4/I2 was simulated using the numerical borehole simulator MULTISIM, which is based on Darcy's law and the continuity equation (TN 98-24). The distance between source and observation borehole was 1 m. Although a response was observed in BGP-3/I1 (cf. Figure 4.7a), a satisfactory fit of the crosshole response was not achieved, even though a complex flow model was chosen. Neither the early arrival time of the pressure signal nor the flattening out of the pressure after increase was reproduced by the simulation. The misfit was interpreted as evidence for the impact of hydro-mechanical coupling (early arrival time of the pressure signal) or for a possible deviation from Darcy's law (threshold pressure gradient for flow at the observation borehole BGP-3). Figure 4.7b demonstrates based on a radial pressure field that the hydraulic gradients at a distance of 1 m from the source borehole are significantly lower than in the immediate vicinity of the source borehole, typically lower than 0.5 m/m. If threshold gradients do exist (which is not proven by the observations), they should be low, possibly smaller than 1 m/m.

Estimate of an upper limit of the hydraulic threshold gradient

Further evidences of a hydraulic threshold gradient are presented in Table 4.3. The threshold gradient necessary to establish Darcy flow in the Opalinus Clay is seemingly in the order of magnitude of 1 m/m. However, for technical reasons no direct measurement of the threshold gradient is possible. The range of uncertainty of the assessed threshold gradients is therefore quite high, i.e. one order of magnitude.

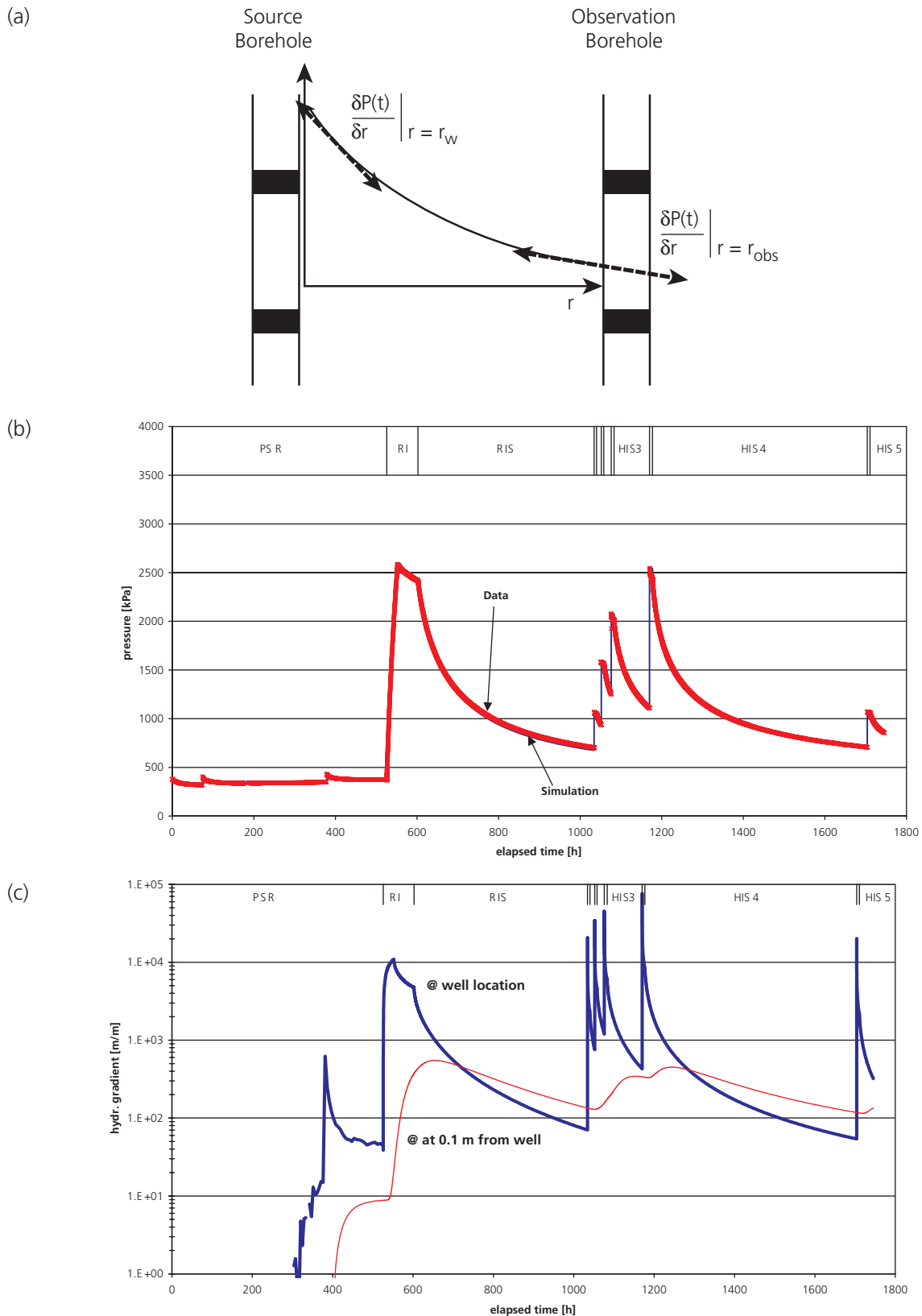


Figure 4.6: Simulation of a sequence of rate injection and head injection tests in BGP-4 as part of the GP experiment (TN 98-24): (a) schematic pressure gradient between boreholes, (b) best-fit simulation by inverse modelling, and (c) hydraulic gradient in the immediate vicinity of the borehole.

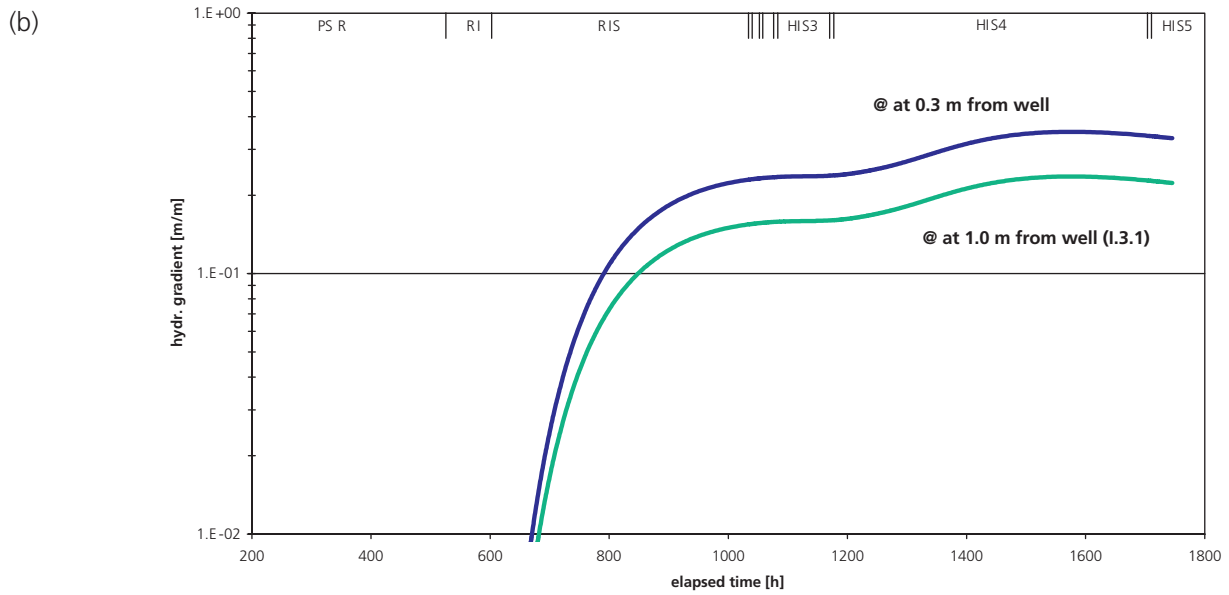
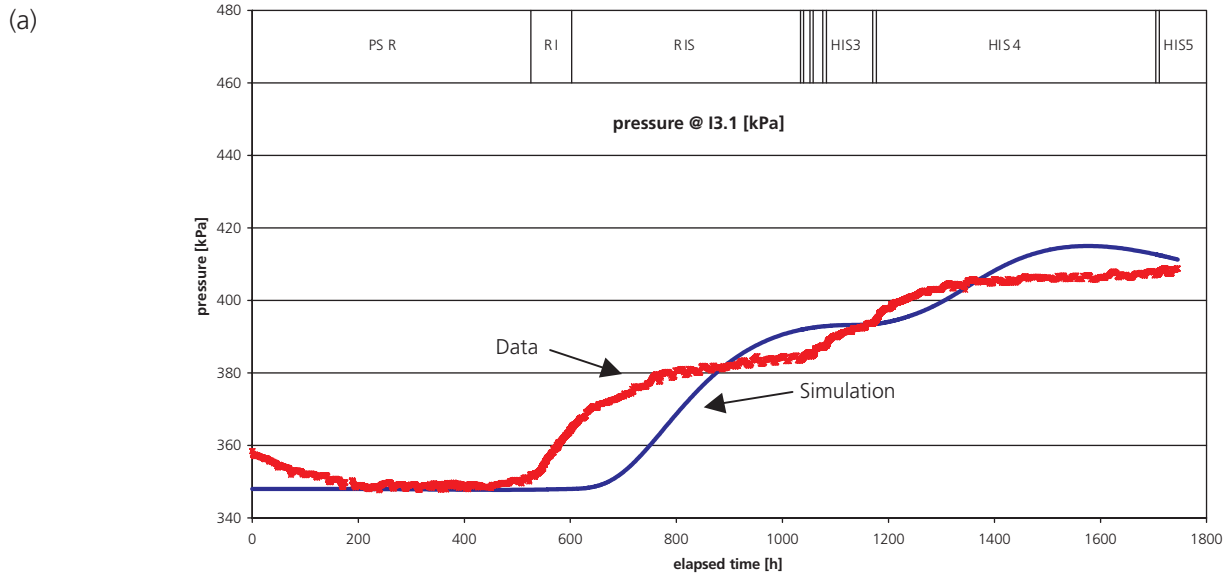


Figure 4.7: Simulation of the crosshole response in BGP-3/11 to a sequence of rate injection and head injection tests in BGP-4 (TN 98-24): (a) a satisfactory fit of the response in BGP-3 by inverse modelling was not achieved; (b) hydraulic gradient at a distance of 0.3 m and at the location of borehole BGP-3/11. The gradients are computed based on a radial flow model.

Hydraulic investigation method	Typical hydraulic gradient imposed [m/m]	Validity of Darcy's law
Permeameter tests on cores	1000–10000	The assumption of Darcy flow is proven experimentally.
Single-hole packer tests	50–500 (gradients during the pressure recovery phases)	The assumption of Darcy flow is proven experimentally.
Hydraulic interference tests	much less than one at the observation borehole	Inconsistency between the pressure evolution observed during the flowing and the pressure recovery phases (especially: abnormal “flattening” of the pressure observed in the observation borehole). These might indicate non-Darcy behavior.
Long-term monitoring of the pressure evolution in the vicinity of the tunnel near field	Radial gradient at the distance of less than 10 m is 1–20	Long-term pressure monitoring in the tunnel nearfield, does not show any indication for deviation from Darcy's law (see preliminary interpretation of the pressure measurements in chapter 4.6)

Table 4.3: Range of validity of Darcy's law and threshold gradient estimates. Typical ranges of hydraulic gradients are listed for different hydrogeological investigation techniques. For those techniques for which no deviation from Darcy's law was observed, it can be inferred that the pressure gradient was above the threshold gradient in the investigated domain.

4.4.2 Osmosis

The phenomenon of osmosis bears relevance for the hydrogeological considerations of the Opalinus Clay in terms of both a potential fluid transport mechanism and a potential cause for instability problems in boreholes and engineered subsurface structures. Literature provides numerous evidences that strongly consolidated clay formations like the Opalinus Clay may act as semi-permeable membranes and that high geochemical gradients in the formation water may drive osmotic flux (e.g. Hanshaw 1962, Young & Low 1965, Fritz 1986, Neuzil 2000). It is also known that such effects may be the cause of borehole instabilities partly due to swelling effects (van Oort 1994, Wong & Heidug 1994). Osmotic flow and osmotic differential pressures have been demonstrated repeatedly in clay formations in both laboratory and field experiments.

Chemo-osmotic flow

Osmosis is a process taking place only in materials with extremely small pores. Its underlying principle is that of a semi-permeable membrane, i.e. water molecules may pass through the porous medium while molecules dissolved in that water may not. If such a semi-permeable membrane separates two solutions with different concentrations, a flux is induced through the membrane as a result of osmosis and an osmotic pressure difference arises between the two sides of the membrane. In analogy to Darcy's law, the osmotic flux v_{Π} is proportional to the gradient of the osmotic pressure π (e.g. Horseman et al. 1996):

$$v_{\Pi}[\text{m/s}] = \zeta \cdot K \frac{\text{grad } \Pi}{\rho \cdot g} \quad (4.2)$$

K and ζ are the hydraulic conductivity and the osmotic efficiency, respectively. Osmotic efficiency is defined as the ratio of the developed hydraulic pressure and the osmotic pressure at zero flux conditions derived from the chemical activity of the water on the sides of the semi-permeable clay membrane.

$$\zeta = \left. \frac{\Delta P}{\Delta \Pi} \right|_{v_{\Pi}=0} \quad \text{where } \Delta \Pi = \frac{R \cdot T}{V_w} \cdot \ln \frac{a_1}{a_2} \quad (4.3)$$

a_1 und a_2 are the chemical activities of the water on the sides of the semi-permeable clay membrane and V_w is the volume of one mole of water.

After Fritz (1982) the van't Hoff equation is applicable for NaCl concentrations < 1 mol:

$$\Delta \Pi \approx v \cdot R \cdot T \cdot \Delta C \quad (4.4)$$

where C is the molar concentration of each of the ions and $v=2$ represents the number of number of ions of the dissociated solute. Assuming a 0.245 mol NaCl solution (equivalent to 14.3 g/l NaCl) the osmotic pressure at room temperature is in the order of 1 MPa (with reference to deionised water). Ultrafiltration is the inverse process of osmosis, describing the concentration gradient, which is

observed when an aqueous phase is pressed through a semi-permeable membrane. Horseman et al. (1996) mention osmosis and ultrafiltration as possible causes for deviations from the linear flow law (hydraulic threshold gradient, cf. chapter 4.4.1).

In the framework of the OP experiment, laboratory and field experiments were conducted in order to determine the osmotic efficiency / pressure of the Opalinus Clay (TN 97-39). Furthermore, Soler (1999) computed the theoretical osmotic pressures resulting from the salinity of the Opalinus Clay and the aquifers below and above.

Osmotic efficiency

In order to determine the osmotic efficiency of the Opalinus Clay under in-situ conditions, the 8 m long vertical borehole BOP-1 in the Reserve niche was

equipped with a PP system (TN 2000-43). The borehole was drilled with air and the testing interval was saturated with a synthetic porewater (Pearson recipe). With the exception of some unforeseen events, the test interval was fully closed off for 2 years, and a thorough equilibration of the testing fluid with the formation was attained (Figure 4.8a). On February the 16th, 2000, the fluid was at once replaced with de-ionised water (Figure 4.8b). Replacement of the fluid in the monitoring interval took place in a closed circulation system to avoid any hydraulic disturbance (i.e. advective flow towards the borehole due to the drop of interval pressure). A marked pressure decrease of around 80 kPa was observed, which is due to the chemical disequilibrium between the formation porewater and the test fluid. A numerical simulation of the experiment rendered a value for the osmotic efficiency of about 12% (TN 2000-44).

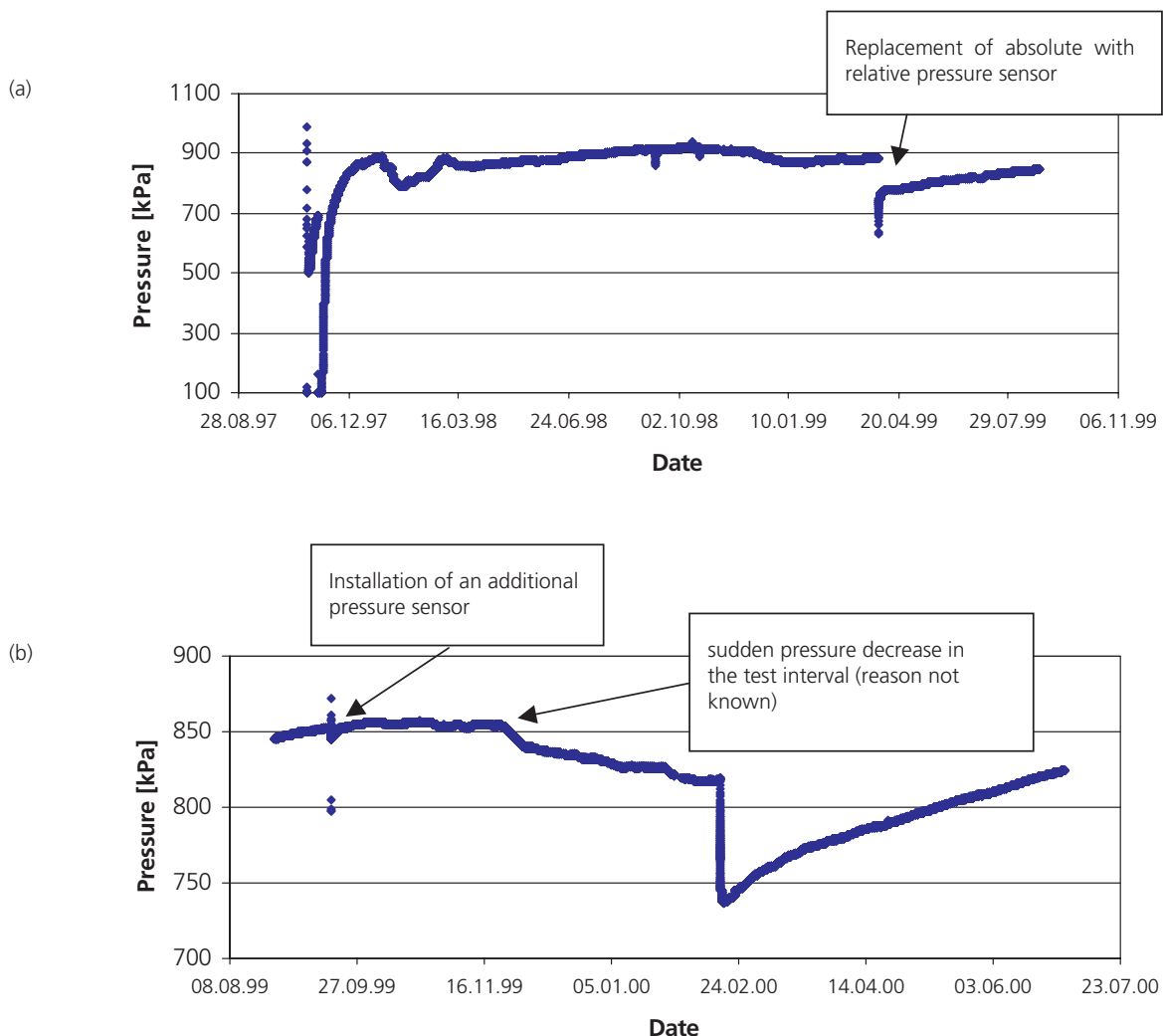


Figure 4.8: Pressures recorded in borehole BOP-1, (a) prior to fluid exchange, and (b) shortly before and after the fluid exchange with de-ionised water on February 16th, 2000.

The lab and in-situ experiments performed within the framework of the OP experiment present relatively low osmotic efficiencies of the Opalinus Clay. The osmotic efficiency was determined on two cores of the Opalinus Clay (shaly facies) under effective stresses of 4.5 MPa and 6.5 MPa (Harrington et al. 2001; TN 97-39, TN 99-81). The resulting values range from 0.03 to 0.10. In the in-situ experiment (TN 2000-42; TN 2000-43, TN 2000-44), the osmotic efficiency was derived from the measured pressure evolution in the testing borehole filled with deionised water. A maximum value of 0.12 was obtained. The impact of chemo-osmosis on packer tests was shown to be small. Further evidences suggesting small impact of osmosis were found:

- The DB experiment investigated the impact of different test fluids (synthetic porewater, KCl-based mud, silicate-polymer mud, see Enachescu et al. 1999). The analysis of the tests does not show a significant dependency of the hydraulic test results on the testing fluid used (cf. chapter 3.4).
- Soler (1999) used the results of the preliminary analyses of porewater samples collected along the reconnaissance gallery to compute osmotic pressures based on the water activities (Figure 4.9). The neighbouring formations on either side, i.e. the Lower Dogger Blaukalke limestones to the SSE and the Lias Gryphaea limestones to the NNW, showed small values of less than 0.1 MPa, while the osmotic pressure toward the centre of the Opalinus Clay formation was found to be up to 1.3 MPa, with an average osmotic gradient in the order of 1–2 m/m.

If it is considered that the clay membrane is not ideal with measured values of the osmotic efficiency of max. $\zeta=0.12$, the corresponding (hydraulic) overpressure will be less than 0.16 MPa and the hydraulic gradient will even be as low as 0.2 m/m. The osmotic fluxes would then have little impact on the hydraulic pressure within the Opalinus Clay at Mont Terri. Note in comparison the hydraulic gradients in the zone of influence of the galleries which are typically larger than 5 m/m in the immediate vicinity of the galleries. Figure 4.9 also indicates that, should chemical osmotic flux occur, it would be directed towards the Opalinus Clay as chemical osmosis promotes the flow of fluid up the salinity gradient.

- Recently, a more comprehensive chloride profile was reported as part of the GM experiment (Pearson et al. 2003; cf. Figure 4.15). The maximum salinity was in the order of 13 g/l (equivalent to 0.35 mol/l). According to the van't Hoff equation the corresponding osmotic pressure is 1.7 MPa (with reference to deionised water) – and, assuming an osmotic efficiency of 12% the hydraulic overpressure is in the order of 0.2 MPa.

4.4.3 Coupled hydro-mechanical processes

Relevance and conceptual framework

The hydromechanical processes are, for several reasons, of marked significance for the hydrogeological studies of the Opalinus Clay. First, they may affect the interpretation of hydraulic tests, leading to biased estimates of hydraulic properties (e.g. overestimation of

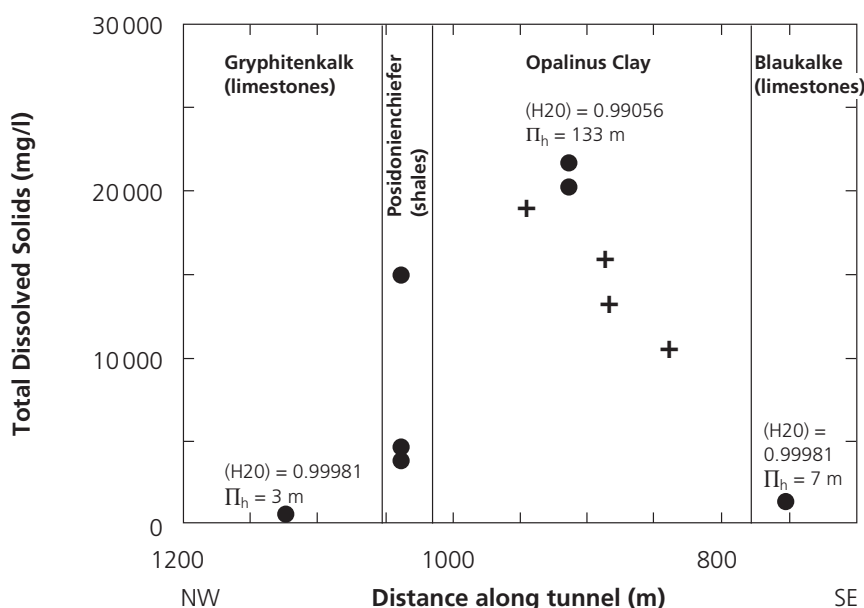


Figure 4.9: Schematic diagram showing Total Dissolved Solids vs. Distance along the Mont Terri reconnaissance gallery. Dots and plus signs are indicating different experimental values. Activity of water (H_2O) and osmotic pressure head (Π_h) are also given for the sample with the highest salinity in the Opalinus Clay, and for two low salinity sample above and below the Opalinus Clay (after Soler 1999).

K-values due to borehole closure effects, breakouts). Second, the mechanical behaviour influences the storage capacity of the Opalinus Clay at the large scale and – to lesser extent – on hydraulic conductivity. Finally, the deformation behaviour of the rock is of great importance in the excavation disturbed zone (Harrington et al. 2001): not only the property of self healing, also is the transition between ductile and brittle strongly related to the stresses in the immediate vicinity of the underground structures. In this study, emphasis is given to the first two issues.

The well-established theories of consolidation and poroelasticity (e.g. Horseman et al. 1996) form the foundation for conceptualisation of hydromechanical processes. Coupling of hydraulic and mechanical quantities is expressed by the concept of effective stress. Assuming a fully saturated porous medium at a given porewater pressure p_{pw} is subjected to mechanical stress σ , the mean effective stress p'_m [Pa] is defined as:

$$p'_m = \frac{1}{3} \cdot (\sigma_1 + \sigma_2 + \sigma_3) - p_{pw} \quad (4.5)$$

where σ_1 , σ_2 and σ_3 represent the principle directions of the stress tensor.

The Opalinus Clay at Mont Terri is an indurated, slightly overconsolidated claystone. Assuming the rock is exposed to changing stress conditions in an elastic deformation regime, a logarithmic relationship holds for the inter-dependence between porosity n [-] and mean effective stress (Wood 1990):

$$n \approx n_o - \kappa \cdot \ln \frac{p'_m}{p'_o} \quad (4.6)$$

where κ is the negative slope of the rebound-reconsolidation line (RRL). The intercept value n_o is conventionally chosen in a way that it represents the porosity at an effective stress $p'_o = 1$ kPa. Drawing on critical state concepts, the drained bulk modulus of an overconsolidated clay, B [Pa], can be estimated from the mean normal effective stress, p'_m , and the negative slope of the rebound-reconsolidation line, κ , using:

$$B = p'_m \left[\frac{1}{(1-n)\kappa} \right] \quad (4.7)$$

The specific storage coefficient S_s , is usually defined as:

$$S_s = \rho_w \cdot g \cdot \left[\frac{1}{B} + \frac{n}{K_w} \right] \quad (4.8)$$

where B and K_w are the compressibility of rock and water, respectively, and ρ_w is the density of water. In the context of groundwater flow modelling the

drained compressibility of the rock is used to determine specific storage, whereas the undrained modulus is more appropriate for hydrotest analysis.

According to the Kozeny-Carman equation (e.g. Horseman et al. 1996) intrinsic permeability k and hydraulic conductivity K [m/s] can be expressed in terms of porosity n and specific surface S :

$$k = \frac{n^3}{(1-n)^2} \left[\frac{1}{\tau^2 \cdot C_s \cdot (\rho_s S)^2} \right]$$

and

$$K \left[\frac{m}{s} \right] \approx 1 \cdot 10^7 \cdot k \left[m^2 \right] \quad (4.9)$$

where τ is the tortuosity and C_s represents a geometry factor with typical values between 2 and 3. Specific surface and porosity can be determined by microstructural analysis of porespace.

Combining equations (4.6) and (4.9) leads to a relationship between permeability and mean effective stress. In the case of elastic deformation, the changes of permeability with stress are rather small. However, when the stress conditions approach a critical state boundary of plasticity, i.e. irreversible deformation, dilatancy or compaction may occur and the permeability changes are much more pronounced and can not be described by equations (4.6) and (4.9).

In oilfield exploration (e.g. Settari & Walters, 2001), it is a well-known procedure to decompose sequentially the hydro-mechanical coupling process into:

- Pore volume coupling - that is, any changes in effective stress (and the resulting volumetric strain) cause changes in the porosity (translating to pressure changes) of the porous medium.
- Permeability coupling, which relates permeability changes to porosity changes due to volumetric deformation

For the hydro-mechanical modelling exercise described below (coupled hydro-mechanical modelling of the interference test in BGP-6), the pore volume coupling alone was used as the changes in permeability due to porosity changes with effective stress were assumed to be negligible (due to lack of data to support otherwise). The approach was simplified by neglecting the porosity-permeability relationship and, instead, introducing so-called transmissibility multipliers. Thus, the coupling between effective stress and pore volume is modelled explicitly, whereas the effective permeability is the product of the intrinsic permeability and a stress dependent dimensionless coefficient

cient. The functional relationship between effective stress and transmissibility multiplier is a smooth function which has to be fitted to the data.

Experimental evidence for coupled hydro-mechanical processes

Interference tests were conducted in the FM niche with the GP experiment in Phase 4, and at the GS site in the new gallery with the GS experiment of Phase 5 in search of evidence for hydro-mechanical processes on the scale of the in-situ experiment. The experimental set-up was similar in both experiments. Figure 4.10a shows the borehole configuration applied in the FM niche: triple packer systems were installed in BGP-5 and BGP-6 for hydraulic testing. Fixed installed micrometers (FIM) with five measuring sections were emplaced in BGP-8 and BGP-9 to monitor displacements along the boreholes (the configuration was

completed by a TDR system for monitoring possible changes of water content during gas injection tests). A three-step constant-head water-injection test (pressure steps HI1, HI2 and HI3) was carried out in interval I2 of borehole BGP-6 (Figure 4.10b) and hydraulic responses were observed in all monitoring intervals of BGP-5 and BGP-6. In addition, displacements were recorded in BGP-8 and BGP-9. Figure 4.10c presents the crossplots of displacements in BGP-8 versus injection pressure in BGP-6/I2. The correlation of displacements and interval pressure is evident. In section F8.2 of BGP-8, a maximum (compressive) strain of -0.02 mm/m is observed. The other sections tend to show dilatant behaviour. In BGP-9 the same pattern is observed, however, the deformations are less pronounced because the distance to the source borehole is longer.

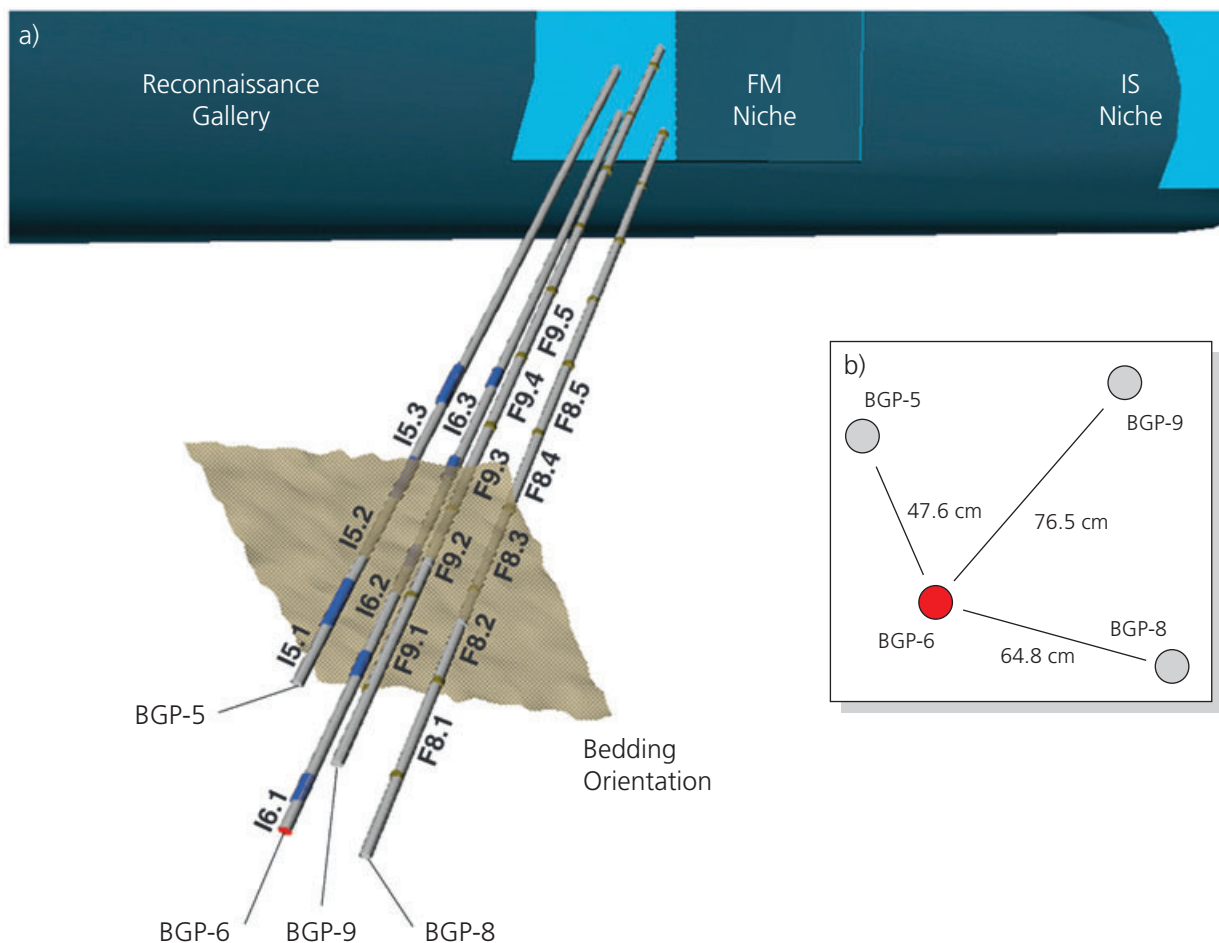


Figure 4.10: Interference test in the FM niche with a water-injection test in BGP-6: test configuration with the four boreholes (a) in 3D with a schematic plane indicating the bedding orientation roughly at right angle to borehole orientation and (b) in plan view perpendicular to BGP-6 at the centre of the test interval. (c) Pressure vs. time plot for the three-step constant-head water-injection test in BGP-6/I2 and (d) corresponding displacement records from FIMs installed in BGP-8 and BGP-9. (c) and (d) on page 46.

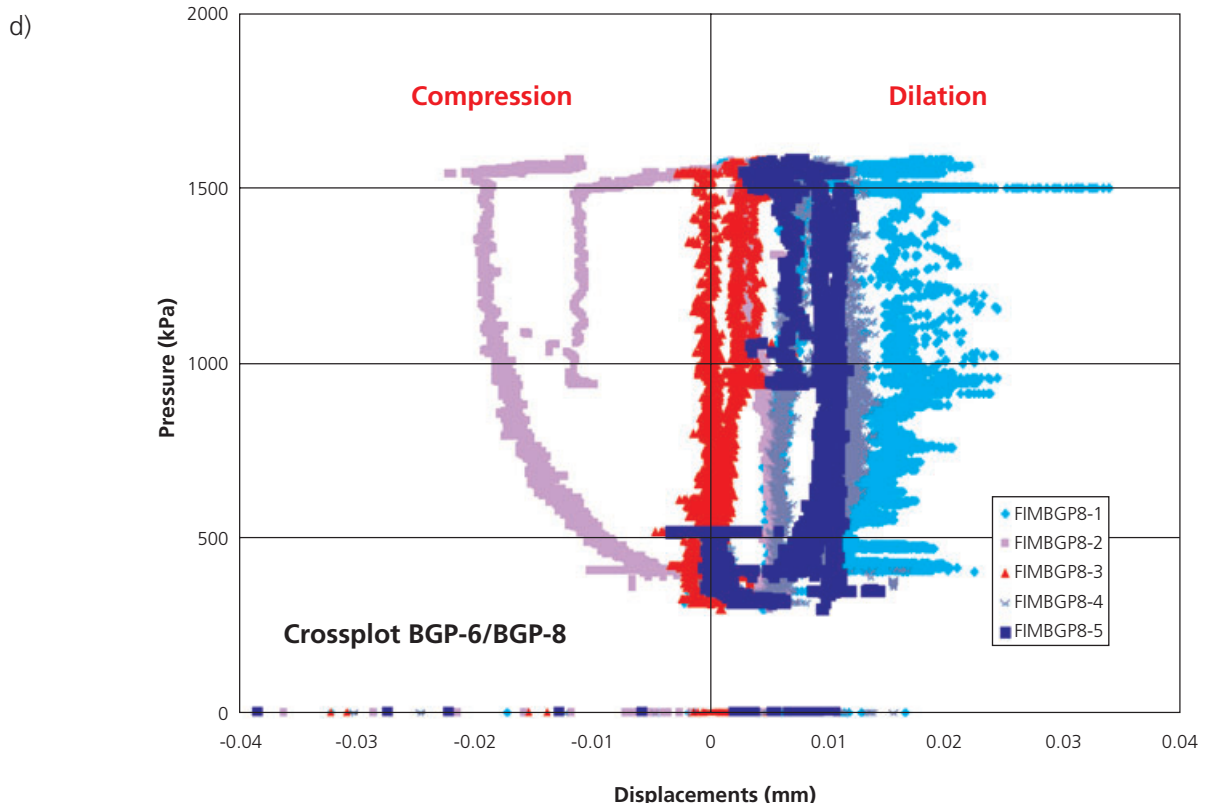
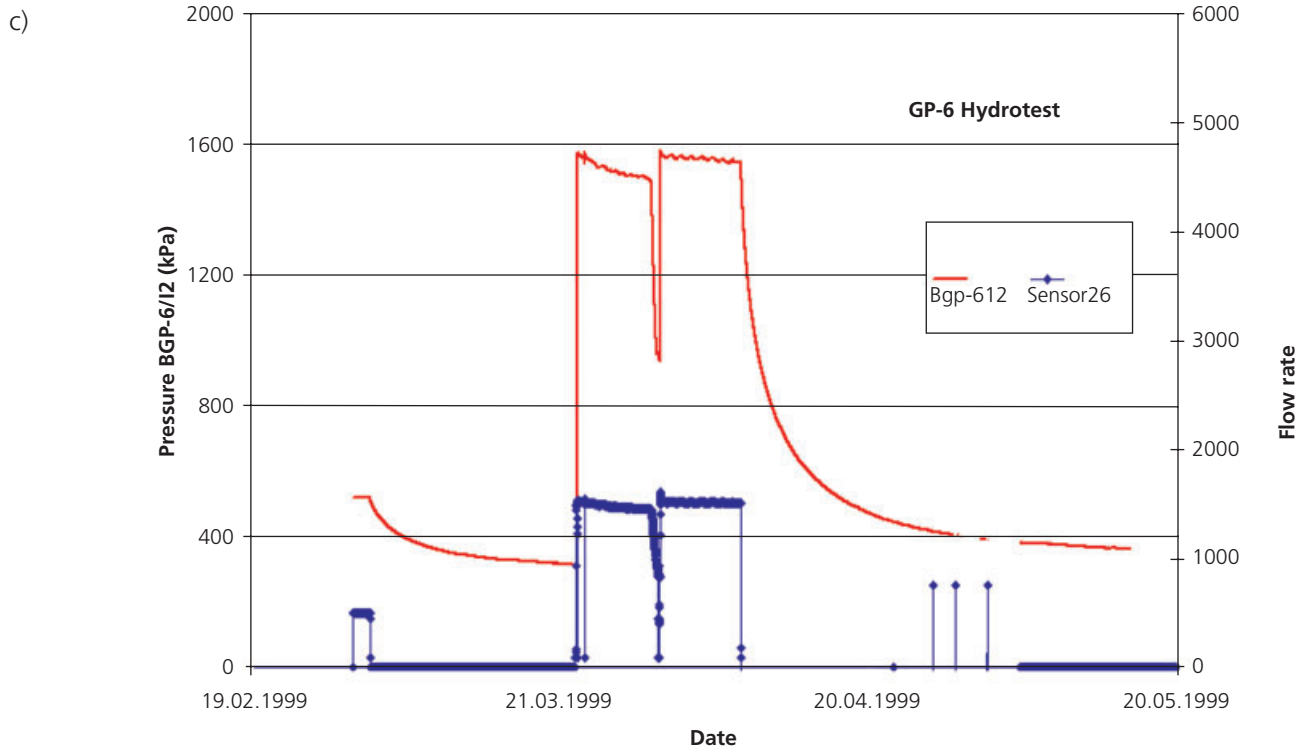


Figure 4.10 continued

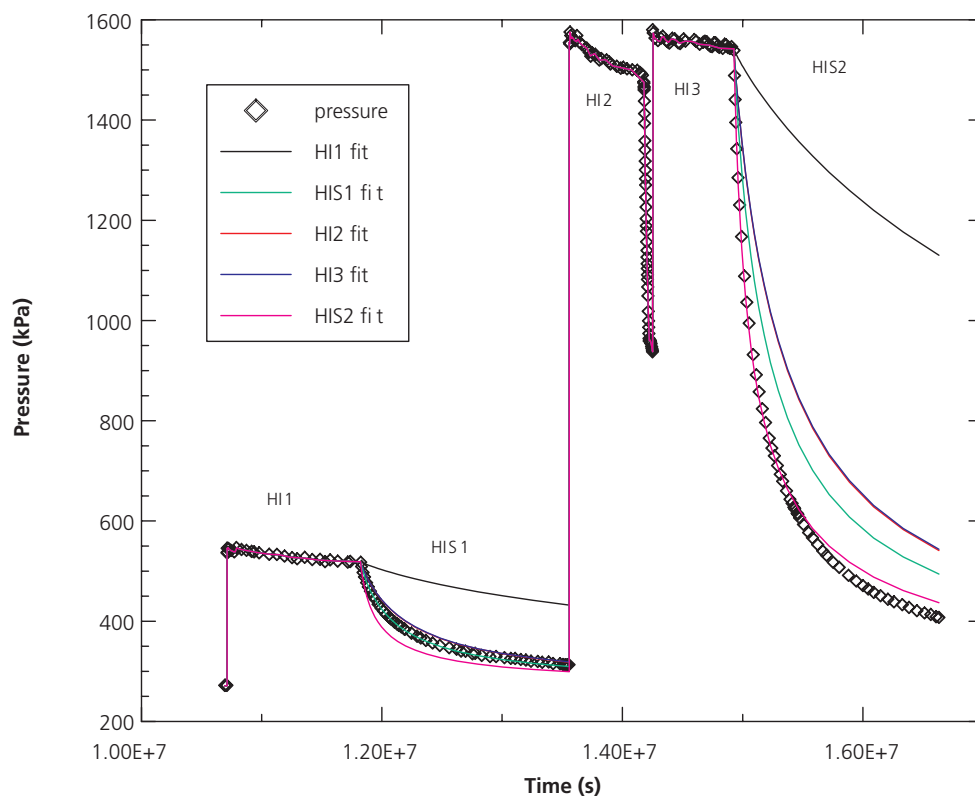
Coupled hydro-mechanical modelling of the hydraulic interference test in BGP-6

The hydro-mechanical analysis of the interference test in BGP-6 was conducted in two steps (cf. TN 2000-21):

- In a first step, a detailed (hydraulic) analysis of the hydrotest response in the test interval I6.2 of borehole BGP-6 was performed with the welltest simulator GTFM (Pickens et al. 1987). The analysis focussed on the measured flow rates during the constant head injection sequences and on the pressure response during the subsequent recovery periods.
- In a second step, the coupled hydro-mechanical code GEOSIM (TN 2000-21) was applied, considering both the hydraulic (e.g., porewater pressure

response) and the geomechanical response. For this task, the test configuration was implemented with a 3D numerical model covering boreholes BGP-6 and BGP-5 for hydraulic responses, and BGP-8 and BGP-9 for geomechanical responses.

The hydraulic test interpretation was aimed at detecting potential changes in hydraulic properties with injection pressure. The detailed analyses were done through diagnostic plot analysis and inverse modelling of individual test events and of the entire hydrotest sequence. Figure 4.11 illustrates the difficulties in matching the entire test sequence by inverse modelling. Fitting the individual test events HI1 / HIS1 and HI2&3 / HIS2&3 leads to acceptable matches, whereas the fit of the entire test sequence is not satisfactory.



P: Static formation pressure
 S_s : Specific storage
 K_{inner} : Hydraulic conductivity of the inner zone in a 2 shell radial composite model
 K_{outer} : Hydraulic conductivity of the outer zone

	K_{outer} (m/s)	K_{inner} (m/s)	Rinner (cm)
HI1	1.18E-14	3.27E-13	12.65
HI2	1.56E-14	2.02E-13	179.95
HI3	3.43E-14	1.99E-13	153.15
HIS1	6.86E-14	3.22E-13	272.05
HIS2	1.53E-13	8.14E-13	582.35

$P = 271$ kPa
 $S_{s \text{ inner}} = S_{s \text{ outer}} = 2E-06$ 1/m

Figure 4.11: Inverse modelling of the packer test conducted in BGP-6 using a finite skin model (inner zone / outer zone) exhibits difficulties in simulating jointly the HI1 / HIS1 sequence and the HI2&3 / HIS2&3 sequence. The analysis of HI1 / HIS1 gives a hydraulic conductivity in the order of 1 to 3 E-14 m/s. The two latter test sequences suggest values in the range 7E-14 and 2E-13 m/s (after TN 2000-21).

Fitting of HI1 / HIS1 leads to K-values in the order of 1 to 3×10^{-14} m/s; putting the weight on H2&3 / HIS2&3, however, gives value between 7×10^{-14} and 2×10^{-14} m/s. This fact suggests dependence between hydraulic conductivity and injection pressure. More generally, a relation between intrinsic permeability and effective stress may be deduced.

Coupled hydro-mechanical modelling was performed with the code GEOSIM (TN 2000-21). In GEOSIM, a sequential coupling procedure was implemented which consists of pore volume coupling followed by permeability coupling. Due to the lack of site specific data, the porosity-permeability coupling was neglected and a simple transmissibility multiplier was introduced. Geomechanical properties of the Opalinus Clay were taken from TN 98-35. Pressure responses in the observation intervals of BGP-5 and BGP-6 were modelled as well as the mechanical responses in BGP-8 and BGP-9. Four different cases were considered:

- Case 1: Opalinus Clay exhibits homogeneous and isotropic hydraulic properties. Geomechanical behaviour is characterised by elastic properties, based on TN 98-35. An additional sensitivity run (Case 1a) was carried out using anisotropic hydraulic conductivity (K enhancement by a factor of 2.5 parallel to bedding).
- Case 2: Flow takes place in mechanically weakened zone which is parallel to the bedding plane and called "fracture zone" in the following. It has a thickness of 2.5 cm. The transmissivity of this fracture zone is stress dependent. The initial transmissivity of the fracture is 2.5×10^{-14} m²/s. Its elastic properties are the same as in Case 1.
- Case 3: Comparable to Case 2, except that softening of the fracture zone during fluid injection is assumed.
- Case 4: Comparable to Case 2, except that the geomechanical behavior is no longer linearly elastic. A hyperbolic model is used, as it was proposed in TN 98-56.

The results of hydro-mechanical modelling are discussed in TN 2000-21. A brief summary is given below.

Case 1 (isotropic properties) results in a poor overall fit of the test sequence both in pressure response and in displacement modelling. The sensitivity run with anisotropic rock properties (Case 1a), however, showed an acceptable overall match. In particular, the general pattern of the simulated displacements at the

FIM locations (compression/extension) was in agreement with the observations. The magnitudes of the simulated displacements were slightly lower than the measured ones.

In Case 2 the potential of a permeability increase as a result of the increase in injection pressure during the hydrotest was examined. That is, as the fluid pressure increases during the constant-head injection tests, the effective stress decreases causing an increase in the fracture transmissivity. The magnitude of the permeability change is a factor 3. Figure 4.12 shows the simulated interval pressures. Note that only the fall-off events (HIS events) were fitted, whereas the HI events were given by prescribed pressure. The overall fit of the interval pressure and the diagnostic plots of the fall-off events are satisfactory. Furthermore, the calculated displacements matched the observed extensions/compressions reasonably well (not presented here, cf. TN 2000-21).

Case 3 corresponds to Case 2, except that the fracture zone was assumed to have a higher compressibility (e.g., decreasing E modulus from 4 GPa to 1 GPa). This softening of the fracture zone during fluid injection was designed to account for potential dilatancy prior to the failure of the samples as suggested in the triaxial tests (TN 98-35 and TN 98-55). The impact of the softer fracture zone did not noticeably affect the fluid pressure response in BGP-6/12. The mechanical effect however is noticeable: an increase in the extension in BGP-8/12 (from about 0.04 to 0.08 mm) is observed, which is significantly greater than the measured displacements.

Case 4 also corresponds to Case 2, except that a hyperbolic geomechanical model is assumed. Similar to Case 3, the impact of the hyperbolic model on the fluid-pressure response is small. The results of the calculated displacements at the corresponding FIM segments in BGP-8 indicate significantly lower extension (0.01 mm) as compared to Case 2. However, variations in the parameters describing the hyperbolic model may result in calculated displacements that show a better fit with the observed data. In conclusion, the introduced complexities of the material law are not required to explain the data.

Concluding remarks

The results of the coupled hydro-mechanical modelling indicate that the observed FIM measurements can be reproduced reasonably well with an overall elastic constitutive model for the clay. However, non-linear behaviour represented by a hyperbolic constitutive model cannot be excluded. More importantly, the coupled modelling indicates that the increased injection

pressure during the HI events caused a significant permeability increase associated with a decrease in effective stress. For the interference test in BGP-6 with a maximum injection pressure of about 1.6 MPa, the permeability enhancement factor was about 3. Hydromechanical modelling of hydraulic interference tests at Mont Terri suffers from the fact that the understanding of stress conditions at the site is quite rudimentary. Neither the principal stress directions, nor stress magnitudes are well known. Moreover, the test boreholes in the FM niche are located close to the tunnel excavations. Thus, complex stress redistribution in the test zone may be expected. Recent geomechanical studies as part of the RA project will place emphasis on an improved understanding of rock stress in the tunnel nearfield. In future phases of the HA project this information will be integrated in the assessment of hydromechanical coupled processes.

4.5 Groundwater flow at different scales

The hydraulic properties of the undisturbed Opalinus Clay formation are governed in part by the hierarchy of pore structures, with the spatial distribution of the various pore structures being scale-dependent. The hydraulic conductivity, too, is a scale-dependent property. In practice – given the low permeability of the Opalinus Clay – hydraulic conductivity may be determined only at small scale. With hydraulic in-situ tests and laboratory experiments it was possible to obtain hydraulic conductivity estimates representative for the centimeter to meter scale. However, attempts to draw conclusions on groundwater flow on the site scale require effective hydraulic conductivity values on the deka- to hectometer scale. In addition to deriving representative hydraulic parameters from testing on the small scale, it is therefore also necessary to establish a (conceptual) modelling approach which allows for the upscaling of these observations to the required region-

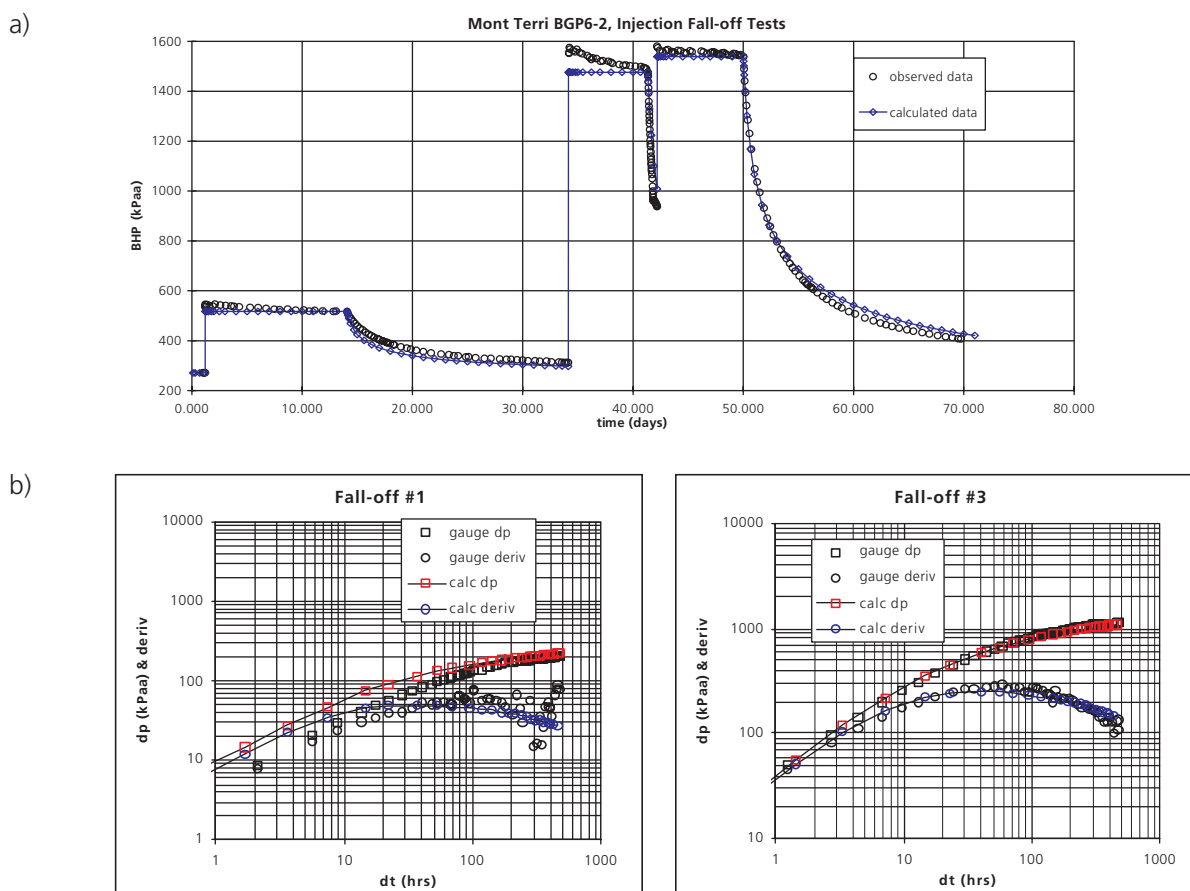


Figure 4.12: Hydro-mechanical modelling of the interference test in BGP-6 – simulated interval pressures. Note that only the fall-off events (HIS events) where fitted, whereas the HI events were given by prescribed pressure: (a) The overall fit of interval pressure and (b) the diagnostic plots of the fall-off events are satisfactory (after TN 2000-21).

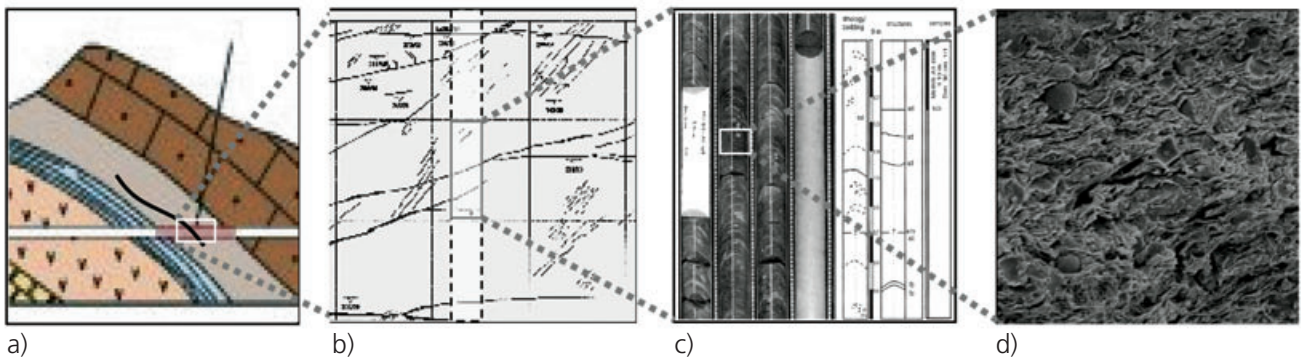


Figure 4.13: Hydraulically relevant structural and stratigraphic elements at various scales of observation: (a) geological formations and regional flexure at the Mont Terri site; (b) facies, fracture zones and single fractures of the decimeter to dekameter scale in the Opalinus Clay formation; (c) lithofacies and bedding as well as various small discontinuities in the order of millimeters to decimeters; and (d) microfractures, and micro/mesopores in the sub-millimeter range (Remark: the figure does not necessarily adhere to the scales introduced above but covers the complete range of scales described).

al scale where no direct measurements are possible. The first step in the analysis of the scale dependency of the hydraulic conductivity is the identification of the hydraulically relevant structural elements at the various scales of observation. In total, four different observation scales have been defined for the Mont Terri site. Their dimensions serve as guidelines rather than exact sizes (Figure 4.13):

- On the site scale (10^1 – 10^3 m) the Opalinus Clay formation represents an aquitard sandwiched between the more permeable formations of the Jurensis Marls and the Lower Dogger Limestones. The Opalinus Clay acts as a hydraulic barrier. The only element which may affect this barrier function at the site scale is the main fault. The impact of the main fault on the hydrogeological system may not be assessed effectively by in-situ experiments. However, it is possible to assess the hydraulic efficiency of the Opalinus Clay barrier qualitatively by means of independent experimental evidences such as the observed pore pressure distribution at the site, pore-water chemistry and isotope profiles.
- Tunnel mapping allows for the differentiation of facies and the detection of discrete structural features on the scale of decimeters to dekameters (10^{-1} – 10^1 m). Within the individual facies, layers of various sand and clay content but of critical lateral extent exist. Hydraulic characterisation of all these features on the decimeter to dekameter scale is carried out through packer testing in boreholes, both in single and cross-hole arrangements. Hydraulic conductivities determined from the results of packer tests with test intervals of several decimeters up to about 10 m in length, are representative for radial extensions of several decimeters to several meters, i.e. corresponding to the radius of influence of the

hydraulic test.

- At the core scale (10^{-3} – 10^{-1} m) and also at the tunnel mapping scale, well structured parallel interlayering of clayey and sandy layers is observed. Layering can be interpreted as an indication for pronounced anisotropy of the hydraulic conductivity at the centimeter to decimeter scale. Permeameter tests allow for the determination of hydraulic conductivity both parallel and perpendicular to the layering.
- The mineralogical composition and the microstructure of the Opalinus Clay were determined in the laboratory for an investigation domain of < 0.002 mm. The microstructure was analysed with various methods like gravimetric methods, helium pycnometry and mercury injection. The equivalent microscopic pore spaces of the Opalinus Clay are classified in the category of micro/meso- and macropores; microfractures may also contribute to porewater flow, although they are rarely observed in the Opalinus Clay. Within the mesopores, the mobility of the porewater is limited by capillary forces and electrical intermolecular forces. Indirect indication of hydraulic conductivity on this microscale is derived from empirical porosity-permeability relationships (e.g. Kozeny-Carman).

4.5.1 Site scale (10^1 – 10^3 m)

On the site scale (dekameters to kilometers), the physical framework for the conceptual hydrogeological model is provided by the local geological setting. The Opalinus Clay is a lithostratigraphic unit of the Mont Terri anticline, a structure belonging to the Folded Jura. Figure 4.14 shows a geological map of the Mont Terri anticline and a cross-section along the Mont Terri road tunnel between St-Ursanne and Courgenay. Today's lithostratigraphic and structural elements are the rudimentary elements responsible for the general

hydrostratigraphy, i.e. the definition of hydrogeological units and determination of water-conducting features. However, one also needs to consider the historical evolution, particularly of tectonic and sedimentological/erosional nature for an enhanced understanding of the presently observed groundwater flow systems.

The primary references published within the Mont Terri investigation program are Vermeille & Bossart (1999a), TN 99-22 as well as contributions to Thury & Bossart eds. (1999). Eventually, an excellent overview of the regional geology and the paleogeology of the site is given in Pearson et al. (2003).

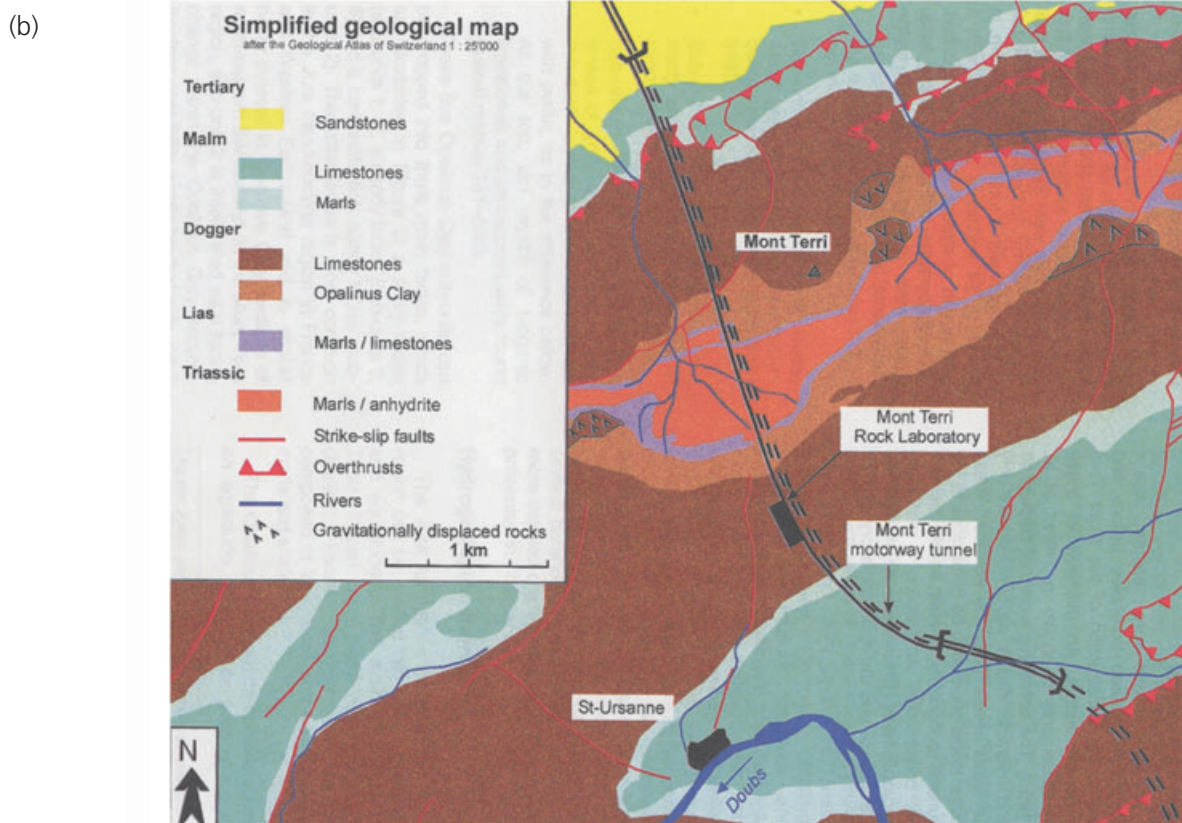
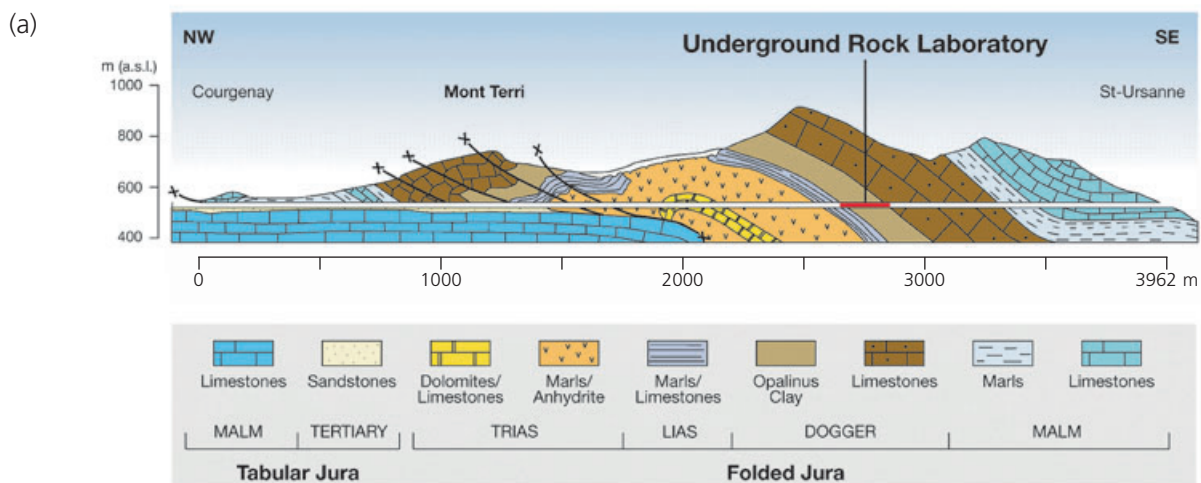


Figure 4.14: (a) Simplified geological cross-section through the Mont Terri anticline along the motorway tunnel, showing the location of the Mont Terri rock laboratory (Thury & Bossart 1999) and (b) simplified map of the Mont Terri anticline.

Definition of hydrogeological units

The purpose of defining the regional hydrostratigraphy is to divide the regional groundwater flow domain into hydrogeological units. These units merge adjacent stratigraphic units of similar hydrogeological properties and are generally classified into aquifers and aquitards. Obviously, the final definition of the hydrogeological units is based on the available hydrogeological data. The hydrogeological investigations for the Mont Terri project focussed almost exclusively on the characterisation of the Opalinus Clay. Little knowledge has been acquired about the adjacent formations. Important sources of information for these formations, therefore, are the records of hydrogeological investigations conducted in the course of construction of the motorway tunnel (TN 99-22). Additional information on the regional hydrogeology has been summarised by Wermeille & Bossart (1999a). Table 4.4 presents the current knowledge base of the hydrogeological setting at site scale.

Clearly identifiable as aquifers are the limestones of the Upper Malm and the limestones of the Lower Dogger. The limestones of the Upper Malm represent a regional aquifer of relevance for the regional water supply. The Lower Dogger limestones form a local aquifer which, nevertheless, produced substantial discharge rates during the construction of the motorway tunnel. The significance of the Jurensis Marls is less clearly defined. Water influx was observed from this formation during construction, but appeared to have originated in localised water conducting features. The measured chloride concentrations in the porewater and along the tunnel present an indirect evidence for this hydrogeological situation (Figure 4.15). The chloride profile shows a gradual decrease in concentra-

tions towards the Lower Dogger which is an indication for more intense groundwater flow in the Lower Dogger. In the Jurensis Marls and the Posidonia Shales some considerable concentrations have been observed in samples obtained from porewater squeezing or leaching, while water samples collected in boreholes tend to imply short-term residence times.

Typical aquitards besides the Opalinus Clay are the Malm Marls, and the marl and anhydrite formations of Trias. The hydraulic barrier function of the Opalinus Clay was investigated rigorously in the Mont Terri investigation program. Not much is known, however, about the other aquitards.

Regional faults

Several thrust faults and strike slip faults intersect the motorway tunnel in the northern section (cf. Figure 4.14). The fault zones were mapped during the exploration phase in 1992 and inflow zones with flow rates of 1–2 l/s observed. The main fault in the Opalinus Clay did not show any water inflow. In addition, the chloride profiles in Figure 4.15 do not suggest enhanced groundwater flow along the main fault, as would be indicated by a drop in salinity.

Tectonic and stratigraphic evolution of the site

Wermeille & Bossart (1999a; Chapter 1.2 in TN 99-73) conducted a comprehensive literature review of the tectonic and stratigraphic evolution of the Folded Jura including the erosional history. The results may be summarised as follows: 40 My ago the area was covered by a sea which led to the deposition of the UMM, the Lower Marine Molasse. The period from 40 My ago to 21.5 My ago saw the subsidence of the

Lithostratigraphy	Hydrogeological classification
Limestones of the Upper Malm (Oxfordian/Kimmeridgian/Thionian)	Regional aquifer (karstified): fissured and karstic limestones; inflow rates > 1 l/s
Malm Marls (Lower Oxfordian/Callovian)	Aquitard: (shaly) marls, limestones, marly clay; impermeable
“Lower Dogger” (Lower Aalean/Lower Bajocian)	Local aquifer (karstified): sandy limestones, fissured and karstic; inflow rates 12–200 l/s
Opalinus Clay (Lower Aalenian)	Aquitard: silty and sandy shales; impermeable
Jurensis Marls and Posidonia Shales (Upper Toarcian)	Hydrogeological unit with localised water circulation (weakly karstified): Marls and limestones; spontaneous water inflows into the tunnel of 1–5 l/s
Triassic marls/anhydrite/dolomites/limestones Aquitard:	Marls, anhydrite, dolomites, limestones; partly fissured and karstic; tight rock with localised inflow rates << 1 l/min

Table 4.4: Hydrogeological classification of the lithostratigraphic units in the Mont Terri region (after Thury & Bossart 1999). Hydrogeological conditions during construction of the motorway tunnel between 1989 and 1999 (after Haapainter & Schaeren TN 99-22).

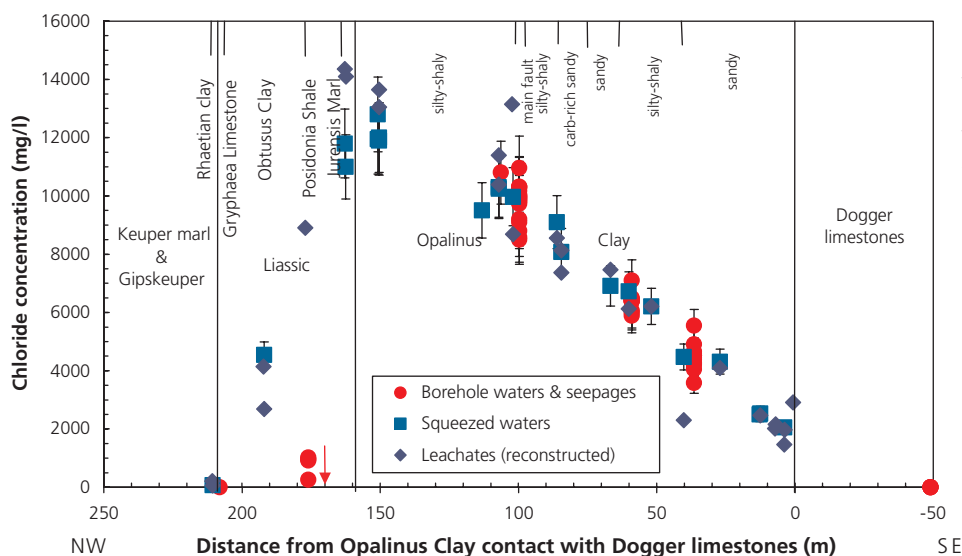


Figure 4.15: Chloride profiles as an indirect evidence for groundwater flow conditions in the Opalinus Clay and in the adjacent stratigraphic formations. The chloride profile shows a gradual decrease in concentrations towards the Lower Dogger, which is an indication for more intense groundwater flow in this formation (after Pearson et al. 2003).

Delémont Basin with the formation of N-S trending faults east of St-Ursanne and the Mont Terri flexure. Sedimentation of the UMM continued initially but was taken over increasingly by the sedimentation of USM, i.e. Lower Fresh Water Molasse, due to freshwater lakes and braided rivers. As the subsidence of the Delémont Basin continued until about 10.5 My ago, the area of St-Ursanne emerged and became hydraulically separated from the Delémont Basin. The erosive period for the Doubs valley also started during this time and a primitive Doubs river formed. The evolutionary history from 10.5 My ago to the present includes the formation of the Folded Jura which was thrust over the flat-lying Tabular Jura into its current position by about 3 My ago. The tectonic process led to the formation of anticlines which also prevented the Doubs river from flowing northwards, eastwards and southwards, i.e. forced it to double back approximately in a westerly direction. In their own interpretive work, Wermeille & Bossart (1999a) derived erosional rates which indicate that the Doubs River at St-Ursanne reached the level of the future Mont Terri underground laboratory between 3 My and 1 My before present. The current overburden at the rock laboratory is about 250–320 m (Thury & Bossart 1999). The estimated overburden in the past was at least 1000 m.

This tectonic and sedimentary evolution has strongly influenced the hydrogeological evolution in the area. It is important to recognize that paleohydrogeological effects may still be evident in the present hydrogeologic regime. According to Wermeille & Bossart (1999a) the two main geological developments with major impact on the paleohydrogeology at the Mont Terri site are (i) the progressive downward erosion

of the Doubs valley, responsible for the change in groundwater flow direction in the Opalinus Clay with a reversal from infiltration to exfiltration along the Doubs river, and (ii) the progressive erosion of the Mont Terri anticline which affected the flow direction and mainly the groundwater chemistry.

The focus of the hydrogeological analyses at the Mont Terri rock laboratory lies on the Opalinus Clay, an aquitard and a sedimentary product of the Jurassic Sea of approximately 180 My ago. Within the bounds of the rock laboratory, the formation is traversed by a major inverse fault zone (Haarpaintner & Schaeren, TN 99-22). The neighbouring formations to the North-west and Southeast of the Opalinus Clay are the aquifers of the Jurensis Marls and Lower Dogger Limestones, respectively. Being situated in the southern limb of the Mont Terri anticline, the strata exposed in the rock laboratory dip with an angle of approximately 45° to the southeast (Thury & Bossart 1999).

4.5.2 The scale of tunnel investigations (10¹ – 10³ m)

At Mont Terri extensive sedimentological mapping of freshly excavated niches, of outcrops in the reconnaissance gallery and of the tunnel walls has resulted in a more detailed lithological partitioning of the Opalinus Clay (Figure 4.16). Geological and hydrogeological characterisation of the tunnel surface mapping covered lithological and structural features on the decimeter to dekameter scale (Figure 4.17). Packer testing in boreholes was used to determine hydraulic properties of the Opalinus Clay on this scale.

Lithology / facies

The Opalinus Clay formation has been divided into three major facies which are generally referred to as the shaly facies, the carbonate-rich sandy facies and the sandy facies (see Figure 4.16). According to Bossart & Wermeille (Chapter 2.1 in Thury & Bossart 1999), the three facies are the result of different sedimentary environments in the shallow basin during the time of deposition. The shaly facies is predominant, making up about 135 m of the new gallery. It, therefore, has been subdivided further into three lithofacies which alternate in the range of decimeters to meters: shale, silty shale and argillaceous marl (TN 99-73, S1.2).

Structural Elements

Particular attention has been paid to the fault zone, representing the "Main Fault" in the central section of the Opalinus Clay formation. In the three galleries excavated parallel to each other, this feature has been observed to be one to several meters thick (see Figure 4.16). It is referred to as the main fault and represents a thrust fault (3rd order fault) with a displacement in the order of 5 m and an extent of at least 60 m (TN 99-73, S1.2). Its orientation is slightly steeper than

that of the bedding and runs subparallel to bedding. The main fault is further characterised by a large number of fault planes, i.e. > 20 1/m. Most of the fault planes within the main fault show slickensides and shear fibres on a polished surface. These small-scale structures consistently indicate overthrusting. Additionally, there are highly deformed intervals similar to fault breccia which show loss of cohesion and completely disturbed bedding (drag folds).

One of the highly tectonised samples from the main fault was impregnated with epoxy resin (chapter 2.3 by Bossart & Adler in Thury & Bossart 1999). Thin section analysis of this section of the main fault revealed that the open fractures likely formed as a result of the tunnel excavation and are not likely candidates for advective water flow. Only the interface between the fracture wall and the fracture infill might have been reactivated in a brittle manner. But the corresponding apertures are small and estimated to be in the micrometer range. Mazurek (2001) concludes as well that the hydraulic character of the main fault is no different than that of the surrounding, undisturbed matrix of the shaly facies.

Strong fabric anisotropy, i.e. layering/bedding planes, is observed in the undisturbed matrix.

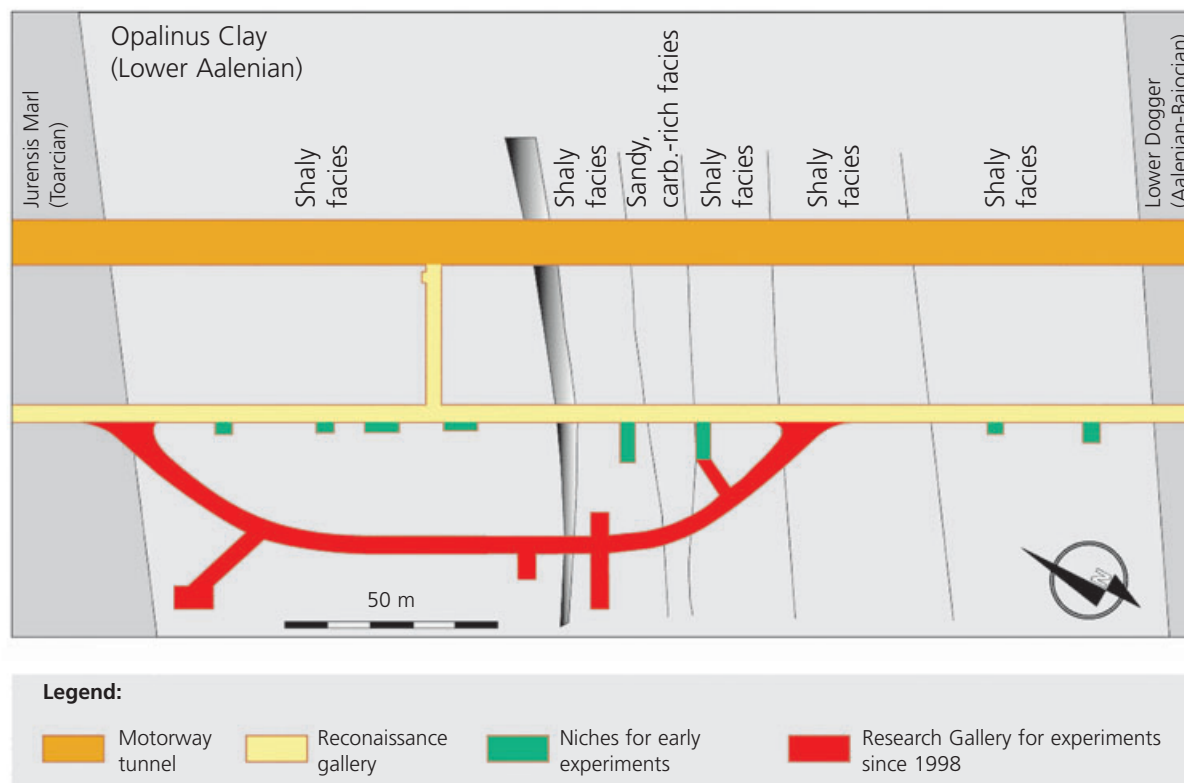


Figure 4.16: The scale of tunnel investigations (10^{-1} – 10^1 m).

Hydraulic relevance of facies and structural elements

Packer tests and permeameter tests were carried out in all facies (cf. Table 4.1 and Table 4.2). Hydraulic conductivities cover a range between 2×10^{-14} and 1×10^{-12} m/s. The K values do not indicate a significant correlation between hydraulic conductivity and the different facies. The measured variabilities in hydraulic conductivity are related to uncertainties in hydraulic testing and test analysis rather than in a systematic change of hydraulic conductivity with changing facies. Extensive hydraulic testing of the main fault was conducted (e.g. packer tests in BFM-C1 and BGP-4, cf. Table 4.1). Fracture frequency along the test intervals was up to 19 1/m. The reported K values are in the range $2 \times 10^{-13} - 5 \times 10^{-13}$ m/s. No significant differences in hydraulic conductivity were detected as compared with undisturbed matrix of the Opalinus Clay.

Lithological unit	Hydraulic conductivity K[m/s]	Specific storage S_s [1/m]
Carbonate-rich sandy facies	$4 \times 10^{-13} - 9 \times 10^{-13}$	$2 \times 10^{-7} - 6 \times 10^{-7}$
Sandy facies	$2 \times 10^{-14} - 2 \times 10^{-13}$	—
Shaly facies	$2 \times 10^{-14} - 2 \times 10^{-12}$	$3 \times 10^{-7} - 3 \times 10^{-5}$

Table 4.5: Ranges of hydraulic properties in the 3 facies of the Opalinus Clay (based on packer test results; cf. Table 4.1).

4.5.3 The scale of core mapping ($10^{-3} - 10^{-1}$ m)

Structural mapping was done concurrently with the lithological mapping for all recovered drillcores. A systematic mapping key was defined in TN 96-02 to classify the features, including bedding, fault planes, joints, veins and artificial discontinuities. The mapping key is essentially the same as used for tunnel mapping. Figure 4.18 shows photo documentation of drillcore mapping and lithological / structural classification schemes. Hydraulically the scale of drillcore mapping can be treated in the same way as the scale of tunnel mapping. Permeameter tests (Table 4.2) did not show significant variability in hydraulic properties on the scale of core mapping.

4.5.4 The sub-millimeter scale

Extensive investigations were carried out to describe mineralogy and microstructure of the Opalinus Clay (Nagra 2002). The investigation methods included:

- mineralogical analyses of drillcores
- various techniques of porosimetry
- various techniques for determination of specific surface (BET, EGME)
- scanning electron microscopy (SEM)
- adsorption / desorption methods

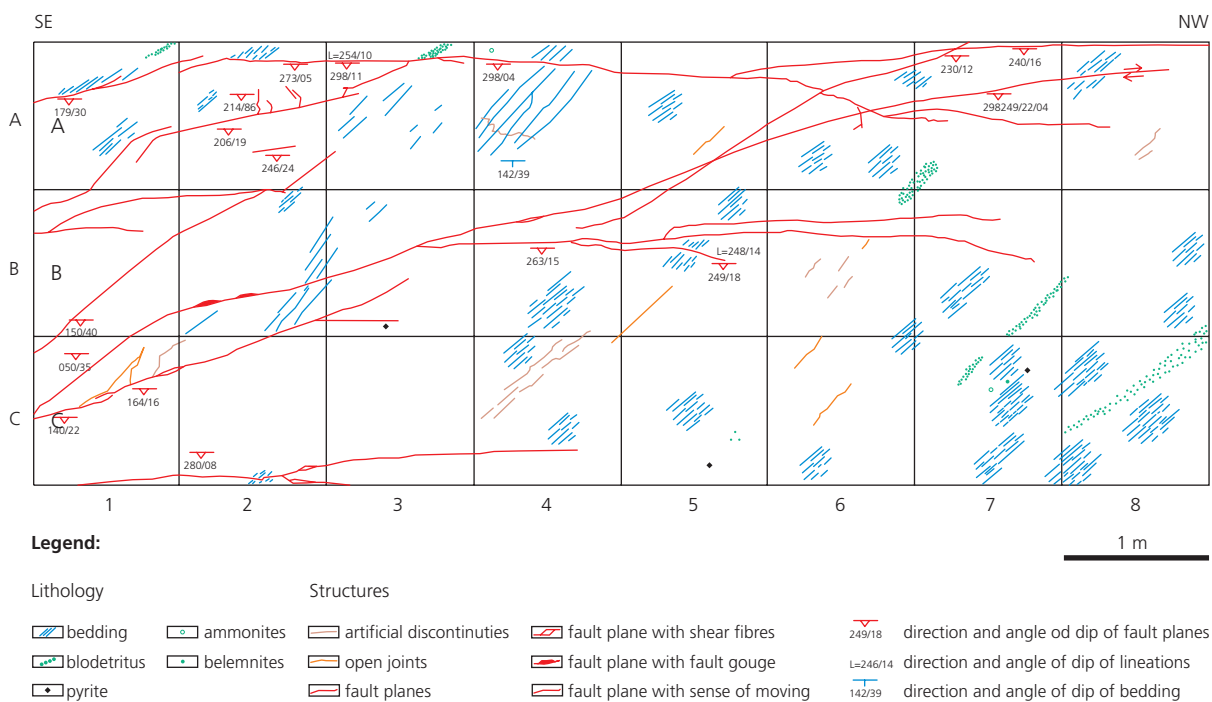


Figure 4.17: Small scale mapping of structural features in the BF niche of the reconnaissance gallery, i.e. in the shaly facies of the Opalinus Clay (Figure 4.13, TN 96-02).

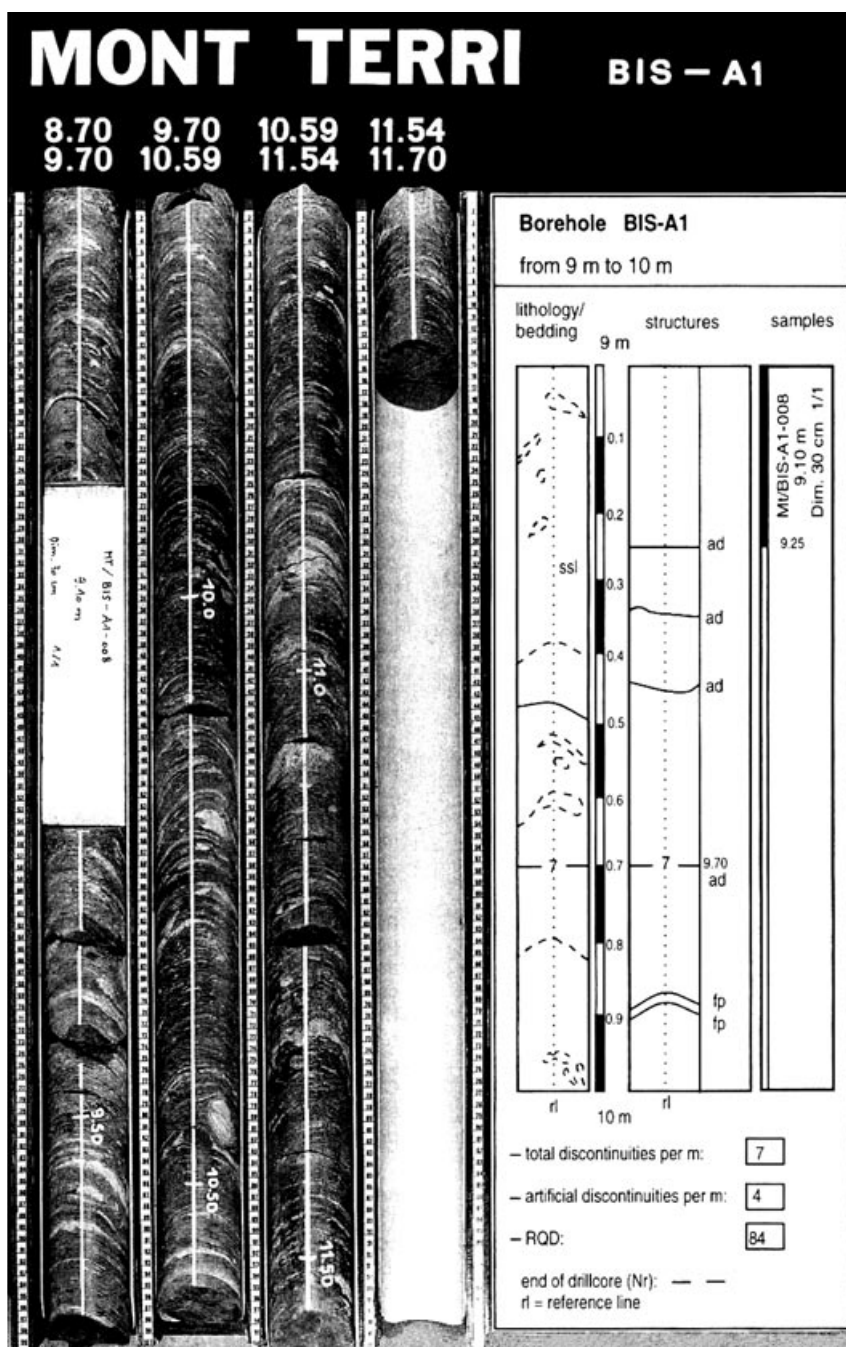


Figure 4.18: Photographic documentation of drillcores and classification of lithological/structural features.

	Calcite	Siderite	Quartz	K-Feldspar	Total layered silicates	Illite	Illite/smectite	Chlorite	Kaolinite
Mean value weight (%)	13	3	14	1	66	23	11	10	22
Standard deviation	±8	±1.8	±4	±1.6	±11	±2	±2	±2	±2
No. of 8 analyses		8	8	8	8	8	8	8	8

Table 4.6: Mineralogy of the clay-rich shaly facies of the Opalinus Clay at Mont Terri after Mazurek (2001). Data from the sandy facies are not included.

From the hydrogeological point of view, mineralogy of the Opalinus Clay is of relevance in the context of coupled hydro-chemical processes such as swelling or chemico-osmotic flow. Table 4.6 gives an overview of the main mineralogical components of the shaly facies at Mont Terri (Nagra 2002). It is evident, that the fraction of the main swelling clay mineral, illite-smectite mixed layers, is quite low.

Some hydrogeologic properties of the Opalinus Clay can be inferred indirectly from the analysis of its microstructure. Figure 4.19 visualises the microscopic arrangement of the clay aggregates using SEM techniques. Feldspar and quartz grains are wrapped in a complex structure. The magnification achieved by conventional SEM techniques is not sufficient to visualise the microscopic system of mesopores (1–30 nm), which represent the main features for fluid transport in the Opalinus Clay. Adsorption/desorption methods and Hg porosimetry are tools for the determination of equivalent pore radii of the microscopic clay structures. As shown in Figure 4.20 and in Table 4.7, equivalent pore radii are in the range of 1–50 nm (mean: 4–11 nm).

Mean equivalent pore radius [nm]	4 – 11
Porosity [-]	0.156
Rock density [g/cm ³]	2.32 – 2.42
Specific surface (BET N2) [m ² /g]	24 – 37
Specific surface (adsorption) [m ² /g]	112 – 147

Table 4.7: Microstructural properties of the Opalinus Clay at Mont Terri after Nagra 2002.

Hydraulic conductivity can be inferred using the Kozeny-Carman relationship (equation 4.9) when porosity and specific surface are known. Specific surface was determined by BET methods as 24–37 m²/g (outer surface) and by adsorption methods as 112–147 m²/g (total surface). The geometry factor C_s is taken to be 2.5 and the tortuosity τ is 1.41. Thus the Kozeny-Carman relationship leads to a range of K values in the order of $1 \times 10^{-13} - 1 \times 10^{-12}$ m/s, which is slightly higher than the permeameter measurements suggest.

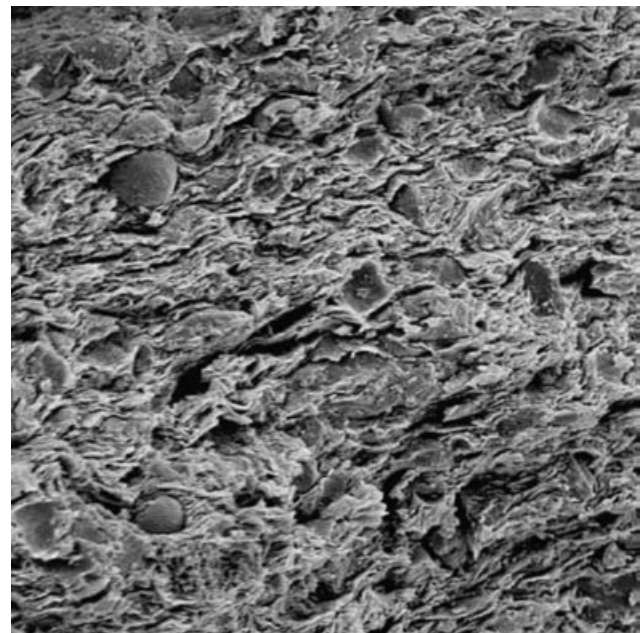


Figure 4.19: Visualisation of the microstructure of Opalinus Clay by SEM (Möri 2000, personal communication).

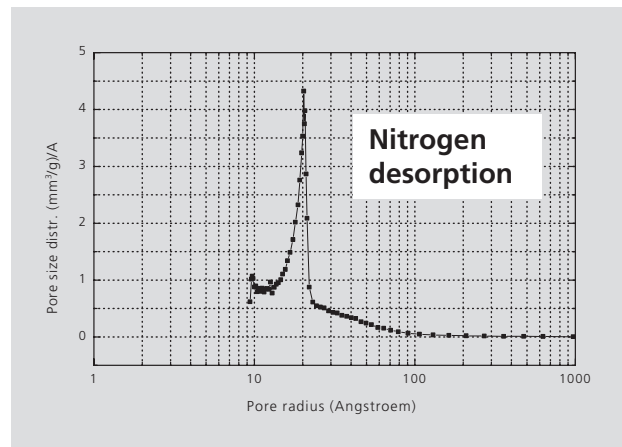
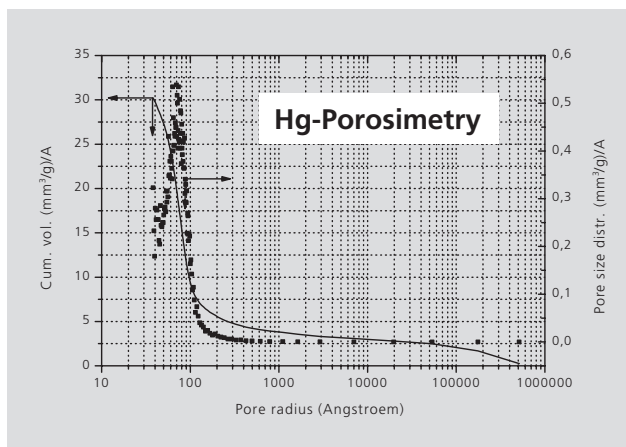


Figure 4.20: Determination of equivalent pore radii by Hg porosimetry and nitrogen desorption (from Bardot et al. 2001).

4.6 Pore pressure distribution at the Mont Terri site

4.6.1 Data base

With the exception of the Opalinus Clay formation, the pore pressures in the Mont Terri site are not very well known. Less than 10 piezometers were installed over the full length of the motorway tunnel previous to its construction in 1992 (i.e. after reconnaissance tunnel excavation in 1989; cf. TN 99-22). Even fewer

observations are available for the time since excavation. Figure 4.21 illustrates the approximate depth of the groundwater level, measured before and after construction in the rock formations adjacent to the Opalinus Clay. In the Triassic and Liassic formations to the Northwest of the Opalinus Clay, pore pressures of 2.0–2.3 MPa (reference level: altitude of the motor way) are reported. In the Lower Dogger aquifer to the Southeast, a pressure of about 0.8 MPa was measured in a borehole in lead of the tunnel excavation.

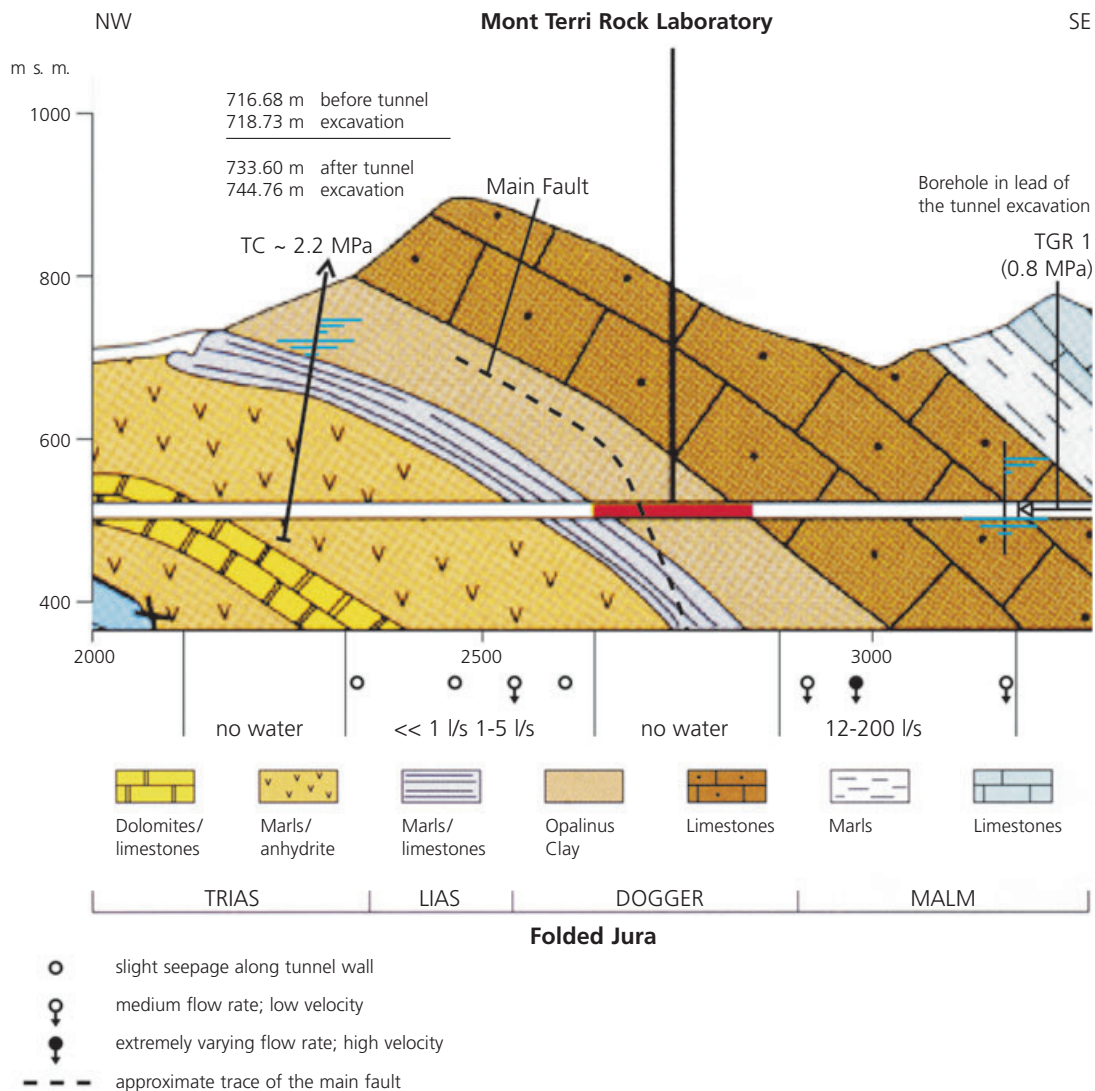


Figure 4.21: Cross-section through the Mont Terri site with piezometric levels (TN 99-22).

Bossart & Wermeille (TN 99-73, Section 1) reason that the drawdown in the vicinity of the Mont Terri rock laboratory due to the excavation of the motorway tunnel is about 30 m as indicated by the water level records. They state further that the expected ground-water level above the rock laboratory corresponds to about 740 m.a.s.l. (around 2.3 MPa) and is not in contradiction with pore pressures observed in the Opalinus Clay. Pore pressures below and above the Opalinus Clay are not known to date.

Since the beginning of the Mont Terri project in 1996, numerous boreholes have been drilled and equipped with long-term monitoring systems to determine pore pressure evolution in the Opalinus Clay formation. In particular, pressure was recorded continually since mid 1997 in the horizontal boreholes BPP-1, BED-B0, BED-B1, BED-B2, BED-B3 and BED-B4 (see Figure 2.2 for locations). Furthermore, the pressure in the vertical BDI borehole was also recorded. Figures 4.22a to e present the pressure records from mid 1997 to early 1999.

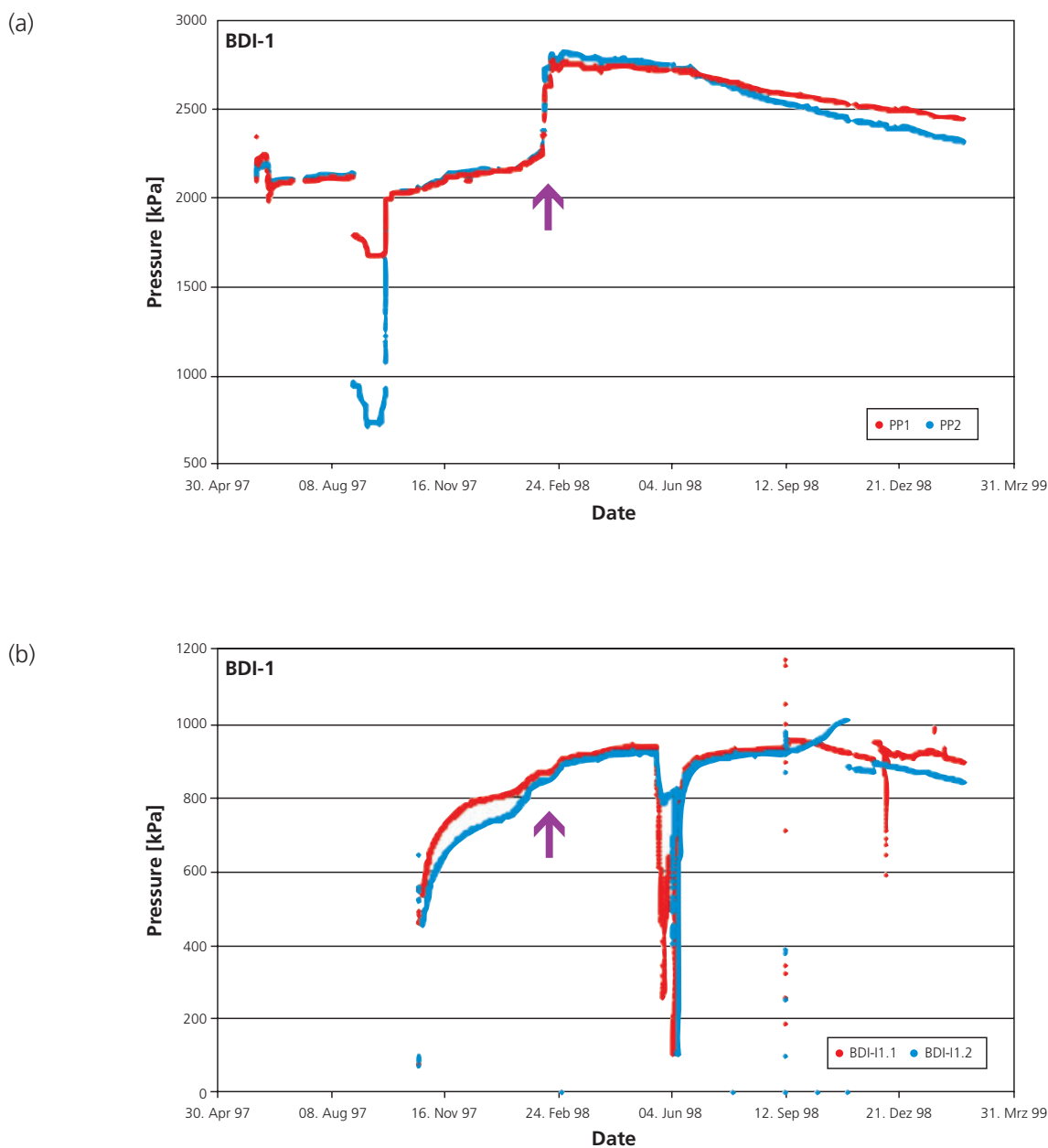
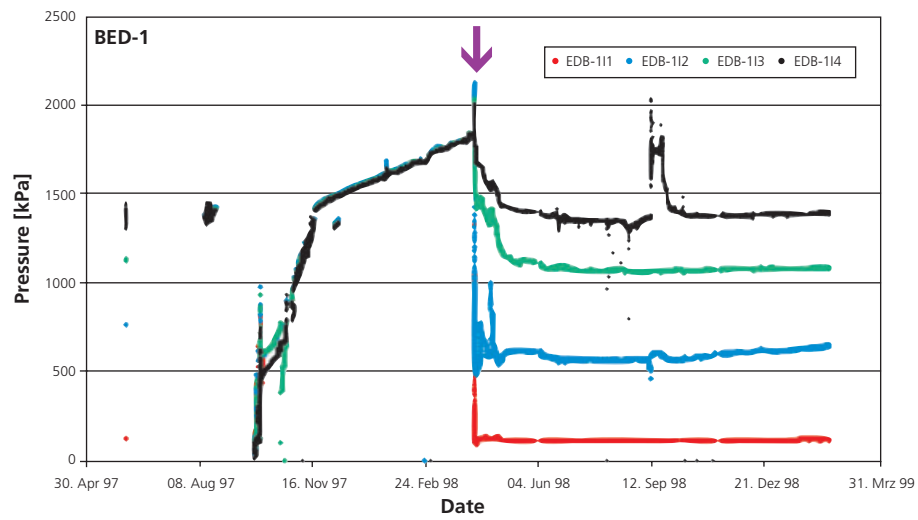
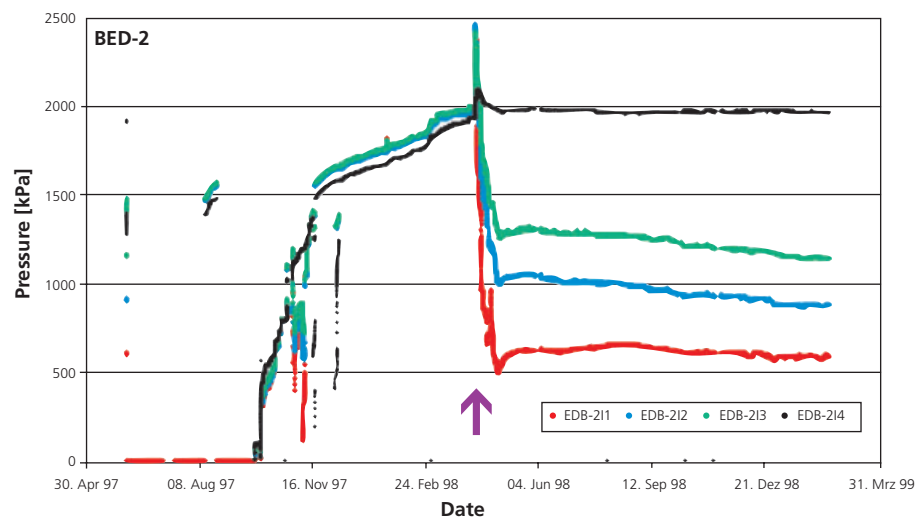


Figure 4.22: Pressure monitoring from mid 1997 to early 1999 in boreholes (a) BPP-1, (b) BED-B1, (c) BED-B2, (d) BED-B3, and (e) BDI-1. The purple arrows indicate the impact signatures caused by the excavation of the new gallery by blasting and a road header. (c), (d) and (e) on page 60.

(c)



(d)



(e)

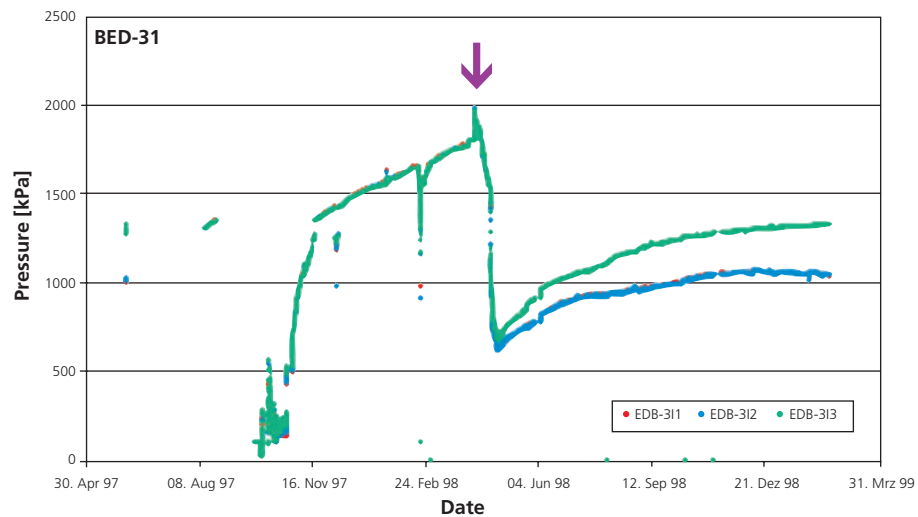


Figure 4.22 continued

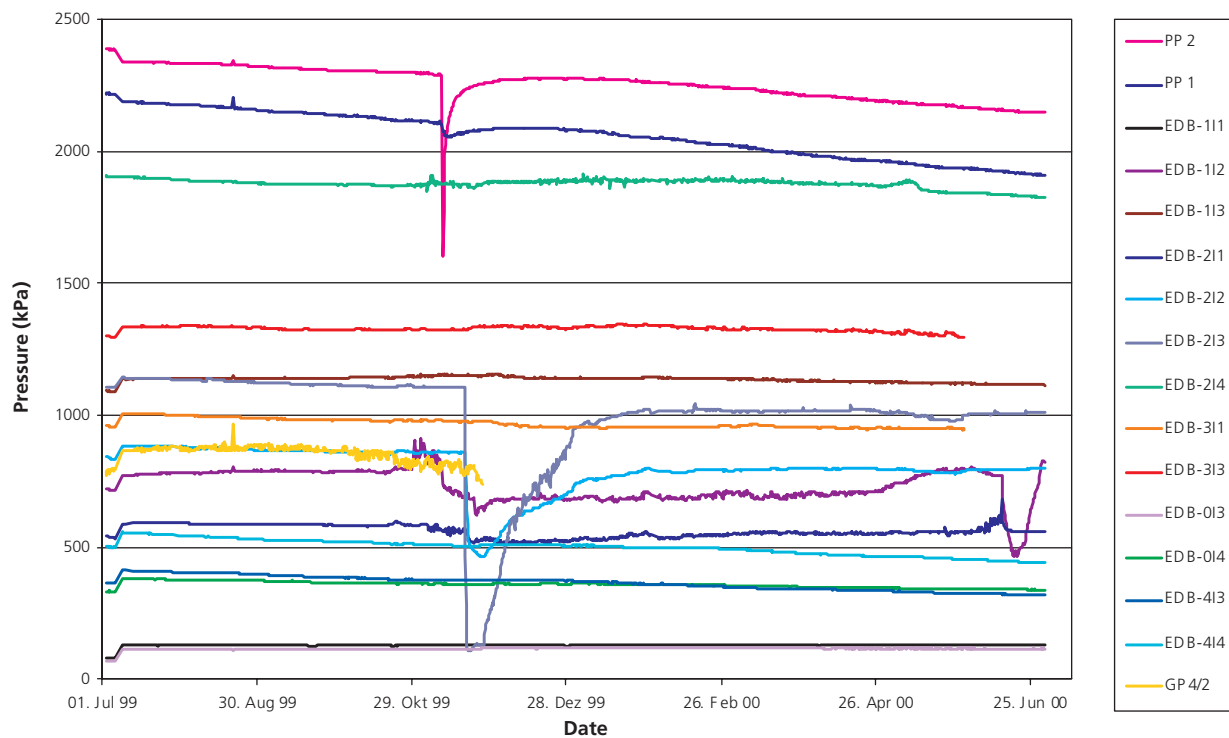


Figure 4.23: The pressure transients in the period from July 1999 to June 2000.

Whereas the changes in pressure prior to spring 1998 denote a gradual re-equilibration with the formation pressure, the sudden increase or decrease observed during spring 1998 is due to the excavation of the new gallery by blasting. Also in the test intervals of the boreholes located the farthest away from the new gallery (e.g. 10 m), the amplitude of the disturbance is quite large on the horizontal boreholes (sometimes larger than 0.5 MPa). In the vertical BDI-1 the impact of the blasting on the pressure is more limited (a few bar pressure increase).

Furthermore, the hydraulic influence of the new gallery is visible in several intervals either clearly situated within the EDZ or in the "hydraulic influence radius" of the new gallery (lower pressure as prior to the excavation).

After installation of the central data acquisition system in Phase 5, the pore pressures in many of the long-term monitoring systems were recorded continuously. Figure 2.2 gives an overview of locations and orientations of the long-term monitoring boreholes. The pressure transients in the time period between June 1999 and June 2000 are given in Figure 4.23. A general trend of decreasing pore pressures is observed in many of the observation intervals, indicating the impact of the tunnel drainage.

4.6.2 Interpretation of the pore pressure distribution in the Opalinus Clay formation

Data observations

From the hydraulic point of view, the pore pressure distribution in the Opalinus Clay might be controlled by any one or several of the following mechanisms:

- differences with respect to the piezometric heads of the adjacent hydrogeological units in the NW and SE directions: Triassic Marls with high freshwater heads corresponding to a pressure of 2.2 MPa at tunnel niveau, and the Dogger aquifer for which merely one measurement of very low value (0.8 MPa) at tunnel niveau is known,
- a hydraulic gradient between the reconnaissance gallery and new gallery causing (slow) drainage of the Opalinus Clay,
- the main fault acting as a "sealing fault" between the NW and SE parts of the Opalinus Clay, i.e. a hypothesis supported by very low permeability values attained in tests conducted in the main fault,
- it cannot be precluded, that geomechanical effects due to stress redistribution after the excavation of the galleries and also to changes within the borehole (e.g. partial collapse of borehole) might have

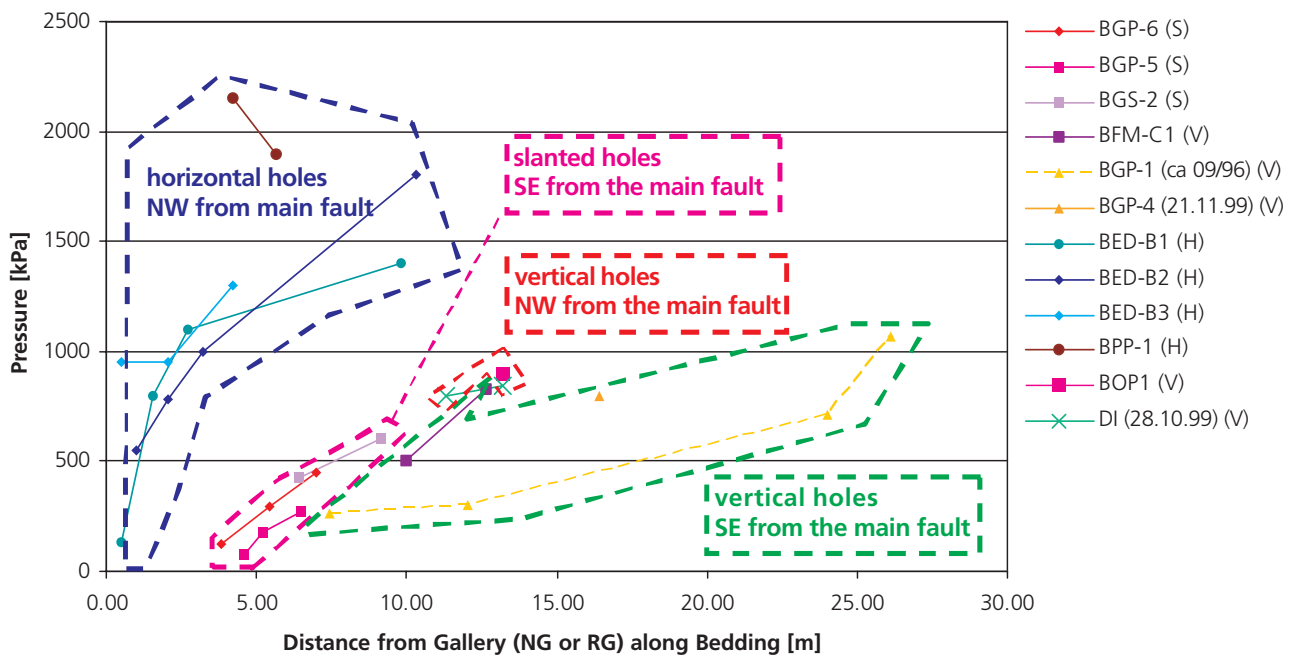


Figure 4.24: Compilation of pressure observations in boreholes of the Mont Terri rock laboratory on 30.06.2000 (unless indicated otherwise in the figure legend), illustrated with respect to the distance along bedding to the nearest gallery.

had an impact on the measured pressure (see Martin & Lanyon 2004),

- it cannot be precluded, that chemico-osmotic flow due to the concentration profile in the site (Figure 4.15) gives rise to an additional anomalous component of the measured pore pressure. The impact of osmotic pressures, however, is small due to the low osmotic efficiency of the rock formation.

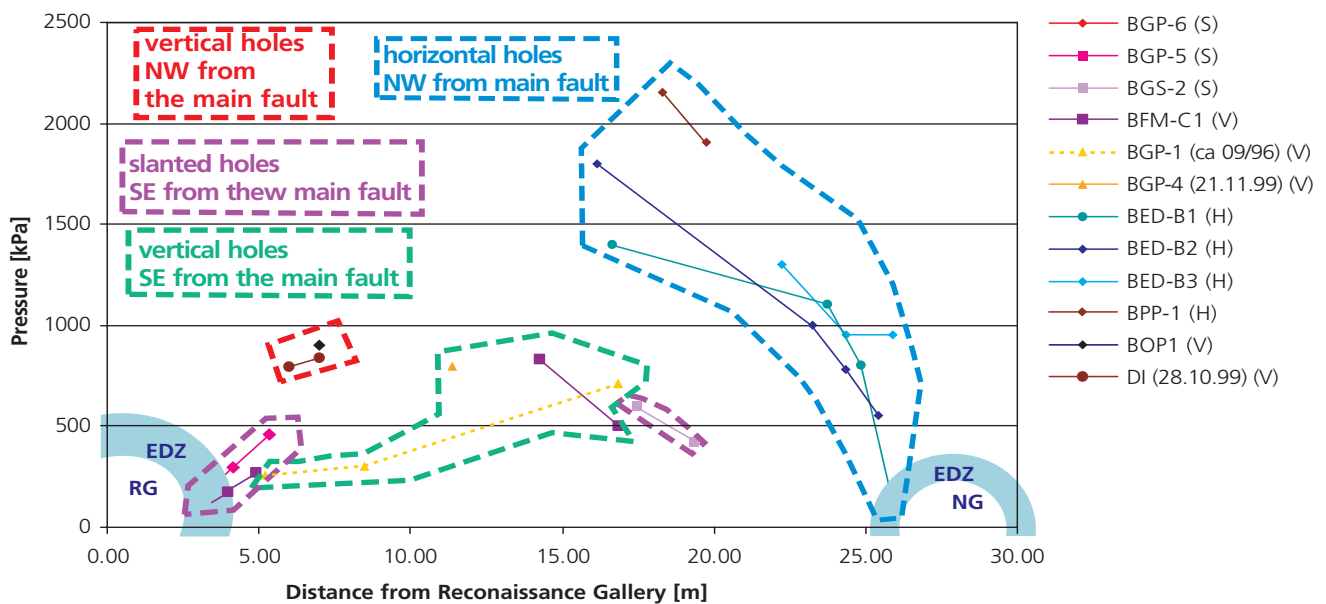
Most likely, it is a combination of these effects which is responsible for the pattern of pressure distribution observed in the Opalinus Clay at the Mont Terri site. The pore pressure measurements gathered by the end of June 2000 are presented in Figure 4.24 and Figure 4.25. Where no values were available by June 2000, younger measurements have been added in the diagrams instead and are indicated as such in the figure legends. The particular point in time was selected as the „longest“ re-equilibration time available. In Figure 4.24 all measurements are presented as distances along bedding either to the reconnaissance gallery or to the new gallery, whichever is closer to the observation interval. Indications of the borehole orientation are also provided in terms of vertical, slanted or horizontal. In Figure 4.25, all measurements are illustrated along an imaginary axis projected between the reconnaissance and the new gallery.

The following observations may be expressed:

- The gradients near the new gallery (boreholes BED: up to 20 m/m) are much higher than those near the reconnaissance gallery (1 m/m). This is consistent with the fact that the reconnaissance gallery was excavated 10 years prior (1989) to the new gallery (1998).
- In horizontal boreholes NW from the main fault and inside the shaly facies, the pressures away from both NG and RG are high up to 2.0 MPa.
- In vertical boreholes SE from the main fault (mainly in the sandy facies), the pressure located more than 7 m away from the RG or NG are low, between 0.3 and 0.8 MPa.
- All the vertical and slanted boreholes deliver pressure observations smaller in magnitude than the horizontal boreholes.

4.6.3 Simple assessment of the galleries' drainage effects with numerical simulations

A 2D transient groundwater flow simulation was performed with the Colenco Code MHYTIC in order to assess the potential drainage effects caused by the reconnaissance and new galleries. It simulated the period from the time of excavation of the reconnaissance gallery in 1989 to mid 2000.



Pressures in Formation adjacent to the Opalinus Clay:

Lias Gryphaea Limestones to the NNW: 2000–2300 kPa

Lower Dogger Blaukalke Limestones to the SSE: 800–1000 kPa (?)

Simulation parameters:

Hydraulic Conductivity $K = 1 \times 10^{-13}$ m/s Specific Storage $S_s = 1 \times 10^{-6}$ 1/m

Borehole orientation:

S: slanted V: vertical H: horizontal

Structural elements:

RG: reconnaissance gallery NG: new gallery EDZ: excavation disturbed zone

Figure 4.25: Compilation of pressure observations gathered in boreholes at the Mont Terri rock laboratory on 30.06.2000 (unless indicated otherwise in the figure legend), illustrated along an axis projected between the reconnaissance gallery and the new gallery.

The 2D finite element domain is presented in Figure 4.26 and is representative of a vertical slice situated in the area of the BED boreholes (see Figure 2.2). The initial pressure head is assumed to be constant and equivalent to 2.2 MPa at the gallery level. The boundary conditions are no flow along the sides and along the bottom, and a constant head of 2.2 MPa along the top boundary. The new gallery is assumed to have been excavated “instantaneously” in mid 1998. The resulting simulated head distributions just before the excavation of the new gallery and by July 2000 are shown in Figure 4.27a and b, respectively. Figure 4.28 presents the projection of the measured pressures and the numerically generated pressure curve on an axis joining the reconnaissance gallery and the new gallery. The following conclusions may be drawn:

- The simulated asymmetric pressure profile is consistent with field observations.
- The simulation matches to a certain extent the pressures observed in the horizontal boreholes and in the vertical boreholes in the first 7 m from the mid-point of the reconnaissance gallery.
- The measurement points assembled in a cloud not matched by the simulations were issued from the downwards vertical and slanted holes with distances to the galleries larger than about 7 m.

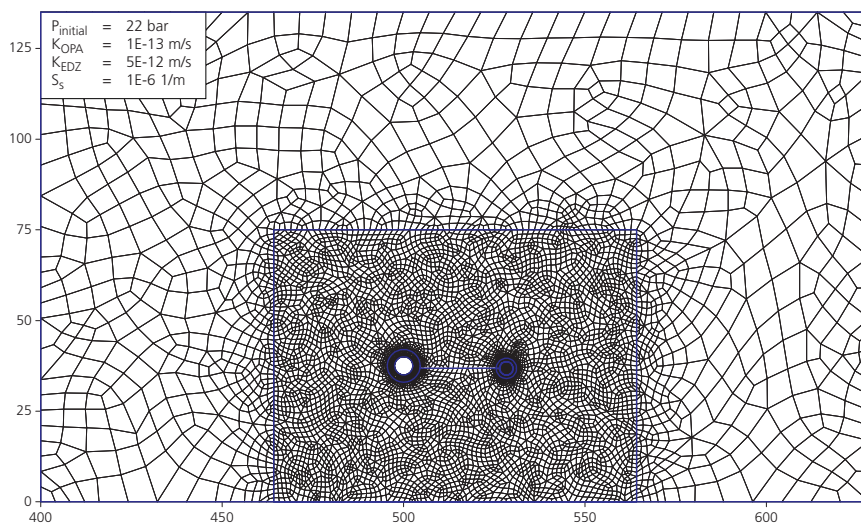


Figure 4.26: Vertical configuration and 2D finite element mesh used to simulate the pressure head on a plane projected perpendicularly through the reconnaissance gallery (left) and the new gallery (right) approximately at tunnel meter RG 970.

Head [m]

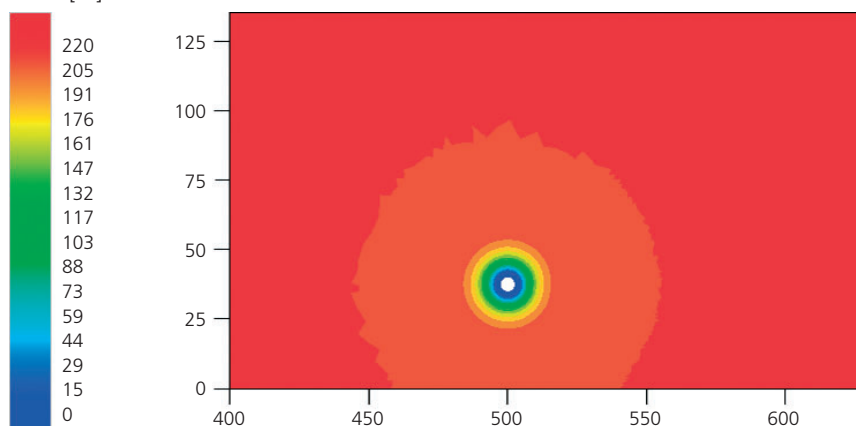
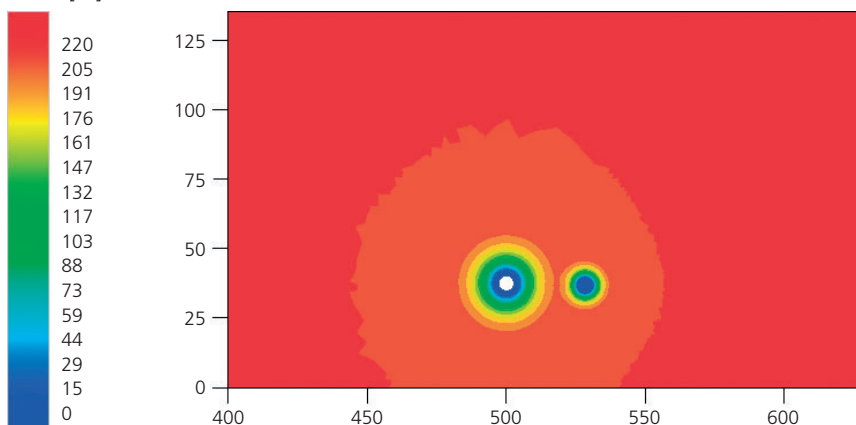
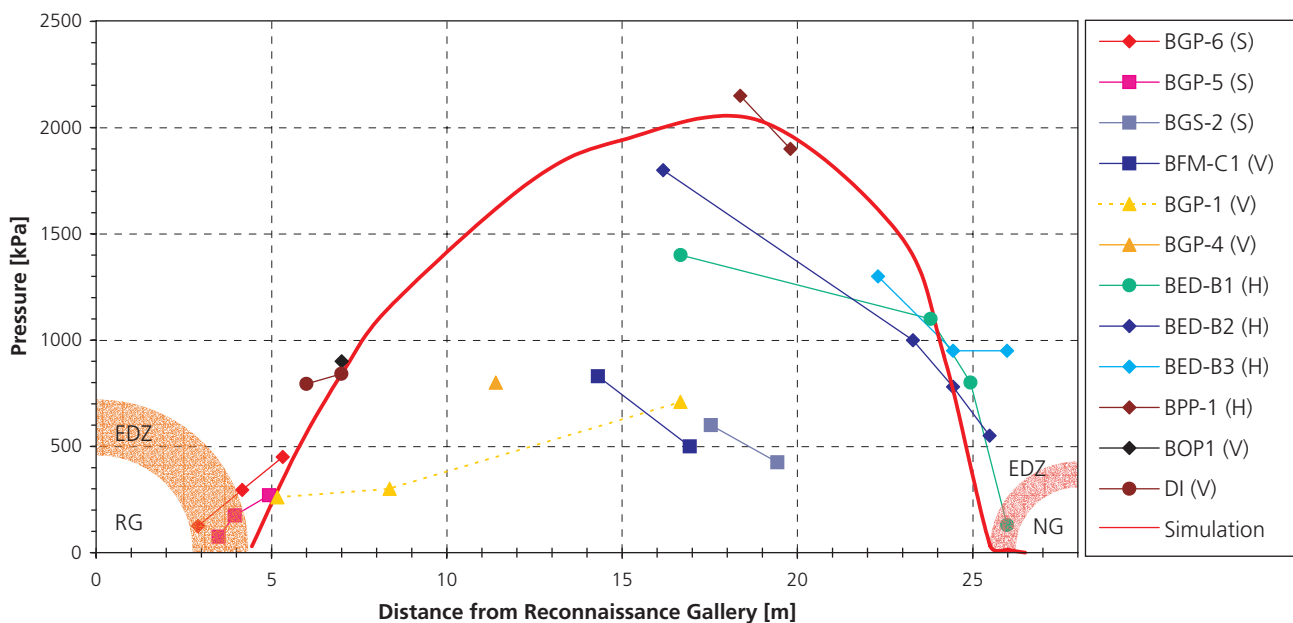


Figure 4.27: Simulation of the distribution of pressure head on a plane projected perpendicularly through the reconnaissance gallery and the new gallery at approximately tunnel meter RG 970. Hypothetical points in time: (a) end of April 1998, (b) end of July 2000.

Head [m]





Pressures in formations adjacent to the Opalinus Clay:

Lias Gryphaea Limestones to the NNW: 2000-2300 kPa

Lower Dogger Blaukalke Limestones to the SSE: 800-1000 kPa

Simulation parameters:

Hydraulic Conductivity $K = 1 \times 10^{-13}$ m/s

Specific Storage $S_s = 1 \times 10^{-6}$ 1/m

Borehole orientation:

S: slanted / V: vertical / H: horizontal

Structural elements:

RG: Reconnaissance Gallery

NG: New Gallery EDZ: Excavation Disturbed Zone

Figure 4.28: Comparison of pressure observations (mostly on 30.06.2000) and the results of the numerical simulation with $K = 1 \times 10^{-13}$ m/s and $S_s = 1 \times 10^{-6}$ 1/m, along an axis projected perpendicularly through the reconnaissance gallery and the new gallery at approximately tunnel meter RG 970.

The measurements located within a few meters of the EDZ of both galleries fit well with the simulation results. Simulations for the region to the NW of the main fault, inside the shaly facies, do fit the high pressures measured (larger than 1.4 MPa) reasonably well. A clear mismatch of the measurement is observed in the vertical boreholes SE of the main fault, mainly situated in the sandy facies.

As no difference in hydraulic conductivity was observed between shaly and sandy facies, two hypotheses can be drawn up with respect to the mismatch observed:

- Either: The part of the Opalinus Clay situated SE of the main fault is largely affected by the low hydraulic head in the adjacent formation of the Dogger limestones and a certain hydraulic separation is created by the main fault which would act as a sealing fault.
- Or: The horizontal borehole intervals are highly affected by the stress field (including borehole collapse) and the pressures measured result from coupling of hydraulic and geomechanic effects.

Effects of chemical osmosis on the pressure measurements do not appear likely because no “abnormal” pressure, i.e. larger than 2.2 MPa, were measured and the osmotic efficiency of the clay membrane is low. A more complex hydraulic model is needed to fully explain the observations. One of these models could be a model consisting of two domains, separated by the main fault as an impervious boundary. The hydraulic head would be 2.2 MPa, i.e. matching the Triassic Marls, to the NNW of the main fault, and 1.0 MPa to the SSE, i.e. conforming with the Lower Dogger. Such a model would be supported by the chloride measurements (c.f. Figure 4.15).

Additional work both in terms of field investigations (e.g., additional pressure observation boreholes at selected locations, for example within the sandy facies and the adjacent formations of the Lower Dogger and Lias aquifers) and in terms of numerical modelling (e.g., 3D hydrogeological modelling, NW/SE gradient) is required to better constrain the hydrogeological situation.

4.7 Evaluation of current hydrogeological site understanding

The geoscientific characterisation of the Opalinus Clay and the adjacent stratigraphic formations at the Mont Terri site was to demonstrate primarily the barrier function of the clay formation. This, in fact, requires an integrated assessment of the available hydrogeological site characterisation data and the cross-comparison with independent evidence to consolidate confidence in the overall performance of the clay formation as a flow barrier. The hydrogeological assessment consists of the following elements:

- identification of relevant hydrogeological features on the site scale
- description of relevant flow mechanisms
- determination of representative hydraulic properties on the site scale
- characterisation of in-situ pore pressure conditions

On the site scale, six *hydrogeological units* were defined (cf. Table 4.3). Focusing on the immediate vicinity of the rock laboratory, the “Lower Dogger” was identified as a local karstified aquifer which exfiltrates substantially into the tunnel systems. The significance of the Jurensis Marls to the North of the Opalinus Clay formation is less clearly defined. Water influx was observed from this formation during construction of the motorway tunnel, but appeared to have originated in localised water conducting features. The measured chloride profiles along the tunnel (cf. Figure 4.15) suggest no significant groundwater flow in this unit.

The Opalinus Clay is a pronounced aquitard. No groundwater influx into the galleries was detected. The chloride profile indicates that diffusion is the dominant transport process. Hydraulic packer testing and permeameter testing exhibit consistently low values of hydraulic conductivity. No significant variations of hydraulic conductivity are seen among the different *facies* of the Opalinus Clay. Even more so, no marked enhancement of hydraulic conductivity is apparent in the vicinity of *tectonic features*: extensive packer testing in the main fault did not reveal any correlation between hydraulic conductivity and fracture frequency along the boreholes.

At elevated hydraulic gradients *groundwater flow is governed by Darcy's law*. Linearity between hydraulic gradient and specific flow was demonstrated in the context of permeameter tests at hydraulic gradients > 1000 . No deviations from Darcy's law were seen in the course of single-hole packer testing at gradients around 50. Hydraulic interference tests, however,

exhibited anomalous crosshole responses, suggesting non-linear flow behavior at hydraulic gradients < 1 . Hence, an estimate for a hydraulic threshold gradient (if in fact existing) might be less than 1. The validity of Darcy's law is supported by the observed cone of pore-pressure decline towards the galleries, suggesting a gravitationally driven groundwater flow at typical hydraulic gradients between 1 and 10, clearly consistent with the hydraulic parameters.

Coupled hydro-chemical and hydro-mechanical processes may affect groundwater flow and transport processes in the Opalinus Clay. Due to its low membrane efficiency, which was determined experimentally (whenever subject to discussion), it is not likely that the pore pressure within the Opalinus Clay of Mont Terri is significantly affected by substantial osmotic flow processes. Hydro-mechanical coupled processes, however, may become relevant when the effective stress in the formation is lowered (e.g. hydraulic testing at elevated injection pressures). In the context of packer testing, evidence was seen for permeability enhancement at elevated injection pressures.

Hydraulic conductivity in the Opalinus Clay exhibits low spatial variability. Independent of the facies and of the degree of tectonic disturbance, K-values of the intact Opalinus Clay (without the EDZ) were measured in the range of $2 \times 10^{-14} - 2 \times 10^{-12}$ m/s (Table 4.5). *Storage coefficients* derived from packer testing were in the range $3 \times 10^{-7} - 3 \times 10^{-5}$ 1/m.

The *pore pressure distribution* at the Mont Terri site is being monitored continuously since Phase 3. Since that time, a continuous decrease of pore pressure has been observed in all observation intervals of the long-term monitoring system. Pore pressure monitoring indicates a clear cone of depression of hydraulic head towards the laboratory galleries. Beyond this, additional trends are observed: the subvertical boreholes generally exhibit lower pressures than the horizontal and the upwards directed boreholes. Also, pore pressure decreases towards the South. Although the spatial distribution of pore pressures at the Mont Terri site is not yet fully understood, it is believed that porewater flow in the Opalinus Clay is governed by the superposed effects of drainage towards the galleries and the pressure boundaries imposed by the adjacent rock formations. Stress redistribution effects due to the excavation of the tunnel might have an influence on the pore pressure currently monitored.

5 Gas Migration Mechanisms in the Opalinus Clay

5.1 Introduction

Radioactive wastes considered for disposal in repositories in deep, low permeability formations are expected to produce a significant amount of gas due to corrosion and microbial degradation processes. Gas generation may continue for long periods after repository closure. The accumulation of the gas may lead to unacceptable build-ups of the gas pressure in the disposal tunnels, if the gas cannot escape through the low permeability host rock.

The investigation of gas migration processes through argillaceous formations is, therefore, a key issue in the assessment of repository performance. The investigations on gas migration carried out at the Mont Terri rock laboratory during Phases 1 through 5 were aimed at collecting a comprehensive data base as a prerequisite for the development of enhanced process understanding. Although a full compatibility of the in-situ conditions at Mont Terri to the conditions at an actual repository site may not be achievable, the basic gas migration mechanisms are expected to be comparable. The Mont Terri site offers the opportunity to do both small scale experiments with drillcores in a laboratory and in-situ experiments in the underground facility.

This part of the hydrogeological synthesis is aimed at reviewing the achievements in the experimental work and in the interpretation of gas migration studies conducted in Phases 1 to 5 of the Mont Terri project. The outline of the chapter is as follows:

- Review of conceptual approaches for gas migration in clay-rich formations.
- Critical assessment of gas related experiments carried out in Phases 1 to 5 through quality assurance with respect to execution, analysis and documentation.

- Survey of the experimental data base for two-phase flow properties of the Opalinus Clay.
- Assessment of the modelling approaches applied in Phases 1 to 5 for the interpretation of gas related experiments.

5.2 Conceptual approaches of gas migration in clay formations

The gas migration in the Opalinus Clay is controlled not only by the hydro-mechanical properties of the rock mass but also by the gas pressure p_g at the generation locus and the hydro-mechanical state of the rock (i.e. saturation with water, porewater pressure, stress state). The in-situ stress of the rock mass is an essential parameter and is described by its three principal components σ_1 , σ_2 and σ_3 . Any gas release through the Opalinus Clay may be accommodated by the following mechanisms:

- advective-dispersive transport of gas dissolved in the porewater
- generalized Darcy flow, i.e. two-phase flow
- microscopic fracturing driven by the gas production rate, i.e. stationary processes
- macroscopic gas- and hydro-fracturing, i.e. instantaneous processes

Table 5.1 presents an overview of the migration mechanisms, pressure regimes and the efficiency of the different mechanisms in the Opalinus Clay. The remainder of this section is dedicated to a discussion of the individual migration mechanisms on a phenomenological base and, where appropriate, in terms of a conceptual modelling approach. Furthermore, the link between gas migration and the deformation of the Opalinus Clay is illustrated.

Gas migration mechanism	Gas pressure regime ¹	Remarks
Advective and dispersive transport of dissolved gas	For any gas pressure p_g	Gas transport by advection is not very efficient in the Opalinus Clay because of the low advective fluxes
Two-phase flow	$p_{ae} < p_g < \sigma_3$	Gas transport efficiency is limited by the high gas entry pressure of clay
Microscopic fracturing	$p_g \approx \sigma_3$	The microfracturing process is controlled by the gas production rate High gas transport capacity due to the pressure- dependent gas permeability
Macroscopic gas frac/ hydro frac	$p_g > \sigma_3 + \text{tensile strength}$	Creation and propagation of macroscopic fracs is initiated and controlled by gas pressure Extremely high transport capacity due to high frac transmissivity

¹ - the values represent rough estimates for the expected pressure ranges

Table 5.1: Overview of potential gas migration mechanisms. The transport capacity of the various mechanisms is influenced by the gas pressure p_g , the minimum main stress σ_3 and the various hydro-mechanical properties of the formation (p_{ae} – gas entry pressure, T_{opa} – tensile strength).

Transport of dissolved gas

Advective and dispersive transport of gas in porewater is a straightforward migration mechanism which is characterised by three fundamental laws: (i) the advective groundwater flow is governed by Darcy's law, (ii) Fick's law represents the diffusion of dissolved gas due to concentration gradients, and (iii) Henry's law describes the solubility of gas in porewater.

The transport of dissolved gas occurs even at low gas pressures; the pressure-dependent solubility of gas in porewater and the increased groundwater flux cause the specific flux of the dissolved gas to increase with an increase in the gas pressure. However, the low hydraulic conductivity of the Opalinus Clay significantly restricts the efficiency of this transport mechanism. The main parameters affecting the transport behavior of dissolved gas are the (gas) diffusion constant, the solubility coefficient, the flow porosity and the hydraulic conductivity.

Two-phase flow

In its conventional form two-phase flow is described as the process whereby the pore volume of a rock formation fills with gas by replacing porewater under the influence of visco-capillary forces (e.g. Baer 1972). This process causes the pore space to deform reversibly, i.e. elastically. Because the pore space of the Opalinus Clay at Mont Terri consists mostly of mesopores (equivalent pore radii: 2 – 50 nm), very high gas pressures are necessary to displace the porewater. The controlling factor for the two-phase flow characteristics of a porous medium is the gas entry pressure p_{ae} with a typical range for the Opalinus Clay of 1–10 MPa. Once the gas entry pressure has been exceeded, the gas mobility is controlled mostly by the intrinsic permeability k of the formation, the permeability-saturation relationship or relative permeability, and the relationship between the capillary pressure and the water saturation. The functional dependency between the pore-space saturation and the relative permeability or the capillary pressure are commonly described with parametric models (e.g. Brooks-Corey model, van Genuchten model, see also TN 98-25). One has to note, though, that only the free or mobile water may be displaced from the pore space whereby the residual water saturation in the Opalinus Clay tends to be at least 50%. The residual gas saturation in the Opalinus Clay, however, is negligible (very low gas content was measured in the Opalinus Clay).

Microfracturing

The tensile strength of the Opalinus Clay is relatively low. Therefore, it is most likely that the rock will not withstand long-term gas pressures with a level higher than the minimum principal stress σ_3 . Based on the expected micro-scale variability of the rock strength it even seems plausible that microfractures will form in the Opalinus Clay before the macroscopic tensile strength of the formation is exceeded. This microscopic fracturing causes an irreversible deformation of the pore space, i.e. dilation, and a detectable increase in intrinsic permeability. While the regime of the conventional two-phase flow sees the intrinsic permeability quasi independent of the absolute gas pressure, for microscopic fracturing the permeability is observed to increase with an increase in gas pressure. This phenomenon of microfracturing occurs when the gas pressure is allowed to grow slowly: the additional pore volume – which is the result of dilation – has to hold a steady balance with the volumetric gas production rate so that a quasi-stationary gas flow may evolve along the newly opened gas flow path.

Macroscopic fracturing

A macroscopic tensile fracture develops when the gas pressure is larger than the sum of the minimum principal stress σ_3 and the tensile strength T_{opa} of the Opalinus Clay, as determined in geomechanical short-term tests. This critical gas pressure is known as the frac-pressure. A macroscopic frac develops only when the gas pressure build-up is fast, i.e. when the formation of microscopic fractures (dilatancy) no longer counterbalances the gas production rate. The macroscopic frac is initiated quasi instantaneously and propagates at about the velocity of a shear wave. The propagation comes to a halt when the gas pressure in the macroscopic fracture becomes less than the value of the minimum principal stress (shut-in pressure). When the gas pressure is increased once more, the re-frac pressure is reached when the previously created fracture is re-opened. The value of the re-frac pressure is intermediate between shut-in pressure and frac pressure. The conceptual, theoretical and experimental framework for fracture propagation is well documented in standard hydrocarbon exploration literature (Valko & Economides 1997).

Propagation of gas induced fracture patterns

Independent of the fracture mechanism, fracture orientation and propagation are controlled primarily by the in-situ stress conditions and the geomechanical/

structural properties of the formation. The following factors of influence are particularly noteworthy:

- In an anisotropic stress field, fracture propagation occurs perpendicular to the direction of minimum principal stress or – in general terms – along the steepest stress gradient.
- Under anisotropic mechanical formation conditions, fracture propagation occurs perpendicular to the direction of minimum tensile strength. One may assume, therefore, that fractures develop preferentially along bedding.
- Geological deformation structures may have geometrical properties which potentially allow them to function as discontinuities. Gas induced fractures may form along these discontinuities. Likewise, the geological structures may be re-activated if their mechanical properties, e.g. tensile strength, cohesion, friction angle, are lowered with respect to the intact Opalinus Clay.

5.3 Quality assurance of gas related experiments

Similar to the suitability assessment of the hydraulic experiments (cf. chapter 3.2) a quality assurance procedure was applied on all gas related experiments that were carried out in Phases 1 to 5. The QA process for the gas related experiments, however, was different in some details because gas migration mechanisms in claystone are much less understood when compared with (single phase) hydrogeological processes. Therefore, the gas related experiments at Mont Terri were mainly aimed at process understanding rather than on the determination of material properties. These differences in emphasis gave reason for developing a slightly different QA approach (TN 00-58). The aspects that were addressed in the QA procedure were (i) field and laboratory methods, as well as (ii) data analysis. Similar to the suitability assessment in chapter 3.2 an attempt has been made to adopt a systematic approach to address the two key points given above for each of the experiments reviewed. Performing the review in a structured way is intended to allow a systematic inter-comparison of the experiments and analyses, thereby bringing out where comparisons can be drawn and ensuring that consistencies or inconsistencies are properly identified. The overall driver for the task was to identify the key gas migration mechanisms and to define the basic dataset for effective gas and two-phase flow parameters for relevant experiments performed as part of Phases 1 to 5 of the Mont Terri project.

Three groups of field experiments were included in the review; these took place in different areas of the Mont Terri rock laboratory. The first group of tests, performed as part of Phases 1 and 2 of the project, concentrated on hydraulic tests and gas threshold pressure tests in boreholes BGP-1, BGP-2, BGP-3 and BGP-4 in the SHGN niche (cf. Figure 2.2; TN 97-28, TN 98-24 and TN 98-25). The next group focused on gas threshold pressure tests and long-term gas injection tests in boreholes BGP5, BGP-6, BGP-8 and BGP-9 in the FM niche (TN 99-07, TN 99-08). The final group of experiments emphasised long-term experiments in boreholes BGS-1, BGS-2, BGS-3 and BGS-4. A series of hydraulic tests were performed in BGS-1 and BGS-2, followed by a long-term gas injection test in BGS-2 (TN 2000-07). Technical Note 2000-10 describes hydraulic fracturing in borehole BGS-2. In addition to the field experiments, permeameter experiments in the laboratory were carried out with core samples. The main objective of these tests was the determination of the hydraulic and gas related properties of the Opalinus Clay (TN 98-15, TN 99-58).

For the first aspect of the quality review, the *field and laboratory methods (FLM)*, a number of key issues were identified that would enable conclusions to be drawn from the work in a systematic manner:

FLM 1: Has standard equipment been used? Is the application of the equipment

- ✓ well within its limits of design?
- ✗ beyond its limits of design?
- ? at the limit of design for the range of parameters expected, or is this not really adequately known or properly understood?

FLM 2: Has a sound experimental methodology been used? This covers such issues as:

FLM 2.1: Has there been adequate time allowed for testing?

(✓ yes, ✗ no, ? not known)

FLM 2.2: Is the test free of issues concerning the stabilisation of pressure or the prehistory?

(✓ yes, ✗ no, ? not known)

FLM 2.3: Has the test been designed appropriately with respect to the general test objectives?

(✓ yes, ✗ no, ? not known)

FLM 3: Do the results look compatible or incompatible with what is expected from the action of various standard processes, as indicated by visual inspection of diagnostic plots? Are there obvious problems (and if so have these been properly identified) such as:

FLM 3.1: Equipment appeared to function satisfactorily?

- (✓ yes, ✗ no, ? not known)
- FLM 3.2: Evidence for coupled processes?
(✓ yes, ✗ no, ? not known)
- FLM 3.3: Wellbore storage has been quantified?
(✓ yes, ✗ no, ? not known)
- FLM 3.4: Is test free of domination by wellbore storage?
(✓ yes, ✗ no, ? not known)
- FLM 4: Is there evidence for adequate motivation for carrying out the experiment in the way it has been carried out?
- FLM 4.1: Were the specific objectives clear from the start?
(✓ yes, ✗ no, ? not known)
- FLM 4.2: Were the objectives achievable given the equipment?
(✓ yes, ✗ no, ? not known)
- FLM 4.3: Were the objectives achieved?
(✓ yes, ✗ no, ? not known)
- FLM 5: Has the methodology tested appropriate flow and gas transport pathways? For each of the experiments:
- FLM 5.1: Has an appropriate conceptual model (or range of conceptual models) been developed for the test?
(✓ yes, ✗ no, ? not known)
- FLM 5.2: Has the 'support scale' of the experiment been identified, i.e. the scale on which the hydrogeological, gas parameters vary?
(✓ yes, ✗ no, ? not known)

For each of the issues FLM 1 to FLM 5, a suite of detailed assessment criteria were defined. In the context of field testing, for example, some of the important FLM 1 assessment criteria were: (i) design of downhole equipment (length of packer seals, guard packers, control of packer pressures, minimisation of

system compressibility, minimisation of test interval volume, independent flow and pressure lines to the test interval) and (ii) design of surface equipment (flow control system, pressure monitoring and data acquisition system). A detailed description of the assessment criteria is given in TN 99-58.

The conclusions from the standard questions given above are recorded in Table 5.2. The checkbox approach to providing an overall review of the complete suite of field experiments necessarily provides only a simplified commentary on the experiments, with an element of subjectivity in the analyses. Further comments to each of the experiments are given in TN 99-58.

The *data analysis (DA) review* was conducted in a way similar to the approach for the review of the *field and laboratory methods*. The intention was to flush out various issues:

- DA 1: How was the analysis performed?
- DA 2: Was there adequate logic behind using one analysis tool rather than another and was this an issue?
(✓ yes, ✗ no, ? not known)
- DA 3: Were appropriate conclusions drawn? For example, were stronger conclusions drawn than were supported by the non-unique nature of the analysis?
(✓ yes, ✗ no, ? not known)
- DA 4: Has the scale of the experiment been determined, as for example embodied in the simplifying assumptions made in the conceptual model used to interpret the experiment, i.e. is this on a sub-cm, sub-m or more generally on what support scale (or radius of interest)?
(✓ yes, ✗ no, ? not known)

Note that reference here is to the scale over

Filed and Laboratory Methods hydro and gas testing	FLM1	FLM2.1	FLM2.2	FLM2.3	FLM3.1	FLM3.2	FLM3.3	FLM3.4	FLM4.1	FLM4.2	FLM4.3	FLM5.1	FLM5.2
BGP-4 Gas	✓	?	?	✓	✓	?	✓	-	✓	✓	✗	✓	✗
BGP-6 Gas (TN99-07)	✓	✓	✓	✓	✓	✓	✓	✓	✓	✓	✓	?	✓
BGS-2 Gas (TN00-07)	✓	✓	✓	✓	?	?	✓	✓	✓	✓	✓	?	?
GP core test (TN98-15)	✓	✗	✓	✓	✗	✓	?	?	?	?	?	✓	✓

Table 5.2: Summary of the quality review of the field and laboratory methods. The symbol ✓ indicates an affirmative or clear response to the question. The symbol ✗ indicates a negative response to the question or incorrect conclusion drawn. The symbol ? indicates an inconclusive or not known response to the posed question.

Data analysis	DA 1	DA 2	DA 3	DA 4	DA 5	DA 6.1	DA 6.2	DA 6.3	DA 6.4	DA 6.5	DA 7
BGP-4 Gas (TN98-25)	IT2, T2	✓	?	?	✓	✓	✓	✓	✓	?	✓
BGS-6 Gas (TN99-07)	SLA, SSA	?	✓	?	✗	✗	✓	✓	✓	?	✓
BSG2 Gas (TN00-07)	I2	?	?	?	✓	✗	✓	✓	?	?	✓

Table 5.3: Summary of the quality review of the data analysis of gas tests performed in Phases 1 to 5. Methods of analysis: TOUGH2 (T2), ITOUGH2 (IT2), INTERPRET2 (I2), Sabet and Horne (SLA), Sabet (SSA), sensitivity analysis (+S). Symbol legend: ✓ yes, ✗ no, ? not known.

which the hydrogeological model assumed has been demonstrated. A scale over which some experimental response has been seen in observation boreholes may well have been identified.

DA 5: Is the conceptual model sufficient to explain the results?

(✓ yes, ✗ no, ? not known)

DA 6: Was adequate attention given to:

DA 6.1: sensitivity of the results to data fit?

(✓ yes, ✗ no, ? not known)

DA 6.2: apparent inconsistencies?

(✓ yes, ✗ no, ? not known)

DA 6.3: consistencies in argument, i.e. have some of the conclusions been supplemented by other information?

(✓ yes, ✗ no, ? not known)

DA 6.4: problems with the test?

(✓ yes, ✗ no, ? not known)

DA 6.5: possibilities of different flow/gas pathways?

(✓ yes, ✗ no, ? not known)

DA 7: Are there any issues to be considered about the quality assurance of the wide range of models referenced (e.g. in TN 98-25)?

(✓ yes, ✗ no, ? not known)

The results of this analysis are given in Table 5.3. As with the analysis shown in Table 5.2, the overview provided in this table is necessarily simplified; further explanation is provided in TN 99-58.

5.4 Experimental data base

Gas related laboratory and field tests have been conducted in the framework of experiments GP, GP-A and GS. Those documents issued by the middle of Phase 5 were included in the quality assurance process described in chapter 5.3. Since that time, two additional documents discussing experimental studies have

been released: (i) a report on the second laboratory experiment with a core sample (TN 99-58) and (ii) a summary report of all field activities in the GP-A/GS experiment (Enachescu et al. 2002). In the next sections, results of the gas related experimental investigations in Phases 1 to 5 will be summarised according to the following outline:

- Gas permeability tests on core samples,
- Gas threshold pressure tests in boreholes,
- Long-term gas-injection tests in boreholes,
- Hydrofracturing and gas fracturing experiments in boreholes.

5.4.1 Gas permeability tests on core samples

Gas permeability tests were conducted as part of the GP experiment (TN 98-15, TN 99-58). The experiments were aimed at

- The evaluation of enhanced gas permeability at high injection pressures, and
- The self-healing capacity of the Opalinus Clay after a gas breakthrough.

A total of four core samples were tested. Their sample ID's are BED-B3 06, BFP-16, BED-C5/7 and BWS-E4 06. The samples were taken from the sandy and shaly facies. The tests were designed to match the expected in-situ stress conditions. The confining pressure was 6 MPa and the downstream porewater pressure was 2 MPa. One core sample each was subjected to flow parallel and perpendicular to bedding. The flow direction for the other two samples was oblique to bedding. It was also ascertained that the core samples were saturated completely before the water/gas injection phase was started. Each test started with a hydrotest phase to determine the intrinsic permeability. Subsequently the gas injection phase was initiated as a constant rate resp. constant head event. Figure 5.1

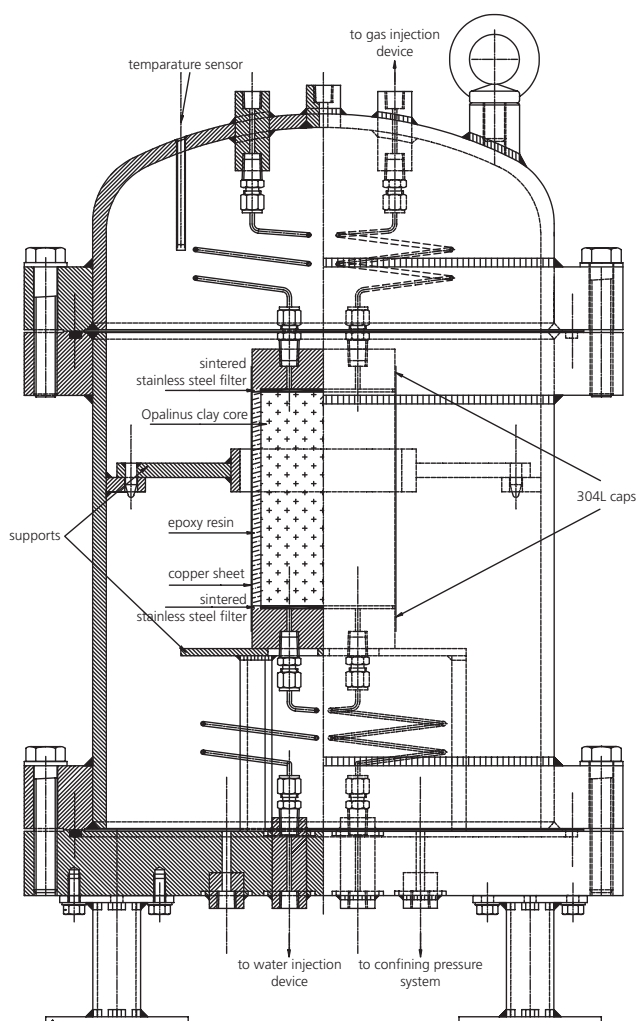


Figure 5.1: Schematic view of SCK-CEN's isostatic cell and sample assembly for the Opalinus Clay samples as part of the GP experiment (after TN 99-58).

shows a schematical sketch of the isostatic cells used for hydraulic testing and gas testing of core samples. The tests were carried out at SCK-CEN's Laboratory. The gas injection periods ranged from 3 to 8 months. The intrinsic permeabilities were consistently in the range of $1 \times 10^{-20} - 2 \times 10^{-20} \text{ m}^2$, with the exception of sample BED-B3 06. This specimen was damaged during the sample preparation process and exhibited a visible fracture in flow direction. The recorded gas entry pressures are all $\leq 0.5 \text{ MPa}$ (cf. Table 4.4). The gas saturation of the core samples after the gas injection phase was generally low (typically below 10%; in case of sample BED-B3 06 the upper limit of gas saturation was determined to be < 0.22).

The disturbed sample BED-B3 06 was tested hydraulically again after the gas injection phase to investigate for potential changes in the hydraulic conductivity. This indicates that the presence of the former gas pathway, represented by the initial planar fracture, did not give rise to an enhanced permeability. Several hypotheses could explain this observation: a self-healing of the sample took place, the lower permeability is due to the de-saturation of the clay, or gas microbubbles might block a portion of the connected porosity. None of these hypotheses can be excluded with the given level of experimental evidence.

Another before-and-after measurement set of hydraulic conductivity was conducted with sample BWS-E4 06. Within the uncertainty limits of the measuring technique, the hydraulic test after gas injection exhibits the same conductivity as the one done before gas testing ($2.1 \times 10^{-20} \text{ m}^2$).

Gas testing of sample BED-C5/7 lasted approximately 6 month. A clear gas breakthrough was achieved. After termination of the gas injection test the sample was dismantled. Visual inspection of the core indicated a sharp separation front between a lighter (unsaturated) and a darker (saturated) zone located at about 4.5 cm from the gas injection side (Figure 5.2). Subsequently, the core was cut into slices and the water

Core sample	Injection period [d]	Direction of flow relative to bedding	Intrinsic permeability ¹⁾ k [m ²]	Gas entry pressure p _{ae} [MPa]
BED-B3 06 2)	60	0°	2.0×10^{-18}	<0.03
BFP 16	110	50°	1.5×10^{-20}	0.5
BWS-E4 06	180	90°	2.0×10^{-20}	0.2
BED-C5/7	174	35°	2.0×10^{-20}	0.2

¹⁾ Intrinsic permeability k (m²) as derived from hydraulic conductivity K (m/s): $k = 1 \text{E-7} \cdot K$

²⁾ Core sample is not representative of undisturbed Opalinus Clay (visible fracture in flow direction)

Table 5.4: Two-phase flow parameters as derived from laboratory experiments on core samples of the Opalinus Clay from the Mont Terri rock laboratory. The intrinsic permeability was derived from hydraulic permeameter tests.

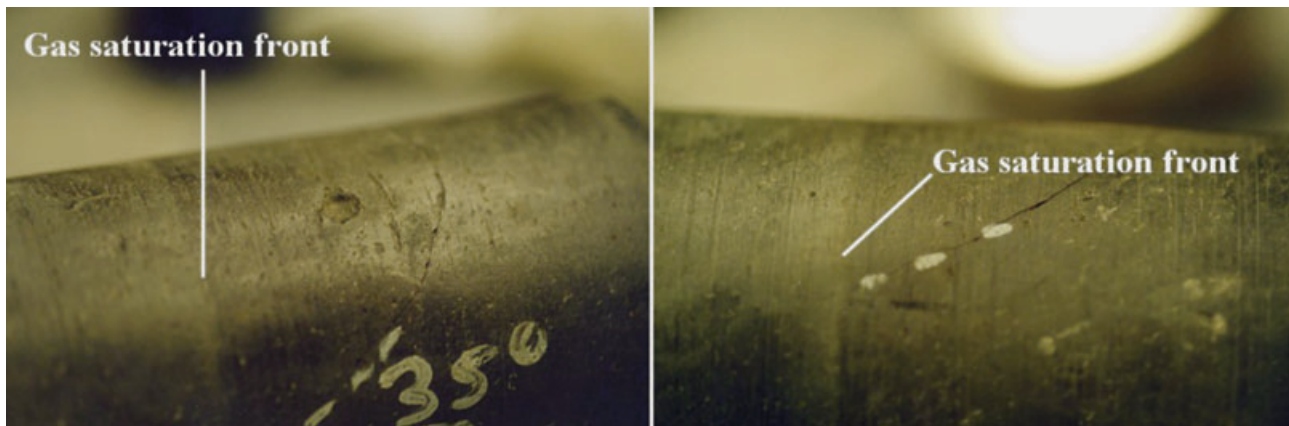


Figure 5.2: Photographs of the BED-C5/7 sample taken right after the gas injection test (after gas breakthrough) and showing a sharp gas saturation front (after TN 99-58).

content of each piece was determined. The water saturation of the different slices varied between 92.8 and 99.8%. This observation is interpreted as follows:

- During the early stages of the gas injection sequence, the gas phase propagates along the system of macropores until it breaks through at the downstream end of the sample. The gas migration mechanism is either water displacement or microscopic pathway dilation. The total volume of gas stored in the sample is negligible.
- A delayed migration into the pore spaces with smaller pore radii starts in the late time stages of the experiment. This delayed migration is extremely slow, nevertheless exhibits an important feature: an increasing amount of gas is stored in the rock sample.

5.4.2 Gas threshold pressure tests

Two gas threshold pressure tests were conducted in boreholes BGP-4 and BGP-6. The purpose of these tests was:

- To determine the gas entry pressure of the Opalinus Clay.
- To provide a data base for a more sophisticated analysis of gas migration in the framework of two-phase modelling and hydro-mechanical modelling (cf. chapter 5.5).

The length of the test interval was 1 m and 4.5 m for boreholes BGP-6 and BGP-4, respectively. The testing sequence consisted in both cases of a hydraulic test, fluid exchange (i.e. replacement of fluid in test interval with gas) and gas injection with a constant flow rate (i.e. “constant rate test”). In BGP-4 the gas injection phase was followed by a long-term pressure recovery

phase. In BGP-6 the constant rate event was turned into a long-term constant pressure event before and then ended with a long recovery period. The determination of the gas entry pressures was done diagnostically (Senger et al. 2002) from the analysis of the gas injection phase (particularly of the deviation from the linear pressure increase during the gas injection phase) and of the recovery phase (Horner plot). In addition, the test in BGP-4 was analysed through numerical modelling (TN 98-25). The specifics are summarised in Table 5.5.

The gas injection test in borehole BGP-4 with its test interval length of 4.5 m was carried out in the “main fault” (cf. Figure 5.3) using a rather high gas injection rate of 0.04 l/min (STP). During the pressure recovery a maximum specific gas flux into the rock of $4 \times 10^{-7} \text{ m}^3/\text{m}^2/\text{min}$ (STP) was determined. Diagnostic analysis of the gas injection phase suggests an air entry pressure of about 0.4 MPa. The Horner plot leads to an estimate for the upper limit of about 1.2 MPa. Finally, inverse modelling of the entire test phase was carried out using the multi-phase flow simulator ITOUGH2 (cf. chapter 5.5): the recommended air entry pressure was in the range 0.4 to 0.8 MPa.

The test in borehole BGP-6 with an interval length of 1 m was conducted in the sandy facies. The gas injection rate was lower than in BGP-4 by the factor of 40. During the constant pressure gas injection event subsequent to the injection phase (cf. chapter 5.4.3), a specific gas flux of into the rock of $1 \times 10^{-5} \text{ m}^3/\text{m}^2/\text{min}$ (STP). A gas entry pressure of 1 MPa was determined from log-log diagnostic analysis of the gas injection phase. It is rather apparent that the attained gas entry pressures are comparable despite the significant differences in the injection rates and the durations of the two tests.

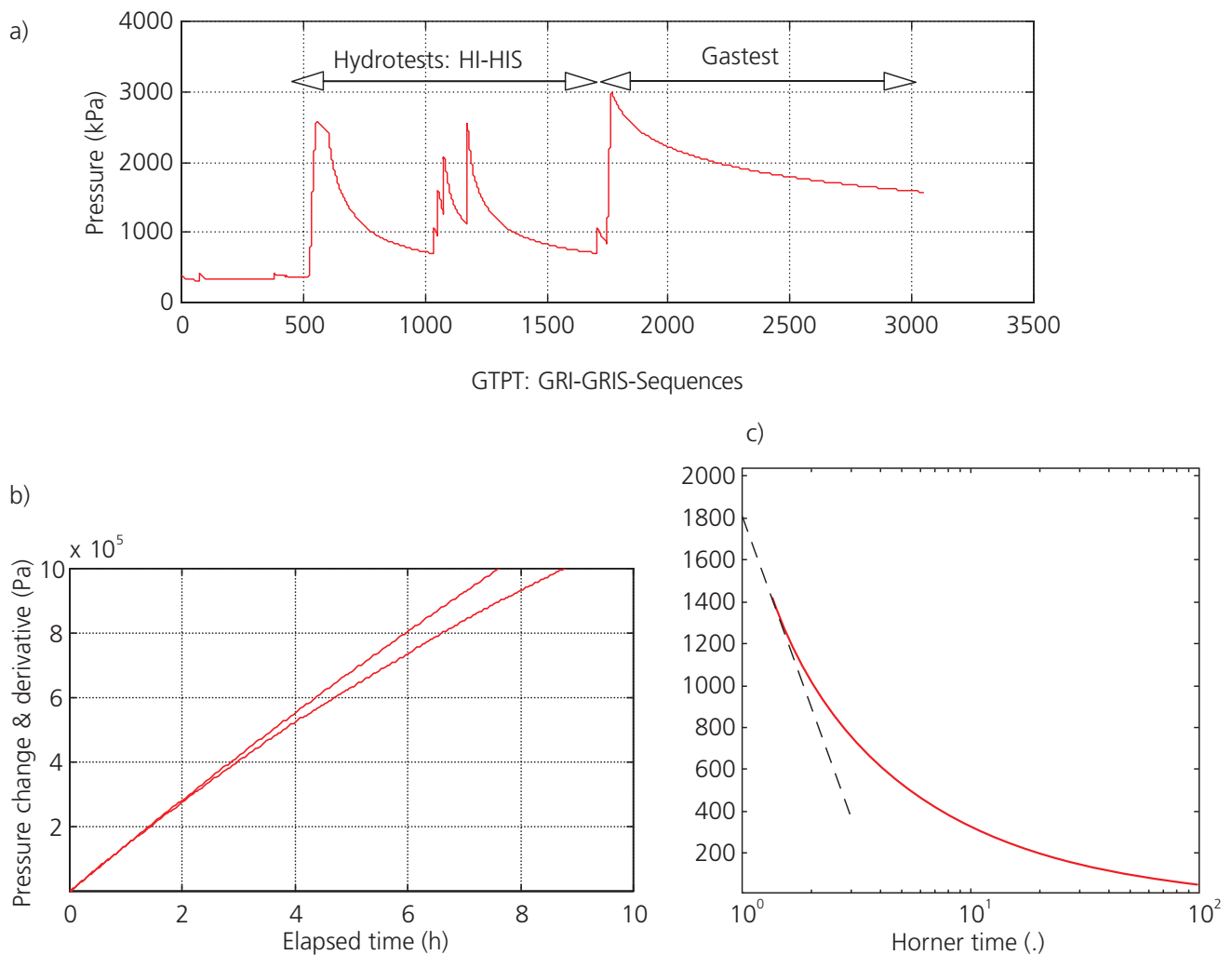


Figure 5.3: Diagnostic analysis of gas threshold pressure test in interval I4.2 of borehole BGP-4: (a) linear plot of the entire test sequence; (b) Cartesian plot of the gas injection phase (deviation from the linear pressure increase during the gas injection phase); (c) Horner plot of the recovery phase (after TN 98-25).

Borehole	Period [h]	Injection rate [l/min STP]	Specific gas flux [$\text{m}^3/\text{m}^2/\text{min STP}$]	Intrinsic permeability [m^2]	Gas entry pressure p_{ae} [MPa]
BGP-4	18	0.04	4×10^{-7} ¹⁾	$2\text{E-}20 - 6\text{E-}20$	0.4–0.8
BGP-6	150	0.001	1×10^{-6} ²⁾	$1.5\text{E-}20$ (hydro)	~ 1.0

¹⁾ Gas flow rate per surface of the test interval during the recovery phase

²⁾ Gas flow rate per surface area during the subsequent constant head gas injection phase

Table 5.5: Two-phase flow parameters as derived from gas threshold pressure tests at the Mont Terri rock laboratory.

The gas entry pressure are surprisingly low, as for pore diameters of 1–50 nm, the Young-Laplace equation would lead to much higher values (factor 10 or more). It seems therefore, that enough macropores (>30 nm)

are available inside the Opalinus Clay, which allow for a lesser capillary resistance to flow. The presence of microcracks around the borehole would also explain those low air entry pressures.

5.4.3 Long-term gas injection tests

Two long-term gas injection tests were conducted as part of the GP and the GP-A experiments in the FM niche and at the GS location, respectively. The experimental design was similar: the injection boreholes were equipped with multi-packer systems while the observation boreholes at a distance of decimeters to a meter were equipped either as piezometers for long-term observations or with multiple extensometers for observations of the axial deformation. The aim of these experiments was two-fold:

- To provide a data base for two-phase modelling of gas migration in the Opalinus Clay (cf. chapter 5.5).

- To provide a data base for modelling hydro-mechanical processes (cf. chapter 5.5).

The gas test of the GP experiment lasted for 24 days (TN 99-08). For a constant pressure of 2.1 MPa, the constant flow rate obtained under stationary conditions was about 0.14 mlN/min. The observations in the other boreholes indicated significant mechanical deformation with up to about 30 $\mu\text{m}/\text{m}$. After completion of the gas injection phase, a hydraulic test was performed in order to assess potential changes in the hydraulic conductivity as a result of gas injection. Within the bounds of measurement precision, the hydraulic conductivities derived before and after gas injection were identical with about $1 \times 10^{-13} \text{ m/s}$.

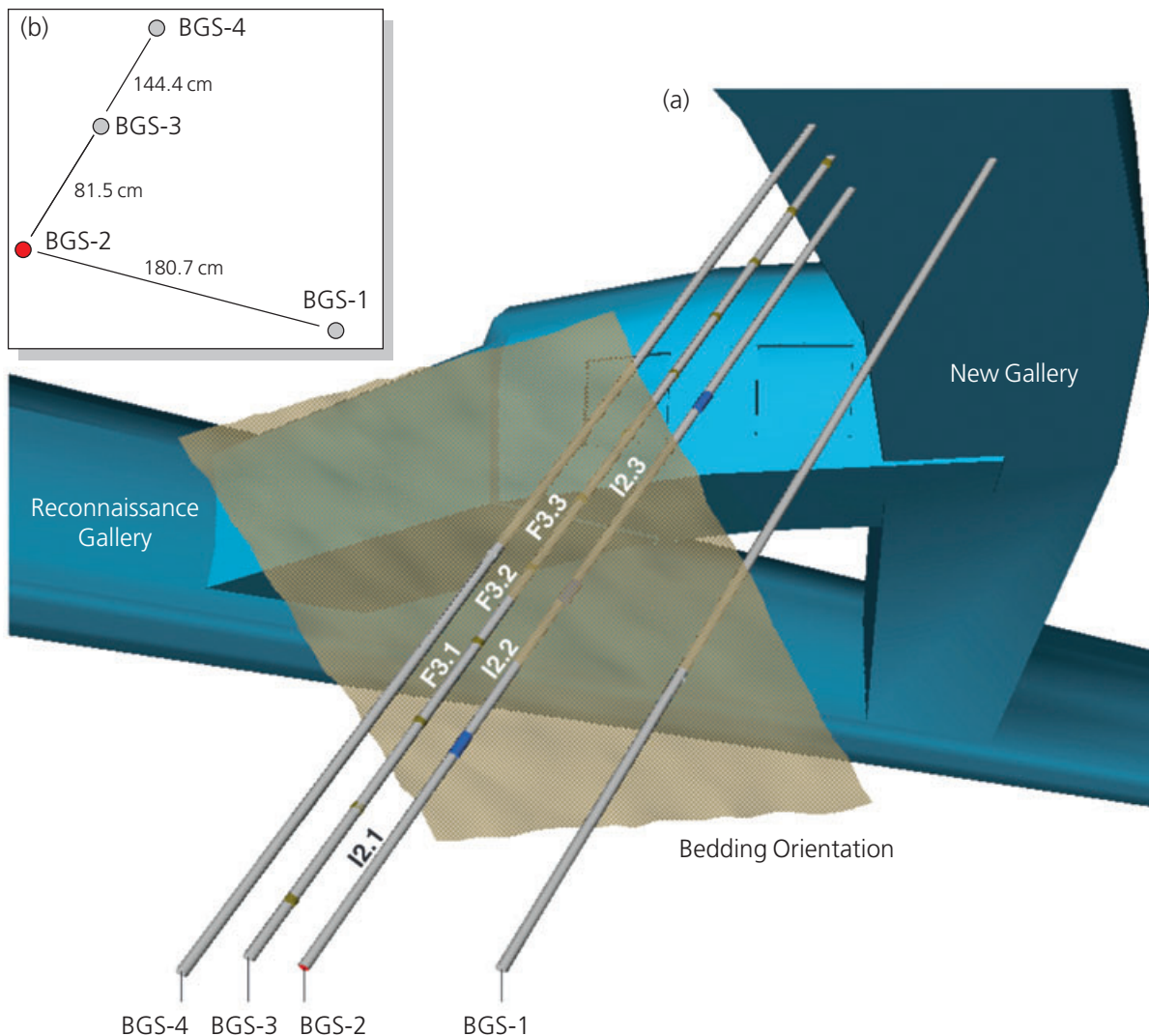


Figure 5.4: Long-term gas injection experiment in the GP-A/GS site. (a) The test configuration consisted of two boreholes: BGS-2 was equipped with a triple packer system, BGS-3 with fixed installed micrometers. (b) Shows a plan view drawn perpendicular to BGS-2 through the centre of test interval I2.2. (c) At gas injection pressures of more than 2 MPa, a significant mechanical response is observed in BGS-3 (after Enachescu et al. 2002). (c) on page 77.

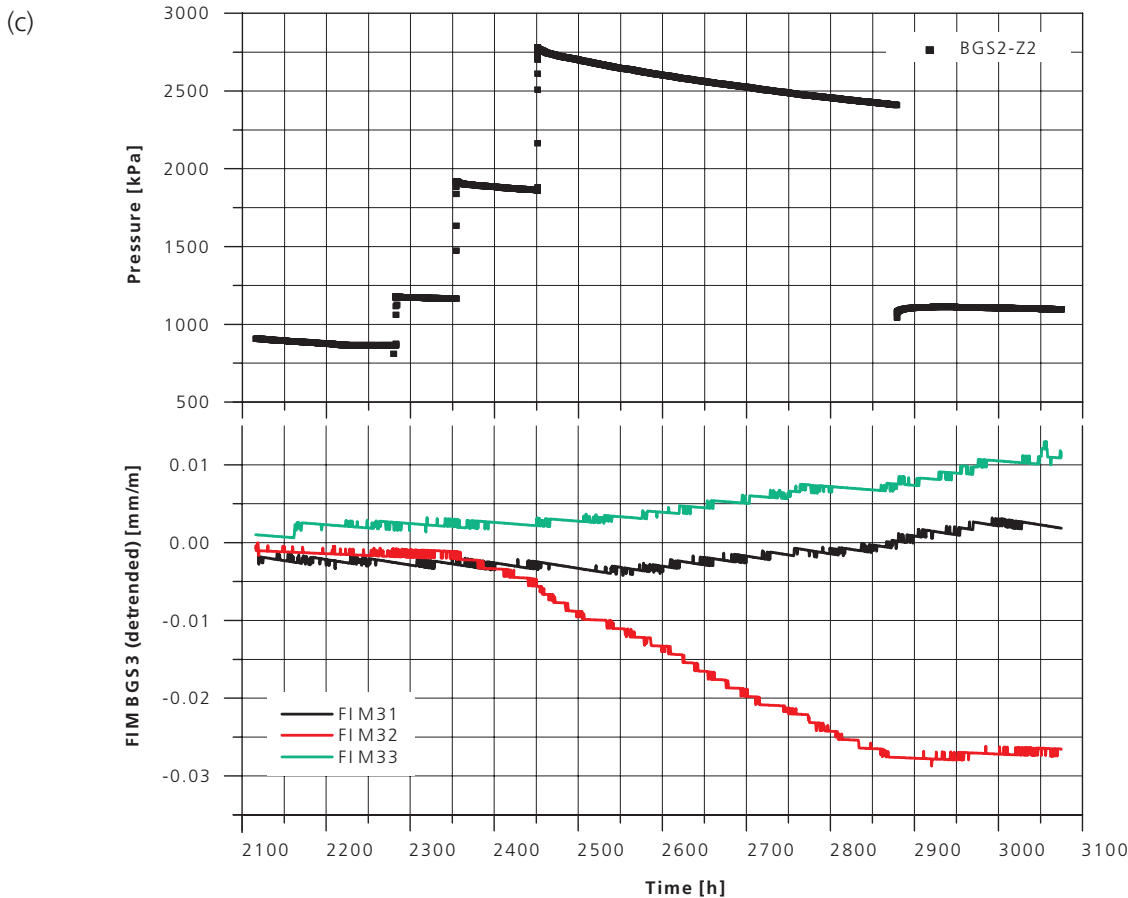


Figure 5.4 continued

The other long-term gas injection test lasted for a total of 30 days and encompassed a testing sequence with three levels (Enachescu et al. 2002). Before testing commenced in the GP-A borehole, the borehole fluid in the test interval of ca. 2.1 l volume was replaced with nitrogen gas. The gas pressure in the test interval was then fixed at differential pressures of about 0.5 MPa, 1.0 MPa and 2.0 MPa, respectively, and the interval closed off. Figure 5.4 shows the development of the interval pressure and of the gas flow rate in the gas injection borehole BGS-2, as well as the deformation in the observation borehole BGS-3 at a distance of 1 m. For a differential pressure of 0.5 MPa the formation appears practically impermeable to gas as the gas entry pressure has not yet been reached. Low flow rates result for a differential pressure of 1 MPa without any significant deformation in the adjacent extensometer boreholes. The highest pressure level is accompanied by marked increases in the gas flow rate and significant deformation of about 20 $\mu\text{m/m}$ which are not reversible after completion of the gas injection test. This gas test was analysed with a coupled hydrodynamic model (Senger et al. 2002).

The pressure recovery observed in the injection borehole and the deformation recorded in the observation borehole could be simulated remarkably well in terms of time and magnitude (cf. chapter 5.5). The quantitative results prove that the intrinsic permeability increases on the highest pressure level by a factor of 5 as a result of the observed dilation.

5.4.4 Hydrofrac and gasfrac experiments

As a follow-up to the long-term gas injection test (Figure 5.4), a complex sequence of hydrofrac and re-frac tests was performed at the GS site, completed by hydrotests and further gas tests. The objectives of this suite of tests were:

- To investigate the pressure regime of hydro-/gas fracturing in the Opalinus Clay (cf. chapter 5.3).
- To determine frac pressure and re-frac pressure at the GS location.
- To determine pressure dependent transmissivity of a hydrofrac.
- To assess the self-healing capacity of the Opalinus Clay.

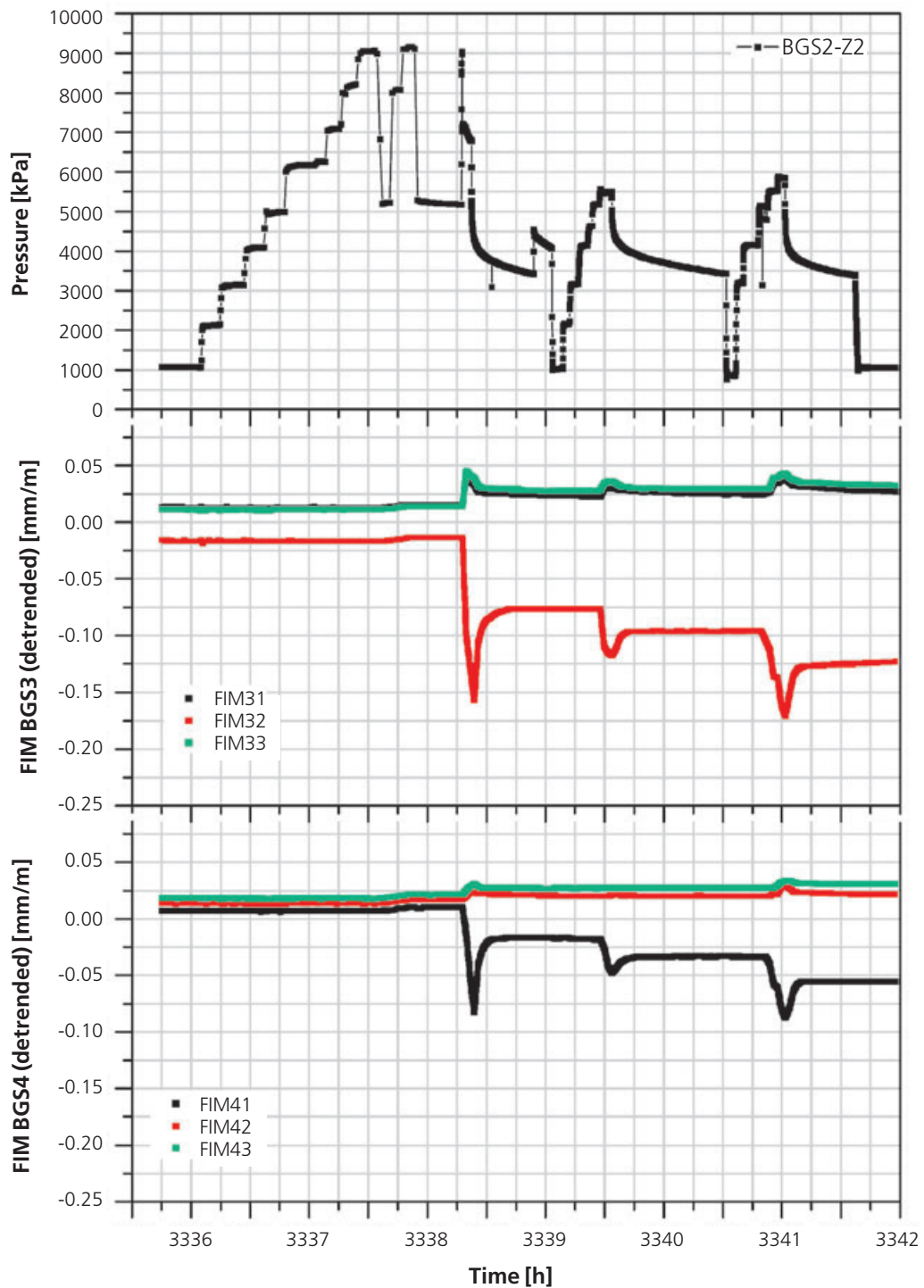


Figure 5.5: Sequence of hydrofrac and re-frac events in test interval I2.2 of borehole BGS-2. Pressure transients in interval I2.2 of borehole BGS-2 and displacements measured in BGS-3 and BGS-4 (after Enachescu et al. 2002).

The hydrofrac/gasfrac sequence was carried out in test interval I2.2 of borehole BGS-2. Pore pressures were monitored in the adjacent observation intervals I2.1 and I2.3 and in borehole BGS-1. Boreholes BGS-3 and BGS-4 were instrumented with extensometers

(Fixed Installed Micrometers/FIM). The orientation of all boreholes was approximately perpendicular to bedding. The expected orientation of the hydrofrac was parallel to bedding. The entire test sequence is listed in Table 5.6.

Stage	Remarks
Stage 1: Hydrofrac	- progressive constant gas pressure steps: (first attempt) 0.8–9 MPa (1.5 h); no fracture event
Stage 2: Hydrofrac (second attempt)	- constant gas pressure steps: 5, 8 and 9 MPa - fracture event at a pressure of 9027 kPa - gas injection continued for 0.08 h at an approximate pressure of 7145–6112 kPa. The total volume injected is 4.7 l - shut in, followed by a pressure reduction to the static formation pressure at approximately 0.8 MPa
Stage 3: Refrac test steps each	- two re-frac cycles with several pressure - shut-in after successful fracture re-opening - pressure drop to static formation pressure (approx. 0.8 MPa) - test interval opened to accommodate back-flow (no backflow measured)
Stage 4: Hydraulic test	- multi-step pulse injection test
Stage 5: Gas pulse test	- gas pulse test (gas pressure below frac pressure)
Stage 6: Gas injection test	- constant rate gas injection - long-term pressure recovery

Table 5.6: Hydraulic fracturing experiment in interval I2.2 of borehole BGS-2: stages of the complex test sequence.

Figure 5.5 shows the pressure transients in test interval I2.2 of borehole BGS-2 during stages 1 through 3. In addition, the mechanical response of the FIM equipment in boreholes BGS-3 and BGS-4 is given. Two cycles of pressurisation are needed to create the hydrofrac. Frac pressure is reached during the second hydrofrac cycle at more than 9 MPa. The frac test was followed by two re-frac cycles. Each cycle consisted of several constant pressure injection events until the fracture re-opened. Subsequently, the test interval was shut-in and, finally, pressure was dropped to the static formation pressure. After the second cycle, the valve to the interval was left open to accommodate back-flow. During the entire equilibration time no back-flow was measured. The re-frac pressure was calculated to 4200 kPa. All Fixed Installed Micrometers (FIM) reacted to the hydrofrac. Zones FIM3.2 and FIM4.1 show a distinct dilation, while zones FIM3.1 and FIM3.3 exhibit contraction. Responses in zones FIM4.2 (slight contraction) and FIM4.3 (slight dilation) are much smaller in magnitude. The mechanical response in FIM3.2 is as high as 15 μm . FIM4.1 exhibits a lower magnitude, because the distance to the gas injection borehole is greater.

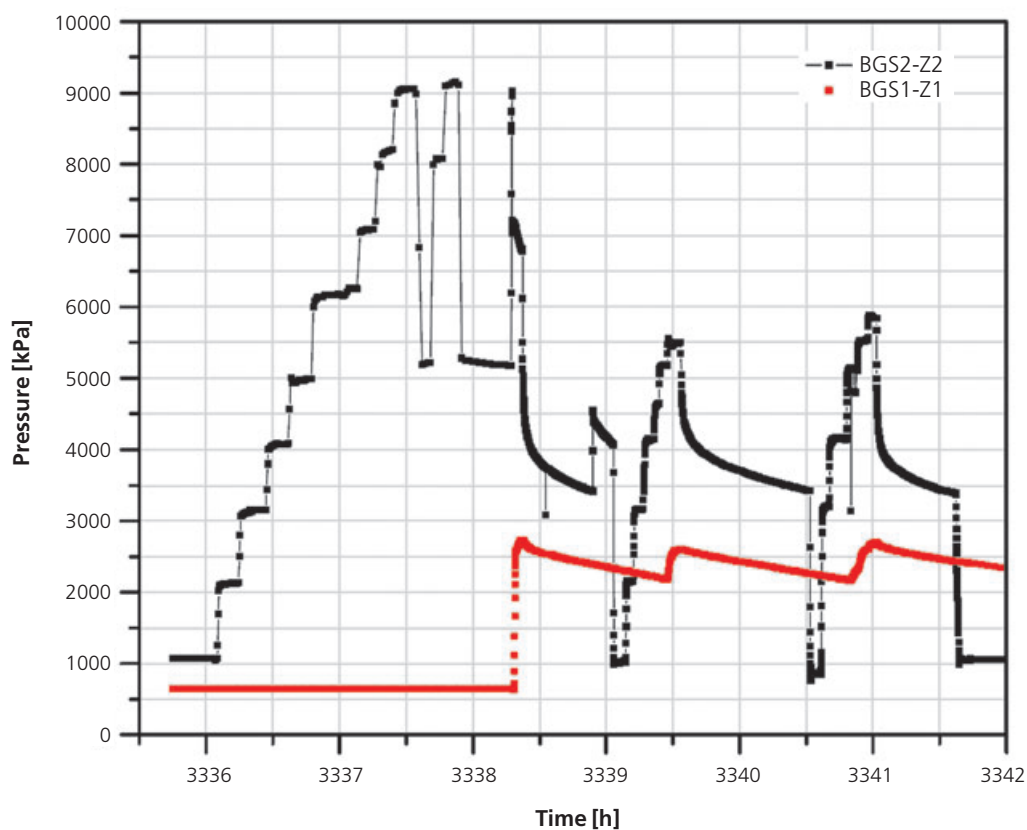


Figure 5.6: Hydraulic response in interval I1.2 of borehole BGS-1 to the hydrofrac and re-frac events in test interval I2.2 of borehole BGS-2 (after Enachescu et al. 2002).

The frac events created an increase in interval transmissivity and a hydraulic communication between intervals I2.1 and I2.2 of borehole BGS-2.

5.5 Modelling of gas related experiments

It was one of the objectives of the gas related field experiments to provide an appropriate data base required for validation of the different conceptual approaches of gas migration (cf. chapter 5.2). Emphasis was given to two-phase flow processes and microscopic pathway dilation because these mechanisms play a key role in the assessment of gas release from the disposal caverns of a repository for radioactive waste.

Two gas experiments were selected for detailed interpretation by numerical modelling, namely the extended gas threshold pressure test in interval I4.2 of borehole BGP-4 (cf. Figure 5.3) and the long-term gas injection test in interval I2.2 of borehole BGS-2 (cf. Figure 5.4). In the following sections, a brief summary of the modelling activities will be given and the achievements will be highlighted. Finally, chapter 5.5.3 is aimed at an assessment of the current level of understanding on gas migration mechanisms in claystones.

5.5.1 Two-phase flow modelling of the gas threshold pressure test in BGP-4 Objectives

A summary and chronology of the BGP-4 testing activities including the hydrotests performed prior to the gas threshold pressure test is reported in TN 97-28. A detailed analysis of the hydrotest events with flow model identification, parameter estimation and extended assessment of parameter uncertainties was documented in TN 98-24. The gas threshold pressure test sequence was also subjected to a detailed two-phase flow analysis (TN 98-25). The objectives of the detailed analysis of the BGP-4 gas threshold pressure test were:

- to interpret the test in terms of constitutive relationships (relative permeability and capillary pressure) based on the conceptual framework of two-phase flow in an Equivalent Poro-elastic Medium (EPM) and taking into account the results of the hydrotests interpretation (TN 98-24)
- to identify signatures in the system response which could be attributed to phenomena not described by an EPM-based two-phase flow modelling approach (e.g. coupled hydro-mechanical behavior)

Interpretation procedure

The interpretation of the gas test was performed according to a standard procedure which has proven successful in the past by Nagra for fractured rocks (Marschall et al. 1998). The procedure includes numerical simulations of pressure transient and water / gas flow transients using the multi-phase flow simulator TOUGH2 and the corresponding tool for inverse modelling ITOUGH2. The key elements of the interpretation procedure are:

- Diagnostic graphical representation of the data for the gas injection and recovery phases.
- Set-up of initial fitting and non-fitting parameters as input parameters for the two-phase flow simulation using TOUGH2.
- Computation of the sensitivity of the two-phase flow model parameters (ITOUGH2).
- Specification of constraints and objective function, and optimisation of fitting-parameter estimates using non-linear regression (ITOUGH2) to obtain best estimates.
- Evaluation of the results of the non-linear regression, and uncertainty analysis.
- Consistency check with the analysis of the hydrotest results from BGP-4.

Two-phase flow parametric models

Capillary pressure/water saturation relationship (CPS):
The two most commonly used CPS models in the two-phase flow literature are given by the Brooks-Corey and the van Genuchten relationships. The model of Brooks & Corey (1964) – here referred to as BC model – is given by:

$$P_c = P_e \cdot S_{ec}^{-1/\lambda} \quad \text{with} \quad S_{ec} = \frac{S_w - S_{wr}}{1 - S_{wr}} \quad (5.1)$$

where:

λ	a pore-size distribution index [-]
P_e	the air entry pressure [Pa]
$P_c = P_g - P_w$	the capillary pressure [Pa]
P_g	the pressure of the gas phase [Pa]
P_w	the pressure of the water phase [Pa]
S_w	the actual water saturation
S_{wr}	the residual water saturation
S_{ec}	the effective saturation as defined above

For a uniform pore-size distribution λ tends to large values, whereas for a wide spread distribution it tends to small values. Typical values for sands range from 2 to 5.

The model of van Genuchten (1980) – here referred to as VG model – is given by:

$$P_c = \frac{1}{\alpha} \cdot (S_{ec}^{\frac{n}{1-n}} - 1)^{\frac{1}{n}} \quad (5.2)$$

where α [1/Pa] and n are shape parameters of the CPS model.

The main difference between the BC model and the VG model is that, when the water saturation S_{ec} tends to 1, the capillary pressure approaches a non-zero value (i.e. the entry pressure: P_e) in the BC model whereas a continuous decrease of the capillary pressure to zero is observed in the VG model. Both parameterizations are fitting curves of the experimental data. For further details about the CPS models described above, the reader is referred to a book by Corey (1994).

Relative permeability/water saturation relationship (RPS): Through theoretical consideration of viscous flow at the pore scale, parametric models have been derived. Their mathematical formulations are recalled briefly. For more detail on this the reader is referred to the two-phase flow literature. The theoretical RPS model of Burdine (1953) has been used in conjunction with the BC model, leading to the following expressions for the relative permeability to water (k_{rw}) and to gas (k_{rg}):

$$k_{rw} = S_e^{(2+3\lambda)/\lambda} \quad (5.3a)$$

$$k_{rg} = (1-S_e)^2 (1-S_e^{(1+2/\lambda)}) \quad (5.3b)$$

where S_e is the apparent saturation, given by:

$$S_e = \frac{S_w - S_{wr}}{1 - S_{gr} - S_{wr}} \quad (5.3c)$$

and S_{gr} is the residual gas saturation which corresponds to the gas saturation which does not contribute to the gas flow.

Similarly, the theoretical RPS model of Mualem (1976) has been used in conjunction with the VG model and leads to the following expressions:

$$k_{rw} = S_e^{1/2} \left[1 - \left(1 - S_e^{\frac{n}{n-1}} \right)^{\frac{n-1}{n}} \right]^2 \quad (5.4a)$$

$$k_{rg} = (1 - S_e)^{1/2} \left(1 - S_e^{\frac{n}{n-1}} \right)^{2(1-1/n)} \quad (5.4b)$$

TOUGH2 is a general purpose simulator for multi-dimensional coupled fluid and heat flows of multi-phase multi-component fluid mixtures in porous and fractured media (Pruess 1991; Pruess 1987). The coupled multi-phase multi-component equations are solved by means of integral finite differences. The solution of the flow of fluids accounts for pressure, viscous, gravity and capillary forces. The equation of motion for each fluid phase is the generalized Darcy equation which represents the phase interference on the basis of relative permeability. Functional relationships are used which describe the relative permeabilities and the capillary pressure as a function of the saturation. Thermodynamic properties of the fluids are represented by steam-table equations while the gaseous phase is treated as an ideal gas and described by local thermodynamic equilibrium. Dissolution of gas into water is described by Henry's law.

In this study, isothermal conditions were assumed and the equation of state module EOS3 (phases: water/air) was used for the simulations of the nitrogen gas injection sequence (GRI) and recovery (GRIS). Because TOUGH2 deals with air mass flow rates, the nitrogen mass flow rates were converted into equivalent air mass flow rates for standard pressure ($P = 100$ kPa) and temperature ($T = 20^\circ\text{C}$) conditions.

The numerical code ITOUGH2 (Finsterle 1997) solves the two-phase flow parameter estimation problem by means of an inverse modelling technique. For the interpretation of the gas threshold pressure test, the pressure data recorded at the test interval during the test are automatically fitted using a minimization algorithm of the differences between simulated and measured data. Both one-phase and two-phase flow parameters can be estimated together with the standard deviations and the correlation coefficients as measures of the parameters uncertainty and interdependence, respectively.

Modelling results

According to the general interpretation procedure (see above), diagnostic test analysis and set-up of input parameters for baseline simulations (forward modelling) formed the early modelling stages. A sensitivity study of the gas injection phase (GRI) and of the subsequent shut-in phase (GRIS) followed, using the inherent capabilities of ITOUGH2: the sensitivity of the pressure transient to the test interval compressibility, the permeability, the formation compressibility and the air entry pressure is high, whereas the one of residual water saturation and the porosity is lower. Noteworthy, the sensitivity coefficients do vary with time resp. with the test events (GRI, GRIS). This fact exhibits a benefi-

cial effect by reducing the degree the non-uniqueness of the solution of the inverse modelling. In order to avoid over-parameterization, inverse modelling was limited to 5 unknown parameters (formation compressibility, test interval compressibility, porosity, permeability, air entry pressure), whereas the parametric two-phase flow model, the pore size factor and the residual water saturation were fixed (VG model: $n = 2$, $S_{rw} = 0.1$, $S_{gr} = 0$ and $S_{gr} = 0.1$, respectively). Further refinement included joint inversion of both, hydraulic and gas test sequence. Finally, the results of inverse modelling can be summarised as follows:

- Strong parameter correlation is seen between gas entry pressure, permeability and porosity. This parameter correlation makes results somewhat ambiguous, although excellent matches of the data are achieved.
- Porosity estimates were between 0.1 and 0.23. It is worth mentioning, that the upper value of 0.23 is not consistent with the porosity estimates gained by laboratory tests.
- Better matches of the data are achieved, when a

finite residual gas saturation is assumed.

- The estimated gas entry pressure of approximately 0.8 MPa matches the results of diagnostic analysis (chapter 5.4) quite well.
- The permeability estimates derived from the interpretation of the gas test sequences are by a factor of 2 to 3 higher than those from the analysis of the hydraulic test prior to gas testing.
- During the GIS test event the gas penetrates not more than a few centimeters into the rock formation. Assuming a uniform radial gas flow through the entire length of the test interval (length: 4.5 m) the gas front is expected to propagate less than 5 cm.

Figure 5.7 shows two simulations of the entire hydrotest and gas threshold pressure test sequence on the basis of the parameter estimates from the gas threshold pressure test analysis. The impact of test interval compressibility from the hydrotest analysis is highlighted, the other parameters being those obtained with the GTP analysis.

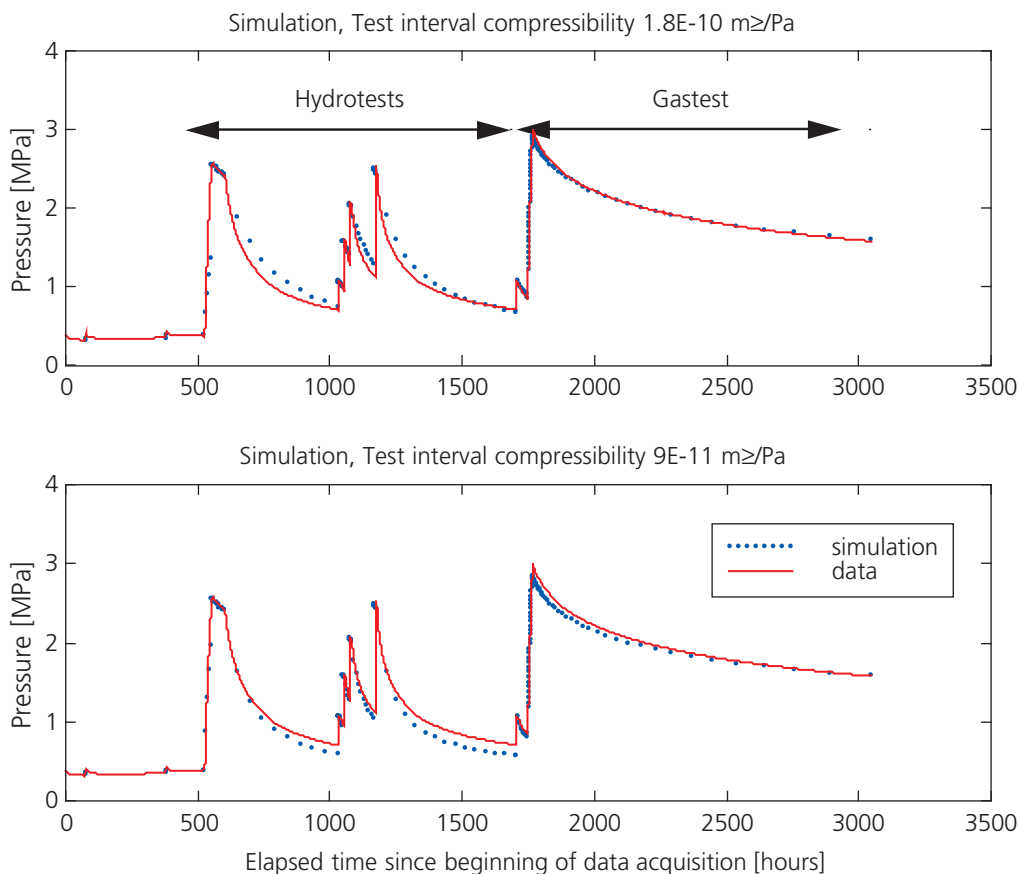


Figure 5.7: Modelling of the extended gas threshold pressure test in interval I4.2 of borehole BGP-4 with a two-phase flow simulator. Note that the entire test sequence is modelled, consisting of a hydrotest, a constant rate gas injection phase and a recovery phase (after TN 98-25).

Concluding remarks

Simulations conducted in the framework of two-phase modelling of the gas threshold pressure test, reproduce the pressure and flow transients observed in test interval BGP-4/I2 satisfactorily. Permeability estimates also compare fairly well with the results of hydraulic testing. Nevertheless, inverse modelling of two-phase flow processes represents an ill-posed problem with non-unique solutions. Consequently, the reliability of parameter estimates and model predictions may be very limited, even if the model calibrations match the data in an acceptable manner.

A way out of this ambiguity is to constrain the problem by introducing independent evidences such as laboratory measurements of porosity, equivalent pore radii (e.g. nitrogen adsorption/desorption), permeability and capillary pressure. Furthermore, a careful analysis of (missing) crosshole responses may help to discard some of the possible solutions. Since the two-phase flow modelling exercise was completed by the end of Phase 3, the geoscientific data base has been broadened significantly and the new evidences might be beneficial in constraining the conceptual uncertainties in two-phase flow modelling. Even so, based on the achievements of this study, the two-phase flow approach seems to be a promising tool for quantitatively characterising gas migration processes in the Opalinus Clay.

5.5.2 Hydro-mechanical modelling of the BGS-2 gas injection experiment Objectives

A summary and chronology of the BGS-2 testing activities, including the hydrotests performed prior to the long-term gas injection test, are reported in TN 00-06, TN 00-07 and in Enachescu et al. (2002). The long-term gas injection test sequence was also subjected to a detailed two-phase flow analysis, combined with simulations of hydro-mechanical coupled processes (Senger et al. 2002). The objectives of the BGP-2 long-term gas test interpretation were:

- to interpret the test in terms of constitutive relationships, i.e. relative permeability and capillary pressure, based on the conceptual framework of two-phase flow in an Equivalent Poro-elastic Medium (EPM) and taking into account the results of the hydrotest interpretations (Enachescu et al. 2002).
- to assess the potential of coupled hydro-mechanical approaches for improving the conceptual understanding of gas migration processes in the Opalinus Clay.

Interpretation procedure and results

The interpretation of the gas test consisted of three major elements (Senger et al. 2002):

- 1) Analysis of the hydrotest sequence using both diagnostic graphical representations and numerical welltest simulators. A standard hydrotest analysis was conducted of the Hydro-1 test phase using nSight (Avis 2000; updated Windows Version of GTFM) to perform an inverse simulation of the pressure response to the entire test sequence in BGS-2/I2.
- 2) Two-phase flow simulations of the gas test with ITOUGH2. For consistency, both the hydrotest and gas test sequence were analysed by inverse modelling. The initial estimates for hydraulic properties were based on the results from the hydrotest and appropriate estimates of two-phase flow parameters.
- 3) Modelling of pressure transients in BGS-1 and BGS-2 and simulation of mechanical responses in the adjacent boreholes BGS-3 and BGS-4 with a fully coupled hydro-mechanical model (GEOSIM, Settari et al. 1999). The results of the Hydro 1 and Gas 1 analyses served as a baseline. The aim of the coupled hydro-mechanical two-phase flow simulation is to identify potential changes in the hydraulic and two-phase flow properties during the gas test that can be related to the displacements observed in BGS-3 and BGS-4.

The analysis of the hydrotest sequence was carried out using the borehole simulators nSight and ITOUGH2. Both codes can be operated in an inverse modelling mode. The best-fit parameters were obtained by inverse simulation of the Cartesian pressure response in BGS-2/I2. Best-fit intrinsic permeability estimates of $1.2 \times 10^{-20} \text{ m}^2$ (nSight) and $2.2 \times 10^{-20} \text{ m}^2$ (ITOUGH2) were determined. The small deviations between the best-fit estimates arise from a slightly different formulation of the storage coefficient in the two codes. Similar to the hydrotest analysis, the gas test was analysed through inverse modelling in a radially-symmetric numerical model using the two-phase flow code ITOUGH2. For the inverse simulation of the gas test sequence, three parameters were estimated, including the permeability and pore compressibility of the formation and the air-entry pressure (P_{ae}) as defined in the van Genuchten two-phase flow parameter model. Other two-phase flow parameters were considered too insensitive to yield well constrained parameters. The results of the inverse simulation indicate a noticeable increase in permeability between the

hydrotest sequence ($k = 2.2 \times 10^{-20} \text{ m}^2$) and the gas test sequence ($k = 5.4 \times 10^{-20} \text{ m}^2$). The estimated air-entry pressure value ($P_{ae} = 148 \text{ kPa}$) was surprisingly low and may not be representative for the undisturbed rock properties: Due to technical problems prior to the first pressure step of the gas test (cf. Figure 5.4), pre-test desaturation of the rock in the vicinity of the borehole cannot be fully ruled out. The first gas test event with its constant pressure plateau may suggest a representative gas entry pressure of about 0.5 MPa. The other two-phase parameters of the van Genuchten model were assumed (i.e., residual water saturation $S_{rw} = 0.2$, residual gas saturation $S_{rg} = 0.001$, van Genuchten parameter $n = 3$). Figure 5.8 shows the results of three simulations of the gas test sequence with different intrinsic permeabilities.

To assess the potential effects of geomechanical processes, the hydrotest and gas test sequences in BGS-2 were simulated with the coupled hydro-mechanical code GEOSIM. Both the hydraulic and two-phase pressure responses in BGS-2 were considered, as well as the geomechanical responses observed in BGS-3 and BGS-4. The focus of the coupled hydro-mechanical analysis under single-phase liquid and two-phase conditions was on improving the

process understanding rather than on obtaining a perfect fit of the observed test data. Of special interest were evidences for stress-permeability relationships. For the coupled hydro-mechanical model, the test configuration was implemented in a 3D mesh geometry with the main coordinate axes parallel to the bedding plane and to the borehole orientation, respectively. The boreholes were explicitly gridded such that the stresses and displacements could be accurately calculated in the near-wellbore region. Due to the lack of a solidified data base of rock stress, isotropic stress conditions were assumed.

There are a number of constitutive relations for different rock materials describing the geomechanical behavior in response to stress changes. However, only a limited number of constitutive models exist which relate changes in stress/strain to changes in hydraulic properties. Those models are typically applied to fractured rock whereby the displacements are related to changes in fracture aperture and a corresponding change in fracture permeability (see Stephanson et al. 1996). For this study, an empirical relationship was used based on the inferred increase in permeability during the gas test sequence. The test data suggest that the permeability increase associated with the rock

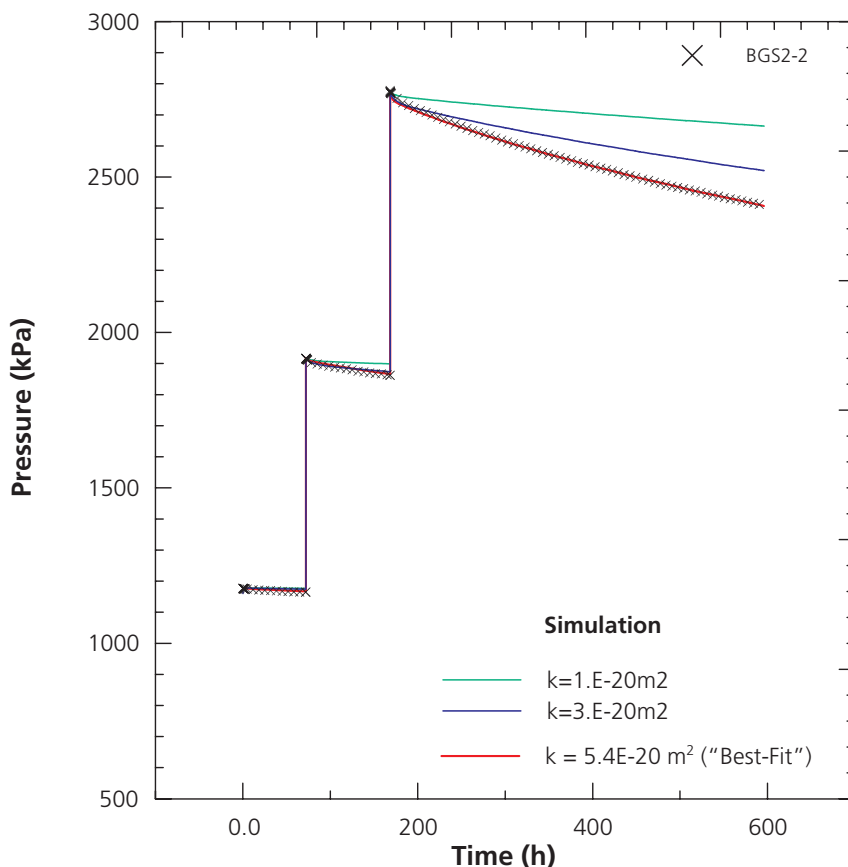


Figure 5.8: Modelling of the gas test sequence in BGS-2/I2 with TOUGH2. The sensitivity of the pressure response to the variation of intrinsic permeability is shown. The third pressure step is most sensitive to permeability. The best-fit intrinsic permeability is 2 to 3 times higher than the best-fit permeability, determined from hydrotest analysis (after Senger et al. 2002).

dilation occurs above a pressure of about 2000 kPa. After the pulse withdrawal test following the last gas pressure event (cf. Figure 5.4), the FIM F3.2 data level off without noticeable rebound suggesting that dilation and the higher permeability are maintained. The resulting change in gas and fluid pressure and the spatial extent of the pressure perturbation away from the injection interval affect the stress distribution which, in turn, causes a geomechanical response as observed in the FIM records.

A number of triaxial tests on the geomechanical behavior of Opalinus Clay cores indicated predominantly elastic properties (TN 98-35, TN 98-55). On the other hand, geomechanical analyses of laboratory tests (TN 98-56) also indicated non-linear elastic behavior as represented by a hyperbolic constitutive model with a stress-dependent elasticity modulus E . For the expected range in differential pressure during the gas test sequence, the hyperbolic constitutive model given in TN 98-56, which was used in the hydro-mechanical analyses (cf. chapter 4.4.3), indicates an overall linear behavior. For this reason, the

base case for the subsequent hydro-mechanical models assumed a linearly elastic geomechanical behavior based on an E modulus of 6 GPa (TN 98-49) which is in the range of the corresponding pore compressibilities estimated from the hydraulic tests and gas tests. For the hydraulic and two-phase flow parameters, the best-fit permeability of $2.2 \times 10^{-20} \text{ m}^2$ from the hydrotest was used as initial value and a pressure-dependent permeability increase was assumed such that the permeability increased from $2.2 \times 10^{-20} \text{ m}^2$ below 2000 kPa to $5.4 \times 10^{-20} \text{ m}^2$ at 2800 kPa that corresponds to the best-fit permeability value from the gas test. The permeability increase was assumed to occur uniformly over the entire test-zone interval connecting BGS-2/I2, BGS-1/I2, BGS-3/F3.2 and BGS-4/F4.2. Vertical permeability in the 3D model was assumed to be one order of magnitude lower than the horizontal permeability. The pressure responses in BGS-2/I2, BGS-1/I2 and BGS-3/F3.2 as well as the calculated displacements parallel to the borehole axis for the corresponding FIM zones in BGS-3 and BGS-4 are shown in Figure 5.9 for the gas test in comparison to the measured data. The

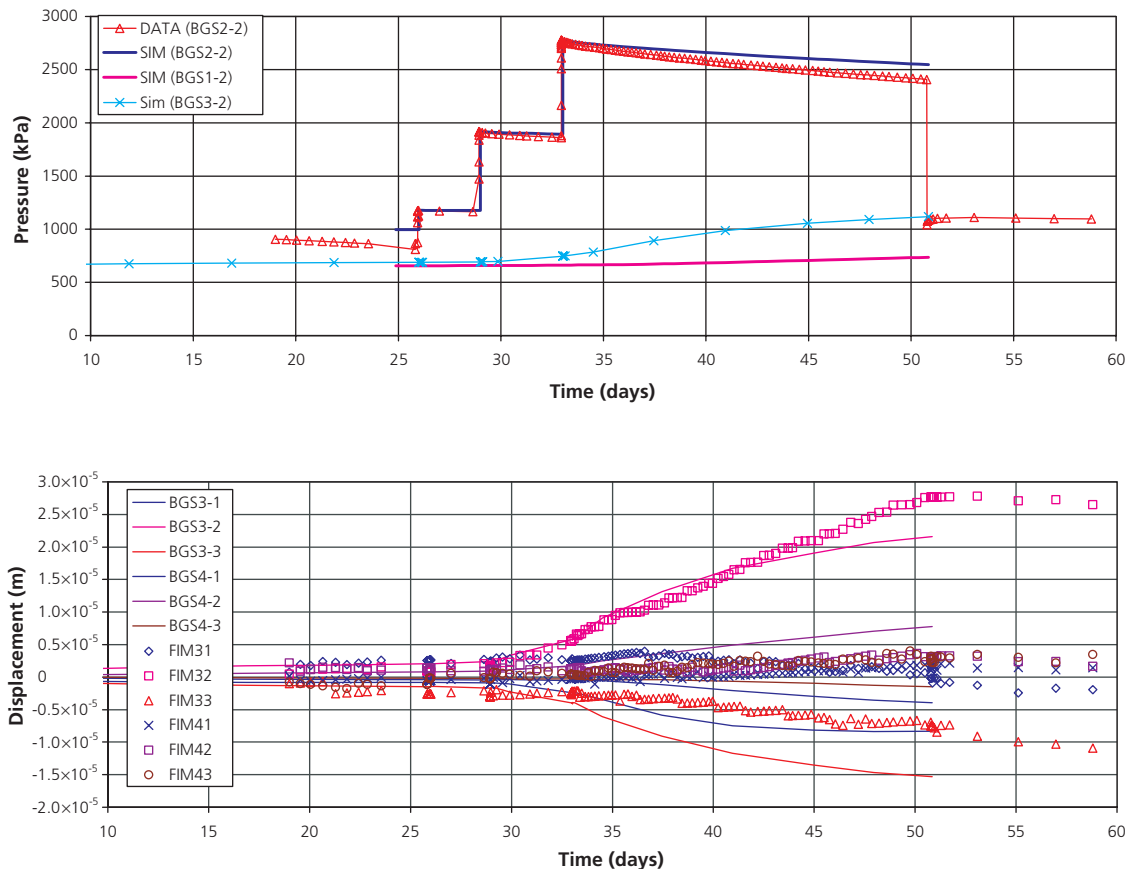


Figure 5.9: Coupled 3D hydro-mechanical simulation: Pressure history in BGS-2/I2, BGS-1/I2 and BGS-2/I3, and FIM data in boreholes BGS-3 and BGS-4. Assumptions: Pressure-dependent permeability over the entire test interval, linear-elastic geomechanical model with an E modulus of 6 GPa (after Senger et al. 2002).

simulated pressures show a reasonably good fit but show less pressure decline during the last pressure step. The corresponding simulated displacements indicate dilation for FIM F3.2 and FIM F4.2, and general compression for the adjacent FIM zones. This compares well with the data, though the magnitude of compression is noticeably greater than the corresponding FIM data. The largest displacements are calculated for the FIM F3.2 zone showing a relatively good fit during the first and the second pressure steps and the early part of the third step. The simulated displacement curve for FIM F3.2 shows a concave shape, with decreasing amounts of dilation, whereas the corresponding FIM F3.2 records indicate a nearly linear increase during the last pressure step.

Several other modelling cases were assessed including a scenario with a limited flow domain ("fracture" model) and a hyperbolic elastic behavior. None of these models showed a significant improvement in the overall performance.

5.6 Evaluation of achievements

In the course of Phases 1 to 5 of the Mont Terri project, a considerable number of laboratory and field experiments were conducted in the general goal of improving the understanding of gas migration processes in the Opalinus Clay. The studies emphasised on

- Improving the conceptual understanding of gas flow mechanisms in the Opalinus Clay.
- Deriving effective parameters to characterise these gas flow mechanisms.
- Assessing possible alterations of rock properties as a consequence of a passed gas phase.

Gas flow mechanisms and effective parameters

Without exception the gas related experiments at Mont Terri have shown that gas transport in the Opalinus Clay starts at low gas pressures, typically in the range 0.2–1 MPa. These pressures are significantly lower than the frac pressure required for macroscopic rock failure to occur. The hydro-frac experiments carried out in borehole BGS-2 (cf. chapter 5.4.4) demonstrate that frac pressures in the order of 9 MPa may be expected. The presumed stress magnitude perpendicular to bedding is in the range of 4–5 MPa.

At low gas pressures, the most probable mechanisms for gas transport are visco-capillary displacement of the porewater (two-phase flow) and microscopic pathway dilation. Two-phase flow is a non-dilatant process

whereby the rock matrix is subjected to small elastic deformations rather than irreversible dilation as the gas migrates through. Evidences for two-phase flow processes at low pressures were found in several in-situ experiments such as the gas testing in boreholes BGP-4, BGP-6, BGS-2). The intrinsic rock permeability was determined by laboratory and in-situ tests. The typical range is between 1×10^{-19} and 5×10^{-21} m². The measured gas entry pressure ranges between 0.2 and 1.3 MPa. Other two-phase flow parameters like the residual water saturation and gas saturation or the pore size factor are quite uncertain. Laboratory experiments indicate, for example, that residual water saturation may be quite high with a value > 0.8. Microscopic pathway dilation is linked to measurable irreversible deformation. Clear evidence was observed during the in-situ gas tests in boreholes BGS-2 and BGP-6. At gas injection pressures above 2 MPa, significant deformation was measured in the adjacent boreholes. Furthermore, a pressure-dependent rock-permeability was measured. The enhancement factor with respect to the intrinsic permeability (two-phase flow) was up to 2.5 (for a gas pressure of 2.5 MPa).

Alterations of the host rock properties

It is not expected that the two-phase flow processes will significantly affect the hydraulic properties of the Opalinus Clay. Two-phase flow is a non-dilatant process. Therefore, porosity does not change significantly during the passage of a gas phase. In laboratory experiments (cf. chapter 5.4.1), no changes of hydraulic conductivity were detected with respect to before and after gas injection.

In contrast, microscopic pathway dilation is a dilatant process and, therefore, might cause an enhancement of intrinsic permeability. In the GP and GS experiments, hydraulic tests were performed in boreholes BGP-6 and BGS-2 before and after the gas injection tests were conducted. A change in the hydraulic conductivity was not identifiable.

6 Summary and Conclusions

At the onset of the Mont Terri project in 1996, experience with hydrogeological testing procedures in clay-rich formations and the data base for the Opalinus Clay was scant. Over the course of Phases 1 to 4 of the Mont Terri research program, a broad geoscientific data base was compiled and a series of site investigation methods was applied. The latter were, to a large extent, adaptations from hard rock exploration both in terms of the equipment, such as hydraulic long-term monitoring systems, and of the hydrotest analysis and interpretation approaches, e.g. petroleum welltest simulators. Phase 5 introduced a new aspect to the research program: an overall review of the data acquired up until then and their interdisciplinary interpretation. The subjects of this publication are the hydrogeologically relevant investigation methods and data. The report's structure follows the particular points of concern:

- Assessment of the achievements of the hydrogeological investigations both in terms of *development of investigation techniques* and in terms of *geoscientific data analysis*
- Development of a *conceptual model of groundwater flow* at the Mont Terri site
- Development of a *conceptual model of gas migration mechanisms* in the Opalinus Clay

As part of the Hydrogeological Analyses (HA) project, the final objective is to provide a first comprehensive synthesis of the hydrogeological setting of the Mont Terri site based on the workings of Phases 1 through 5.

6.1 Summary of achievements

Phases 1 through 5 of the Mont Terri project saw the execution of many experiments for a variety of different purposes. Key aspects of the *hydrogeological investigations* were (i) the development and testing of site characterisation techniques for clay-rich media, (ii) the demonstration of the barrier function of the Opalinus Clay on the site scale and (iii) the advancement of the understanding of gas transport mechanisms in the Opalinus Clay. Some of the key achievements are highlighted here:

- A quality assurance procedure (“suitability assessment”, cf. chapter 3.2) was implemented, aimed at identifying and assessing those Mont Terri Technical Notes which convey hydraulically relevant information. The QA procedure was designed as a pre-defined and traceable procedure, equally applicable to all experiments conducted at the Mont Terri rock

laboratory. It is recommended that this procedure be adopted for the QA of all hydrogeological data acquired in future phases.

- Different types of hydraulic long-term monitoring systems were tested in boreholes at the Mont Terri rock laboratory, e.g. classical inflatable multipacker systems, the PP system and minipacker piezometers. Even though each system had been designed for specific modes of application, certain clay-specific design criteria are advised to be considered by all (cf. chapter 3.3). Particularly relevant specifications are (i) the minimisation of the effective volume of the observation interval, (ii) the introduction of mechanical support along the entire observation interval to prevent borehole collapse, (iii) an appropriate selection of the materials for the downhole equipment to prevent corrosion and to allow for representative porewater sampling.
- Extensive experimental efforts were undertaken to assess for possible artefacts in the results of hydraulic packer testing as a consequence of the drilling techniques (e.g. drilling fluids) and testing methodologies (e.g. borehole history, test fluid; cf. chapter 3.4) applied. The experiments demonstrated that chemico-osmotic effects may have a minor impact on the transmissivity of the “inner zone”, i.e. the zone immediately surrounding the borehole. However, the estimates of the formation properties are not affected significantly. Test perturbations were apparent in the borehole which had been drilled with air.
- A preliminary conceptual hydrogeological model of the Mont Terri site was developed and the understanding of the groundwater flow regime has been enhanced (cf. chapter 4.6). The hydrogeological units of main concern for the underground laboratory and its vicinity are the karstified “Lower Dogger” aquifer and the Opalinus Clay formation, a highly efficient flow barrier. The hydraulic significance of the Jurensis Marls and Posidonia Shales to the North has not been established very well. The main fault, which intersects the rock laboratory, does not affect the barrier function of the Opalinus Clay. The hydraulic conductivity of the Opalinus Clay generally shows low spatial variability and lies in the range of 2×10^{-14} – 2×10^{-12} m/s. The expected range of specific storage is 4×10^{-7} – 3×10^{-5} 1/m. The primary driving force for porewater flow in the Opalinus Clay at the Mont Terri site is gravity: the long-term observations of hydraulic head depict a clear cone of depression towards the gallery system. Furthermore, the “Lower Dogger” aquifer to the South represents a sort of constant pressure boundary for the hydraulic system.

- The investigations of gas transport mechanisms focussed on both laboratory and in-situ experiments (chapter 5). Experimental evidences are found for non-dilatant (classical two-phase flow) and for dilatant (microscopic and macroscopic fracturing) gas transport. The observed gas entry pressure for the Opalinus Clay was generally low (< 1 MPa). Microscopic pathway dilation with an enhancement of gas permeability was observed at pressures (2 to 3 MPa) considerably lower than the refrac pressure. Hydrofrac experiments exhibited frac pressures of 9 MPa and refrac pressures in the order of 4 to 5 MPa.

6.2 Unresolved issues and outlook

The appreciation of hydraulic formation properties and hydrogeological processes active in the Opalinus Clay has grown substantially throughout Phases 1 to 5 of the Mont Terri research program. Site characterisation techniques and interpretation methods have been consolidated, groundwater flow mechanisms have been assessed successfully and hydraulic formation properties have been determined. Finally, the barrier function of the Opalinus Clay was verified in principle on the site scale.

Nevertheless, some issues of hydrogeological relevance remain unresolved and require further studies:

- The pore pressure distribution in the aquifer systems above and below the Opalinus Clay formation is not well known. In particular, the role of the Jurensis Marls as a potential aquifer system has not been well defined.
- Although the main features of porewater flow and pore-pressure distribution in the Opalinus Clay are understood reasonably well, there are some unresolved questions. The large scale anisotropy in hydraulic conductivity is still uncertain. Furthermore, storage coefficients have been determined only on the scale of laboratory experiments and by packer testing. It is expected that site-scale hydrodynamic models which account for the 3D nature of the groundwater system will undoubtedly enhance the integrated understanding of flow processes active at the Mont Terri site.
- Impact of in-situ stress conditions on pore-pressure distribution and groundwater flow at the site: It is expected that stress re-distribution around the galleries may cause extended zones with enhanced hydraulic conductivity, i.e. so-called “stress-dependent permeability”. Furthermore, tight fractures may be activated when the effective stress in the site is

lowered (e.g. due to pore pressures or due to stress unloading in the vicinity of the tunnel). In the context of a performance assessment, such permeability or transmissivity enhancement at low effective stress is an issue of high importance because these processes may reduce considerably the barrier function of the Opalinus Clay. Due to the poor understanding of in-situ stress conditions at the site, an assessment of coupled hydro-mechanical processes in the excavation disturbed zone is still premature. The results from the Rock Mechanical Analyses project will likely feed into the future task of conceptualising the hydro-mechanical processes active in the Opalinus Clay.

- Consolidation behavior, permeability-porosity relationships and poro-elastic properties of the Opalinus Clay: Stress-strain relationships under undrained conditions were investigated in various rock mechanical experiments. However, merely a few consolidation tests were carried out under drained conditions. Such experiments are required to better understand the burial history of the site. Laboratory testing, e.g. oedometer tests, isostatic and triaxial cell tests, and in-situ testing are recommended to consolidate the available data base.

7 References

- AVIS, J. (2001): nSIGHTS well test simulator: Users Manual. Duke Engineering & Services.
- BARDOT, F., SAADA, A., GABORIAU, H. & VILLIÉRAS, F. (2001): Sondierbohrung Benken: Textural characterization of Opalinus Clay – Use of nitrogen and water adsorption and desorption isotherms. Unpubl. Nagra Int. Rep., Wettingen, Switzerland.
- BEAR, J. (1972): Dynamics of fluids in porous media. American Elsevier, New York.
- BEAUHEIM, R.L., ROBERTS, R.M., DALE, T.F., FORT, M.D. & STENSURUD, W.A. (1993): Hydraulic Testing of Salado Formation Evaporites at the Waste Isolation Pilot Plant Site: Second Interpretive Report. SAND92-0533. Albuquerque, NM: Sandia National Laboratories.
- BOCK, H. (2001): RA Experiment: Data report on rock mechanics. Mont Terri Project Technical Report TR 2000-02 St-Ursanne, Switzerland.
- BOCK, H. (2002): RA Experiment: Rock mechanics analyses and synthesis: Conceptual model of the Opalinus Clay. Mont Terri Project Technical Report TR 2001-03 St-Ursanne, Switzerland.
- BOUCHET, A. & RASSINEUX, F. (1996): Mineralogical study of four samples of shales from Mont Terri (Switzerland). Rapp. ERM 96 151 AB 325, Réf. ANDRA B RP O.ERM 96-009.
- BRADLEY, G., CROISÉ, J., ENACHESCU, C., HORSEMAN, S.T., JEFFERIES, M., LAVANCHY, J.M., NOY, D. & SHUTTLE, D. (1998): Sondierbohrung Benken – Scoping Study of the Hydraulic Testing in the Opalinus Clay. Unpubl. NAGRA Int. Rep., Wettingen, Switzerland.
- BROOKS, R.H. & COREY, A.T. (1964): Hydraulic properties of porous media, Hydrol. Pap., 3, 1-27, Colo. State Univ., Fort Collins, USA.
- BURDINE, N.T. (1953): Relative permeability calculations from pore-size distribution data. Trans. Amer. Inst. Min. Metall. Pet. Eng., 198, 71-78.
- COREY, A. (1994): Mechanics of immiscible fluids in porous media. Ed. Water Resources publication, Third Edition, Colorado, USA.
- CROISÉ, J., MARSCHALL, P. & SENGHER, R. (1998): Gas-water flow in a shear zone of a granitic formation: interpretation of field experiments. DisTec'98 - Tracer Hydrogeology. Balkema, Rotterdam, Netherlands.
- DUKE ENGINEERING & SERVICES. (1998): GEOSIM Reservoir / Geomechanical / Fracturing Coupled Modeling System – User Documentation. Duke Engineering & Services (Canada), Inc., Calgary, Canada.
- ENACHESCU, C., BLÜMLING, P., CASTELAO, A. & STEFFEN, P. (2002): Mont Terri / GP-A and GS Experiments - Synth. Rep. Unpubl. Nagra Int. Rep., Wettingen, Switzerland.
- FRITZ, S.J. (1986): Ideality of clay membranes in osmotic processes: A review. Clays & Clay Mins. 34(2), 214-223.
- GREENBERG, J.A., MITCHELL, J.K. & WITHERSPOON, P.A. (1973): Coupled Salt and Water Flows in a Groundwater Basin. Journal of Geophysical Research 78 (27), 6341-6353.
- HANSHAW, B.B. (1962): Membrane properties of compacted clays. Ph. D., Harvard University, USA.
- HARRINGTON, J.F., HORSEMAN, S.T. & NOY, D.J. (2001): Swelling and osmotic flow in a potential host rock. Process assessment and scenario studies. 6th Int. Workshop Key Issues on Waste Isolation Research, Paris, 11/2001.
- HORSEMAN, S.T., ALEXANDER, J. & HOLMES, D.C. (1991): Implications of Long-Term Transient Flow, Coupled Flow and Borehole Effects on Hydrogeological Testing in the Opalinus Clay: Preliminary Study with Scoping Calculations. NAGRA Technical Report 91-16, Wettingen, Switzerland.
- HORSEMAN, S.T., HIGGO, J.J.W., ALEXANDER, J. & HARRINGTON, J.F. (1996): Water, Gas, and Solute Movement through Argillaceous Media. NEA Working Group on Measurement and Physical Understanding of Groundwater Flow Through Argillaceous Media. Report CC-96/1.
- MARSCHALL, P., CROISÉ, J., FISCHER, U., SENGHER, R. & WYSS, E. (1998): Gas flow through water-saturated shear zones: field and laboratory experiments and their interpretation. Proceedings of the 21st Int. Symposium on the Scientific Basis for Nuclear Waste Management - MRS '97. Davos, Switzerland.
- MARTIN, D. & LANYON, B., with contributions of BLÜMLING, P. & BOSSART, P. (2004): EDZ in Clay Shale: Mont Terri Rock Laboratory. Mont Terri Project Technical Report TR 2001-01, St-Ursanne, Switzerland.
- DE MARSILY, G. (1986): Quantitative hydrogeology. Academic Press, New York.
- MAZUREK, M. (2001): Sprödstrukturen und potentielle Migrationspfade im Opalinuston und seinen Rahmengesteinen. Unpubl. Nagra Int. Rep., Wettingen, Switzerland.
- MILLER, R.J. AND LOW, P.F. (1963): Threshold gradient for water flow in clay systems. Soil Society of America Proc., 27/6.
- MUALEM, Y. (1976): A new model for predicting the hydraulic conductivity of unsaturated porous media, Water Resour. Res., 12(6), 513-522.
- NAGRA (2002): Projekt Opalinuston – Synthese der geowissenschaftlichen Untersuchungsergebnisse. Entsorgungsnachweis für abgebrannte Brennelemente, verglaste hochaktive sowie langlebige mittelaktive Abfälle. Nagra Technical Report NTB 02-03, Wettingen, Switzerland.
- NEUZIL, C.E. (1994): Characterization of flow properties, driving forces and pore-water chemistry in the ultra-low permeability Pierre Shale, North America.

- OECD/NEA Workshop on the Determination of Hydraulic and Hydrochemical Characteristics of Argillaceous Rocks, Nottingham, UK. ISBN 92-64-14485-4.
- NEUZIL, C.E. (2000): Osmotic generation of 'anomalous' fluid pressures in geological environments. *Nature*, 403.
- PEARSON, F.J., ARCOS, D., BATH, A., BOISSON, J.-Y., FERNÁNDEZ, A.M., GAEBLER, H.E., GAUCHER, E., GAUTSCHI, A., GRIFFAULT, L., HERNAN, P. & WABER H.N. (2004). Geochemistry of water in the Opalinus Clay formation at the Mont Terri Rock Laboratory. *Berichte des BWG – Serie Geologie*, No. 5, Bern, Switzerland.
- PICKENS, J.F., GRISAK, G.E., AVIS, J.D., BELANGER, D.W. & THURY, M. (1987): Analysis and Interpretation of Borehole Hydraulic Tests in Deep boreholes: Principles, Model Development and Applications. *Water Resources Research*, 23/7, 1341-1375.
- PRUESS, K. (1987, 1991): TOUGH, TOUGH2, User's Manual. Report LBL-20700, Lawrence Berkeley Laboratory, University of California, Berkeley, CA, USA.
- SENGER, R., MARSCHALL, P. & LAVANCHY, J.M.. (1998): Gas threshold pressure tests in deep boreholes for determining two-phase flow properties of the host rock at the proposed L/ILW repository, Switzerland. *Proceedings of the 21st Int. Symposium on the Scientific Basis for Nuclear Waste Management - MRS '97*. Davos, Switzerland.
- SENGER, R., DOMSKI, P. & WALTERS, D. (2002): OPA Geosynthesis: Coupled processes associated with gas flow through Opalinus Clay. Unpubl. Nagra Int. Rep., Wettingen, Switzerland.
- SETTARI, A. & WALTERS, D.A. (2001): Advances in coupled geomechanical and reservoir modeling with applications to reservoir compaction. *Society of Petroleum Engineers*, Paper SPE 51927.
- SOLER, J.M. (1999): Coupled transport phenomena in the Opalinus Clay: Implications for radionuclide transport. *Nagra Technical Report NTB 99-09*, Wettingen, Switzerland.
- STEPHANSON, O., JIN, L., & TSANG, C.F. (1996): Coupled Thermo-Hydro-Mechanical Processes of Fractured Media: Mathematical and Experimental Study, in, *Developments in Geotechnical Engineering*, 79. Elsevier, Amsterdam.
- SWARTZENDRUBER, D. (1962a): Non-Darcy flow behaviour in liquid-saturated porous media. *J. Geophys. Res.* 67/13.
- SWARTZENDRUBER, D. (1962b): Modification of Darcy's law for the flow of water in soils. *Soil Sciences* 93/1.
- THURY, M. & BOSSART, P. (1999): The Mont Terri rock laboratory, a new international research project in a Mesozoic shale formation, in Switzerland. *Engineering Geol.* 52, 347-359.
- THURY, M. & BOSSART, P., eds. (1999): Mont Terri rock laboratory. Results of the hydrogeological, geochemical and geotechnical experiments performed in 1996 and 1997. Swiss National Hydrological and Geological Survey, Geological Report No. 23, Bern, Switzerland.
- VALKO, P. & ECONOMIDES, M.J. (1997): Hydraulic fracture mechanics. John Wiley, New York.
- VAN GENUCHTEN, M.Th. (1980): A closed-form equation for predicting the hydraulic conductivity of unsaturated soils. *Soil Sci. Soc. Amer. J.*, 44, 892-898.
- VAN OORT, E. (1994): A novel technique for the introduction of drilling fluid induced borehole instability in shales. In: *Eurock '94*, Rotterdam, Holland. Balkema, 293-308.
- VINARD, P. & MCCORD, J. (1991): Factors Possibly Affecting Formation Static Pressure Estimates at Wellenberg. Unpubl. Nagra Int. Rep., Wettingen, Switzerland.
- VOIGT, H.D. & BAMBERG, H.F. (1995): Hydrodynamische Eigenschaften poröser Medien. In: *Geohydrodynamische Erkundung von Erdöl-, Erdgas- und Grundwasser-Lagerstätten* (F. Häfner, H.D. Voigt, H.F. Bamberg, M. Lauterbach, eds.), Wissenschaftlich-Technischer Informationsdienst, Zentrales Geologisches Institut Berlin, Jahrgang 26/1995 – Heft 1. Berlin, Deutschland.
- WAWERSIK, W.R., CARLSON, L.W., HENFLING, J.A., BORNS, D.J., BEAUHEIM, R.L., HOWARD, C.L. & ROBERTS, R.M. (1997): Hydraulic Fracturing Tests in Anhydrite Interbeds in the WIPP, Marker Beds 139 and 140. SAND95-0596. Albuquerque, NM: Sandia National Laboratories.
- WERMEILLE, S. & BOSSART, P. (1999) : Paleohydrological study on the surroundings of the Mont Terri Rock Laboratory. *Mont Terri Project Technical Report TR 99-01*, Institut Géotechnique SA, St-Ursanne.
- WONG, S.W. & HEIDUG, W.K. (1994): Borehole stability in shales: A constitutive model for the mechanical and chemical effects of drilling fluid invasion. In: *Eurock '94*, Rotterdam, Holland. Balkema, 251-257.
- WOOD, D.M. (1990): Soil behaviour and critical state soil mechanics. Cambridge University Press.
- YOUNG, A. & LOW, P.F. (1965): Osmosis in argillaceous rocks. *Am. Assoc. Pet. Geol.* 49(7), 1004-1008.

Mont Terri Technical Notes

- TN 96-02: A. Möri & M. Adler: Small scale mapping of niches (Excavation work during phase 1, spring 1996). Geotechnical Institute; Mont Terri internal, unpublished report.
- TN 96-03: Straumann et al.: Excavation of phase 1 niches: technical and engineering aspects. E+B; Mont Terri internal, unpublished report.

- TN 96-04: H. Dollinger & A. Möri: Phase 1 drilling and field mapping of drillcores. Geotechnical Institute; Mont Terri internal, unpublished report.
- TN 96-05: P. Holub "Borehole logging, Phase 1". Geotest; Mont Terri internal, unpublished report.
- TN 96-11: P. Bossart & M. Adler: Fluid logging and borehole fluid effects (experiments FM-A and BF). Geotechnical Institute; Mont Terri internal, unpublished report.
- TN 96-17: A. Rübel, J. Lippmann, K. Osenbrück & Ch. Sonntag: Stable isotopes and noble gases in pore water and rock samples of the Opalinus Clay at Mt. Terri (WA-B experiment) – Part I: Stable isotopes and noble gases in pore water". Institut für Umweltphysik, Universität Heidelberg. B.E. Lehmann & I.N. Tolstikhin: Part II: Helium and argon isotopes in rock samples. Physics Institute of the University of Berne & Geological Institute of the Kola Science Centre in Apatity, Russia; Mont Terri internal, unpublished report.
- TN 96-18: E. Wyss: GP (phase 1): Screening pulse tests in BGP-1. Solexperts; Mont Terri internal, unpublished report.
- TN 96-20: H. Dollinger, P. Bossart & Ch. Bühler: DT Drilling technique, Phase 1. Geotechnical Institute & Solexperts; Mont Terri internal, unpublished report.
- TN 96-21: S.T. Horseman: Guidelines for chemico-osmotic experiments in OPA. British Geological Survey; Mont Terri internal, unpublished report.
- TN 96-26: E. Wyss: GP (phase 1): Triple packer system and pressure recovery period PSR1. Solexperts; Mont Terri internal, unpublished report.
- TN 96-27: E. Wyss: GP (phase 1): Hydraulic test sequences RI1-RIS1, PSR2, PSR3 & RI1-RIS2. Solexperts; Mont Terri internal, unpublished report.
- TN 96-30: K. Watanabe & H. Kazama: Preliminary analysis of evaporation measurements in the Mont Terri Laboratory (Nov. 28 – Dec. 4 1996). Saitama University, Faculty of Engineering, Japan; Mont Terri internal, unpublished report.
- TN 97-01: G. Volckaert & T. Fierz: PP Experiment: design & functional tests. SCK·CEN & Solexperts; Mont Terri internal, unpublished report.
- TN 97-02: G. Volckaert & T. Fierz: PP Experiment: preliminary in situ test. SCK·CEN & Solexperts; Mont Terri internal, unpublished report.
- TN 97-03: G. Volckaert & T. Fierz: PP Experiment: in situ installation and first results. SCK·CEN & Solexperts; Mont Terri internal, unpublished report.
- TN 97-04: A. Möri, M. Adler & S. Wermeille: Phase 2 drilling and field mapping of drillcores. Geotechnical Institute; Mont Terri internal, unpublished report.
- TN 97-06: B. Vöggtli & P. Bossart: DT Experiment: swelling experiment on OPA drillcores. Geotechnical Institute; Mont Terri internal, unpublished report.
- TN 97-07: M. Adler & P. Bossart: FM-A Experiment: Results of fluid logging in borehole BFM-A2. Geotechnical Institute; Mont Terri internal, unpublished report.
- TN 97-08: A. Möri & P. Bossart: FM-B: Visualisation of in-situ matrix and flow porosity in the Opalinus Clay. Geotechnical Institute; Mont Terri internal, unpublished report.
- TN 97-18: U. Mäder: Flow mechanisms FM-C: diffusion type laboratory experiments on OPA from Mt. Terri – interim report. Rock-Water Interaction Group, University of Berne; Mont Terri internal, unpublished report.
- TN 97-21: A. Rübel, J. Lippmann, K. Osenbrück & Ch. Sonntag: Stable isotopes and noble gases in pore water of the Opalinus Clay at Mt. Terri (WS-B Experiment, Borehole BWS-A3). Institut für Umweltphysik, Universität Heidelberg; Mont Terri internal, unpublished report.
- TN 97-24: L. Schwark: WS-B Experiment: Organic geochemical and petrological characterisation of organic matter from the Opalinus Clay at the Mont Terri site. University of Köln; Mont Terri internal, unpublished report.
- TN 97-26: J.F. Harrington & S.T. Horseman: Osmotic Pressure Experiment (OP): Scoping experiments on osmotic transport in Opalinus Clay – Interim report. British Geological Survey; Mont Terri internal, unpublished report.
- TN 97-28: E. Wyss: Experiment GP, Phase 2: Hydraulic tests and gas threshold pressure test in a major tectonic fault. Solexperts; Mont Terri internal, unpublished report.
- TN 97-29: H. Rohler: Experiment GP, Phase 2: Ion-selective borehole logging – Borehole BGP-4. ETH Zürich; Mont Terri internal, unpublished report.
- TN 97-32: J. Adams & R. Gemperle: ED-A: Results of hydraulic tests performed with the Modular Mini-Packer System (MMPS). Solexperts; Mont Terri internal, unpublished report.
- TN 97-36: P. Holub: Borehole logging, Phase 2. Geotest; Mont Terri internal, unpublished report.
- TN 97-38: A. Pasquiou & J.C. Robinet: Hydrodynamic characterization of the Opalinus Clay. Eurogeomat; Mont Terri internal, unpublished report.
- TN 97-39: J.F. Harrington & S.T. Horseman: Laboratory experiments on hydraulic and osmotic flow in Opalinus Clay. British Geological Survey; Mont Terri internal, unpublished report.
- TN 98-11: K. Watanabe, H. Imai, H. Saegusa & F. Shidahara: Evaporation logging in-situ measurement. Saitama University, Hazama Corporation & PNC;

- Mont Terri internal, unpublished report.
- TN 98-15: L. Ortiz Amaya: GP Core laboratory tests. SCK-CEN; internal, unpublished report.
- TN 98-24: P.S. Domski, R.M. Roberts, R.K. Senger, J. Croisé & J.M. Lavanchy: Analysis of the BGP-1 RI2 & RIS2 and BGP-4 hydrotests conducted at the Mont Terri Rock Laboratory. Duke Engineering and Services & Colenco Power Engineering; Mont Terri internal; unpublished report.
- TN 98-25: J.M. Lavanchy & R.K. Senger: GP Experiment: Analysis of the BGP-4 GRI & GRIS gas threshold pressure", J. Croisé, D. Gilby. Colenco Power Engineering & Duke Engineering and Services; Mont Terri internal, unpublished report.
- TN 98-35: F. Rummel, Th. Hettkamp & U. Weber: DM Experiment: Laboratory experiments for the determination of deformation mechanisms and a constitutive law for time dependent deformation behavior of the Opalinus Clay (Phase 3). Mesy GmbH, Bochum; Mont Terri internal; unpublished report.
- TN 98-40: P. Holub: Borehole logging, Phase 3. Geotest; Mont Terri internal, unpublished report.
- TN 98-41: M. Mazurek: Mineralogical composition of Opalinus Clay at Mont Terri – A laboratory inter-comparison. University of Berne; Mont Terri internal, unpublished report.
- TN 98-46: D.J. Noy: Parameter estimates from 1D modelling of osmotic experiments. British Geological Survey; Mont Terri internal, unpublished report.
- TN 98-48: P. Bossart & M. Thury: WS-A Experiment: estimation of hydraulic conductivity based on inflow measurements. Institut Géotechnique & SNGHS; Mont Terri internal, unpublished report.
- TN 98-49: M. Hohner & P. Bossart: Geological, mineralogical, geochemical, geomechanical and hydraulic parameters of OPA derived by in-situ and laboratory experiments (Phases 1, 2 and partly 3). University of Barcelona & Geotechnical Institute; Mont Terri internal, unpublished report.
- TN 98-55: F. Rummel, Th. Hettkamp, U. Weber: DM Experiment: Laboratory experiments for the determination of deformation mechanisms and a constitutive law for time dependent deformation behavior of the Opalinus Clay (Phase 3). Mesy GmbH, Bochum; Mont Terri internal, unpublished report.
- TN 98-56: Konietzky: DM Experiment: Numerical back analysis of triaxial lab tests for the Opalinus Clay. ITASCA; Mont Terri internal, unpublished report.
- TN 98-58: T. Fierz: EDB Experiment: Rawdata report – Pore water pressures and deformation measurements. Solexperts; Mont Terri internal, unpublished report.
- TN 98-62: C. Enachescu, A. Schmid & J.V. Wozniwicz: DB Experiment: Deep borehole hydraulic testing. Golder Associates; Mont Terri internal, unpublished report.
- TN 98-63: H.P. Weber: Deep borehole experiment, geological description of drillcores. NAGRA; Mont Terri internal, unpublished report.
- TN 98-64: A. Mais: DI Experiment: mercury porosimetry and H₂O determination. University of Fribourg; Mont Terri internal, unpublished report.
- TN 99-05: T. Fierz & A. Portmann: GP Experiment: Instrumentation of borehole BGP-5 (Triple Packer System) and borehole BGP-6 (PP Piezometer). Solexperts; Mont Terri internal, unpublished report.
- TN 99-06: T. Fierz & M. Eichler: GP Experiment: Instrumentation of boreholes BGP-8 and BGP-9 with FIMs (fix installed micrometers). Solexperts; Mont Terri internal, unpublished report.
- TN 99-07: H.R. Fisch & M. Piedevache: GP Experiment (Phase 4): Results of hydraulic testing. Solexperts; Mont Terri internal, unpublished report.
- TN 99-08: H.R. Fisch & M. Piedevache: GP Experiment: Results of gas testing. Solexperts; Mont Terri internal, unpublished report.
- TN 99-18: A. Rübel, J. Lippmann & Ch. Sonntag: WS-A Experiment: Profiles of stable isotopes and noble gases in pore water across OPA. Institut für Umweltphysik, Universität Heidelberg; Mont Terri internal, unpublished report.
- TN 99-20: S. Wermeille, A. Möri, H. Steiger, M. Adler, M. Alig & B. Rathmayr: Phase 4, drilling campaign 4a and 4b: Drilling and field mapping of drillcores. Geotechnical Institute; Mont Terri internal, unpublished report.
- TN 99-22: R.T. Haarpaintner & G. Schaeren: Conditions géologiques et hydrogéologiques générales. Bureau Technique Norbert, Géologues-conseils; Mont Terri internal, unpublished report.
- TN 99-33: P. Holub: BF Experiment: Caliper and fluid logging. Geotest; Mont Terri internal, unpublished report.
- TN 99-49: H.R. Fisch: FM-C Experiment: Results of hydraulic testing in borehole BFM-C1. Solexperts; Mont Terri internal, unpublished report.
- TN 99-58: L. Ortiz: GP Experiment: Phases 4 and 5 (1998-2000) – Results of the laboratory hydraulic and gas testing. SCK-CEN; Mont Terri internal, unpublished report.
- TN 99-73: Various contributors: Second Mont Terri Workshop (1-4 June 1999): Compilation of abstracts and transparencies. 5 volumes; Mont Terri internal, unpublished report.
- TN 99-81: D.J. Noy & S.T. Horseman: OP Experiment: Design calculation. Determination of the osmotic pressure response of borehole BOP-1 to a change of borehole fluid. British Geological Survey; Mont

- Terri internal, unpublished report.
- TN 2000-01: J.L. Fuentes: HE Experiment: Status report and compilation of field data. AITEMIN; Mont Terri internal, unpublished report.
- TN 2000-06: K. Jäggi & P. Steffen: GS and GP-A Experiments: Mobilisation and borehole instrumentation of BGS-1 and BGS-2. SJ Geotec; Mont Terri internal, unpublished report.
- TN 2000-07: C. Enachescu, K. Jäggi, A. Schmid & J. Wozniwicz: GP-A Experiment: Pre-frac hydraulic and gas longterm tests in borehole BGS-2. Golder Associates & SJ Geotec; Mont Terri internal, unpublished report.
- TN 2000-10: C. Enachescu, K. Jäggi, R.J. Pine & A. Schmid: GS Experiment: Hydraulic fracturing in borehole BGS-2. Golder Associates and SJ Geotec; Mont Terri internal, unpublished report.
- TN 2000-11: T. Lagler & V. Siegel: GS Experiment: Optical imaging of BGS-1 and BGS-2. BLM; Mont Terri internal, unpublished report.
- TN 2000-12: T. Fierz & R. Wälchli: GS Experiment: Instrumentation of boreholes BGS-3 and BGS-4 with FIMs (Fix Installed Micrometers). Solexperts; Mont Terri internal, unpublished report.
- TN 2000-13: T. Fierz: GS Experiment: Deformation measurements in boreholes BGS-3 and BGS-4 with FIMs (Fix Installed Micrometers). Solexperts; Mont Terri internal, unpublished report.
- TN 2000-21: R. Senger, P. Domski, D. Walters & T. Setari: HA Experiment: Development of a coupled process model of fluid flow in the Opalinus Clay. Duke Engineering; Mont Terri internal, unpublished report.
- TN 2000-22a: L. Schlickenrieder & J. Croisé: HA Experiment: Conceptual Hydrogeological Model of the Site / Part A – Review of the Hydrogeological Data Base. Colenco; Mont Terri internal, unpublished report.
- TN 2000-42: H.R. Fisch & P. Bossart: OP Experiment: Fluid exchange in borehole BOP-1 with deionised water. The field data set. Solexperts & Geotechnical Institute; Mont Terri internal, unpublished report.
- TN 2000-43: D.J. Noy: OP Experiment: Simulation of fluid exchange carried out in borehole BOP-1". British Geological Survey; Mont Terri internal, unpublished report.
- TN 2000-44: D.J. Noy: OP Experiment: Simulation of fluid exchange carried out in borehole BOP-1. British Geological Survey; Mont Terri internal, unpublished report.
- TN 2000-58: D. Holton, A.R. Hoch & W.R. Rodwell: Mont Terri hydrogeological analyses: Coupled models of gas flow. AEA Technology; Mont Terri internal, unpublished report.

An Experimental and Modelling Study of Chemico-osmotic Effects in the Opalinus Clay of Switzerland

D.J. Noy, S.T. Horseman, J.F. Harrington, P. Bossart & H.R. Fisch

Recommended quotation:

Noy, D. J. et al. (2004): An Experimental and Modelling Study of Chemico-osmotic Effects in the Opalinus Clay of Switzerland. In: Heitzmann, P. ed. (2004): Mont Terri Project – Hydrogeological Synthesis, Osmotic Flow. Reports of the Federal Office for Water and Geology (FOWG), Geology Series No. 6.

Abstract

This programme of work on osmotic flow in Opalinus Clay comprised three main activities, a laboratory pilot study on samples, an *in situ* experiment in a borehole at the Mt Terri Rock Laboratory and a theoretical study supported by mathematical modelling.

The pilot study demonstrated that the shale behaves as a leaky semi-permeable membrane and that it was possible to generate a measurable flow of water by exposing a sample to a solute concentration gradient in the absence of a pressure gradient.

The equations for chemico-osmotically coupled flow and solute transport developed by Greenberg et. al. (1973) were used to assess the results of the laboratory experiments. Some aspects of the transient flows and the long term swelling behaviour seen in the data cannot be explained by the original equations and a modification to the definition of compressibility was proposed which improved the representation of these transient effects.

The modified equations were then applied to the interpretation of an *in situ* field experiment, undertaken at the Mont Terri Rock Laboratory, in which the fluid chemistry within a sealed borehole test interval was first equilibrated with the host rock pore-water and then changed suddenly for either fresh water or a hypersaline brine. A substantial pressure transient, with a magnitude of several metres of equivalent freshwater head, was observed, lasting for several months, which was due solely to the change of fluid chemistry. Matching the magnitude and duration of the response with the solution to the theoretical model equations provided estimates for the osmotic coupling coefficients of Opalinus Clay.

In addition to demonstrating the magnitude of the chemico-osmotic effects in Opalinus Clay and obtaining estimates for the osmotic efficiency, the study also provided evidence for two further important features of these processes. Firstly, the osmotic efficiency of the *in situ* material is greater than that of a laboratory samples. This may be a consequence of the greater disruption caused to the latter by the sampling process. Secondly, the osmotic efficiency of the *in situ* material is lower at high solute concentrations than when the pore fluid is dilute, confirming observations made by previous researchers.

Acknowledgements

We would like to thank the Mont Terri Partners, who have financed the osmotic pressure experiment, and who were quite generous when the budgets of the experiment were exceeded once again. These are: ANDRA (B. Vignal), IRSN (J.-Y. Boisson), NAGRA (M. Hugli and K. Kennedy) and SCK·CEN (B. Neerdael).- Furthermore we would like to thank the experiment delegates for their encouraging comments and good discussions. These are mainly A. Gautschi from Nagra, J.-M. Matray from IRSN and P. DeCannière from SCK·CEN. This report was reviewed by P. Soler, J.-M. Matray and P. DeCannière. We would like to thank the reviewers for their constructive reviews.

Contents

Abstract	97
Acknowledgements	98
Contents	99
List of tables	100
List of figures	101
1 Introduction	102
2 Theoretical model	105
2.1 Numerical solution	107
3 Laboratory study	109
3.1 Apparatus.....	109
3.2 Procedures	110
3.3 Test conditions	110
3.4 Results	111
4 Field experiment	114
4.1 Experimental set-up	114
4.2 Procedures	115
4.3 Results	115
5 Interpretation	117
5.1 Laboratory study	117
5.2 Borehole experiment.....	117
6 Conclusions	124
7 References	125
Mont Terri Technical Notes	126

List of tables

Table 3.1: Results of the controlled flow rate (CFR) test stages on the two specimens	111
Table 3.2: Results of the osmotic flow (OF) test stages on the two specimens	111
Table 4.1 Chemical analyses of the formation water in borehole BWS-A1 and samples of the test fluids.....	116
Table 5.1: Summary of parameters used in numerical modelling. Porosity was taken as 0.13 in all com- puter simulations and (*) refers to concentrations on either side of the laboratory sample NS01. (†) Phase 3 prediction was carried out using all the parameters from the Phase 2 interpretation except that the borehole solute concentration was set to 1.497 mol.dm ⁻³	117

List of figures

Figure 1.1 Plan of the Mt. Terri Underground Rock Laboratory showing the site of the Osmotic Pressure ("OP") Experiment and the sampling location for the laboratory test material in the SHGN niche	102
Figure 3.1: Schematic of the apparatus for the laboratory pilot study.....	109
Figure 3.2: Schematic of the pressure vessel and specimen assembly for the laboratory pilot study.....	110
Figure 3.3: Osmotic flow transient from stage 2 of NS01. Osmotic flow started shortly after the saline solution at one side of the disc was replaced with distilled water. The flow transient asymptotically approaches the steady-state flow condition	112
Figure 3.4: Volumetric strain against average effective stress for NS01 when subject to the pressure variations of CFR test stages 7 to 11, inclusive. Strain was calculated from net pump flows and corrected for apparatus compliance and the compressibility of liquid in the upstream system.....	112
Figure 4.1: Schematic of the equipment for the field experiment in the Mt. Terri Rock Laboratory in Switzerland. Pressure transducers are labelled P1 to P5.	114
Figure 4.2: The pressure evolution for Phase 2, replacement of the test section fluid with de-ionised water. The data have been plotted starting from 1 February 2000	116
Figure 4.3: The pressure evolution for Phase 3, replacement of the test section fluid with hyper-saline brine. The data have been plotted starting from 1 March 2002.....	116
Figure 5.1: Model predictions of flows and volumetric strain as a function of time using equations (15) and (21) compared to the data from laboratory pilot study NS01 Stage 2. Negative volumetric strain indicates swelling of the sample (the data for volumetric strain are off scale in this plot, c.f. Figure 5.2).....	118
Figure 5.2: Model predictions of flows and volumetric strain as a function of time using equations (25) and (26) compared to the data from laboratory pilot study NS01 Stage 2. Negative volumetric strain indicates swelling of the sample	119
Figure 5.3: Field data from Phase 2 of the BOP-1 borehole experiment compared to the model prediction using an osmotic efficiency derived from the laboratory study (see Table 5.1 - Phase 2 prediction).....	120
Figure 5.4: Data from Phase 2 of the BOP-1 borehole experiment compared to the model prediction based on optimised parameters (see Table 5.1)	120
Figure 5.5: Field data from Phase 3 of the BOP-1 borehole experiment compared to the model prediction using optimised parameters derived from the Phase 2 interpretation (see Table 5.1).....	121
Figure 5.6: Field data from Phase 3 of the BOP-1 borehole experiment compared to the model prediction based on optimised parameters (see Table 5.1)	121

1 Introduction

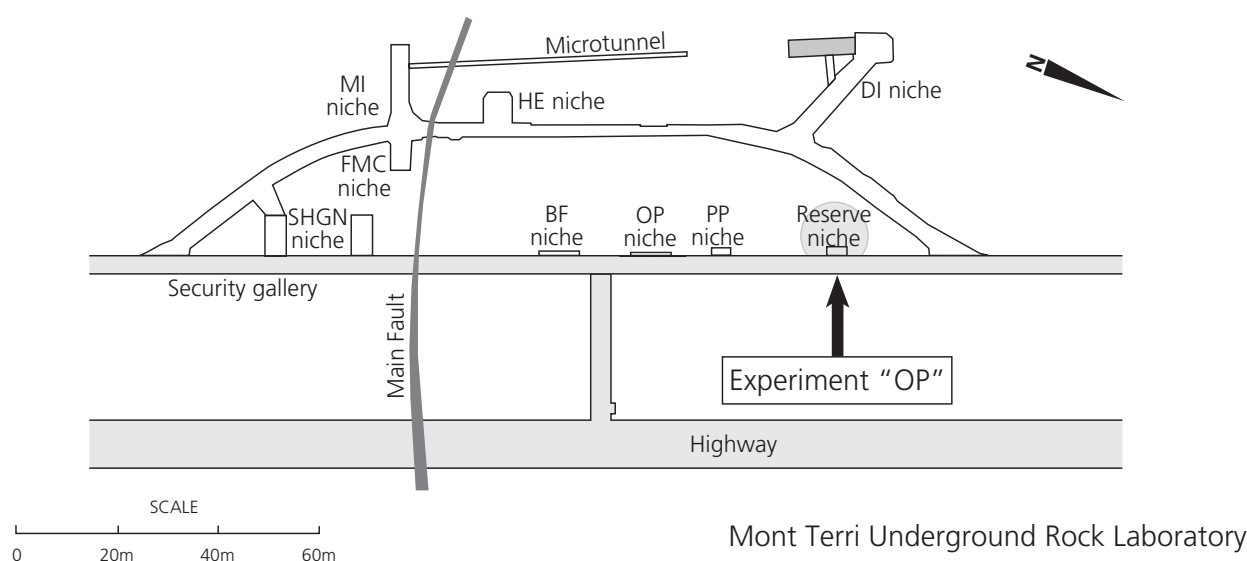
This report describes a study of chemico-osmotic effects in the Opalinus Clay formation aimed at estimating its osmotic efficiency. The study is comprised of three experimental stages (one laboratory based and two conducted *in situ*) with theoretical assessment and interpretation of each stages. In addition, the interpretations of the first two stages were used to make blind predictions of the outcomes of the following experimental stage.

The Opalinus Clay is a Middle Jurassic (Aalenian) marine shale which underlies large areas of north-western Switzerland. The formation is being studied by a multi-national consortium of companies as a typical example of a rock-type which might prove suitable as a repository host-medium for the geological disposal of radioactive waste (Thury and Bossart, 1999). Tunnelling operations for the N16 Transjuran Motorway connecting Belfort in France to the Swiss highway network afforded an excellent opportunity for research teams to investigate the hydrogeological, geochemical and geotechnical characteristics of this argillaceous rock formation under representative *in situ* conditions. The 3.9 km long Mt. Terri Tunnel links the towns of Delémont and Porrentruy and passes through a mountain ridge which, in structural geological terms, represents the northernmost anticline of the Jura Mountains. The Mt. Terri Rock Laboratory is located in a tunnel (known as the Security Gallery) driven parallel to the main motorway tunnel and through a 230 m long section of the Opalinus Clay. A number of side-

branches (or niches) were excavated in this section to provide suitable sites for experimental work (Figure 1.1). The shale formation dips at between 20° and 60° to the south-east and has a local thickness of around 160 m. The depth below ground surface varies between 250 and 320 m.

The Opalinus Clay at Mont Terri has been divided into five lithostratigraphical sub-units, largely on the basis of shale, sand and carbonate contents (Thury, 1999). The most shaly of these sub-units lies at the base of the formation and is around 80 m thick. It comprises argillaceous and marly shales with micas and nodular, bioturbated layers of marl. Clays and micas make up around 65% of the rock and the typical mineralogical composition is 10% illite-smectite mixed-layer clay, 17% illite, 30% kaolinite, 8% chlorite, 20% quartz, 7% calcite, 3% feldspars, 2% siderite, 1% dolomite/ankerite, 1% pyrite and 0.4% organic carbon. Porosity determined from weight loss by drying at 40°C is in the range 13 to 19%.

Osmosis can be defined as a bulk movement of solvent from a region where a solution has a low concentration of solutes to a region where the solute concentration is greater. Since the additional of solutes lowers both the chemical potential and the activity of the solvent, osmosis can also be interpreted as a flow down the chemical potential gradient of the solvent. In order to obtain osmotic flow, it is necessary to place a semi-permeable membrane between the two solutions. This membrane allows water molecules to pass,



Mont Terri Underground Rock Laboratory

Figure 1.1 Plan of the Mt. Terri Underground Rock Laboratory showing the site of the Osmotic Pressure ("OP") Experiment and the sampling location for the laboratory test material in the SHGN niche.

but restricts the passage of the solute. Chemico-osmosis is a specific example of a variety of so-called "coupled" transport processes in which a flux is driven by a "non-conjugate" thermodynamic force (Fargue et al., 1989; Soler, 1999). Other examples affecting the movement of the liquid phase are thermo-osmosis and electro-osmosis.

The membrane properties of clays are mainly due to electrical restrictions on the movement of the solute ions through the narrow pore spaces between negatively-charged clay mineral surfaces (Fritz, 1986). The charge on the surface of a clay particle together with the charge due to the balancing cations is referred to as the electrical double layer. If the cations are freely diffusing in solution, a very characteristic distribution of charge develops which is termed the diffuse double layer (DDL). Ions within the DDL are subject to two opposing tendencies. Electrostatic forces attract the cations towards the charged surface whereas diffusion tends to make them drift away to regions of lower concentration. Anions behave in the opposite way. Double Layer Theory provides a mathematical framework for the analysis of such problems. The Debye length is a measure of the thickness of the diffuse layer and is found to depend on temperature, the valence of the ions and the concentration of external equilibrium solution (Everett, 1988). When clay particles are in close proximity, the diffuse layers on each surface become overlapped and the negative electrical potential within the pore channels tends to repel any anions that attempt to enter or pass through them. This phenomenon is known as anion or Donnan exclusion (Bolt and de Haan, 1962). During solute transport, the dissociated ions of a salt must move together so as to maintain electroneutrality in the bulk solution. This means that any restriction on the mobility of the anions will also impose a restriction on the movement of the cations. The overall effect is that neutral water molecules can pass through a clay, but the motion of charged species in solution is impeded.

Experimental evidence of membrane behaviour in compact clay systems is now sufficiently conclusive that it cannot be ignored (Hanshaw, 1962; Kemper and Evans, 1963; Young and Low, 1965; Kemper and Rollins, 1966; Letey and Kemper, 1969; Banin and Low, 1971; Greenberg, 1971; Kharaka and Berry, 1973; Fritz and Marine, 1983).

Some of the more recent experimental work on chemico-osmotic effects in shales has been prompted by oil industry concerns about the effect of water-based drilling muds on the stability of exploration and production wells drilled through shale formations (Chenevert, 1970; Sherwood, 1993; Schlemmer et al., 2002). Wong and Heidug (1994) describe a laboratory

experiment designed to simulate some of the processes occurring in the borehole. Two porous plates with concave inner surfaces were arranged on opposite curved sides of a 15 mm diameter cylindrical shale sample so as to form two fluid chambers, each in contact with the rock. An axial load was applied to the sample and a constant confining stress was applied to the plates. The two chambers were filled with distilled water at 3.0 MPa pressure. Brine was then introduced into one of the chambers while maintaining the pressure constant. The pressure changes in the other chamber were monitored with time. In the most extreme response reported in this paper, the pressure fell from 3.0 MPa to only 0.2 MPa in around 10 hours. After this initial decline, the pressure gradually increased with time over a period of 200 hours. The authors do not state the salt concentration used in the experiment.

Van Oort (1994) describes a very similar experiment on the Cretaceous Pierre Shale of North America. A cylindrical sample was consolidated in a triaxial cell at a temperature of 65°C and a confining pressure of 5 MPa. Porous discs at each end of the sample enabled a fixed backpressure (i.e. external water pressure) of 0.35 MPa to be applied to the sample during consolidation process. The pressure in the upstream porous disc was then suddenly increased to 3.5 MPa. The pressure in the downstream disc was monitored with time and followed a path which asymptotically approached 3.5 MPa. After a period of about 230 hours it had reached 3.25 MPa. At this time, the fluid in the upstream disc was replaced by a 4.85 mol.dm⁻³ CaCl₂ brine, while maintaining the upstream pressure constant. The downstream pressure declined rapidly with time. After about 50 hours it had dropped by 1.95 MPa to around 1.3 MPa. It then slowly increased to 2.05 MPa over the remaining 320 hours or so of the experiment.

These two laboratory experiments confirm that shale samples act as non-ideal osmotic membranes. Water molecules rapidly migrated up the solute concentration gradient causing the low-concentration chamber (or filter) to show a pressure decrease. Because of the non-ideality of the shale membrane, salt was then able to slowly diffuse through the shale in the reverse direction. This gradually eliminated the concentration gradient, so that the osmotic pressure differential between the chambers became smaller with the passage of time.

Neuzil (1994; 2000) reports some field experiments on the effect of osmotic movement of water on head measurements in the Pierre Shale. Four boreholes were drilled, cased and completed with 20 m screens. Waters of differing chemistries were added to these

boreholes. Two contained saline solution (50 g dm^{-3} NaCl), one a solution more or less matched to the pore-water chemistry of the rock (5 g dm^{-3}) and the fourth almost pure water ($<0.1 \text{ g dm}^{-3}$). The water levels were monitored for a period of 7 years. The levels in the two boreholes containing the hypersaline solution rose by 3 and 4 metres, respectively. Little change was observed in the borehole containing the pore-water duplicate and there was a small decrease in level ($\sim 0.2 \text{ m}$) in the hole containing fresh water. Neuzil states "It is clear that osmotic pumping of pore fluids has occurred in this experiment, showing that the Pierre Shale *in situ* has the properties of an osmotic membrane". This is a very important experimental finding and probably represents the first *in situ* experiment to clearly demonstrate the phenomenon of chemico-osmosis in shale. Neuzil also monitored the salinity of each borehole solution with time. The hypersaline solution showed a significant decrease in salinity. The pore-water duplicate showed a fairly minor decrease. In the case of the fresh water, the salinity increased significantly with time. It is clear from the relatively small magnitude of the water level changes with time and the changes in salinity of the borehole fluids that the clay membrane is non-ideal and the osmotic movement of water up the concentration gradient of the pore solution is accompanied by the diffusional transport of ions in the reverse direction.

A number of researchers have suggested that chemico-osmosis might be the source of anomalous heads in some low permeability sedimentary sequences (Berry, 1960; Marine and Fritz, 1981; Neuzil, 2000). Hyperfiltration or reverse-osmosis has also been examined as a possible mechanism affecting brine chemistry in sedimentary basins (Berry, 1960; Coplen and Hanshaw, 1973; Graf, 1982). The implications of osmotic flow to the migration of radionuclides from a repository have also been examined by Soler (1999; 2001).

The theoretical description of the coupled flows have been based upon concepts of irreversible thermodynamics as presented by Kirkwood (1954) for biological membranes. The applicability of these concepts to the coupled flow of solute and water in sedimentary systems was demonstrated by Abd-el-Aziz and Taylor (1964), Letey and Kemper (1969), and Olsen (1969). These ideas have been adapted by Greenberg et. al. (1973) for application to general hydrogeological environments. The equations they developed are used in this report to assess a set of laboratory experimental observations carried out on samples of Opalinus Clay. It is shown that some aspects of the transient flows and the long term swelling behaviour seen in the data

cannot be explained by the original equations and a modification to the definition of compressibility is proposed which shows some improvement.

The modified equations are then applied to the interpretation of an *in situ* field experiment, undertaken at the Mont Terri Rock Laboratory, in which the fluid chemistry within a sealed borehole section is first equilibrated with the host rock pore-water and then changed suddenly for first fresh water and then, after a further period of equilibration, for a hypersaline brine. A substantial pressure transient, with a magnitude of several metres of equivalent freshwater head, is observed, lasting for several months, which is due solely to this change of fluid chemistry. Matching the magnitude and duration of the response with the solution to the theoretical model equations provides estimates of the osmotic coupling coefficients for the Opalinus Clay.

In summary, Section 2 of this report describes the theoretical approach used to interpret the chemico-osmotic coupled processes of fluid flow and solute transport. Section 3 outlines the initial laboratory pilot study and its main results, while Section 4 provides details of the three phases of the *in situ* experiment. Section 5 details the steps taken to interpret the various experimental results and Section 6 summarises the main conclusions from the study. During the course of this study a number of Technical Notes were published covering design and manufacture of field and laboratory equipment, development and modification of computer codes, and interim interpretations. A compilation of these notes is provided in the References.

2 Theoretical modell

Following Greenberg et al (1973), we adopt an extension of Darcy's law based on the ideas of irreversible thermodynamics which introduces the effects on groundwater of a solute concentration gradient

$$q = -\frac{k}{\mu}(\nabla p + \rho g \hat{z}) - k_{hc} \nabla c \quad (1)$$

where q is the volumetric flow rate, k is the intrinsic permeability, μ is the fluid viscosity, ρ is the fluid density, g is the acceleration due to gravity, \hat{z} is a unit vector along the z -axis, k_{hc} is the osmotic coupling coefficient, p is the fluid pressure, and c is the solute concentration. It may be noted that the choice of signs in equation (1) means that k_{hc} will always take a negative value. This emphasizes that osmosis acts in the opposite sense to Darcy flows relative to its respective driving potential (i.e. the solute gradient vs. the head gradient). To obtain the groundwater flow equation, equation (1) is combined with the fluid continuity equation and expressions for the solid and fluid phase compressibilities. The fluid continuity equation is

$$\frac{\partial(\phi \rho)}{\partial t} = -\nabla \cdot (\rho q) \quad (2)$$

where ϕ is the porosity. The left-hand side of equation (2) may be expanded to give

$$\phi \frac{\partial \rho}{\partial t} + \rho \frac{\partial \phi}{\partial t} = -\nabla \cdot (\rho q) \quad (3)$$

The compressibility of the solid phase skeleton may be defined by

$$\alpha = -\frac{1}{V} \frac{\partial V}{\partial \bar{\sigma}_{eff}} \quad (4)$$

where V refers to the total volume of an element of the porous medium and $\bar{\sigma}_{eff}$ is the mean effective stress defined by the Terzaghi relationship

$$\bar{\sigma} = \bar{\sigma}_{eff} + p \quad (5)$$

where $\bar{\sigma}$ is the mean total stress (Bear 1972). Provided that the total stress remains constant, we have $d\bar{\sigma}_{eff} = -dp$, which enables us to write

$$\alpha = \frac{1}{V} \frac{\partial V}{\partial p} \quad (6)$$

Writing the rock element volume $V = V_s + V_p$, where V_s is the solid volume (assumed constant) and V_p is the

pore volume, then we can express the porosity as

$$\phi = \frac{V_p}{V_s + V_p} \quad (7)$$

Hence, re-arranging for V_p in terms of V_s and ϕ gives

$$V = V_s + \frac{\phi V_s}{(1-\phi)} = \frac{V_s}{(1-\phi)} \quad (8)$$

Differentiating we have

$$\frac{\partial V}{V} = \frac{\partial \phi}{(1-\phi)} \quad (9)$$

Substituting equation (9) into equation (6) gives

$$\alpha \frac{\partial p}{\partial t} = \frac{1}{(1-\phi)} \frac{\partial \phi}{\partial t} \quad (10)$$

The compressibility of the fluid phase may be defined as

$$\beta \frac{\partial p}{\partial t} = \frac{1}{\rho} \frac{\partial \rho}{\partial t} \quad (11)$$

Combining equation (3) with equations (10) and (11) gives

$$\phi \beta \rho \frac{\partial p}{\partial t} + \alpha (1-\phi) \rho \frac{\partial p}{\partial t} = -\nabla \cdot (\rho q) \quad (12)$$

Introducing the equivalent freshwater head, $h = (p/\rho_0 g) + z$, where ρ_0 is the density of fresh water, and using equation (1) gives

$$\begin{aligned} (\phi \beta + \alpha(1-\phi)) \rho \rho_0 g \frac{\partial h}{\partial t} &= -\nabla \cdot (\rho q) = \\ \nabla \cdot \left(\rho \frac{k \rho_0 g}{\mu} \nabla h - \rho_0 g \hat{z} + \rho g \hat{z} \right) &+ \nabla \cdot (\rho k_{hc} \nabla c) \end{aligned} \quad (13)$$

The specific storage, S_s , and hydraulic conductivity, K , of the

$$S_s = \rho_0 g (\phi \beta + \alpha(1-\phi)) \quad K = \frac{k \rho_0 g}{\mu} \quad (14)$$

so that equation (13) becomes

$$\rho S_s \frac{\partial h}{\partial t} = \nabla \cdot (\rho K \nabla h - \rho_r \hat{z}) + \nabla \cdot (\rho k_{hc} \nabla c) \quad (15)$$

where

$$\rho_r = \left(\frac{\rho}{\rho_0} - 1 \right) \quad (16)$$

Greenberg et al (1973) show that the mass flux of solute, J , includes osmotic coupling terms in addition to the usual advective and diffusive transport terms,

$$J = -\left(cK'_{ch}(\nabla h + \rho_r \hat{z}) + D \nabla c\right) \quad (17)$$

where

$$K'_{ch} = k_{hc} \left(\frac{\rho_0 g}{RT} \right) + K \quad (18)$$

$$D' = D + ck_{hc} \quad (19)$$

and D is the effective diffusion coefficient, R is the gas constant, and T (K) is the absolute temperature. The continuity equation for solute mass is

$$\frac{\partial(\phi c)}{\partial t} = -\nabla \cdot J \quad (20)$$

Expanding the left-hand side as in equation (2) and using the definition of solid phase compressibility in equation (10) and the mass flux given in equation (17) gives the equation for solute transport as

$$\begin{aligned} \phi \frac{\partial c}{\partial t} + [\alpha(1-\phi)\rho_0 g] c \frac{\partial h}{\partial t} = \\ \nabla \cdot \left(cK'_{ch}(\nabla h + \rho_r \hat{z}) \right) + \nabla \cdot (D' \nabla c) \end{aligned} \quad (21)$$

Equations (15) and (21) together describe a coupled system which exhibits a chemico-osmotic type of behaviour. Initial assessments of the data presented below in Section 3 used these equations. However, it was found that the solutions were unsatisfactory in a number of aspects, particularly in the lack of any long term volume changes due to swelling. A modification to the above development is therefore suggested. It may be noted that equation (1) can be written in the form

$$q = -K \left(\nabla \left(h + \frac{k_{hc}}{K} c \right) + \rho_r g \hat{z} \right) \quad (22)$$

which in turn suggests that the Darcy flow in this modified form of the equation is responding to the gradient of an effective head, h' , given by

$$h' = h + \frac{k_{hc}}{K} c \quad (23)$$

The particular modification to the above development of Greenberg et al (1973) that is suggested is to extend the use of this effective head to the definition

of the solid phase compressibility given in equation (10). The new equation for the compressibility is thus

$$\frac{\partial \phi}{\partial t} = \alpha(1-\phi) \rho_0 g \left(\frac{\partial h}{\partial t} + \frac{k_{hc}}{K} \frac{\partial c}{\partial t} \right) \quad (24)$$

Making use of this leads to a modified form of equation (15)

$$\begin{aligned} \rho S_s \frac{\partial h}{\partial t} + \rho \left(\alpha(1-\phi) \rho_0 g \frac{k_{hc}}{K} \right) \frac{\partial c}{\partial t} = \\ \nabla \cdot (\rho K \nabla h + \rho_r \hat{z}) + \nabla \cdot (\rho k_{hc} \nabla c) \end{aligned} \quad (25)$$

It can be seen that the second term of this equation contains the solid phase component of the specific storage multiplied by the ratio of the osmotic coupling coefficient to the hydraulic conductivity. Similarly, the solute transport equation (21) becomes

$$\begin{aligned} \left(\phi + c \left[\alpha(1-\phi) \rho_0 g \right] \frac{k_{hc}}{K} \right) \frac{\partial c}{\partial t} + [\alpha(1-\phi) \rho_0 g] c \frac{\partial h}{\partial t} = \\ \nabla \cdot \left(cK'_{ch}(\nabla h + \rho_r \hat{z}) \right) + \nabla \cdot (D' \nabla c) \end{aligned} \quad (26)$$

It is found that the new terms in equations (25) and (26) lead to changes in the transient behaviour of the system that are consistent with that seen in the data and predict a significant degree of swelling as a result of changes in the solute concentration.

It may be noted that the equations presented here consider the osmotic flux to arise from the concentration gradient of a single solute. This relatively simple empirical approach should be adequate provided that the groundwater chemistry is simple (i.e. a single, or strongly dominant, dissolved component) and provided that the parameters are used consistently from cases to case, such as using an interpretation of experimental data in a prediction of borehole behaviour. However, to address more complex fluid chemistries a more rigorous approach will need to be developed, based upon the idea that the groundwater flows in response to a gradient of chemical potential. The chemical potential may then be expressed in terms of the pressure and the concentrations of all solutes to yield equations which could be reduced to those used here with appropriate simplifying assumptions. Such a development is beyond the scope of the current study. Finally, it may be noted that the terms "osmotic permeability" and "osmotic efficiency" are sometimes used when discussing chemico-osmotic effects. The relationship of these parameters to those used in the equations above may be conveniently explored by

considering the osmotic flow across a sample of thickness L in the presence of a solute concentration gradient but no pressure gradient. Equation (1) becomes

$$q = -k_{hc} \frac{\Delta c}{L} \quad (27)$$

where Δc is the concentration difference (mol.m^{-3}) across the sample, and k_{hc} is the osmotic coupling coefficient with dimensions ($\text{m}^5\text{mol}^{-1}\text{s}^{-1}$). This osmotic flow can also be written in terms of an "osmotic pressure" difference, $\Delta\Pi_0$ (Pa) by analogy with Darcy's law as

$$q = -\frac{k_{\Pi}}{\mu} \frac{\Delta\Pi_0}{L} \quad (28)$$

where k_{Π} is the "osmotic permeability" and μ (Pa.s) is the viscosity. The relationship between solute concentration and osmotic pressure is given by the van't Hoff equation

$$\Delta\Pi_0 = n\Delta c \cdot RT \quad (29)$$

where n is the number of dissociated ions formed when the salt goes into solution, R ($=8.314 \text{ J.mol}^{-1}\text{K}^{-1}$) is the gas constant, T (K) is the absolute temperature. Equating the flows in equations (27) and (28) and using equation (29) gives

$$k_{\Pi} = k_{hc} \left(\frac{\mu}{nRT} \right) \quad (30)$$

The "osmotic efficiency" of Kemper and Rollins (1966) is found by equating the flow rate due to an hydraulic pressure difference to the flow rate due to an osmotic pressure difference. The osmotic efficiency is then given by the ratio of the water pressure to the osmotic pressure. Combining Darcy's law for pressure driven water flow with equation (28) for the osmotic flow and rearranging gives

$$\frac{\Delta p}{\Delta\Pi_0} = -\frac{k_{\Pi}}{k} = -\frac{\left[\frac{k_{hc}\mu}{nRT} \right]}{\left[\frac{K\mu}{\rho g} \right]} = -\frac{k_{hc}}{K} \left[\frac{\rho g}{nRT} \right] \quad (31)$$

Thus, taking a slightly saline $\rho = 1030 \text{ kg.m}^{-3}$, $g = 9.81 \text{ m.s}^{-2}$, $R = 8.314 \text{ J.mol}^{-1}\text{K}^{-1}$, $T = 298 \text{ K}$ and $n = 2$ gives the

$$\text{Osmotic efficiency} \approx -2 \frac{k_{hc}}{K} \quad (32)$$

It may be noted that the parameter n in the van't Hoff

equation (29) may be reduced from the value of 2 assumed here in more concentrated solutions due to ion pairing effects. This would cause the true osmotic efficiency to be somewhat higher than is estimated from equation (32).

2.1 Numerical solution

The pair of equations (15) and (21), or the modified equations (25) and (26), form a system of coupled non-linear partial differential equations. To obtain solutions, the equations were discretized using central finite differences for the spatial derivatives, in Cartesian coordinates for the laboratory experiments and in radial coordinates for the borehole experiments.

The equations were also simplified by assuming a constant fluid density so that only a single spatial dimension needed to be considered, x or r , respectively. For the laboratory experiments it was sufficient to provide specified head and solute concentration values as the boundary conditions.

For the borehole experiments it is necessary to supplement the main equations with equations that represent the response of the sealed borehole section to the flows of fluid and solute. Fluid flows into the sealed borehole section, including for generality an external injection rate, work against the borehole storage to create changes to the head in the section. Thus the new equation required is

$$S_w \frac{\partial h_w}{\partial t} = Q_w - 2\pi r_w L \left(-K \frac{\partial h}{\partial r} - k_{hc} \frac{\partial c}{\partial r} \right)_{r=r_w} \quad (33)$$

where S_w is the borehole storage, defined as the rate of change of fluid volume per unit change of borehole head, Q_w is the rate of external injection of fluid into the sealed section (negative for abstraction), L is the length of the sealed Section, h_w is the head in the borehole and r_w is the borehole radius. It can be seen by comparison with equation (1) that the bracketed term on the right hand side of equation (33) is just the modified Darcy flux at the borehole wall.

In a similar way, an equation for the solute mass balance at the borehole boundary may be written as

$$V_w \frac{\partial c_w}{\partial t} = 2\pi r_w L \left(D \frac{\partial c}{\partial r} + cK_{ch} \frac{\partial h}{\partial r} \right)_{r=r_w} \quad (34)$$

where V_w is the volume of fluid in the test section and c_w is the solute concentration there. Thus, equations (33) and (34) provide the rate equations for the borehole boundary nodes and complete the system of coupled non-linear ordinary differential equations which

are integrated in time using Gear's backward difference formulae with either of the subroutine packages LSOIBT (Hindmarsh, 1982) or DASSL (Petzold, 1982). The codes OSMO1 and OSMO1R implement the solutions for Cartesian and radial geometries respectively (Noy, 1998).

3 Laboratory study

The objectives of the laboratory pilot study were to examine both the transient and steady-state osmotic flow of water through disc-shaped specimens of Opalinus Clay subject to a fixed solute concentration gradient. The required outputs were the osmotic efficiency and the resulting osmotic permeability of the shale. This demanded independent measurement of the hydraulic conductivity. Given the known swelling response of de-stressed shale when exposed to water, the apparatus was designed so that an isotropic confining stress could be applied to the shale discs during the flow measurements.

3.1 Apparatus

The apparatus consisted of five main components: (1) a sample assembly, (2) a pressure vessel and associated confining pressure system, (3) a fluid injection system, (4) a back-pressure system, and (5) a microcomputer-based data acquisition system (Figure 3.1). The pressure vessel, shown in Figure 3.2, comprised an Autoclave Engineers bolted single-closure reactor vessel, made from 316 stainless steel and pressure tested to 40 MPa. The shale disc was sandwiched

between two end-caps, each with a sintered stainless steel porous disc, and then jacketed in heat-shrink Teflon tubing to exclude confining fluid and provide a flexible pressure seal. Jubilee hose clamps and thin copper shims were used to compress the Teflon tubing against a Viton "O"-ring in each end-cap so as to provide a leak-tight seal. Each end-cap has a central inflow duct and a circular groove cut into the loading-bearing surface which was linked to an outflow duct. This arrangement allows the permeant to be flushed from the porous disc and connecting tubes when the solution chemistry is changed.

Flow rates were monitored or controlled using a pair of ISCO-500 Series D syringe pumps operating from a single digital control unit. The pump controller has an RS232 serial port that allows volume, pressure and flow rate data to be transmitted to an equivalent port of a personal computer. A program written in QBASIC prompted the pump controller to transmit data to the computer at pre-set time intervals. Data acquisition rates ranged from one scan per 15 minutes to one per 30 minutes. All pressure transducers were calibrated against a Druck PTX610 pressure transmitter using the manufacturer's calibration data.

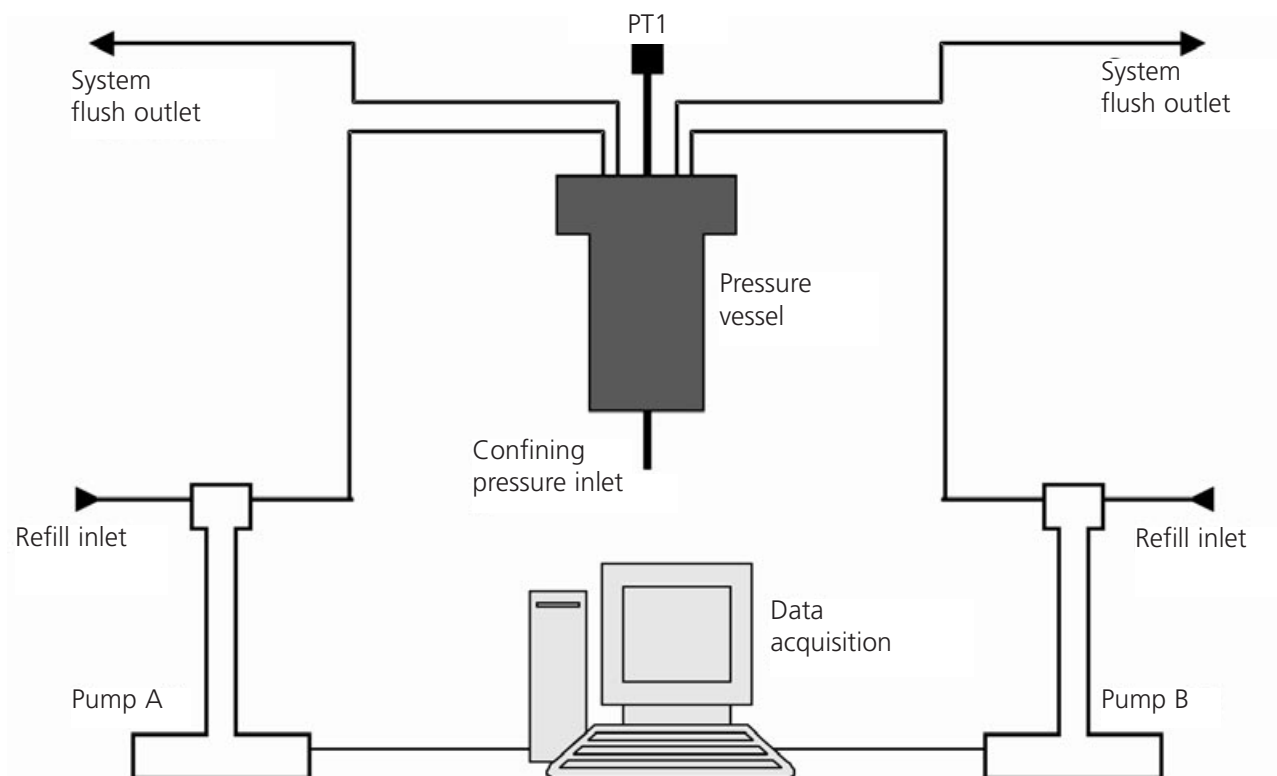


Figure 3.1: Schematic of the apparatus for the laboratory pilot study.

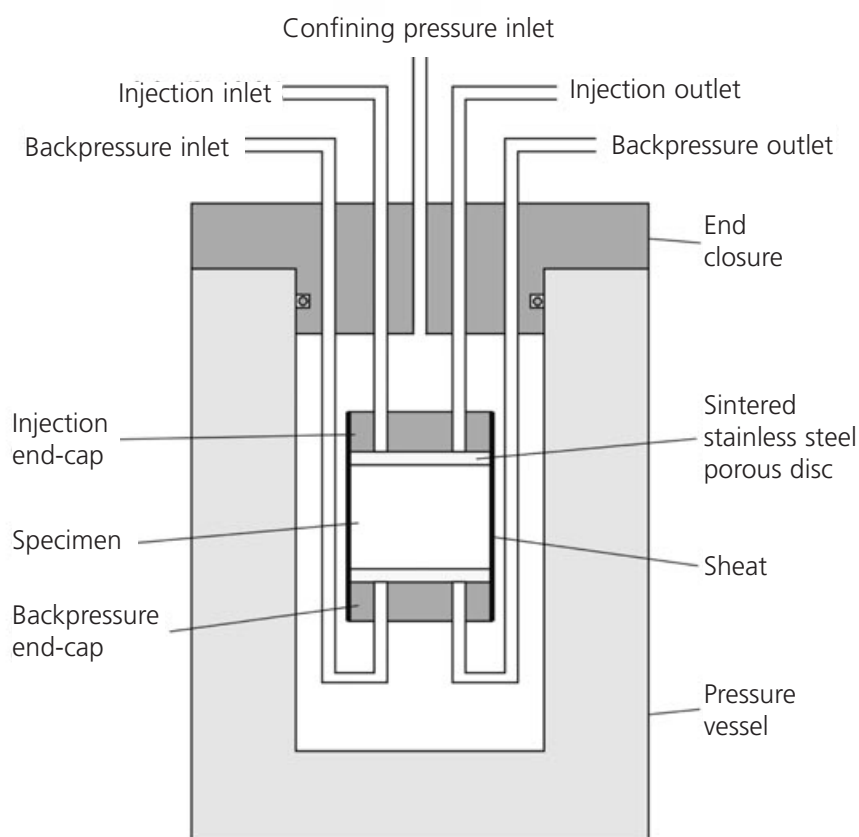


Figure 3.2: Schematic of the pressure vessel and specimen assembly for the laboratory pilot study.

3.2 Procedures

A block sample of Opalinus Clay was taken from SHGN niche of the Mt. Terri Rock Laboratory (Figure 1.1). The block was placed in a heat-sealable aluminized plastic bag. The bag was flushed with nitrogen prior to heat-sealing to prevent oxidation of secondary minerals during shipment. On receipt at BGS, two discs of nominal diameter 5.0 cm and thickness 1.0 cm were prepared from the block using a combination of dry coring, sawing and surface grinding. These discs were orientated so that the direction of flow during the experiments would be normal to the plane of the bedding.

The two porous discs were saturated with saline solution of appropriate chemistry (see below) before being placed in contact with the shale.

The test history for each specimen comprised a sequence of test stages (see Tables 3.1 and 3.2). During an equilibrium (EQ) stage, the specimen was exposed to the saline solution on both faces, with the same pressure at both ends. An osmotic flow (OF) stage was accomplished by replacing the solution at one end of the specimen with distilled water at the same pressure. Since there was no pressure gradient

across the disc during an OF stage, the measured water flow was solely due to osmosis. A constant flow rate (CFR) stage was used to evaluate the hydraulic permeability of the specimen and involved pumping the saline solution through the disc at a number of controlled flow rates, with the same solution present as a backpressuring fluid at the downstream end. Anticipating that the osmotic flow rates would be very small, the test programme was carefully designed to minimize systematic errors. Eight separate determinations of osmotic flow were made on the two specimens. The syringe pumps were interchanged and direction of flow varied to reduce uncertainties associated with pump performance and possible leakage of the apparatus. The experiments were performed in an air-conditioned laboratory at a temperature of 20 ± 0.3 °C.

3.3 Test conditions

The vertical total stress acting in the shale at the depth of the tunnel niche was estimated to be 5.5 MPa. This value was selected for the isotropic confining pressure in the experiments, except for stages 13

to 18 of NS01 where confining pressure was increased to 7.5 MPa. A fixed backpressure of 1.0 MPa was specified for all test stages. Guided by the results of previous pore-water squeezing experiments on Opalinus Clay, a 14.3 g dm^{-3} NaCl solution was made up to simulate the natural pore-water of the shale (Cave et al., 1998). The molar concentration of this solution is $0.245 \text{ mol.dm}^{-3}$ which, according to equation (29), gives an osmotic pressure of 1.19 MPa.

3.4 Results

Hydraulic permeabilities were calculated from the CFR test data by taking the pressure drop across the specimen at the steady-state asymptote of the pressure transient. The pressure transients were also analyzed using equation (15), neglecting the second term on the right since there was no concentration gradient in these test stages.

Table 3.1 summarizes the results of the controlled flow rate (CFR) test stages on the two specimens. The average effective stress is the difference between the isotropic confining stress and the average pore pressure. Hydraulic conductivity values calculated from flow under a steady-state pressure gradient were close

to those obtained by mathematical analysis of the pressure transients. The mean hydraulic conductivity, K , normal to bedding was $7.7 \times 10^{-14} \text{ m} \cdot \text{s}^{-1}$ and the mean specific storage, S_s , from all reliable determinations was 4.1×10^{-4} .

Table 3.2 summarizes the results of the osmotic tests stages on the two specimens. Osmotic flows were calculated by time-averaging the flow rates of the upstream and downstream pumps in the region of the steady-state asymptote of the flow transient. The osmotic permeability, k_{Π} , normal to bedding was calculated using equations (28) and (29). The osmotic coupling coefficient, k_{hc} , was then calculated using equation (30). Figure 3.3 illustrates the osmotic flow transient from stage 2 of NS01. The experimental noise seen in the curves is typical of the entire dataset and is indicative of practical difficulties in measuring the exceptionally small osmotic flow rates.

Volumetric strains were calculated assuming the mineral grains to be incompressible, taking the difference between the volume of water pumped in and the volume pumped out of the specimen and dividing the result by the original specimen volume. A correction was applied for apparatus compliance and compression of the liquid in the upstream system. Bulk compressibility, α , was estimated from the stress-strain

Specimen	Test stage	Average effective stress (MPa)	Controlled flow rate (ml.hr ⁻¹)	Hydraulic conductivity $K \text{ (m} \cdot \text{s}^{-1} \times 10^{14})$		Specific storage $S_s \text{ (m}^{-1} \times 10^4)$
				From steady-state gradient	From transient analysis	
NSO1	7	4.40	1.0	7.4	5.9	6.2
	8	4.32	2.0	7.8	7.0	4.3
	9	4.23	3.0	7.5	6.3	4.2
	10	4.31	2.0	7.2	-	-
	11	4.40	1.0	6.9	6.6	4.1
	17	6.39	1.0	6.6	6.3	3.4
	18	6.28	2.0	6.4	5.4	3.2
NSO2	5	4.41	1.0	8.4	8.7	3.9
	6	4.34	2.0	9.2	11.2	3.9
	7	4.28	3.0	10.0	11.1	4.1
	8	4.33	2.0	9.0	-	-
	9	4.37	1.0	6.2	-	-

Table 3.1: Results of the controlled flow rate (CFR) test stages on the two specimens.

Specimen	Test stages	Average effective stress (MPa)	Average osmotic flow rate ($\mu\text{L} \cdot \text{hr}^{-1}$)	Osmotic Permeability, $k_{\Pi} \text{ (m}^2 \cdot 10^{22})$	Osmotic coupling coefficient $k_{hc} \text{ (m}^2 \cdot \text{mol}^{-1} \cdot \text{s}^{-1} \times 10^{15})$	Osmotic efficiency
NSO1	2-5	4.50	0.4	4.6	-2.3	0.061
	14-15	6.50	0.3	3.5	-1.7	0.045
NSO2	2-3	4.50	0.1	1.3	-0.6	0.016

Table 3.2: Results of the osmotic flow (OF) test stages on the two specimens.

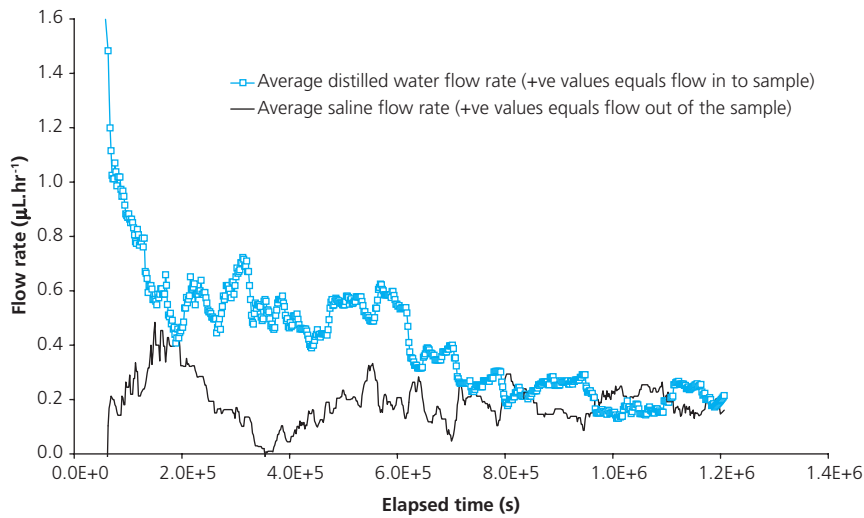


Figure 3.3: Osmotic flow transient from stage 2 of NS01. Osmotic flow started shortly after the saline solution at one side of the disc was replaced with distilled water. The flow transient asymptotically approaches the steady-state flow condition.

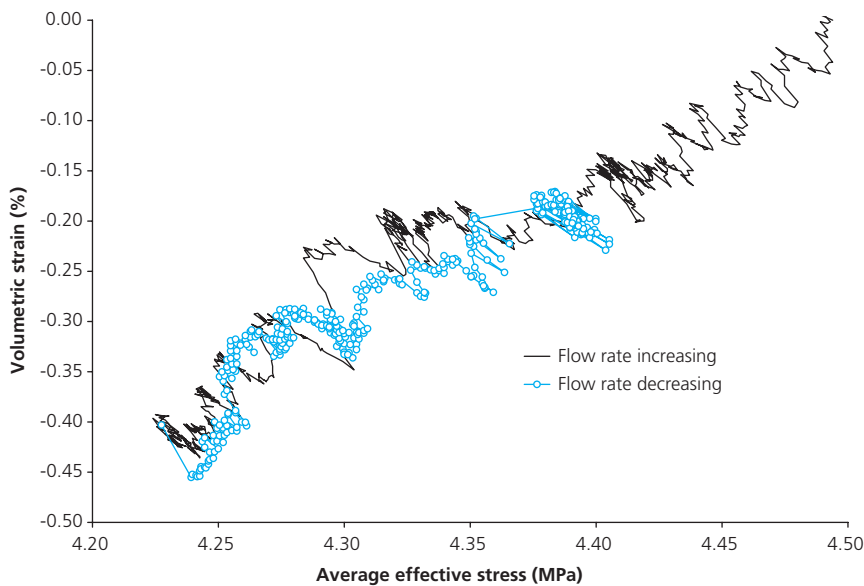


Figure 3.4: Volumetric strain against average effective stress for NS01 when subject to the pressure variations of CFR test stages 7 to 11, inclusive. Strain was calculated from net pump flows and corrected for apparatus compliance and the compressibility of liquid in the upstream system.

plots using least-squares regression analysis and then compared with the values calculated directly from specific storage using Equation (14).

With the application of an isotropic effective confining stress of 4.5 MPa, specimen NS01 exhibited time-dependent swelling for a period of around 5 days. The volumetric strain calculated on the basis of full saturation was around -1.3%, where the negative sign denotes a volume increase. When effective confining stress was increased to 6.5 MPa, a small amount of consolidation was observed. The observed tendency of the shale to swell at the lower stress and consolidate at the higher stress when exposed to a solution matched to the original pore-water suggests that the

(pre-excavation) mean normal effective stress at the sampling location in the Mt. Terri Rock Laboratory is bracketed by the values 4.5 and 6.5 MPa.

When one side of the specimen NS01 was exposed to distilled water, the shale swelled by -0.8% over a period of 10 days. Similar behaviour was observed for specimen NS02 which swelled by -0.9% over 26 days. Clearly, a simple change in the salinity of the pore-water can lead to a change in specimen volume. This observation prompted the modifications to the numerical model discussed in Section 5.1.

Figure 3.4 shows a plot of volumetric strain against average effective stress for specimen NS01 during controlled flow rate test stages 7 to 11, inclusive.

Increases in flow rate led to positive pressure transients which were accompanied by swelling. Flow rate decrements led to negative pressure transients accompanied by consolidation.

The strains associated with changes in pore-water pressure were found to be fairly reversible. These data give a compressibility, α , for a history of variable pore-water pressure and constant total stress of $1.3 \times 10^{-8} \text{ Pa}^{-1}$. Stages 17 and 18 at the higher effective stress gave a similar value of $1.7 \times 10^{-8} \text{ Pa}^{-1}$. Compressibility calculated from specific storage using Equation (14) was $5.4 \times 10^{-8} \text{ Pa}^{-1}$ for stages 7 to 11, inclusive, and $3.8 \times 10^{-8} \text{ Pa}^{-1}$ for stages 17 and 18.

All compressibility values are very high for a shale, suggesting that the volumetric strains must be largely determined by quasi-elastic deformation processes such as swelling and crack dilation. In order to test this hypothesis, a 3-D swelling test was performed on a 40 mm cube of the niche SHGN material (ISRM, 1981). The cube was immersed in distilled water and

the resulting swelling strains were measured in three mutually-perpendicular directions using Baty spring-loaded mechanical dial gauges. Within 15 minutes of immersing the cube, fractures began to open and small gas bubbles were expelled from the rock. The cube swelled preferentially in a direction normal to bedding by the combined processes of clay swelling, slaking and bedding plane crack dilation. The total volumetric strain after eight days of monitoring was -2.9% . The volumetric strains of the specimens during hydraulic and osmotic testing were clearly of the same order of magnitude as those during the swelling test. It is interesting to note that stage 13 of NS01 gave a significantly lower compressibility of $1.7 \times 10^{-9} \text{ Pa}^{-1}$ for the condition of variable total stress and constant pore-water pressure. It therefore appears that a change in pore-water pressure at fixed total stress has a significantly larger effect on specimen volume than does a change in total stress at fixed pore-water pressure.

4 Field experiment

The main objective of the *in situ* experiment was to examine the sensitivity of the equilibrium pressure (or head) in a borehole in Opalinus Clay to changes in the salinity of the borehole fluid. Experimental guidelines were that: (a) the pressure measurements should be undertaken within a packed-off test section of a vertical borehole, (b) the packer assembly should be mechanically stiff (i.e. non-compliant), (c) there should be negligible leakage of test fluid, (d) the volume of the test interval should be minimized to reduce the time duration of the pressure transients, (e) the test interval and associated pipework should not contain a compressible gas phase, and (f) temporal changes in the salinity of the test fluids should be monitored (Horseman, 1996).

The field experiment was sited in the OP niche which is adjacent to the Security Gallery of the Mt Terri Rock Laboratory (see Figure 1.1). The Opalinus Clay in this locality corresponds with the lowermost shaly unit identified by Thury (1999). The shale displays strong bedding anisotropy, dips at about 40 degrees towards SSE and is fairly homogenous, with few tectonic fractures. Unloading fractures within the excavation disturbed zones of the tunnel and experimental niche do not extend more than 1 m into the floor.

For the purposes of discussion here, the experiment has been divided into three phases. Phase 1 covers the period starting from 25 September 1997 when the borehole was drilled. Phase 2 starts on 16 February 2000 when de-ionised water was introduced into the test interval and Phase 3 starts on 6 March 2002 when the hypersaline brine solution was introduced.

4.1 Experimental set-up

Borehole BOP-1 was drilled on 25 September 1997 using compressed air as a flushing medium. The 101 mm diameter borehole was drilled vertically downwards to a depth of 8 m. Borehole stability was excellent and no macroscopic borehole breakouts were observed after drilling. The interval 6.2 to 8.0 m was found to comprise unfractured homogeneous gray shale and was selected for the test.

Figure 4.1 is a schematic of the equipment for the experiment. A hydraulic packer and slotted screen were positioned to give a test interval with a length of 1.5 m, a diameter of 0.096 m and a fluid volume of 0.00425 m³. The test interval was fitted with a piezometer.

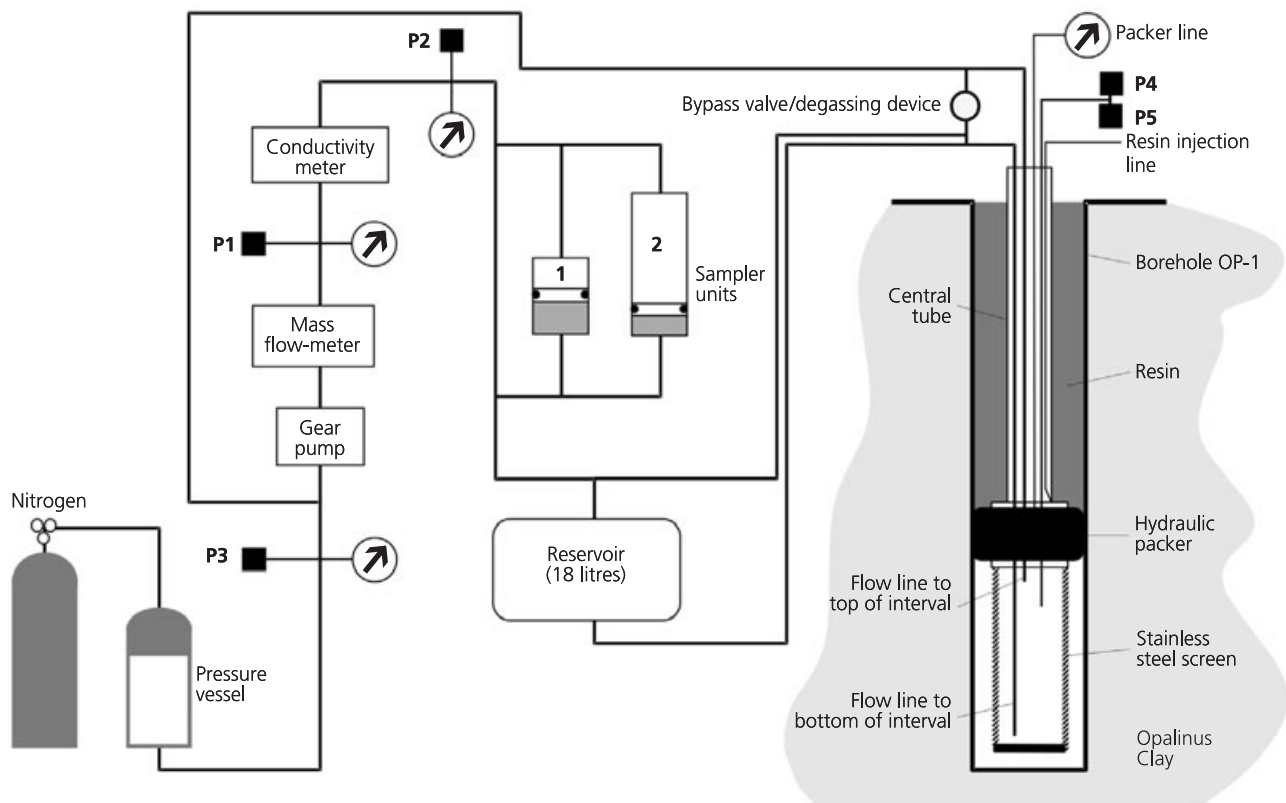


Figure 4.1: Schematic of the equipment for the field experiment in the Mt Terri Rock Laboratory in Switzerland. Pressure transducers are labelled P1 to P5.

The main technical challenge of the experiment was how to exchange the test fluid with a new fluid without changing the downhole pressure. This was considered necessary because the hydromechanical responses associated with any change in interval pressure might lead to unnecessary complications in the interpretation of the data. After some preliminary experimentation, it was found that the test interval could be effectively flushed by passing through the system a volume of fluid at least three times that of the test interval. The reservoir shown in the schematic is made up of inclined stainless steel tubes linked together to give a total capacity of 0.018 m³. This reservoir also served as a receiver for the displaced fluid. The exchange was accomplished using gear pumps, with a mass flow meter to determine flow rate. The two sampling units allowed some of the fluid in the test interval to be withdrawn for chemical analysis. An electrical conductivity meter was used to indicate the progress of a fluid exchange. The interval pressure was maintained by adjusting the pressure of nitrogen gas in the headspace of a pressure vessel linked into the up-hole pipework. Guided by experience during the first fluid exchange, the surface equipment was slightly modified at the end of Phase 2 to enable trapped air to be more easily removed. A data acquisition system was installed in the niche to continuously monitor: (a) interval pressure, (b) pressure at selected points in the up-hole circuit, (c) pump flow rate, and (d) electrical conductivity.

4.2 Procedures

The packer was inflated to a pressure of 2 MPa using water. The packer pressure fell by 0.5 MPa over the first day and then remained stable. The tightness of the packer seal was checked by applying an under-pressure of 80 mbar using a vacuum pump. Finally, the annulus between packer and borehole mouth was filled with an epoxy resin in order to provide a really tight test interval.

The flow and pressure measuring lines were flushed with CO₂ and then filled with a water. Since the solubility of CO₂ in water is much greater than that of air, this procedure was adopted to remove any free gas from the up-hole system. The water used in this first phase of the experiment was a synthetic pore solution known in the Mt Terri Project as "Pearson Type A1 water". The composition of this solution is close to that of the formation pore-water (Pearson et al., 1999).

After borehole completion, the pressure evolution was monitored for approximately two years. During this

first phase of the experiment, the test fluid became fully equilibrated with the surrounding Opalinus Clay pore-water. In the second phase, the original test fluid was sampled and replaced with de-ionised water and the fluid was allowed to equilibrate with formation water for another two years. In the third and last phase, the test fluid was replaced with a 100 g dm⁻³ NaCl solution.

4.3 Results

The fully equilibrated test interval pressure at the end of Phase 1 was 900 ± 20 kPa. The data reveal a small seasonal periodicity, with slightly higher pressures in summer and lower in winter. All pressure values quoted in this section were measured by a transducer reading absolute pressure.

The pressure evolution for Phase 2 after replacement of the original test fluid with de-ionised water is shown in Figure 4.2. At the time of shut-in of the test interval the pressure was 893 kPa. Pressure began to fall and reached a minimum of 812 kPa after 52 hours, a drop of 81 kPa. After reaching the minimum pressure, the interval pressure began to slowly increase, reaching a value of about 850 kPa by the end of March 2000. Pressure continued to slowly increase.

The pressure evolution for Phase 3 after replacing the test fluid with the hypersaline solution is shown in Figure 4.3. At the time of shut-in, the interval pressure was 930 kPa. Pressure then began to rise, reaching a maximum of 1082 kPa after 221 hours, an increase of 152 kPa. After reaching the maximum pressure, the pressure slowly began to decrease, reaching a value of about 1050 kPa by end of April 2002. There were no signs of equilibration and the interval pressure continued to slowly decrease.

Chemical analyses of the test fluid samples at the time of fluid replacement are presented in Table 4.1. Also shown is an analysis of formation water from borehole BWS-A1 which was drilled in the same shaly facies of the Opalinus Clay as the osmosis borehole. Other than easily explained differences in alkalinity and total organic carbon, the fully-equilibrated test fluids at end of Phases 1 and 2 have a compositions which are very close to the formation water from borehole BWS-A1. Since the fluid introduced into the test interval at the start of Phase 2 was distilled water, the analysis shows that the main chemical constituents of the pore-water were able to freely diffuse into the test interval over a period of two years. When measured over this timescale, the shale membrane is clearly very leaky. The test fluid composition at the start of Phase 3 dif-

Species	Concentration (mg · dm ⁻³)			
	Pore-water	Test fluid	Test fluid	Test fluid
	BWS-A1	End Phase 1	End Phase 2	Start Phase 3
Sodium	5610	5750	5330	34900
Potassium	65	55	48	17
Magnesium	344	476	455	17
Calcium	570	715	635	35
Strontium	36	32	39	<10
Chloride	10395	10240	9340	52400
Bromide	36	33	32	<40
Sulphate	1251	1314	1175	25
Alkalinity (HCO ₃ ⁻)	36	332	298	63
Total organic carbon	38	5	5	1
Total dissolved solids	18381	18952	17357	87508

Table 4.1 Chemical analyses of the formation water in borehole BWS-A1 and samples of the test fluids.

fers from that of the made-up brine suggesting that some degree of mixing occurred during the fluid exchange.

Taken collectively, the results of the *in situ* experiment demonstrate that hydraulic head measurements in the Opalinus Clay show a measurable but quite small sensitivity to changes in the chemistry of the fluid in the test interval. The transient responses associated with osmotic flow appear to be temporary and of limited

duration and eventually diffusive leakage through the leaky shale membrane eliminates the concentration gradient. There are obvious similarities between the field-scale responses from the Mt Terri Rock Laboratory and the laboratory-scale pressure responses in the tests performed by Wong and Heidug (1994) and van Oort (1994), suggesting that this behaviour is not specific to the Opalinus Clay.

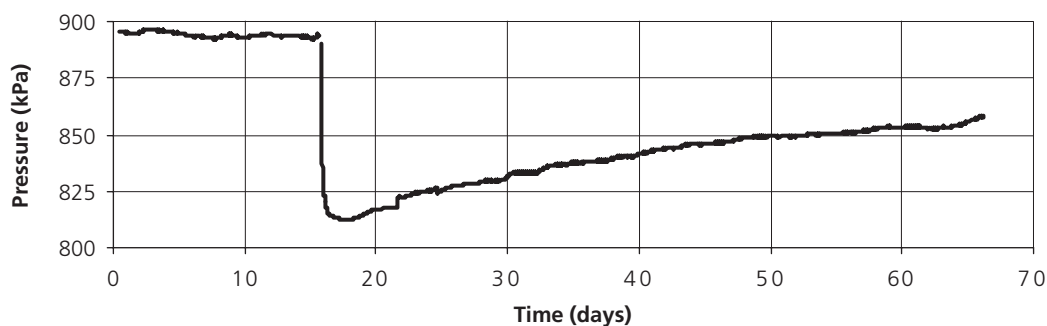


Figure 4.2: The pressure evolution for Phase 2, replacement of the test section fluid with de-ionised water. The data have been plotted starting from 1 February 2000.

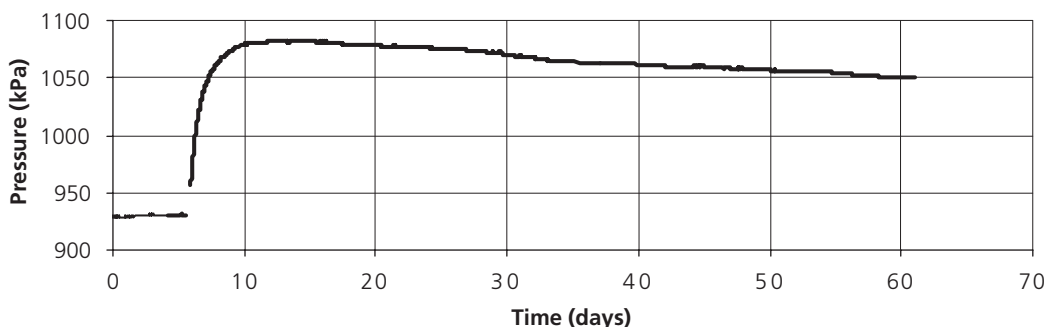


Figure 4.3: The pressure evolution for Phase 3, replacement of the test section fluid with hypersaline brine. The data have been plotted starting from 1 March 2002.

5 Interpretation

5.1 Laboratory study

The pilot study experiments clearly demonstrate the existence of osmotically-driven water flow in Opalinus Clay samples. Long term steady state flow rates that have been measured are readily converted to estimates of the osmotic permeability using the gradient of the solute concentration. However, it was a more detailed examination of the transient behaviour of the system that suggested the modified theoretical treatment indicated by equations (24)-(26).

The response obtained by the solution of equations (15) and (21), the original version of the model, using the parameter values listed in Table 5.1, is shown in Figure 5.1. There are two important features to note about these plots. Firstly, the modelled flow rates in and out of the sample quite quickly reach a state in which they are close to the eventual steady state and there is a prolonged period during which the flow out of the sample slightly exceeds that of the flow in. Secondly, the estimated volumetric strain rapidly attains a maximum value of about 0.02% and then relaxes gradually back towards zero. This model does not predict any long term volumetric swelling of the sample. In contrast, the solution to equations (25) and (26), using the same set of parameter values, is shown in Figure 5.2, together with the data from Stage 2 of the tests on sample NS01. It can be seen that the modelled transient approach to the steady state is of a more protracted duration and at all times the flow rate into the sample exceeds that out of it. Although the data are very noisy, it does appear that the new model provides a more realistic representation of the system response. The predictions of the new model for the volumetric strain are much more clearly reflecting the data from the experiment since they show the development of a long term volumetric strain of 0.8% on a timescale similar to that measured.

It was concluded that the pilot study provided good support for the suggested application of the effective head defined in equation (23) to the definition of compressibility as given in equation (24) since it both provides an improved representation of the transient flows and an explanation for the observed swelling of the shale samples in response to a change of pore fluid chemistry. Equations (25) and (26) were therefore used for all remaining model calculations.

5.2 Borehole experiment

As indicated above in Section 4, the *in situ* borehole test was carried out in three phases with extended periods in between to allow the borehole fluid and formation pore-water to return to their *in situ* composition. For the second phase the fluid in the borehole test section was replaced with de-ionised water and for the third phase the test section fluid was replaced with a hypersaline brine. By making use of the laboratory results it was possible for the interpretation of each phase to proceed by means of an initial predictive calculation based on previous data followed by parameter estimation calculations in which a good fit to the data was sought.

The compositions of the test fluids are shown in Table 4.1 and it is found that the total dissolved solids (TDS) in the three fluids amount to about $19.0 \text{ g} \cdot \text{dm}^{-3}$, $17.4 \text{ g} \cdot \text{dm}^{-3}$ and $87.5 \text{ g} \cdot \text{dm}^{-3}$ respectively. In each case the dominant component is the dissolved NaCl, although the *in situ* pore-water is clearly somewhat more complex, as would be expected, with significant concentrations of calcium, magnesium, sulphate, and bicarbonate. For the purposes of the model calculations, the TDS values were converted to NaCl concentrations of $0.324 \text{ mol} \cdot \text{dm}^{-3}$ and $0.298 \text{ mol} \cdot \text{dm}^{-3}$ for the pore-waters and $1.497 \text{ mol} \cdot \text{dm}^{-3}$ for the brine.

Parameter	Laboratory study interpretation	Borehole experiment		
		Phase 2 prediction	Phase 2 interpretation †	Phase 3 interpretation
Borehole solute concentration ($\text{mol} \cdot \text{dm}^{-3}$)	0(*)	0	0	1.497
Formation solute concentration ($\text{mol} \cdot \text{dm}^{-3}$)	0.245(*)	0.298	0.298	0.298
Hydraulic conductivity ($\text{m} \cdot \text{s}^{-1}$)	7.5×10^{-14}	1.9×10^{-13}	1.9×10^{-13}	1.9×10^{-13}
Diffusion coefficient ($\text{m}^2 \cdot \text{s}^{-1}$)	1.0×10^{-10}	1.0×10^{-10}	1.4×10^{-10}	3.3×10^{-11}
Solid phase compressibility (Pa^{-1})	3.2×10^{-7}	3.4×10^{-9}	3.4×10^{-9}	3.4×10^{-9}
Osmotic coupling coefficient ($\text{m}^5 \cdot \text{mol}^{-1} \cdot \text{s}^{-1}$)	-1.73×10^{-15}	-4.38×10^{-15}	-7.72×10^{-15}	-3.45×10^{-15}
Osmotic efficiency	0.046	0.046	0.081	0.036
Borehole storage (m^2)	N/A	9.22×10^{-7}	2.80×10^{-7}	4.25×10^{-7}

Table 5.1: Summary of parameters used in numerical modelling. Porosity was taken as 0.13 in all computer simulations and (*) refers to concentrations on either side of the laboratory sample NS01. (†) Phase 3 prediction was carried out using all the parameters from the Phase 2 interpretation except that the borehole solute concentration was set to $1.497 \text{ mol} \cdot \text{dm}^{-3}$.

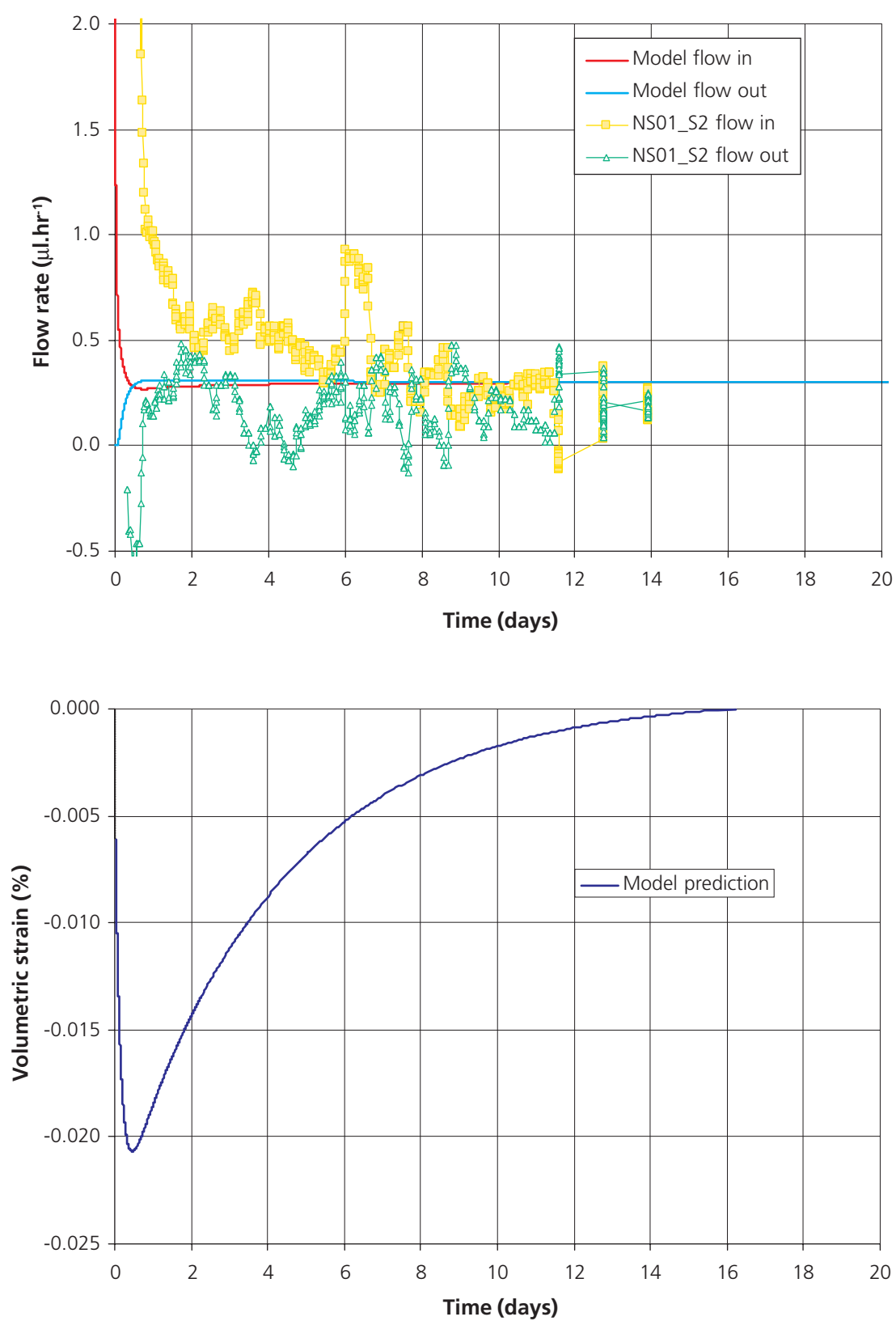


Figure 5.1: Model predictions of flows and volumetric strain as a function of time using equations (15) and (21) compared to the data from laboratory pilot study NS01 Stage 2. Negative volumetric strain indicates swelling of the sample (the data for volumetric strain are off scale in this plot, c.f. Figure 5.2).

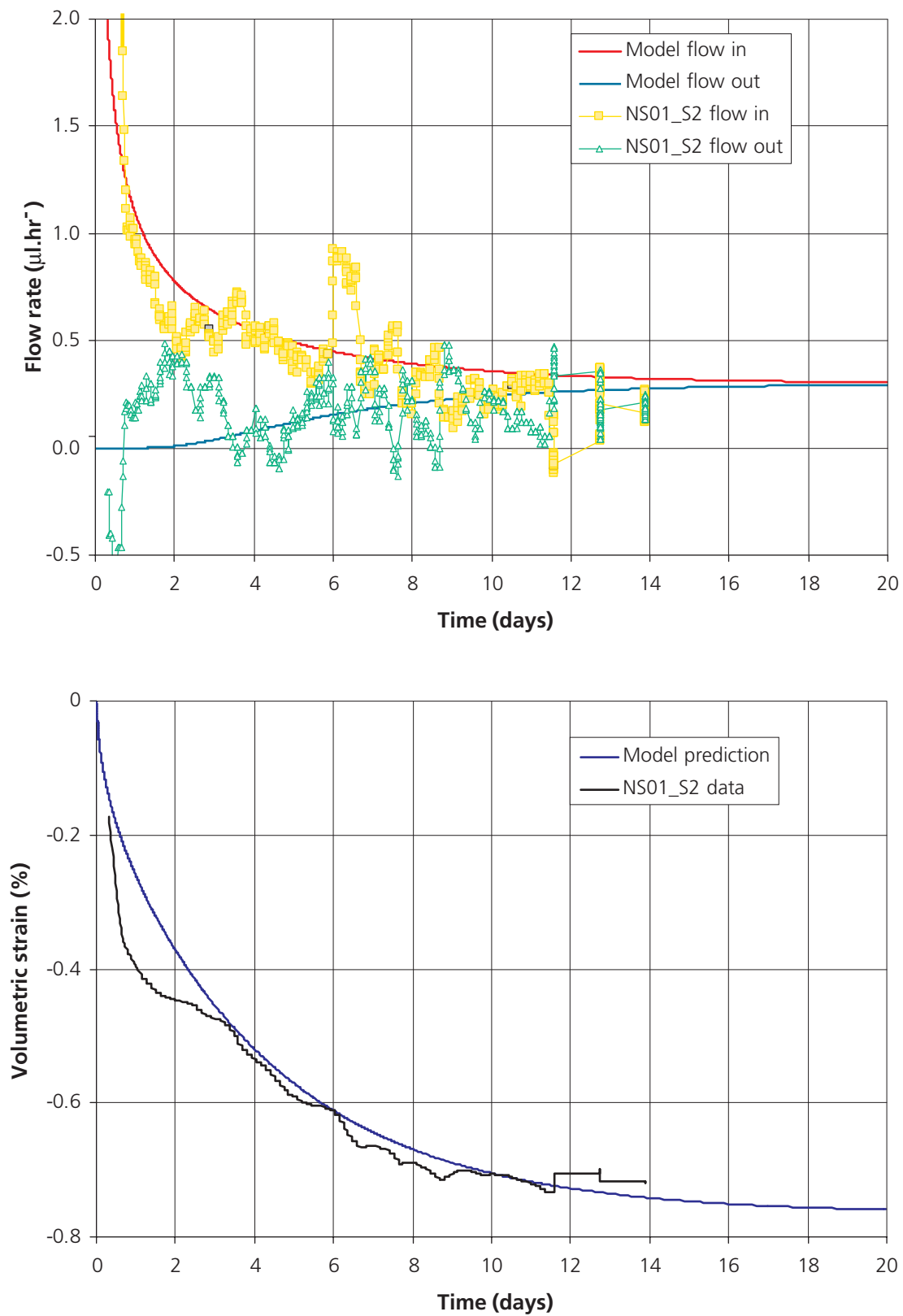


Figure 5.2: Model predictions of flows and volumetric strain as a function of time using equations (25) and (26) compared to the data from laboratory pilot study NS01 Stage 2. Negative volumetric strain indicates swelling of the sample.

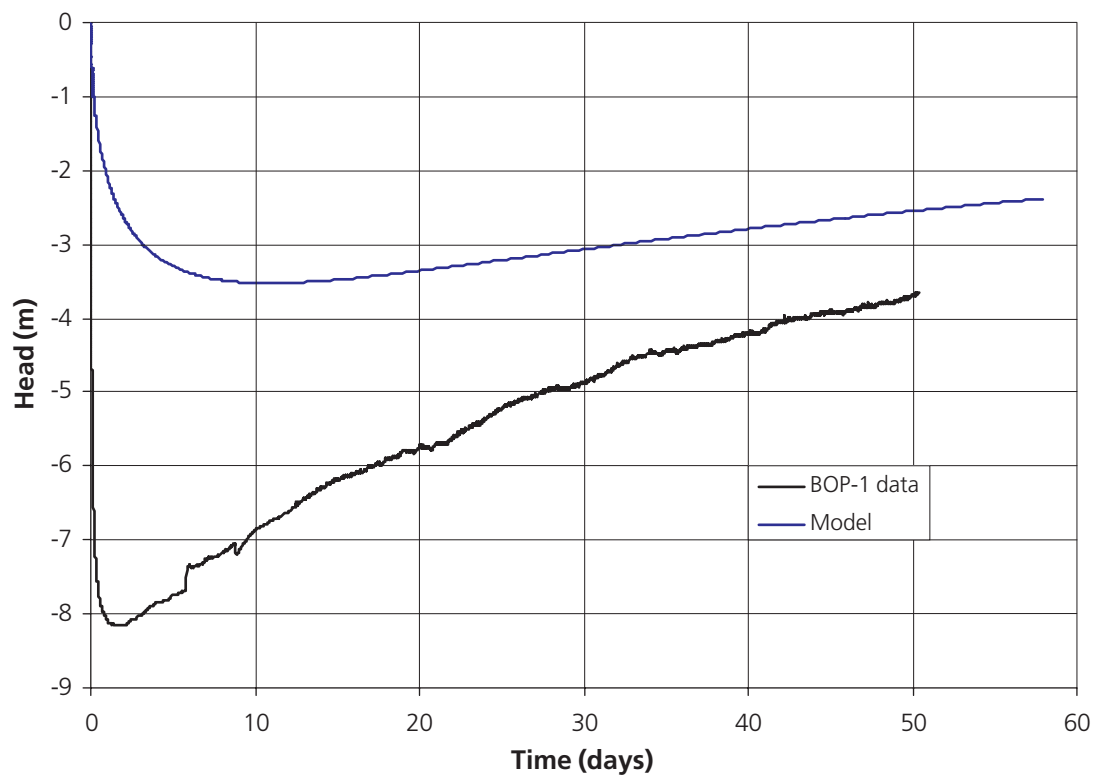


Figure 5.3: Field data from Phase 2 of the BOP-1 borehole experiment compared to the model prediction using an osmotic efficiency derived from the laboratory study (see Table 5.1 - Phase 2 prediction).

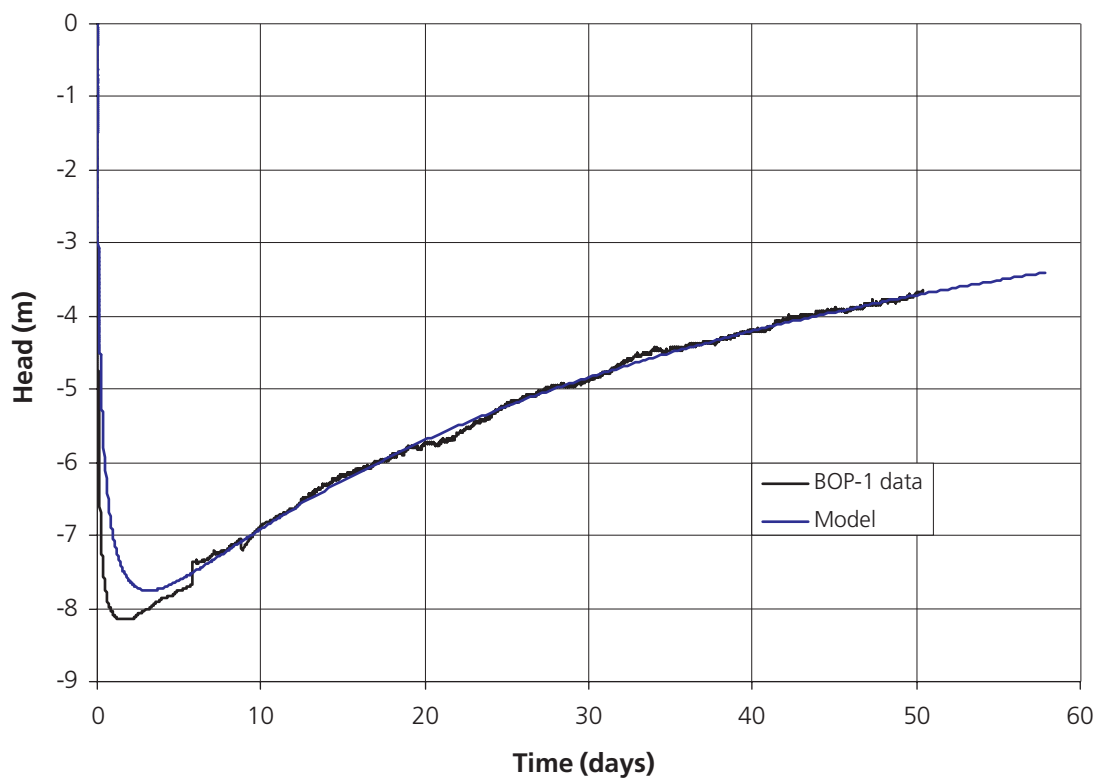


Figure 5.4: Data from Phase 2 of the BOP-1 borehole experiment compared to the model prediction based on optimised parameters (see Table 5.1).

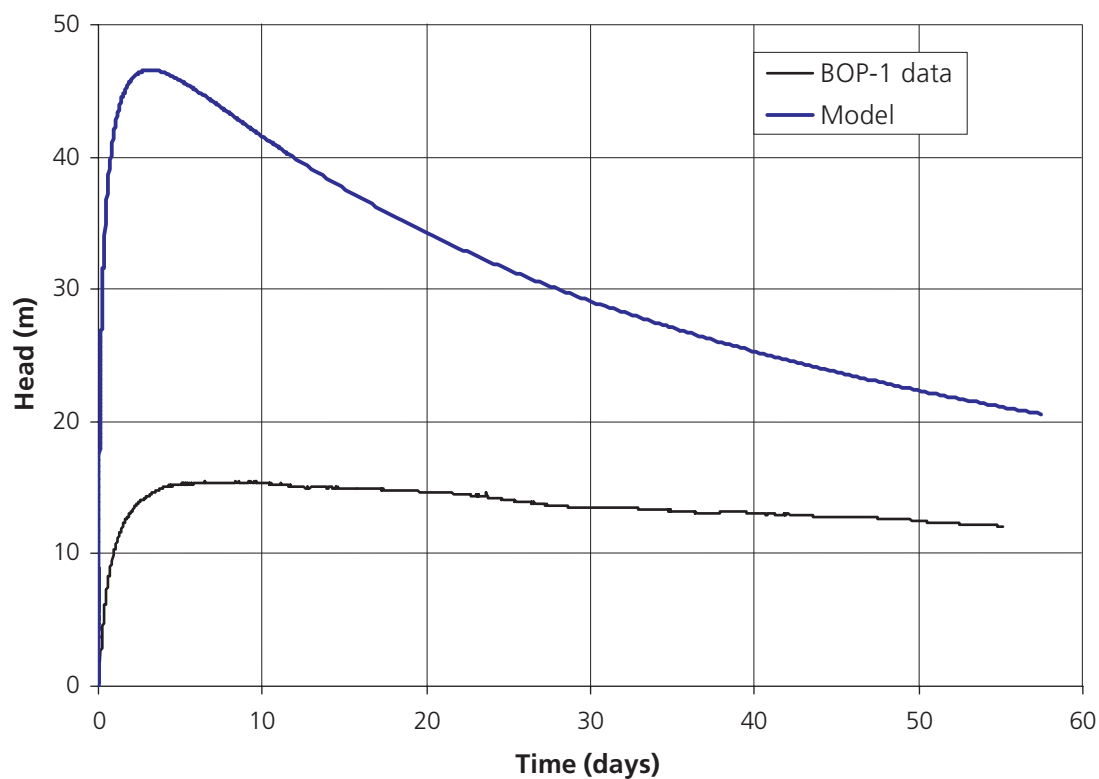


Figure 5.5: Field data from Phase 3 of the BOP-1 borehole experiment compared to the model prediction using optimised parameters derived from the Phase 2 interpretation (see Table 5.1).

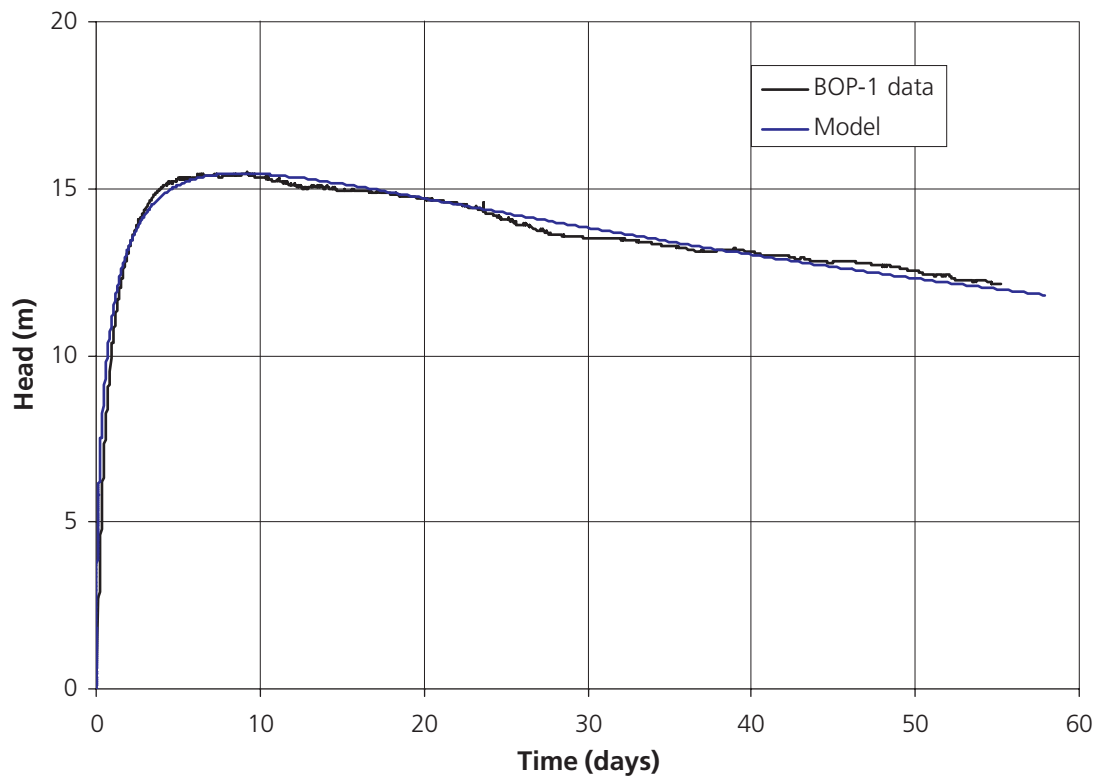


Figure 5.6: Field data from Phase 3 of the BOP-1 borehole experiment compared to the model prediction based on optimised parameters (see Table 5.1).

The initial predictive model of the first phase of the experiment was calculated using parameter values partly derived from the interpretation of the laboratory experiment described in Section 5.1. In addition, estimates of hydraulic conductivity, specific storage and borehole storage were available from independent tests of the formation (Wyss et al., 1999). The hydraulic conductivity of the formation was substantially higher than that of the laboratory sample, so it was assumed that the osmotic efficiency should be held constant. The full set of parameters used in the calculation is given in Table 5.1 (Phase 2 prediction) and the results are shown in Figure 5.3. It can be seen that the model response differs from the data in three important aspects: (a) the magnitude of the response seen in the data is much greater than was obtained from the model, (b) the data shows a much faster approach to maximum drawdown than is seen in the model, (c) the rate of recovery seen in the data is greater than predicted by the model. The sensitivity of the model to changes in the various parameters was explored by making changes to each in turn. The following responses were observed:

- i) Increasing the hydraulic conductivity reduces the magnitude of the osmotic response but has little effect on the timescale of the return to equilibrium.
- ii) Increasing the diffusion coefficient causes the osmotic drawdown to recover more quickly whilst at the same time slightly reducing the magnitude of the maximum response.
- iii) Reducing the borehole storage has no effect on the long term recovery of the system, but does increase the rate at which the initial drawdown is expressed. The net effect is thus to slightly increase the magnitude of the maximum drawdown and sharpen the trough about the maximum response.
- iv) Increasing the magnitude of the osmotic permeability, or increasing the osmotic efficiency, increases the magnitude of the overall response but has little effect on the timescale of the return to equilibrium.

Using these responses as a guide it was possible to obtain the fit to the data shown in Figure 5.4 using the parameter values listed in Table 5.1 (Phase 2 interpretation). It can be seen that an excellent fit to the data has been obtained. Comparing the new parameter values to those in Table 5.1 (Phase 2 prediction) shows that the osmotic efficiency of the formation had to be raised by a factor of about 1.8 and the borehole storage reduced by a factor of 3.3. In addition, the diffusion coefficient was increased slightly. It

seems reasonable to suppose that the reduced osmotic efficiency of the laboratory sample relative to the *in situ* formation may be in part be due to the disruption caused by the sampling process.

A predictive calculation for Phase 3 was made using the same parameter values as for the Phase 2 interpretation but with the initial solute concentration in the borehole set to the $1.497 \text{ mol.dm}^{-3}$ of the brine that was exchanged into the packed borehole test interval. The result is shown in Figure 5.5, together with the data obtained from this phase of the experiment. It can be seen that the time to peak response in the data was greater than that predicted and the magnitude of the response was much smaller, peaking at about 15.4 m after 8 days, compared to the predicted peak of about 46.6 m after 3 days. Also, the rate of decline of the pressure was much slower than predicted, with the data showing only a 20% reduction from peak value after 50 days, whereas the model predicts a decline of about 50% in that time.

Using the sensitivities of the model to the parameter values noted above as a guide once more it was possible to obtain a good fit to the data, as shown in Figure 5.6, using the revised parameter values listed in Table 5.1 (Phase 3). Comparing these values with those in Table 5.1 (Phase 2 interpretation) it will be seen that the osmotic efficiency of the formation is a factor of 2.3 lower under the hypersaline conditions than under the freshwater conditions. Also, the diffusion coefficient is a factor of 4.2 lower. The borehole storage is a factor of 1.5 higher than was found before, but this is still much lower than the initial estimates.

Thus, it would seem that the osmotic permeability, and hence the osmotic efficiency, is greater at low solute concentrations than at high values. This would be consistent with the experimental findings of Fritz and Marine (1983) on osmotic flow in bentonite. The variation of the osmotic permeability with solute concentration is likely to arise from interactions between the ions in solution and the fabric of the clay minerals at the microscopic scale. One possibility would be that the high ionic strength fluid causes the separation between clay platelets to decrease in line with Double Layer Theory predictions, leading to widening of the interconnected flow channels through the clay fabric. The electrical restrictions on the passage of ions along these flow channels would decrease as their aperture increases, leading to a reduction in osmotic efficiency. These hypothesized changes in clay fabric do not explain why the diffusion coefficient should be lower in the presence of the hypersaline solution.

6 Conclusions

The programme of work on osmotic flow in Opalinus Clay comprised three main activities, a laboratory pilot study on samples, an *in situ* experiment in a borehole at the Mt Terri Rock Laboratory and a theoretical study supported by mathematical modelling.

The pilot study demonstrated that the shale behaves as a leaky semi-permeable membrane with an osmotic efficiency in the range 1.5 to 6%. It is thus possible to generate a measurable flow of water when a sample is exposed to a solute concentration gradient in the absence of a pressure gradient. When pore-water was replaced by distilled water, the sample swelled by up to 0.9%. Clearly, a simple change in pore-water salinity can lead to a change in shale volume.

The results of the laboratory study were initially analysed using equations for chemico-osmotically coupled flow and solute transport developed by Greenberg et. al. (1973). Some aspects of the transient flows and the long term swelling behaviour seen in the data could not be explained by the original equations and a modification to the definition of compressibility was proposed which improves the representation of these transient effects.

The *in situ* borehole experiment in the Mt Terri Rock Laboratory lasted nearly five years and utilized a specially-designed packer system in which the chemistry of the sealed test interval could be controlled and changed without disturbing the pressure regime. After filling the test interval with an aqueous solution matched to the natural formation water, the pressure evolution was monitored for approximately two years. The test interval pressure at the end of this phase was 900 ± 20 kPa.

In the second phase, the original test fluid was sampled and replaced with de-ionised water and the fluid was allowed to equilibrate with formation water for another two years. Immediately after shut-in pressure began to fall, reaching a minimum of 812 kPa after 52 hours. Interval pressure then began to slowly increase. The magnitude of the *in situ* response obtained was significantly greater than that predicted on the basis of the parameters from the laboratory pilot study. It was found that both the osmotic efficiency and the diffusion coefficient were larger in the *in situ* formation than in the laboratory sample.

In the third and last phase, the test fluid was replaced with hypersaline solution. In contrast to the previous response, pressure then began to rise after shut-in, reaching a maximum of 1082 kPa after 221 hours. After reaching the maximum, interval pressure slowly began to decrease. The initial predictive model calculation for this phase was based on the interpretation and parameters of the previous phase. The observed response was smaller than the predicted. Parameters

were adjusted and the model re-calculated to fit the data. This demonstrated that both the osmotic efficiency and the diffusion coefficient were lower under the high salinity pore-water conditions of the last phase.

The osmotic efficiency of the Opalinus Clay was generally lower than might be anticipated for this well-compacted argillaceous rock. A possible explanation for low osmotic efficiency and the unusually large compressibility seen in laboratory testing is that the test material contained a network of microcracks which opened up during de-stressing, sample preparation and testing. The aperture of such cracks (typically μm -scale) would be sufficiently large to allow the solutes to diffuse through the rock virtually unimpeded by the relatively short-range (typically nm-scale) electrostatic interactions with the clay mineral surfaces.

It is possible that the shale around the borehole wall was also damaged by unloading and deformation. It is entirely feasible that undisturbed rock remote from the excavations could display a lower compressibility and a significantly higher osmotic efficiency.

7 References

- ABD-EL-AZIZ, M. & TAYLOR, S.A. (1964): Simultaneous flow of water and salt through unsaturated porous media, 1: Rate equations. *Soil Sci. Soc. America Proc.* 29, 141.
- BANIN, A. AND LOW, P.F. (1971): Simultaneous transport of water and salt through clays, 2: Steady-state distribution of pressure and applicability of irreversibility of thermodynamics. *Soil Sci. America Proc.* 112, 69-88.
- BEAR J. (1972): *Dynamics of fluids in porous media.* Elsevier, New York.
- BERRY F.A.F. (1960): Geologic evidence suggesting membrane properties of shales. *Bull. Amer. Assoc. Petroleum Geol.* 44(6), 953-954.
- BOLT, G.H. & DE HAAN, F.A.M. (1962): Anion exclusion in soils. In: *Soil Chemistry, Developments in Soil Science*, Elsevier, Amsterdam.
- CAVE, M.R., REEDER, S., ENTWISLE, D.C., BLACKWELL, P.A., TRICK, J.K., WRAGG, J. & VICKERS, B. (1998): Chemical characterisation of squeezed pore-waters and aqueous leachates from Opalinus Marl core material from the Mont Terri tunnel, Switzerland. In: Bossart, P. (ed.): *Basic geochemical data from water sampling (WS) experiments, Phases 1 and 2. Mont Terri Project Technical Report 97-02*, Swiss National Hydrological and Geological Survey, Bern.
- CHENEVERT, M.E. (1970): Shale alteration by water adsorption. *J. Petroleum Tech.*, 1141-1148.
- COPLIN, TB. AND HANSHAW, B.B. (1973): Ultrafiltration by a compacted clay membrane. I. Oxygen and hydrogen isotopic fractionation. *Geochim. Cosmochim. Acta* 37, 2295-2310.
- EVERETT, D.H. (1988): *Basic Principles of Colloid Science.* Royal Society of Chemistry Publications.
- FARGUE, D., GOBLET, P. & JAMET, PH. (1989): Étude sous l'angle thermodynamique des processus de transfert potentiels non-dominants des radionucléides dans les géosphère. Final Rapport LHM/RD/89/52, Centre D'Informatique Géologique, École Nationale Supérieure des Mines de Paris.
- FRITZ, S.J. (1986): Ideality of clay membranes in osmotic processes: A review. *Clays & Clay Minerals* 34/2, 214-223.
- FRITZ, S.J. & MARINE, I.W., 1983. Experimental support for predictive osmotic model of clay membranes. *Geochim. Cosmochim. Acta* 47, 1515-1522.
- GRAF, D.L. (1982): Chemical osmosis, reverse chemical osmosis and the origins of subsurface brines. *Geochim. Cosmochim. Acta* 46, 1431-1448.
- GREENBERG J.A. (1971): Diffusional flow of salt and water in soils. Ph.D. thesis, University of California, Berkeley, USA.
- GREENBERG, J.A., MITCHELL, J.K. AND WITHERSPOON, P.A. (1973): Coupled salt and water flows in a groundwater basin. *J. Geophys. Res.* 78, 6341 - 6353.
- HANSHAW, B.B. (1962): Membrane properties of compacted clays. Ph.D. thesis, Harvard University, USA.
- HINDMARSH, A.C. (1982): ODEPACK, a systematized collection of ODE solvers. Lawrence Livermore National Laboratory Report, UCRL-88007.
- HORSEMAN, S.T. (1996): Guidelines for chemico-osmotic experiments in Opalinus Clay. Unpublished Technical Note TN96-21, Mont Terri Project, Switzerland.
- ISRM (1981): Rock Characterization, Testing and Monitoring. In: Brown E.T. (ed.): *International Society of Rock Mechanics, Commission on Testing Methods.* Pergamon Press, Oxford.
- KEMPER, W.D. & EVANS, N.A. (1963): Movements of water as affected by free energy and pressure gradients, III, Restriction of solutes by membranes. *Soil Sci. Soc. America Proc.* 27, 485-490.
- KEMPER, W.D. & ROLLINS, J.B. (1966): Osmotic efficiency coefficients across compacted clays. *Soil Sci. Soc. America Proc.* 30, 529-534.
- KHARAKA, Y.K. & BERRY F.A.F. (1973): Simultaneous flow of water and solutes through geological membranes - I. Experimental investigation. *Geochim. Cosmochim. Acta* 37, 2577-2603.
- KIRKWOOD, J.G. (1954): Transport of ions through biological membranes from the standpoint of irreversible thermodynamics. In: Clarke, H. (ed.): *Ion Transport Across Membranes.* Academic Press, New York.
- LETEY J, AND KEMPER, W.D. (1969): Movement of water and salt through a clay-water system: Experimental verification of Onsager reciprocal relation. *Soil Sci. Soc. America Proc.* 33, 25-29.
- MARINE, W.I. AND FRITZ, S.J. (1981): Osmotic model to explain anomalous hydraulic heads. *Water Resources Research* 17, 73-82.
- NEUZIL, C.E. (1994): How permeable are clays and shales? *Water Resources Research* 30, 145-150.
- NEUZIL C.E. (2000): Osmotic generation of "anomalous" fluid pressures in geological environments. *Nature* 403, 182-184.
- NOY D.J. (1998): A user guide for OSMO1R: a program for solution of radial groundwater flow and solute transport with chemico-osmotic coupling. British Geological Survey Technical Report WE/98/37, Keyworth, Nottingham.
- OLSEN H.W. (1969): Simultaneous fluxes of liquid and charge in saturated kaolinite. *Soil Sci. Soc. America Proc.* 33, 338-344.
- PEARSON, F.J., SCHOLTIS, A., GAUTSCHI, A., BAEYENS, A., BRADBURY, M. AND DEGUELDRE, C. (1999): Chemistry of porewater. In: THURY M. AND BOSSART P. (eds): *Mont Terri Rock Laboratory: results of the hydrogeological, geochemical and geotechnical experiments per-*

- formed in 1996 and 1997. Swiss National Hydrological and Geological Survey, Geological Reports No. 23, Bern.
- PETZOLD, L.R. (1982): A description of DASSL: a differential/algebraic system solver. Sandia National Laboratories report SAND82-8637.
- SCHLEMMER, R., FRIEDHEIM, J.E., GROWCOCK, F.B., BLOYS, J.B., HEADLEY, J.A. & POLNASZEK, S.C. (2002): Membrane efficiency in shale: an empirical evaluation of drilling fluid chemistries and implications for fluid design. Presented at IADC/SPE Drilling Conference, Dallas, Texas, Feb. 2002, Paper 74557.
- SHERWOOD J.D. (1993): Biot poroelasticity of a chemically active shale. *Proc. Royal Soc. London A* 440, 365-377.
- SOLER, J.M. (1999): Coupled transport phenomena in the Opalinus Clay: implications for radionuclide transport. Paul Scherrer Institut Report 99-07. Also published as Nagra Technical Report NTB 99-09.
- Soler, J.M. (2001): The effect of coupled transport phenomena in the Opalinus Clay and implications for radionuclide transport. *J. Contaminant Hydrology* 53, 63-84.
- THURY, M. (1999): Extended summary. In: Thury, M. and Bossart, P. (eds): Mont Terri Rock Laboratory: results of the hydrogeological, geochemical and geotechnical experiments performed in 1996 and 1997. Swiss National Hydrological and Geological Survey, Geological Reports No. 23, Bern.
- THURY, M. AND BOSSART P. (1999): The Mont Terri Rock Laboratory, a new international research project in a Mesozoic shale formation in Switzerland. *Engineering Geol.* 52, 347-359.
- VAN OORT, E. (1994): A novel technique for the introduction of drilling fluid induced borehole instability in shales. In: *Eurock '94*, Balkema, Rotterdam, 293-308.
- WONG, S.W. AND HEIDUG, W.K. (1994): Borehole stability in shales: A constitutive model for the mechanical and chemical effects of drilling fluid invasion. In: *Eurock '94*, Balkema, Rotterdam, 251-257.
- WYSS, E., MARSHALL, P. & ADAMS, J. (1999): Hydraulic parameters and formation pressures in matrix and faults. In: Thury, M. and Bossart, P. (eds): Mont Terri Rock Laboratory: results of the hydrogeological, geochemical and geotechnical experiments performed in 1996 and 1997. Swiss National Hydrological and Geological Survey, Geological Reports No. 23, Bern.
- YOUNG, A. & LOW, P.F. (1965): Osmosis in argillaceous rocks. *Bull. Amer. Assoc. Petroleum Geol.* 49/7, 1004-1008.

Mont Terri Technical Notes

- TN 96-21: S.T. Horseman: Guidelines for chemico-osmotic experiments in OPA. British Geological Survey; Mont Terri internal, unpublished report.
- TN 97-39: J.F. Harrington and S.T. Horseman: Laboratory experiments on hydraulic and osmotic flow in Opalinus Clay. British Geological Survey; Mont Terri internal, unpublished report.
- TN 98-48: D.J. Noy: Parameter estimates from 1D modelling of osmotic experiments. British Geological Survey; Mont Terri internal, unpublished report.
- TN 99-81: D.J. Noy and S.T. Horseman: OP Experiment: Design calculation. Determination of the osmotic pressure response of borehole BOP-1 to a change of borehole fluid. British Geological Survey; Mont Terri internal, unpublished report.
- TN 2000-44: D.J. Noy: OP Experiment: Simulation of fluid exchange carried out in borehole BOP-1. British Geological Survey; Mont Terri internal, unpublished report.
- TN 2002-19: D.J. Noy: Osmotic Pressure Experiment: Fluid exchange with a high saline solution. British Geological Survey; Mont Terri internal, unpublished report.
- TN 2002-21: H.R. Fisch and P. Bossart: Experiment OP: Fluid exchange in borehole BOP-1 with a 100 g dm⁻³ NaCl fluid. The field data set. Solexperts & Geotechnical Institute; Mont Terri internal, unpublished report.

